



The Open
University



“Marine biotechnologies for the decontamination and restoration of degraded marine habitats”

PhD Candidate: Filippo Dell’ Anno (F7057844)

Thesis submitted for the degree of Doctor of Philosophy, XVIII Cycle
November 2019

The Open University, Milton Keynes (UK), School of Life, Health and Chemical
Sciences

Stazione Zoologica Anton Dohrn Naples (Italy), Department of Marine
Biotechnology

Supervision Pannel:

Director of Studies: Dr. Adrianna Ianora (Stazione Zoologica Anton Dohrn, IT)

Internal Supervisor: Dr. Clementina Sansone (Stazione Zoologica Anton Dohrn, IT)

External Supervisor: Prof. Antonio Dell' Anno (Università Politecnica delle Marche, IT)

Advisor: Prof. Alan Dobson (University College Cork, Ireland)

Examiners:

External Examiner: Prof. Peter Golyshin (Bangor University, UK)

Internal Examiner: Dr. Paolo Sordino (Stazione Zoologica Anton Dohrn, IT)

Chair: Dr. Alessandra Gallo (Stazione Zoologica Anton Dohrn, IT)

Abstract

This research presents the results obtained using a bioremediation approach aiming to enhance natural remediation of the Bagnoli-Coroglio area, a post industrial site in the Gulf of Naples, Italy, characterized by the presence of several pollutants released in almost a century by the ILVA steel plant. In particular, the thesis evaluates the benthic microbial taxonomic composition of this area after ten decades of pollution. Results indicate the prevalence of the Phyla Proteobacteria, (36.7%), Planctomycetes (20.5%) and Bacteroidetes (9.6%) and the presence of a core microbiome suggesting that pollutants and other abiotic factors may have contributed to shape benthic prokaryotic communities. The thesis also evaluates the biotechnological potential of single isolates bacteria (*Halomonas* sp., *Alcanivorax* sp., *Epibacterium* sp., *Pseudoalteromonas* sp., and *Virgibacillus* sp.) and mixtures of these species isolated from polluted sediments collected from Bagnoli-Coroglio area and the Sarno river mouth, another polluted site in the Gulf of Naples. Laboratory tests highlighted the ability of mixed cultures and single taxa to degrade PAHs (Polycyclic Aromatic Hydrocarbons) and precipitate heavy metals from culture media. Results of Sequential Selective Extraction (SSE) analysis emphasized the ability of mixed cultures to reduce the mobility of As, Cd and Zn by changing their partitioning in the geochemical fractions. Full genome sequencing of isolated strains has allowed for the genetic and molecular characterization of mechanisms underlying processes of degradation and detoxification of xenobiotics. In particular, many genes involved in hydrocarbon degradation pathways and in heavy metal detoxification systems have been identified. My results suggest a potential biotechnological

application of these strains in waste-water treatment as well as decontamination of polluted sediments.

Acknowledgements

I would like to thank my supervisory team: Dr. Adrianna Ianora, Prof. Antonio Dell' Anno and Dr. Clementina Sansone. Their help was precious and fundamental to complete my thesis. A warm thanks to my Advisor, Prof Alan Dobson, who during these years has given me valuable advice to guide my research. I am also very grateful to Prof. Marla Trinidad and Dr. Lonnie van Zyl from IMBM (University of Western Cape, SA) who allowed me to deeply investigate the genomic features belonging to the isolated bacteria, during a three month secondment funded by the EU Ocean Medicines (H2020, MSCA-RISE) project. Finally, I would like to thank my family who, unconditionally, supported me during these years, and Francesca that makes my life every day brighter.

Table of contents

Table of contents

Chapter 1: General Introduction.....	1
1.1) Bioremediation: state of art.....	1
1.2) PAHs bacterial remediation.....	10
1.3) Heavy metals bacterial remediation.....	18
1.4) Towards an Omicss bioremediation approach	29
1.5) Aims of the thesis.....	33
Chapter 2: Effects of multiple pollution stressors on microbial diversity: The case study of the Bagnoli-Coroglio area (Gulf of Naples, South Tyrrhenian Sea).....	35
1) Introduction.....	36
2) Material and Methods.....	38
2.1) Study area.....	38
2.2) Prokaryotic Abundance and Biomass.....	40
2.3) Illumina sequencing and bioinformatic procedures for sediment microbiome analyses.....	41
2.4) Statistical analyses.....	42
3) Results and discussion.....	43
3.1) Chemical characterization.....	43
3.2) Prokaryotic Abundance.....	46
3.3) Alpha diversity.....	49
3.4) Taxonomic composition.....	52
4) Conclusion.....	64
Chapter 3: Biotechnological potential of bacteria isolated from two highly anthropic-impacted coastal areas from the Gulf of Naples.....	65

Abstract.....	65
1)Introduction.....	67
2)Material and Methods.....	69
2.1) Sediment sampling.....	69
2.2) Bacteria isolation from sediments from both sites.....	71
2.3) Bacteria characterization and identification.....	72
2.4) Analysis of sequenced data.....	72
2.5) Bacteria growth versus metals and PAHs concentrations.....	72
2.6) Evaluation of Polycyclic Aromatic Hydrocarbons (PAHs) degradation and removal rate of heavy metals in liquid solution.....	73
2.7) Evaluation of Polycyclic Aromatic Hydrocarbons (PAHs) degradation and removal rate of heavy metals during coupled water-sediment experiments.....	75
3)Results and Discussion.....	76
3.1) Bioremediation of Bacteria Isolated from the Sarno River Site.....	76
3.1.1) Identification of bacterial isolates and bacterial growth in the presence of contaminants	76
3.1.2) Evaluation of PAHs degradation and heavy metal precipitation of bacterial cultures (as single isolate and in mixtures).....	89
3.1.3) Effects of bacterial cultures addition (as isolates and as mixtures) on hydrocarbon degradation and heavy metal partitioning in contaminated sediments from Bagnoli-Coroglio.....	95
3.2) Bioremediation of Bacteria Isolated from the Bagnoli-Coroglio Site.....	99
3.2.1) Identification of bacterial isolates and bacterial growth in the presence of contaminants.....	99
3.2.2) Evaluation of PAHs degradation and heavy metal precipitation capacity of bacterial cultures (as isolates and and in mixtures).....	115
3.2.3) Effects of bacterial cultures addition (as isolates and as mixtures) on hydrocarbon degradation and heavy metal partitioning in contaminated sediments from Bagnoli-Coroglio	121
4)Conclusion.....	127

Chapter 4: Genomic characterization and functional analysis of bacterial isolates..128

Abstract.....	128
1) Introduction.....	129
2) Materials and Method.....	131
2.1) Bacterial culturing.....	131
2.2) Genomic DNA preparation and Genome sequencing.....	131
2.3) Annotation and comparative genomics.....	132
3) Results and discussion.....	134
3. 1) General description of the Genomes.....	140
3.1.1) <i>Halomonas</i> sp. SZN1.....	140
3.1.2) <i>Alcanivorax</i> sp. SZN2.....	144
3.1.3) <i>Pseudoalteromonas</i> sp. SZN3.....	148
3.1.4) <i>Epibacterium</i> sp. SZN4.....	151
3.1.5) <i>Oceanicaulis</i> sp. SZN5.....	155
3.1.6) <i>Alkaliphilus</i> sp. SZN6.....	158
3.2) Genetic basis of PAHs degradation.....	161
3.2.1) Ring Hydroxylating dioxygenase.....	166
3.2.2) Cytochrome P450.....	173
3.2.3) Catechol pathway.....	179
3.2.4) Protocatechuate pathway.....	182
3.2.5) Homogentisate pathway.....	187
3.2.6) Homoprocatechuate pathway.....	192
3.2.7) Phenilacetic pathway.....	197
3.3) Genetic bases for Metal detoxification.....	201
4) Conclusion.....	211
Chapter 5: General conclusions.....	213
6) Bibliography.....	221

List of Figures

- Figure 1.1.** Map of the four sampling sites analysed in the current study: 1) Impianto Sollevamento Dazio, 2) Scarico Conca di Agnano; 3) Canale Bianchettaro; 4) Galleria scarico Impianto Coroglio.....39
- Figure 1.2.** Heat-maps showing the concentrations reported of Biopolymeric organic C (a), Carbohydrates (b), lipids (c), phytopigments (d) and protein (e) along the littoral area of Bagnoli-Coroglio.....43
- Figure 1.3.** Prokaryotic Abundance (a) and Biomass (b) counting in epifluorescence bacterial cells labelled with SYBR Green according to Danovaro et al. 2009. Bacterial cells have been collected at three different depths (0-3 cm, 3-6 cm, 6-9 cm) at four different sites as indicated in the map. Biomass has been calculated basing on the different prokaryotic size.....48
- Figure 1.4.** Amplicon Sequence Variance richness (a), effective species number (b) and Evenness values (c) calculated for samples collected at three different depths (0-3 cm, 3-6 cm, 6-9 cm) in the four analysed station of Bagnoli-Coroglio area.51
- Figure 1.5.** Abundances of the most represented Phylum in the study area of Bagnoli-Coroglio. Blue bars refer to percentage of sequences while red bars refer to percentage Otus observed.....57
- Figure 1.6.** Abundances of the most represented phylum and classes in the study area of Bagnoli-Coroglio. Blue bars refer to percentage of sequences while red bars refer to percentage Otus observed.....58
- Figure 1.7.** Percentage of distribution of bacterial Classes at different four stations and layers (0-3 cm, 3-6 cm, 6-9 cm) studied in Bagnoli Coroglio area.....59
- Figure 1.8.** Percentage of distribution of Orders belonging to the Gamma Proteobacteria at four different station and layers (0-3 cm, 3-6 cm, 6-9 cm) analysed in Bagnoli-Coroglio area.....60
- Figure 1.9.** Distribution of the most abundant families belonging to the Order Xanthomonadales at different stations and layers (0-3 cm, 3-6 cm, 6-9 cm) analysed in Bagnoli-Coroglio area.....61

Figure 1.10. Cluster Dendrogram (d) built using Bray-Curtis distances matrix, using R Package Vegan. The dendrogram clustered the different layers belonging to the four analysed station relying on their similarity.....	63
Figure 2.1. Map of the study area with the position of the sampling site of Sarno River Mouth.....	70
Figure 2.2. The Bagnoli-Coroglio Sediment sampling strategy (ABBACO research project). The blue dots outside the inner grid represents superficial sampling points. The triangles inside the grid represents sampling points where coring activity has been carried on.....	70
Figure 2.3. Agar plates with Mix culture (A), the two isolates <i>Halomonas</i> sp. (B), <i>Alcanivorax</i> sp. (C) and the agarose gel after 16s RNA amplicon (D) (Lanes 1, 2, 3, respectively contain DNA ladder, <i>Halomonas</i> SZN1 16s rRNA, <i>Alcanivorax</i> SZN2 16s rRNA.....	77
Figure 2.4. 16s RNA tree of <i>Halomonas</i> sp. SZN1 and <i>Alcanivorax</i> sp. SZN2 built using the best twenty 16s RNA sequences retrieved from NCBI database. Tree has been created with the Maximum Likelihood Method using MEGA 7 software after alignment conducted with Muscle algorithm.....	78
Figure 2.5. Minimum Inhibition Concentrations (MIC) testing Pb at concentrations of 100, 1000 and 10000 ppm on Consortium A2 (A), <i>Halomonas</i> sp. SZN1 (B), and <i>Alcanivorax</i> sp. SZN2 (C) expressed as Optical density (OD) values with time.....	82
Figure 2.6. Minimum Inhibition Concentrations (MIC) testing PAHs at concentrations of 100, 1000 and 10000 ppm on Consortium A2 (A), <i>Halomonas</i> sp. SZN1 (B), and <i>Alcanivorax</i> sp. SZN2 (C) expressed as Optical density (OD) values with time.....	83
Figure 2.7. Minimum Inhibition Concentrations (MIC) testing As at concentrations of 100, 1000 and 10000 ppm on Consortium A2 (A), <i>Halomonas</i> sp. SZN1 (B), and <i>Alcanivorax</i> sp. SZN2 (C) expressed as Optical density (OD) values with time.....	85
Figure 2.8. Minimum Inhibition Concentrations (MIC) testing Zn at concentrations of 100, 1000 and 10000 ppm on Consortium A2 (A), <i>Halomonas</i> sp. SZN1 (B), and <i>Alcanivorax</i> sp. SZN2 (C) expressed as Optical density (OD) values with time.....	86
Figure 2.9. Minimum Inhibition Concentrations (MIC) testing Cd at concentrations of 100, 1000 and 10000 ppm on Consortium A2 (A), <i>Halomonas</i> sp. SZN1 (B), and <i>Alcanivorax</i> sp. SZN2 (C) expressed as Optical density (OD) values with time.....	87
Figure 2.10. Minimum Inhibition Concentrations (MIC) testing Cu at concentrations of 100, 1000 and 10000 ppm on Consortium A2 (A), <i>Halomonas</i> sp. SZN1 (B), and <i>Alcanivorax</i> sp. SZN2 (C) expressed as Optical density (OD) values with time.....	88

Figure 2.11: Biomass growth measurements at four different time, of the MIX culture (Consortium A2), <i>Halomonas</i> sp. SZN1 and <i>Alcanivorax</i> sp. SZN2 incubated with a mix of heavy metals (A), PAHs (B) and no amendments (C).....	92
Figure 2.12: pH variations at four different hours, of the mix culture (Consortium A2), <i>Halomonas</i> sp. SZN1, and <i>Alcanivorax</i> sp. SZN2 incubated with a mix of Heavy metals(A), PAHs (B) and no amendments (C).....	93
Figure 2.13: A) Percentage of PAHs degradation after the incubation time (27 days) with <i>Halomonas</i> sp. SZN1 and <i>Alcanivorax</i> sp. SZN2 and its mixture. (B) Heavy metal precipitation after the incubation time (27 days) with <i>Halomonas</i> sp. SZN1 and <i>Alcanivorax</i> sp. SZN2 and its mixture.....	94
Figure 2.14. Percentage of PAHs removal rates in sediments after inoculation with <i>Halomonas</i> sp. SZN1 and <i>Alcanivorax</i> sp. SZN2 and a mixture of both strains (Consortium A2).....	97
Figure 2.15. As (A), Cd (B), Pb (C), Cu (D) and Zn (E) distribution in the four sediment fractions following Selective Sequential Extraction.....	98
Figure 2.16. Agar plates with Mix cultures: Consortium 2B (A), Consortium 4 (B), Consortium 41 (C); the three isolates <i>Epibacterium</i> sp. SZN4 (D), <i>Pseudoalteromonas</i> sp. SZN3 (E), and <i>Virgibacillus</i> sp. SZN7 (F) and the agarose gel after 16s RNA amplification (G) (Lanes 1, 2, 3, 4, respectively contain DNA ladder, <i>Epibacterium</i> 16s rRNA, <i>Pseudoalteromonas</i> 16s rRNA, and <i>Virgibacillus</i> 16s.....	100
Figure 2.17. 16s RNA tree of <i>Epibacterium</i> sp. SZN3, <i>Pseudoalteromonas</i> sp. SZN3, and <i>Virgibacillus</i> sp. SZN7, built using the best twenty 16s RNA sequences retrieved from NCBI database. Tree has been created with the Maximum Likelihood Method using MEGA 7 software after alignment conducted with Muscle algorithm.....	103
Figure 2.18: Minimum Inhibition Concentrations (MICs) testing As (A), PAHs (B), Pb (C), Cd (D), Cu (E), and Zn (F), on Consortium 2B at concentrations of 100, 1000 and 10000 ppm, expressed as Optical density (OD) values with time.....	107
Figure 2.19: Minimum Inhibition Concentrations (MICs) testing As (A), PAHs (B), Pb (C), Cd (D), Cu (E), and Zn (F), on Consortium 4 at concentrations of 100, 1000 and 10000 ppm, expressed as Optical density (OD) values with time.....	108
Figure 2.20: Minimum Inhibition Concentrations (MICs) testing As (A), PAHs (B), Pb (C), Cd (D), Cu (E), and Zn (F), on Consortium 41 at concentrations of 100, 1000 and 10000 ppm, expressed as Optical density (OD) values with time.....	109
Figure 2.21: Minimum Inhibition Concentrations (MICs) testing As (A), PAHs (B), Pb (C), Cd (D), Cu (E), and Zn (F), on <i>Epibacterium</i> sp. at concentrations of 100, 1000 and 10000 ppm, expressed as Optical density (OD) values with time.....	111

Figure 2.22: Minimum Inhibition Concentrations (MICs) testing As (A), PAHs (B), Pb (C), Cd (D), Cu (E), and Zn (F), on *Pseudoalteromonas sp.* at concentrations of 100, 1000 and 10000 ppm, expressed as Optical density (OD) values with time.....112

Figure 2.23: Minimum Inhibition Concentrations (MICs) testing As (A), PAHs (B), Pb (C), Cd (D), Cu (E), and Zn (F), on *Virgibacillus sp.* at concentrations of 100, 1000 and 10000 ppm, expressed as Optical density (OD) values with time.....113

Figure 2.24: Biomass growth measurements, at four different timings, of Consortium 4 (4), Consortium 41 (41), Consortium 2B (2B), *Epibacterium sp.* SZN4, (1), *Pseudoalteromonas sp.* SZN3, (3), *Virgibacillus sp.* SZN7(7) incubated with a mix of heavy metals (A), PAHs (B) and no amendements(C).....117

Figure 2.25: pH measurements, at four different hours, of Consortium 4 (4), Consortium 41 (41), Consortium 2B (2B), *Epibacterium sp.* SZN4, (1), *Pseudoalteromonas sp.* SZN3, (3), *Virgibacillus sp.* SZN7 (7) incubated with a mix of heavy metals (A), PAHs (B) and no amendements (C).....118

Figure 2.26: PAH degradation rates (A) and heavy metals removals (B) of Consortium 4 (4), Consortium 41 (41), Consortium 2B (2B), *Epibacterium sp.* SZN1, (1), *Pseudoalteromonas sp.* SZN3, (3), *Virgibacillus sp.* SZN7, (7) at the end of incubation time (27 days).....119

Figure 2.27. Percentage PAHs degradation rates in sediments at the end of the incubation time (27 days) compared to controls.....124

Figure 2.28. As (A), Cd (B), Pb (C), Cu (D) and Zn (E) distribution in the four sediment fractions following Selective Sequential Extraction at the end of incubation time (27 days).....124

Figure 3.1. Illumina Miseq Output after sequencing. The different colours of the dots represent a different number of estimated clusters for consortia 2B (A), A2 (B), 41 (C) and 4 (D).....136

Figure 3.2. Circular representation of *Halomonas sp.* SZN1 genome. The different rings represent (from outer to inner) predicted protein-coding sequences (CDS) on the forward (outer wheel) and the reverse (inner wheel) strands (circle 2 and 3) colored according to the assigned COG classes (circle 1, 4), G+C content (circle 5), GC skew (circle 6), genomic position (circle 7). The COG colors represent functional groups (A, RNA processing and modification; B, chromatin structure and dynamics; J, Translation, ribosomal structure and biogenesis; K, Transcription; L, Replication, recombination and repair; D, Cell cycle control, cell division, chromosome partitioning; O, Posttranslational modification, protein turnover, chaperones; M, Cell wall/membrane/envelope biogenesis; N, Cell motility; P, Inorganic ion transport and metabolism; T, Signal transduction mechanisms; U, Intracellular trafficking, secretion, and vesicular transport;

V, Defense mechanisms; W, Extracellular structures; Y, Nuclear structure; Z, Cytoskeleton; C, Energy production and conversion; G, Carbohydrate transport and metabolism; E, Amino acid transport and metabolism; F, Nucleotide transport and metabolism; H, Coenzyme transport and metabolism; I, Lipid transport and metabolism; Q, Secondary metabolites biosynthesis, transport and catabolism; R, General function prediction only; S, Function unknown).....142

Figure 3.3. The red bars indicate the Genomic Islands found in *Halomonas* sp. SZN1. The most interesting GC island was in the genome region between 1.96 Mb and 1.995.....143

Figure 3.4. Circular representation of *Alcanivorax* sp. SZN2 genome. The different rings represent (from outer to inner) predicted protein-coding sequences (CDS) on the forward (outer wheel) and the reverse (inner wheel) strands (circle 2 and 3) colored according to the assigned COG classes (circle 1, 4), G+C content (circle 5), GC skew (circle 6), genomic position (circle 7). The COG colors represent the functional groups (A, RNA processing and modification; B, chromatin structure and dynamics; J, Translation, ribosomal structure and biogenesis; K, Transcription; L, Replication, recombination and repair; D, Cell cycle control, cell division, chromosome partitioning; O, Posttranslational modification, protein turnover, chaperones; M, Cell wall/membrane/envelope biogenesis; N, Cell motility; P, Inorganic ion transport and metabolism; T, Signal transduction mechanisms; U, Intracellular trafficking, secretion, and vesicular transport; V, Defense mechanisms; W, Extracellular structures; Y, Nuclear structure; Z, Cytoskeleton; C, Energy production and conversion; G, Carbohydrate transport and metabolism; E, Amino acid transport and metabolism; F, Nucleotide transport and metabolism; H, Coenzyme transport and metabolism; I, Lipid transport and metabolism; Q, Secondary metabolites biosynthesis, transport and catabolism; R, General function prediction only; S, Function unknown).....146

Figure 3.5. The red bars indicate the Genomic Islands found in *Alcanivorax* sp. SZN2. From the automatic annotation provided by island viewer only one gene (beta-ketoadipyl CoA thiolase; 1673405-1674613 bp), linked to central hydrocarbon degradation pathway has been identified.....147

Figure 3.6. Circular representation of *Pseudolateromonas* sp. SZN3 genome. The different rings represent (from outer to inner) predicted protein-coding sequences (CDS) on the forward (outer wheel) and the reverse (inner wheel) strands (circle 2 and 3) colored according to the assigned COG classes (circle 1, 4), G+C content (circle 5), GC skew (circle 6), genomic position (circle 7). The COG colors represent the functional groups (A, RNA processing and modification; B, chromatin structure and dynamics; J, Translation, ribosomal structure and biogenesis; K, Transcription; L, Replication, recombination and repair; D, Cell cycle control, cell division, chromosome partitioning; O, Posttranslational modification, protein turnover, chaperones; M, Cell

wall/membrane/envelope biogenesis; N, Cell motility; P, Inorganic ion transport and metabolism; T, Signal transduction mechanisms; U, Intracellular trafficking, secretion, and vesicular transport; V, Defense mechanisms; W, Extracellular structures; Y, Nuclear structure; Z, Cytoskeleton; C, Energy production and conversion; G, Carbohydrate transport and metabolism; E, Amino acid transport and metabolism; F, Nucleotide transport and metabolism; H, Coenzyme transport and metabolism; I, Lipid transport and metabolism; Q, Secondary metabolites biosynthesis, transport and catabolism; R, General function prediction only; S, Function unknown).....149

Figure 3.7. The red bars indicate the Genomic Islands found in *Pseudoalteromonas* sp. SZN3. No genes involved in metal tolerance and hydrocarbon degradation were detected in the identified genome islands.....150

Figure 3.8. Circular representation of *Epibacterium* sp. SZN4 genome. The different rings represent (from outer to inner) predicted protein-coding sequences (CDS) on the forward (outer wheel) and the reverse (inner wheel) strands (circle 2 and 3) colored according to the assigned COG classes (circle 1, 4), G+C content (circle 5), GC skew (circle 6), genomic position (circle 7). The COG colors represent functional groups (A, RNA processing and modification; B, chromatin structure and dynamics; J, Translation, ribosomal structure and biogenesis; K, Transcription; L, Replication, recombination and repair; D, Cell cycle control, cell division, chromosome partitioning; O, Posttranslational modification, protein turnover, chaperones; M, Cell wall/membrane/envelope biogenesis; N, Cell motility; P, Inorganic ion transport and metabolism; T, Signal transduction mechanisms; U, Intracellular trafficking, secretion, and vesicular transport; V, Defense mechanisms; W, Extracellular structures; Y, Nuclear structure; Z, Cytoskeleton; C, Energy production and conversion; G, Carbohydrate transport and metabolism; E, Amino acid transport and metabolism; F, Nucleotide transport and metabolism; H, Coenzyme transport and metabolism; I, Lipid transport and metabolism; Q, Secondary metabolites biosynthesis, transport and catabolism; R, General function prediction only; S, Function unknown).....153

Figure 3.9. The red bars indicate the Genomic Islands found in *Epibacterium* sp. SZN4. The following genes *CzcA*, *czrB*, *NccC*, *CopA*, *cueR*, *merR*, *merT*, *merA* involved in mechanisms of resistance to Zinc, Cadmium Nickel, Copper and Mercury were identified in the region between 4.25M and 4.65M.....154

Figure 3.10. Circular representation of *Oceanicaulis* sp. SZN5 genome. The different rings represent (from outer to inner) predicted protein-coding sequences (CDS) on the forward (outer wheel) and the reverse (inner wheel) strands (circle 2 and 3) colored according to the assigned COG classes (circle 1, 4), G+C content (circle 5), GC skew (circle 6), genomic position (circle 7). The COG colors represent functional groups (A, RNA processing and modification; B, chromatin structure and dynamics; J, Translation, ribosomal structure and biogenesis; K, Transcription; L, Replication, recombination and

repair; D, Cell cycle control, cell division, chromosome partitioning; O, Posttranslational modification, protein turnover, chaperones; M, Cell wall/membrane/envelope biogenesis; N, Cell motility; P, Inorganic ion transport and metabolism; T, Signal transduction mechanisms; U, Intracellular trafficking, secretion, and vesicular transport; V, Defense mechanisms; W, Extracellular structures; Y, Nuclear structure; Z, Cytoskeleton; C, Energy production and conversion; G, Carbohydrate transport and metabolism; E, Amino acid transport and metabolism; F, Nucleotide transport and metabolism; H, Coenzyme transport and metabolism; I, Lipid transport and metabolism; Q, Secondary metabolites biosynthesis, transport and catabolism; R, General function prediction only; S, Function unknown).....156

Figure 3.11. The red bars indicate the Genomic Islands found in *Oceanicaulis* sp. SZN5. MATE multi-drug resistance genes linked to metals resistance were identified in the region 1.142 M and 1.154 M 159

Figure 3.12. Circular representation of *Alkaliphilus* sp. SZN6 genome. The different rings represent (from outer to inner) predicted protein-coding sequences (CDS) on the forward (outer wheel) and the reverse (inner wheel) strands (circle 2 and 3) colored according to the assigned COG classes (circle 1, 4), G+C content (circle 5), GC skew (circle 6), genomic position (circle 7). The COG colors represent functional groups (A, RNA processing and modification; B, chromatin structure and dynamics; J, Translation, ribosomal structure and biogenesis; K, Transcription; L, Replication, recombination and repair; D, Cell cycle control, cell division, chromosome partitioning; O, Posttranslational modification, protein turnover, chaperones; M, Cell wall/membrane/envelope biogenesis; N, Cell motility; P, Inorganic ion transport and metabolism; T, Signal transduction mechanisms; U, Intracellular trafficking, secretion, and vesicular transport; V, Defense mechanisms; W, Extracellular structures; Y, Nuclear structure; Z, Cytoskeleton; C, Energy production and conversion; G, Carbohydrate transport and metabolism; E, Amino acid transport and metabolism; F, Nucleotide transport and metabolism; H, Coenzyme transport and metabolism; I, Lipid transport and metabolism; Q, Secondary metabolites biosynthesis, transport and catabolism; R, General function prediction only; S, Function unknown).....159

Figure 3.13. The red bars indicate the Genomic Islands found in *Alkaliphilus* sp. SZN6. MATE multi-drug resistance gene, involved in mechanisms of resistance to metals, was identified in the region comprised 429K and 448K.....160

Figure 3.14. Heat map of genes and relative copy numbers identified by RAST in the five draft genomes analyzed. On the left column are indicated genes involved in the metabolism of aromatic compounds. The different colour intensity is related to number of gene copies. (white: “no genes”; dark green “max. number of genes”).....163

Figure 3.15. Aromatic hydrocarbon degradation pathway. A) catechol and protocatechuate produced as central intermediates of aerobic pathways. B) Degradation

pathway of Benzoate. Benzoate can be degraded through a dioxygenase or a monooxygenase. Both the enzymes capable of such reactions (Ring Hydroxylating Dioxygenase and Cytochrome P 450 monooxygenase) have been identified in the draft genomes of *Halomonas* sp. SZN1, *Alcanivorax* sp. SZN2, *Pseudolateromonas* sp. SZN3, *Epibacterium* sp. SZN4. The cis hydroxylation via dioxygenase favours the formation of Salicylate and the subsequent Catechol formation through salicylate hydroxylase found in *Alcanivorax* sp. SZN2, *Halomonas* sp. SZN1, and *Epibacterium* sp. SZN4. The catechol became substrate of catechol 1,2 dioxygenase (only in *Halomonas* sp. SZN1) that led to formation of cis cis muconic acid and β ketoadipic acid. This compound enters the β -keto adipate pathway that, through the β - keto adipate succinyl CO-A transferase and β keto adipyl thiolase (*Halomonas* sp. SZN1, *Epibacterium* sp. SZN4, *Pseudoalteromonas* sp. SZN3, and *Oceanicaulis* sp. SZN5), led to the formation of Acetyl CoA and succinyl CoA. The trans hydroxylation via monooxygenase led to the formation of protocatechuate intermediate. This pathway begins with a hydroxylation in position 3 of 4-Hydroxybenzoate by hydroxybenzoate hydroxylase, found only in the genomes of *Halomonas* sp. SZN1, and *Epibacterium* sp. SZN4, which leads to the formation of the compound 3,4 hydroxybenzoate. The next step is catalyzed by the protocatechuate enzyme 3, 4 dioxygenase able to convert 3, 4 hydroxybenzoate in β carboxy muconate which through the activity of 3 carboxy ci-cis muconolactone cycloisomerase is transformed in γ Carboxy muconolactone. The protocatechuate 3, 4 dioxygenase sequence found in *Halomonas* sp. SZN1, and *Epibacterium* sp. SZN4. The subsequent decarboxylation reaction catalyzed by the enzyme 4 carboxy muconolactone decarboxylase is described only in *Halomonas* sp. SZN1, *Epibacterium* sp. SZN4, and *Oceanicaulis* sp. SZN5. This leads to the formation of 3 oxoadipate enol lactonase which is transformed in 3 oxoadipate by the activity of β keto adipate enol lactonase, an enzyme identified in the genomes of *Halomonas* sp. SZN1, *Alcanivorax* sp. SZN2, and *Epibacterium* sp. SZN4. The last two steps of the pathway are catalyzed by enzymes whose sequences have been reported only in *Alcanivorax* sp. SZN2, and *Halomonas* sp. SZN1; more specifically, the activity of 3 oxo adipate Co-A transferase promotes the formation of 3 oxo adipyl CoA which becomes a substrate of β keto adipyl CoA thiolase catalysing the production of succinyl CoA, a compound involved in the citric acid cycle.....164

Figure 3.16. Comparison of strain sequences from my *Halomonas* sp. SZN1 draft genome and the three closest sequences identified in the National Centre for Biotechnology Information (NCBI) data bank. Ring hydroxylating dioxygenase (RHD) is indicated as ORF 2. Contig 29 is the genomic region where the gene encoding for RHD was identified in my draft genome. The right panel lists genes that are encoded by *Halomonas* sp. SZN1 (ORFs 1-10) and those that are encoded by reference genomes (ORFs 11-30).....169

Figure 3.17. Comparison of strain sequences from my *Alcanivorax* sp. SZN2 draft genome and the three closest sequences identified in the National Centre for Biotechnology Information (NCBI) data bank. Ring hydroxylating dioxygenase is indicated as ORF 4. Contig 9 is the genomic region where the gene encoding for RHD was identified in my draft genome. The right panel lists genes that are encoded by the

draft genome of *Alcanivorax* sp. SZN2 (ORFs 1-10) and those that are encoded by reference genomes (ORFs 11-30).....170

Figure 3.18. Comparison of strain sequences from my *Pseudoalteromonas* sp. SZN3 genome and the three closest sequences identified in the National Centre for Biotechnology Information (NCBI) data bank. Ring hydroxylating dioxygenase is indicated as ORF 8. Contig 18 is the genomic region where the gene encoding for RHD was identified in my draft genome. The right panel lists genes that are encoded by the draft genome of *Pseudoalteromonas* sp. SZN3 (ORFs 1-11) and those that are encoded by reference genomes (ORFs 12-19).....170

Figure 3.19. Comparison of strain sequences from my *Epibacterium* sp. SZN4 draft genome and the three closest sequences identified in the National Centre for Biotechnology Information (NCBI) data bank. Ring hydroxylating dioxygenase is indicated as ORF 8. The right panel lists genes that are encoded by the draft genome of *Epibacterium* sp. SZN4 (ORFs 1-13) and those that are encoded by reference genomes (ORFs 14-22).....171

Figure 3.20. Phylogenetic tree built with MEGA 7 using the best twenty hits after blasting the ring hydroxylating dioxygenase belonging to *Halomonas* sp. SZN1 (*Alcanivorax* sp. SZN2, *Epibacterium* sp. SZN4, *Pseudoalteromonas* sp. SZN3) and *Oceanicaulis* sp. SZN5 on Swiss Prot Data bank.....172

Figure 3.21. Comparison of strain sequences from my *Halomonas* sp. SZN1 draft genome and the three closest sequences identified in the National Centre for Biotechnology Information (NCBI) data bank. Cytochrome P450 is indicated as ORF 6. Contig 15 is the genomic region where the gene encoding for Cytochrome P450 was identified in my draft genome. The right panel lists genes that are encoded by the draft genome of *Halomonas* sp. SZN1 (ORFs 1-14) and those that are encoded by reference genomes (ORFs 15-27).....175

Figure 3.22. Comparison of strain sequences from my *Alcanivorax* sp. SZN2 draft genome and the three closest sequences identified in the National Centre for Biotechnology Information (NCBI) data bank. Cytochrome P450 is indicated as ORF 12. Contig 76 is the genomic region where the gene encoding for Cytochrome P450 was identified in my draft genome. The right panel lists genes that are encoded by the draft genome of *Alcanivorax* sp. SZN2 (ORFs 1-20) and those that are encoded by reference genomes (ORFs 21-29).....176

Figure 3.23. Comparison of strain sequences from my *Epibacterium* sp. SZN4 draft genome and the three closest sequences identified in the National Centre for Biotechnology Information (NCBI) data bank. Cytochrome P450 is indicated as ORF 5. Contig 44 is the genomic region where the gene encoding for Cytochrome P450 was identified in my draft genome. The right panel lists genes that are encoded by the draft genome of *Epibacterium* sp. SZN4 (ORFs 1-14) and those that are encoded by reference genomes (ORFs 15-25).....177

Figure 3.24. Phylogenetic tree of built with MEGA 7 using the best twenty hits after blasting the Cytochrome P450 belonging to *Halomonas* sp. SZN1, *Alcanivorax* sp. SZN2, and *Epibacterium* sp. SZN4 on SwissProt Databank.....178

Figure 3.25. Phylogenetic tree built with MEGA 7 using the best twenty hits after blasting the Hydroxiquinol 1,2 dioxygenase belonging to *Halomonas* sp. SZN1 on Swiss Prot data bank.....181

Figure 3.26. Comparison of strain sequences from my *Halomonas* sp. SZN1 draft genome and the three closest sequences identified in the National Centre for Biotechnology Information (NCBI) data bank. Protocatechuate 3-4 dioxygenase sun unit beta and alpha are indicated as ORF 4 and 5. Contig 30 is the genomic region where the genes encoding for Protocatechuate 3-4 dioxygenase sun unit beta and alpha were identified in my draft genome. The right panel lists genes that are encoded by the draft genome of *Halomonas* sp. SZN1 (ORFs 1-13) and those that are encoded by reference genomes (ORFs 14-16).....183

Figure 3.27. Comparison of strain sequences from my *Epibacteriums* sp. SZN4 draft genome and the three closest sequences identified in the National Centre for Biotechnology Information (NCBI) data bank. Protocatechuate 3-4 dioxygenase sun unit beta and alpha are indicated as ORF 8 and 9. Contig 8 is the genomic region where the genes encoding for Protocatechuate 3-4 dioxygenase sun unit beta and alpha were identified in my draft genome. The right panel lists genes that are encoded by the draft genome of *Halomonas* sp. SZN4 (ORFs 1-13) and those that are encoded by reference genomes (ORFs 14-16).....184

Figure 3.28. Phylogenetic tree built with MEGA 7 using the best twenty hits after blasting the *protocatechuate 3, 4 dioxygenase* belonging to *Halomonas* sp. SZN1 and *Epibacterium* sp. SZN4 on Swiss Prot data bank185

Figure 3.29. Comparison of strain sequences from my *Pseudoalteromonas* sp. SZN3 draft genome and the three closest sequences identified in the National Centre for Biotechnology Information (NCBI) data bank. Homogentisate 1-2 dioxygenase is indicated as ORF 5. Contig 15 is the genomic region where the genes encoding for Homogentisate 1-2 dioxygenase was identified in my draft genome. The right panel lists genes that are encoded by the draft genome of *Pseudoalteromonas* sp. SZN3 (ORFs 1-9) and those that are encoded by reference genomes (ORFs 10-12).....188

Figure 3.30. Comparison of strain sequences from my *Epibacterium* sp. SZN4 draft genome and the three closest sequences identified in the National Centre for Biotechnology Information (NCBI) data bank. Homogentisate 1-2 dioxygenase is indicated as ORF 7. Contig 69 is the genomic region where the genes encoding for Homogentisate 1-2 dioxygenase was identified in my draft genome. The right panel lists genes that are encoded by the draft genome of *Epibacterium* sp. SZN4 (ORFs 1-14) and those that are encoded by reference genomes (ORFs 15-19).....189

Figure 3.31. Phylogenetic tree built with MEGA 7 using the best twenty hits after blasting the Homogentisate 1, 2 dioxygenase belonging to *Halomonas* sp. SZN1, *Epibacterium* sp. SZN4, *Pseudoalteromonas* sp. SZN3 and *Oceanicaulis* sp. SZN5 on Swiss Prot databank.....190

Figure 3.32. Comparison of strain sequences from my *Alcanivorax* sp. SZN2 draft genome and the three closest sequences identified in the National Centre for Biotechnology Information (NCBI) data bank. The genes involved in Homoprotocatechuate pathway are indicated from ORF 7 to ORF 19. Contig 65 is the genomic region where the genes encoding for Homoprotocatechuate pathway were identified in my draft genome. The right panel lists genes that are encoded by the draft genome of *Alcanivorax* sp. SZN2 (ORFs 1-20) and those that are encoded by reference genomes (ORFs 21-38).....193

Figure 3.33. Comparison of strain sequences from my *Halomonas* sp. SZN1 genome and the three closest sequences identified in the National Centre for Biotechnology Information (NCBI) data bank. The genes involved in Homoprotocatechuate pathway are indicated from ORF 4 to ORF 14. Contig 29 is the genomic region where the genes encoding for Homoprotocatechuate pathway were identified in my draft genome. The right panel lists genes that are encoded by the draft genome of *Halomonas* sp. SZN1 (ORFs 1-17) and those that are encoded by reference genomes (ORFs 18-47).....194

Figure 3.34. Phylogenetic tree built with MEGA 7 using the best twenty hits after blasting the 3, 4 dihydroxy phenylacetate 2, 3 dioxygenase belonging to *Halomonas* sp. SZN1 and *Alcanivorax* sp. SZN2 on Swiss Prot data Bank.....195

Figure 3.35. Comparison of strain sequences from my *Halomonas* sp. SZN1 genome and the three closest sequences identified in the National Centre for Biotechnology Information (NCBI) data bank. The genes involved in Phenilacetic pathway are indicated from ORF 10 to ORF 19. Contig 29 is the genomic region where the genes encoding for Phenilacetic pathway were identified in my draft genome. The right panel lists genes that are encoded by the draft genome of *Halomonas* sp. SZN1 (ORFs 1-19) and those that are encoded by reference genomes (ORFs 20-36).....198

Figure 3.36. Phylogenetic tree built with MEGA 7 using the best twenty hits after blasting the phenylacetyl CoA oxygenase reductase belonging to *Halomonas* sp. SZN1, *Alcanivorax* sp. SZN2 and *Epibacterium* sp. SZN4 on Swiss Prot data bank.....199

Figure 3.37. Heat map of genes and relative copy numbers identified by RAST in the six draft genomes analyzed. On the left column are indicated genes involved in “resistance to antibiotics and toxic compounds”. The different colour intensity is related to number of gene copies. (white: “no genes”; dark green “max. number of genes).....205

Figure 3.38. Comparison of strain sequences from my *Pseudoalteromonas* sp. SZN3 genome and the three closest sequences identified in the National Centre for Biotechnology Information (NCBI) data bank. The genes involved in metal resistance are indicated from ORF 2 to ORF 14. Contig 10 is the genomic region where the genes encoding for metal resistance were identified in my draft genome. The right panel lists genes that are encoded by the draft genome of *Pseudoalteromonas* sp. SZN3 (ORFs 1-15) and those that are encoded by reference genomes (ORFs 16-19).....206

Figure 3.39. Comparison of strain sequences from my *Epibacterium* sp. SZN4 draft genome and the three closest sequences identified in the National Centre for Biotechnology Information (NCBI) data bank. The genes involved in metal resistance are indicated as ORF 1, 3, 4, 5, 16, 18, 19, 22, 24, 25, 26, 27, 28, 29. Contig 22 is the genomic region where the genes encoding for metal resistance were identified in my draft genome. The right panel lists genes that are encoded by the draft genome of *Epibacterium* sp. SZN4 (ORFs 1-31) and those that are encoded by reference genomes (ORFs 32-36).....207

Figure 3.40. Comparison of strain sequences from my *Halomonas* sp. SZN1 genome and the three closest sequences identified in the National Centre for Biotechnology Information (NCBI) data bank. The genes involved in mercury resistance are indicated as ORF 6, 7, 8, 9, 10, 11. Contig 30 is the genomic region where the genes encoding for mercury resistance were identified in my draft genome. The right panel lists genes that are encoded by the draft genome of *Halomonas* sp. SZN1 (ORFs 1-15) and those that are encoded by reference genomes (ORFs 16-23).....208

Figure 3.41. Comparison of strain sequences from my *Alcanivorax* sp. SZN2 genome and the three closest sequences identified in the National Centre for Biotechnology Information (NCBI) data bank. The genes involved in Arsenic resistance are indicated as ORF 11, 12, 13, 14. Contig 30 is the genomic region where the genes encoding for mercury resistance were identified in my draft genome. The right panel lists genes that are encoded by the draft genome of *Alcanivorax* sp. SZN2 (ORFs 1-18) and those that are encoded by reference genomes (ORFs 19-24).....208

Figure 3.42. Comparison of strain sequences from my *Halomonas* sp. SZN1 genome and the three closest sequences identified in the National Centre for Biotechnology Information (NCBI) data bank. The genes involved in Arsenic resistance are indicated as ORF 6, 7, 10, 11, 12. Contig 68 is the genomic region where the genes encoding for Arsenic resistance were identified in my draft genome. The right panel lists genes that are encoded by the draft genome of *Halomonas* sp. SZN1 (ORFs 1-15) and those that are encoded by reference genomes (ORFs 16-29).....209

Figure 3.43. Comparison of strain sequences from my *Epibacterium* sp. SZN4 genome and the three closest sequences identified in the National Centre for Biotechnology Information (NCBI) data bank. The genes involved in Arsenic resistance are indicated as ORF 5, 6, 7, 18. Contig 74 is the genomic region where the genes encoding for Arsenic resistance were identified in my draft genome. The right panel lists genes that

are encoded by the draft genome of *Epibacterium* sp. SZN4 (ORFs 1-11) and those that are encoded by reference genomes (ORFs 12-24).....210

List of tables

Table 2.1. Coordinates, pH, eh and T° of the four sampled stations.....	40
Tab 2.2. Distribution of the different fractions of organic matter in Bagnoli-Coroglio sediments.....	45
Table. 2.3: List of ASVs present in all samples at all sites.....	62
Table 3.1. List of identified strains per culture consortia	137
Table 3.2. Similarity % of marker genes in recombinase A (recA), DNA gyrase subunit B (gyrB) and RNA polymerase subunit B (rpoB).....	137
Table 3.3: Results of the average nucleotide allignment. Each reference genome was chosen following the output generated by blast of the 3 largest contigs for each genome, assembled with MYCC.....	138
Table 3.4: General genomic features of <i>Halomonas</i> sp.....	141
Table 3.5. General genomic features of <i>Alcanivorax</i> sp.....	145
Table 3.6. General genomic features of <i>Pseudoalteromonas</i> sp.....	148
Table 3.7. General genomic features of <i>Epibacterium</i> sp.....	152
Table 3.8. General genomic features of <i>Oceanicaulis</i> sp.....	155
Table 3.9. General genomic features of <i>Alkaliphilus</i> sp.....	158
Table 3.10. Summary table of the features shown by the draft genomes. In detail, ANI is the acronym of Average Nucleotide Identity; RHD is the acronym of Ring Hydroxylating Dioxygenase; CYP 450 is the acronym of Cytochrome P450.....	212
Table 4.1. List of cultures and their ability to grow at different concentrations (100, 1000, 10000 ppm) of As, Pb, Cd, Zn, Cu and PAHs.....	215
Table 4.2. List of cultures and their ability to precipitate Heavy Metals (As, Pb, Cd, Zn, Cu) and degrade PAHs in Marine Broth solutions after 27 days of incubation.....	216

Table 4.3. List of cultures and their ability to degrade Hydrocarbons after 27 days of incubation in contaminated Bagnoli –Coroglio sediments.....217

Table 4.4. List of cultures and their ability to reduce Heavy Metal bioavailability (As, Pb, Cd, Zn, Cu) after 27 days of incubation with Bagnoli-Coroglio sediments.....218

Glossary:

Bioaccumulation: gradual accumulation of substances, such as pesticides other chemicals, in an organism.

Bioaugmentation: addition of archaea or bacterial cultures required to speed up the rate of degradation of a contaminant.

Biodegradation: breakdown of organic matter by microorganisms, such as bacteria and fungi

Bioimmobilization: contaminants reduction of mobility and bioavailability

Bioleaching: Bioleaching is the extraction of metals from their ores through the use of living organisms. Bioleaching is one of several applications within biohydrometallurgy and several methods are used to recover copper, zinc, lead, arsenic, antimony, nickel, molybdenum, gold, silver, and cobalt. Bioleaching can involve numerous ferrous iron and sulfur oxidizing bacteria, including *Acidithiobacillus ferrooxidans* (formerly known as *Thiobacillus ferrooxidans*) and *Acidithiobacillus thiooxidans* (formerly known as *Thiobacillus thiooxidans*). As a general principle, Fe^{3+} ions are used to oxidize the ore. This step is entirely independent of microbes. The role of the bacteria is the further oxidation of the ore, but also the regeneration of the chemical oxidant Fe^{3+} from Fe^{2+} .

Biomobilization: contaminants increase in mobility and bioavailability

Bioremediation: Bioremediation is a process used to treat contaminated media, including water, soil and subsurface material, by altering environmental conditions to stimulate growth of microorganisms and degrade the target pollutants.

Biostimulation: Biostimulation involves the modification of the environment to stimulate existing bacteria capable of bioremediation. This can be done by addition of various forms of rate limiting nutrients and electron acceptors, such as phosphorus, nitrogen, oxygen, or carbon

Biotransformation: chemical modification made by an organism on a chemical compound.

List of abbreviations:

ASV, Amplicon Sequence Variant

CEC, cation exchange capacity

DDT, dichlorodiphenyl-trichloroethane

ESN, effective number of species

HPLC, high-performance liquid chromatography

HTS, high throughput sequencing

LC-MS, Liquid chromatography–mass spectrometry

MA, Marine Agar

MB, Marine Broth

NGS, Next Generation Sequencing

OD, optical density

OTU, operational taxonomic unit

PAH, polycyclic aromatic hydrocarbon

PCB, Polychlorinated biphenyl

PCDD, polychlorinated dibenzo-p-dioxin

PCDF, polychlorinated dibenzo-furans

POM, Particulate organic matter

SIN, site of national interest

SSE, Sequential Selective Extraction

TOC, Total Organic Concentration

Chapter 1

1) General Introduction

1.1) Bioremediation: state of art

Compounds like polycyclic aromatic hydrocarbons (PAHs), polychlorinated byphenyls (PCBs) and different forms of heavy metals and metalloids are released into the environment through incomplete combustion of organic matter (Wuana and Okieimen 2011), the runoff from soil (Aly Salem et al. 2013) and improper industrial discharges or waste disposal practices. Such toxic compounds represent a severe threat to human and ecosystem safety and health (Ben Chekroun et al. 2014, particularly in coastal and transitional ecosystems characterized by high contamination levels due to high anthropic pressure and reduced hydrodynamism (Zheng et al. 2011). The accumulation of high concentrations of pollutants in the sediments can determine significant impacts on biodiversity and the functioning of ecosystems and may affect the production of products and services and the use of resources.

Contaminated sediments represent a serious problem of great interest at a global scale, due to the identification of large areas with high levels of pollutants. Today a list of 39 Priority Sites to be reclaimed, included in the Italian National Reclamation Program, has been identified across the national territory, most of which are located in coastal and transition marine areas. High levels of contamination are also associated with sediments in harbor areas that due to handling to maintain the depth of navigation, cause management problems for their relocation. Historically most dredged harbor sediments

are discharged into neighboring coastal areas and / or used as landfill. Several studies have shown a clear biological impact due to dredging activities and sea-discharge activities of such matrices, which lead to a physical impact (i.e. induced by the immersion itself of dredging, burial, suffocation of benthic marine organisms) and toxicological effects determined by the associated contaminants (Regoli et al. 2002; Trannum et al. 2004; Tornero and Hanke 2016). Ecological changes resulting from the release of dredged material have also important effects on the provisioning of ecosystem' s goods and services for human well-being in the short and long term (Mandal, Chatterjee, and Gosh 2011).

The need to find management alternatives to sea discharge has led, in recent years to the production of different patents, for the reclamation of these matrices through ex-situ treatments. However, national (see DL 152/2006) and international (WFD 2000/60 EU; European Marine Strategy Framework Directive) policies are increasingly seeking management alternatives capable of limiting sediment handling interventions, and promoting the decontamination of these matrices by using eco-compatible in situ technologies. Among these, bioremediation technologies appear to be promising for their eco-compatibility, their efficiency in reducing contamination levels and their versatility for use in different types of contaminants and in different environmental contexts (Megharaj and Naidu 2017).

In order to detoxify polluted sediments, many physicochemical techniques have been developed such as reverse osmosis, electrodialysis, ultrafiltration, ion-exchange and chemical precipitation (Crini and Lichtfouse 2018).

Unfortunately, these methods present several disadvantages such as high costs, the generation of toxic sludges (Ahalya et al. 2003) and the inability to apply many of these techniques *in situ*. A valid solution to the problem may be represented by bioremediation which is an eco-friendly strategy based on the capability of prokaryotes, fungi and photosynthetic organisms (e.g. plants and microalgae) to enhance natural processes involved in the removal of contaminants thereby reducing their ecotoxicological threat (Brar et al. 2017). Although bioremediation may in many instances be quite slow and may not completely remove toxic materials, it nonetheless represents the most promising method because based on cheap-technology with low environmental impact.

Among the principal prokaryotes used in these processes the most abundant genera are *Alcaligenes*, *Bacillus*, *Enterobacter*, *Flavobacterium*, *Pseudomonas* (Ojuederie and Babalola 2017) and *Achromobacter*, *Acinetobacter*, *Alteromonas*, *Arthrobacter*, *Burkholderia* (Xu et al. 2018) as well as Obligate Hydrocarbonoclastic Bacteria (OHCB) such as *Alcanivorax*, *Thalassolituus*, *Cycloclasticus*, *Oleispira* (Yakimov, Timmis, and Golyshin 2007) that are widely known to successfully to be involved in hydrocarbons breakdown. Moreover, organisms such as Microalgae and Fungi have demonstrated bioremediation capabilities. Genera belonging to Microalgae such as *Spirulina*, *Chlorella*, *Spirogyra*, *Scenedesmus*, *Oscillatoria quadripunctulata*, *Chlorococcum*, *Stigonema*, *Gloeocapsa* and *Tetraselmis* (Ayse, et al. 2005; Arunakumara, et al. 2008; Yao et al. 2012; Ajayan, et al. 2011) have been shown to be able to remove heavy metals such as As, Cd, Co, Cr, Ni, Pb, Hg and Zn. According to Lei et al. (2007); Takáčová et al. (2014); García de Llasera et al. (2016) and Ghosal et al. (2016) microalgae belonging to the

genera *Selenastrum*, *Scenedesmus*, *Chlorella* are effective microorganisms in PAHs degradation since they displayed a degradation activity towards naphthalene, phenanthrene and pyrene. Another possible strategy for the reclamation of polluted sites is mycoremediation since Fungi have been described as capable to survive in extreme conditions, as well as to produce a multitude of enzymes such as catalase, peroxidase, laccase and Cytochrome P450, suitable for detoxification and biodegradation (Morel et al. 2013; Durairaj et al. 2015). Fungi isolated from PAHs contaminated soils such as *Aspergillus*, *Curvularia*, *Drechslera*, *Fusarium*, *Lasiodiplodia*, *Mucor*, *Penicillium*, *Rhizopus* and *Trichoderma* have been described as capable to degrade aromatic compounds (Lladó et al. 2013; Balaji, Arulazhagan, and Ebenezer 2014; Chang et al. 2016) while species such as *Aspergillus niger*, *flavus* and *foetidus* as well as genera like *Cryptococcus*, *Penicillium* and *Curvularia* have been described to be tolerant, and effective in the removal of heavy metals such as Pb, Hg, and U through biosorption (Chakraborty et al. 2013; Mumtaz et al. 2013; Kurniati et al. 2014; Deshmukh et al. 2016). The mechanisms allowing removal of metals and hydrocarbons, for Bacteria, Algi and Fungi, rely on a first passage mediated by exopolysaccharides which allows the uptake of contaminants on the cell surface or eventually their complexation into less bioavailable forms (Deshmukh et al. 2016; Liu et al. 2016; Casillo et al. 2018). The metals once adhered to the membrane or cell wall (depending on the microorganism) can remain adherent or internalized (microalgae and fungi) and chelated by molecules belonging to the phytochelatin classes (Perales-Vela et al. 2006; Sharma et al. 2015; Khullar and Sudhakara Reddy 2019)

Generally, bioremediation processes can be enhanced by bio-stimulation of autochthonous assemblages (e.g. by adding different chemical compounds and or electron donors/acceptors) or by bio-augmentation, which consists in adding selected microorganisms that are able to degrade/mobilize contaminants (Catania et al. 2015). Bioremediation mechanisms, that can occur both under aerobic and anaerobic conditions, can differ due to the type of contaminant and the kind of matrix. For this reason, the degradation of organic pollutants involves aerobic/anaerobic respiration and fermentation metabolism while transformation/sequestration of heavy metals (which do not undergo degradation) are based on bio-accumulation, biotransformation, and bioleaching activities (Kumar et al.2019). The mechanisms of absorption of heavy metals and organic pollutants by microorganisms, although still largely unknown, seems to occur through physicochemical interactions with an uptake rate that is inversely proportional to the compound's hydrophobicity (Zgurskaya et al.2016). Chemical and physical factors can enhance or inhibit this process. Indeed, small variations in pH can lead to formation of cationic and anionic species in both metals and organic contaminants that can be complexed with molecules having opposite charges expressed on the membrane or released in solution by microorganisms (Ayangbenro and Babalola 2017). Temperature also influences the stability of the ions in solution and thus the bioavailability of the contaminants. For example, an increase in temperature from 25 to 40 °C changes the absorption rate of the heavy metal Pb from 0.596 to 0.728 mg/g (Arjoon et al. 2013). All these variables need to be carefully considered during the decontamination of marine sediments.

Numerous studies have shown that biodegradation processes of organic contaminants in sediments can be accelerated by adding appropriate compounds and/or electron acceptors/donors that can stimulate native microbial communities (Zhuang et al. 2019). For example, it is known that hydrocarbon biodegradation processes are mainly limited by the availability of N and P and dissolved molecular oxygen (Head et al. 2006). However, many authors have shown that biodegradation of hydrocarbons by microorganisms can also take place under reduced conditions by using alternative electron acceptors (sulphates, nitrates, Fe, Mn,) (Meckenstock et al. 2004). In particular, microcosm experiments on harbor sediments contaminated by PAHs showed a significant reduction of different PAHs concentrations through the application of reducing sulphate bacteria (Nasser et al. 2017). This suggests that biostimulation strategies should be selected on the basis of the metabolic needs of the microbial community. In this regard, several studies have shown that the addition of inorganic nutrients to oil-contaminated sediments can stimulate the biodegradation efficiency of certain classes of compounds, while others, such as heavy metals, are somewhat refractory to biodegradation (Swannell et al. 1996).

Subsequent studies have confirmed that environmental manipulation due to the addition of stimulant compounds modifies natural microbial communities with cascading effects on their biodegradation capacity (Head et al. 2006). Therefore, in order to formulate more suitable and efficient bioremediation *in situ* strategies, it is necessary to understand and define existing relationships between biodegradation rates, contaminants involved (in the case of complex mixtures of compounds) and dynamics of the microbial community in structural and functional terms (Ibarrolaza et al. 2009).

Understanding these relationships requires a highly interdisciplinary approach and adequate analytical tools to enable the development of appropriate models of contaminant degradation in relation to biostimulation interventions.

The development of appropriate *in situ* bioremediation strategies for sediment reclamation must take into account the performance of organic contaminants biodegradation processes and also the potential effects that biotreatment may have on the fate of heavy metals (Dell'Anno et al. 2003; Lloyd 2003). This should be carefully considered when sediments show significant contamination not only from organic but also from inorganic compounds. Different studies have shown that microorganisms play a key role in the mobilization/immobilization of heavy metals in sediments (Gadd 2010; Valls and De Lorenzo 2002). These effects can be attributed to the direct action of microorganisms on the different geochemical components to which the metals are associated and to the variations of redox potential generated by their metabolism (Malik 2004; Tabak et al. 2005). In particular, there is evidence that in anaerobic conditions the dissimilation of Fe and Mn oxides and hydroxides in sediments by Fe and Mn reducing microorganisms affects carbon cycling as well as speciation of redox sensitive metals in the environment (Novotnik et al. 2019). In contrast, sulphides produced by anaerobic sulphate-reducing bacteria metabolism represent one of the major buffer systems for stabilizing metal cations by the formation of metallic-sulfur complexes (Ayangbenro and Babalola 2017). Moreover, degradation processes of organic matter by heterotrophic microorganisms can increase the mobility of the metals associated (Neagoe et al. 2012). Considering not only the effects of microbial biotransformation on organic but also on

inorganic contaminants is a prerequisite for the development of biotechnological strategies that are actually eco-compatible.

An effective bioremediation strategy should consider the bioremediation of metals and organic contaminants as a co-occurring process. For example, microbial processes aimed at hydrocarbon degradation may change heavy metal mobility, influencing their bioavailability and toxicity for the biota (White, Sayer, and Gadd 1997; Lloyd 2003). Therefore, in bioremediation treatments of marine sediments contaminated with hydrocarbons and heavy metals attention should be paid both to the extent of hydrocarbon degradation and to the potential risks associated to changes of metal speciation (Dell'Anno et al. 2003).

Biotreatments can cause changes in the composition of the prokaryotic community living in the sediment. Bacterial communities in marine sediments are mainly composed by *Alpha-*, *Gamma-* and *Deltaproteobacteria*, *Holophaga/Acidobacteria*, *Planctomycetales*, *Bacteroidetes*, *Verrucomicrobia*, *Actinobacteria*, and *Firmicutes* (Gray and Herwig 1996; Polymenakou et al. 2005; Musat et al. 2006; Zhang et al.2008), while archaeal communities are mostly formed by Euryarchaeota (Röling et al. 2004). The main genera of prokaryotes involved in hydrocarbon degradation are *Alcanivorax*, *Cycloclasticus*, *Oleiphilus*, *Oliespira*, *Pelagibacter*, *Pseudomonas*, *Roseobacter*, *Thalassolituus*, *Vibrio* and species belonging to the phylum *Flexibacter-Cytophaga-Bacteroides* (Hedlund and Staley 2006; Rappé et al. 2002; Yakimov et al. 2005; Head et al.2006; McKewet al. 2007). It has been observed that the application of strategies for sediment remediation can determine shifts in the composition of the prokaryotic community, with the selection of certain strains rather than others (Head et al. 2006;

McKew et al. 2007). Bioremediation performance may be affected by the particular composition of the microbial community. Röling et al. (2002), found that in microcosm experiments using different levels of inorganic nutrients lead to the selection of very different bacterial communities, but the extent of hydrocarbon degradation was similar in all the experimental microcosms. The establishment of synergistic relationships, co-metabolic processes, and other interactions within a heterogeneous microbial community is an important aspect for the effectiveness of bioremediation strategies (Yu et al. 2005; McKew et al. 2007).

Therefore, given the complexity of identifying efficient, ecologically, economically viable and technically applicable biotechnologies for *in situ* recovery of contaminated sediments, it is necessary to develop new research in this field through integrated approaches and interdisciplinary competencies.

1.2) PAH bacterial remediation

The contamination of marine sediments by petroleum hydrocarbons is widespread in coastal regions of the world and represents a major concern for the potential detrimental consequences on ecosystems health and provision of goods and services (Lozada et al. 2014). Indeed, PAHs, which are the most common petroleum contaminants in the environment are considered to be potentially mutagenic and carcinogenic (Mao et al. 2012). Abdel-Shafy and Mansour 2016, (2016) reported that hydrocarbons such as Benzo [a] pyrene are genotoxic and implicated in human breast cancer. However, the focus has been placed on the biodegradation of low molecular weight PAHs whilst little research has been carried out on the biodegradation of high molecular weight PAHs that have been found to be of more relevance from a health perspective. Therefore, in recent years, effort has been devoted to explore remediation options based on treatments of sediments that are able to reduce contaminant concentrations to threshold levels below which no detrimental effects on living biota are expected to occur. Among these, environmental-friendly bioremediation technologies are arousing interest in the scientific community, for their potential in the safe remediation of oil-polluted areas, such as marine sediments (Xu et al. 2005).

Field and laboratory experiments demonstrated that biodegradation processes of oil-contaminated sediments may be accelerated by enhancing biomass and / or activity of hydrocarbon-degrading microorganisms through biostimulation as well as bioaugmentation strategies (Azubuiké, Chikere, and Okpokwasili 2016). In order to design an optimal bioremediation strategy, it is important to understand the factors that

enhance microbial metabolism and hydrocarbon degradation, a knowledge which could help restore the environment to a pre-pollution state as early as possible.

One of the main factors affecting oil bioremediation is the physical nature of the crude oil: for instance, a single large oil slick has a smaller surface area for oil-eating microbes to access compared to numerous small-sized oil slicks and also, heavy and viscous hydrocarbon compounds may prove to be recalcitrant as lighter hydrocarbons are easier for microbes to digest due to the higher rate of diffusion through the oil-water interface (Zaki, Authman, and Abbas 2015). It is even important to investigate the chemical nature of the spilled petroleum because some unbranched alkanes can be degraded in a few weeks but branched alkanes and multiple-ringed aromatic hydrocarbons can be more resistant to microbial degradation. Asphalthenes are considered to be the most recalcitrant, and thus, could accumulate in the environment (Pourfakhraei et al. 2018). The rate of degradation depends on the availability of nutrients. The two most limiting elements are nitrogen and phosphorus that are incorporated into cellular biomass and stimulate hydrocarbon metabolism (McKew, Coulon, Osborn, et al. 2007; Calvo et al. 2009), but even the lack of sulphur and potassium can affect bioremediation rates (Evans et al. 2004). Other factors that have to be considered during bioremediation are water temperature, oxygen concentration, sediment particle size and mineralogical composition. Indeed, the temperature of the surrounding water in which the oil occurs determines the rate of hydrocarbon degradation. It has been observed that crude oil degradation is faster in warm water because heat promotes the breakdown of the spilled petroleum that becomes more attainable to oil-degrading microbes following Arrhenius kinetics rules. In cold environments, sub-zero temperatures cause the shut

down of transport channels of cells and may even freeze the entire cytoplasm, thus, rendering most known oleophilic microbes metabolically inactive. However, many oleophilic microbes are cold-tolerant, as most of the ocean is deep and cold (2-4 C°) but have to deal with the problem of the freeze-thaw seasonal cycle between winter and summer, which limits the bioavailability of the spilled petroleum (Yang et al. 2009).

Oxygen concentration is a crucial factor in bioremediation processes, since most of oleophilic microbes are aerobes (such as *Pseudomonas* and *Proteus*) and only a few are anaerobes (such as *Geobacter*). Therefore, environments with low and or depleted oxygen concentrations such as oxygen minimum zones, surface sediments of highly eutrophic ecosystems and sub-surface sediments, have lower rates of hydrocarbon biodegradation compared to fully oxygenated systems (Mille et al, 1988) .

Size matrix also influences bioremediation effectiveness since it determines the rate of sediment permeability, which indirectly affects the rate of petroleum biodegradation. Fine sediment particles such as silt / clay have small interstitial spaces which make the soil impermeable, thus, retaining the spilled petroleum at the surface and reducing the bioavailability of microbial nutrients and oxygen (Ahmad et al. 2019). Moderately drained soils are the optimum requirements for the rapid bioremediation of oil-polluted soils. pH is an additional factor influencing bioremediation as it can slow down and/or inhibit microbial activity. Generally higher bioremediation performance occurs at pH values around 6-8 (Ayangbenro et al. 2018). Even the presence of antagonistic oleophilic bacteria can reduce bioremediation rates since some species can release metabolites that inhibit the growth and development of other oleophilic bacteria. Understanding the interdependence of microbial populations is a requirement for the successful

application of bioremediation strategies (Abatenh et al. 2017). Therefore, it should be considered a complex array of factors in order to define efficient bio treatments whether they are conducted in an oxic or an anoxic environment.

It has been observed that bacteria favor aerobic conditions for degradation of PAHs via oxygenase-mediated metabolism (Ghosal et al. 2016b). Usually, the first step in the aerobic bacterial degradation of PAHs is the hydroxylation of an aromatic ring via a dioxygenase which is a multi-component enzyme generally consisting of reductase, ferredoxin, and terminal oxygenase subunits. This enzyme leads to the formation of cis-dihydrodiol, which is re-aromatized to a diol intermediately by the action of a dehydrogenase enzyme. These diol intermediates may then be cleaved by intra diol or extra diol ring-cleaving dioxygenases through either an ortho-cleavage or meta-cleavage pathway, leading to intermediates such as catechols or protocatechuate that are ultimately converted through β -keto adipate pathway to citric acid cycle (CAC) intermediates (Shahsavari et al. 2019). Other pathways involved in bacteria degradation are gentisate, homogentisate, and homoprotocatechuate metabolic routes whose genes have been described in metagenomes and transcriptomes of *Pseudomonas aeruginosa* PAO1, *Klebsiella Pneumoniae* AWD5 and within a bacteria consortium consisting of *Pseudomonas*, *Aquabacterium*, *Chryseobacterium*, *Sphingobium*, *Novosphingobium*, *Dokdonella*, *Parvibaculum*, and *Achromobacter* (Yan and Wu 2017; Rajkumari, Paikhomba Singha, and Pandey 2018; Garrido-Sanz et al. 2019). Bacteria can also degrade PAHs via the cytochrome P450-mediated pathway, with the production of trans-dihydrodiols (Ostrem Loss and Yu 2018) or under anaerobic conditions, e.g. under nitrate-reducing conditions (Carmona et al. 2009).

There is increasing evidence indicating that biodegradation of hydrocarbons takes place also in anoxic conditions (Rabus et al. 2016). This opens new perspectives for the *in situ* treatment of contaminated sediments where reducing conditions below the sediment surface limit the usefulness of O₂ as an electron acceptor (Hastings et al. 2016), which could be supplied to stimulate the degradation of petroleum hydrocarbons. Under reducing conditions, other options have to be evaluated for enhancing the *in situ* biodegradation of organic contaminants.

In anoxic marine sediments, reductions of sulfate, Mn(IV) and Fe(III) are the primary terminal electron-accepting processes (Vandieken, Finke, and Thamdrup 2014). Thus, the microbial metabolism of hydrocarbons under anaerobic conditions may be effective for remediation of sediments only if the hydrocarbon oxidizers are sulfate, Fe(III), or Mn(IV) reducers. In this regard, previous studies demonstrated that, among the different anaerobic processes, hydrocarbon degradation coupled with sulfate reduction prevails in marine anoxic sediments (Coates et al. 1997) since sulfate is abundant in coastal sediments while Fe(III) is less available in massively contaminated sediments (Stauffert, Cravo-Laureau, and Duran 2014). Thus, the degradation of hydrocarbons in anoxic marine matrix under sulfate-reducing conditions has been thought to be the most suitable treatment (Dell'Anno et al. 2009). Despite different bacterial strains have been identified to degrade a wide variety of petroleum-based contaminants in anaerobic conditions, information on how to enhance microbial growth and biodegradation performance in anoxic marine sediments is still limited.

Other possible promising tools for the enhancement of bioremediation processes in highly polluted environments are the use of microorganisms able to produce surfactant

compounds (Radmann et al. 2015) that can be defined as amphiphilic molecules presenting hydrophobic and hydrophilic features (Lee et al. 2008). These molecules can promote bioremediation processes by increasing the contact angle between sediments and pollutants, which induces the separation of hydrophobic contaminants from the sediment and, at the same time, makes them more soluble by partitioning them into internal hydrophobic cores of surfactant micelles (Cameotra and Makkar 2010). Thus, biosurfactants can enhance the removal of contaminants from the sediment matrix through chemical interactions and by increasing solubility and mobility of organic pollutants (*i.e.* bioavailability). Nikolopoulou et al. (2013) have shown data confirming the effectiveness of rhamnolipids in the remediation of crude oil contaminated matrixes. After adding rhamnolipids to a solution of crude oil and sand (5 g: 1000 g) a degradation rate of 30% for fluorene, almost 20% for phenanthrene and 10% for dibenzothiothene was observed after 15 days. Another biosurfactant able to enhance the biodegradation of crude oil is a glycolipid produced by *Candida bombicola* that allows 80% biodegradation of saturates and 72% of aromatics (Kang et al. 2010). A series of dynamic column elution tests conducted by Bordas, Lafrance, and Villemur, (2005) suggest that rhamnolipids at a high concentration (5.0 g/L) could remove ~70% of the pyrene in soil. Pyrene removal from the contaminated soil can be enhanced through the addition of a biosurfactant extracted from *P. aeruginosa SP4*. The addition of 250 mg/L biosurfactant, determined a pyrene removal rate of 84.6% compared to 59.8% for the control sample without any surfactants (Jorfi et al. 2013). A study conducted by Cheng, Zhao, and Wong (2004) showed a reduction in the absorption of PAHs in the soil or an increase in its desorption rate, through the combined use of non-ionic surfactants (Tween 80) and

biosurfactants in soil-aqueous systems under thermophilic conditions. The data showed that the concentration of the surfactant, which must be above the respective CMC (critical micelle concentration), increased the solubilization/desorption of PAHs from the soil to the aqueous phase in a dose-dependent manner. Therefore, the use of a mixture of surfactants should be further investigated since it could be a promising synergistic tool for the bioremediation of PAH contaminated soils.

Coastal marine sediments subjected to strong anthropogenic inputs are sometimes characterized not only by high concentrations of petroleum hydrocarbons, but also by high heavy metal contents, whose fate in the environment is influenced by microbial-mediated processes (Ezekwe and Utong 2017). Microbial processes may, indeed, either increase or decrease heavy metal mobility, thus influencing their bioavailability and toxicity (Caporale and Violante 2016). Therefore, the bioremediation of marine sediments contaminated by organic and inorganic pollutants should not only identify the best conditions for increasing the biodegradation yields of organic xenobiotics, but also assess the potential risks associated to changes in heavy metal speciation (Dell'Anno et al. 2003).

The need for reliable techniques capable to degrade petroleum derivatives have led to the release in 1981 of the first patent (US Patent 4259444) of a living organism involving engineered *Pseudomonas* strains. To date, another living organism (*Geobacillus* sp.) has been patented (US 20130295650A1) capable to degrade organic recalcitrant compounds such as PAHs, PCB, polychlorinated dibenzo-p-dioxins and polychlorinated dibenzofurans (PCDD/Fs). Although the application of this patent provides the ability to remedy both *ex situ* and *in situ* sediment samples, numerous factors, such as the yield of

bioremediation over time, the samples pretreatment with chemical solvents and the need for 60 degrees to reach the optimum temperatures for *Geobacillus* sp. activity, highlight the need to patent biological systems of simpler applicability.

1.3) Heavy metal bacterial remediation

In all aquatic systems, the sediment is the compartment where metals and other pollutants accumulate and may enter food webs, with detrimental effects for the environment and human health (Lim et al. 2008). Although the contamination of sediments is often due to both the presence of organic and inorganic pollutants, metals are of growing concern in the field of water quality management. Understanding the dynamics of metal behavior in water environments has been a major focus to environmental scientists for years and the interest in this area continues to grow, as regulatory agencies are faced with the regulation, mitigation and remediation of water bodies and contaminated sediments (Carvalho 2017). Indeed, the remediation of contaminated sediments remains a key challenge, especially in connection with the interest in biotechnological approaches, which would offer environmentally friendly and cost-feasible strategies.

Whereas organic pollutants have been the objective of a very large number of studies that have produced a large number of patents, effective techniques for metal decontaminants are reduced to post mining remediation. This is very likely due to a partial understanding of the complex behavior of metals in environmental matrices including sediments that are, in turn, affected by complex geochemical and biological processes. Thus, understanding key variables controlling metal “behavior” under different conditions is a pre-requisite for planning successful biotreatments for the bioremediation of sediments contaminated with metals (Fonti, Dell’Anno, and Beolchini 2015).

Industrial and commercial activities and low hydrodynamics are the main factors for the accumulation of high concentrations of metals and metalloids (e.g. As) in the sediments of marine coastal areas (Zouch et al. 2018).

The sediment is an essential, integral and dynamic part of marine systems. It consists of a complex and heterogeneous matrix of many different components and phases, including crystalline minerals, hydrous metal oxides, salts, calcareous biogenic particles and organic substances (Brils 2008). The composition of shallow marine sediments changes from site to site, because it is closely related to the geology and hydrography of the adjacent land areas, to the local climate and the socio-economic significance of the water systems they come from (Preda and Cox 2005). Trace metals, such as Cd, Hg, Zn, Ni, Cr, Pb, Cu, and semi-metals, like As, enter water systems due to multiple processes: atmospheric deposition, erosion of bed-rock minerals, in-stream of industrial effluents and other anthropogenic sources (Colacicco et al. 2010). Once metals reach the water column, sediments act as a sink, since they adsorb and accumulate metals by several mechanisms: particle surface absorption, ion exchange, co-precipitation and complexation with organic substances. The distribution of metal contaminants in the various phases of the sediment affects their behavior in the water system, including, their mobility, bio-availability and toxicity (Devi and Bhattacharyya 2018).

Metals and metalloids that accumulate into the sediment can reach concentrations that are much higher than in the water column and become a very important secondary source of contamination, with detrimental effects on the ecosystem and on human health. Resuspension phenomena lead to the release of soluble metals entrapped into the sediment or to changes in the oxidation/reduction state which cause the release of

insoluble metals by the different components of the sediment (Toes et al. 2008). Resuspension phenomena induced by dredging activity can lead to the remobilization of historically accumulated metals in deeper sediment layers, which contributes to elevated metal concentration in the overlying waters. As a consequence, metals and semi-metals become bio-available to benthic organisms and the whole ecosystem (Chon, Ohandja, and Voulvoulis 2012). Furthermore, trace metals entering natural waters become part of the water-sediment system and their distribution, potential release into the water-phase and bio-availability is highly affected by the physiochemical characteristics of the sediment and the bioavailability of pollutants (Olaniran, Balgobind, and Pillay 2013), in a dynamic set of physical-chemical interactions and equilibria. The releasing intensity of metal contaminants from the sediment into the water is controlled by properties of the sediment, like oxidation-reduction state, concentration and type of complexing agents, particle size distribution, concentration of acid volatile sulfides but also by other factors, like pH of the water, levels of bioturbation and by rainfall and runoff events (Zhang et al. 2014; Burton et al. 2008).

Coastal aquatic ecosystems characterized by high commercial and industrial exploitation are usually characterized by high concentrations of metals and semi-metals. Among these, harbor systems need to be periodically dredged in order to maintain the navigation depth and facilitate sailing. Nevertheless, dredging activities may also suspend a significant amount of metals and induce oxidation-reduction changes that may increase the bio-availability of metals and favor their entry into the food web (Eggleton and Thomas 2004). However, when dredging operations are unavoidable, these produce very large volumes of contaminated sediments and will lead to the

problem of the management of such materials. On the basis of an estimate by Junakova and Junak (2017) around 100 and 200 million cubic meters of contaminated sediment might be produced yearly in Europe.

Conventional remediation strategies can include *in-situ* sediment remediation strategies and relocation actions. In the first group, natural recovery consists in allowing natural attenuation processes without human intervention, and *in situ*-capping with either inert or reactive barriers, without dredging activities. In other cases, such as for confined disposal facilities and contained aquatic disposal, dredging is followed by disposal in submerged or partially saturated facilities. Relocation actions include mainly landfill disposal and dumping at sea (Adriaens, Li, and Michalak 2006). Natural recovery has become unsustainable, for political and social reasons, as well as problems associated with difficulties to quantify contaminant transport pathways. Application of *in-situ* capping and *in-situ* confined aquatic disposal are limited due to uncertainties about long-term stability under various environmental conditions. Landfill disposal, confined disposal facilities or dumping at sea are still the most applied management strategies, despite they also offer several disadvantages, including limited space capacity, costs and low sustainability, and environmental compatibility (Agius and Porebski 2008).

Alternative approaches have received increased attention. Environmentally friendly techniques from treatment strategies for soils and other environmental matrices have been investigated for applications with sediments. Nevertheless, sediments are more difficult to treat than other waste materials, so the only technique widely used for sediment treatment is the separation of less polluted sand fractions, in order to minimize the contaminated volumes that require dumping. On the contrary, treatment

and reuse of dredged sediments is politically encouraged and considered as part of sediment management, but its application is still very limited and often characterized by very high costs and low feasibility (Akcil et al. 2014).

In this context, bioremediation strategies have been recently considered as a promising answer to the problem of sediments contaminated also by metals (Igiri et al. 2018).

As explained above, metal contaminants are not absolutely fixed in the sediment and can be mobilized in response to redox changes, such as those due to dredging activities and/or disposal actions, and may enter food webs with detrimental effects for the entire ecosystem and human health (Peng et al. 2009). Unlike organic pollutants, metals cannot be degraded. They are infinitely persistent and not subjected to biological and chemical degradation processes occurring in the sediment, since metals can only be transformed into more soluble/insoluble compounds and/or in less toxic species. Indeed, changing their speciation has consequences on their solubility and transport properties, which together determine their bio-availability and affect their toxicity (de Paiva Magalhaes et al. 2015). As a consequence, any bioremediation strategy should be aimed at increasing their solubility (bio-mobilization) or increasing their stability and reducing their bioavailability (bio-immobilization) and toxicity.

Biological processes leading to bio-immobilization and bio-mobilization of metals are components of natural biogeochemical cycles and may be exploited for the treatment of contaminated sediments (Jing and Kjellerup 2017). Metal mobilization can be mediated by a range of microorganisms and processes, including autotrophic and heterotrophic leaching, chelation by microbial metabolites and methylation. Similarly, many organisms can contribute to immobilization bio-sorption, intracellular

sequestration and bio-mineralization by precipitation as insoluble compounds (Tabak et al. 2005). Microorganisms, mainly prokaryotes, seem to find successful applications in bioremediation strategies. Microorganisms involved in bio-transformation strategies of metal contaminated sediments may be indigenous in the contaminated area or they may be isolated from different systems and brought to the contaminated site. In the first case, microorganisms are already adapted to local environmental conditions and bioremediation strategies consist basically in stimulating and exploiting the microbial function leading to bioremediation objectives (Biostimulation). In the second case, microorganisms are chosen on the basis of their metabolic properties, including their tolerance to high concentrations of metals and other contaminants, and added to contaminated sediments to enhance bio-transformation (Bioaugmentation) (Adams et al. 2015). This could require changes in natural environmental conditions (e.g. concentration of oxygen, pH, etc..) to favor microbial activity (Garbisu et al. 2017).

Bioremediation strategies can be applied directly in the contaminated site, without moving the sediment ("*in-situ*"), in the contaminated area but with small scale mixing of the sediment ("*on site*" or "*in-place*"), or in areas or reactors designed for sediment treatment, that require removal and transportation ("*ex-situ*").

Bioleaching is considered a promising *ex situ* strategy for metal bio-mobilization from contaminated sediments (Sabra et al. 2013). Bioleaching finds applications mainly in mining industries, and is considered a potential technique also for soil and sediment treatment. It is based on the exploitation of chemolithotrophic Fe/S oxidizing bacteria (e.g. *Acidithiobacillus ferrooxidans*), isolated from acid coal mine drainage, that are able

to oxidize elemental sulfur, and reduced sulfur compounds and/or ferrous ions, leading to metal solubilization through their metabolic products (Rawlings and Johnson 2007).

Bio-immobilization strategies involving indigenous prokaryotes of the sediment consist mainly in bio-mineralization of metals into the sediment to reduce metal mobility, and consequently their toxicity. For example, indigenous sulfate-reducing bacteria in the sediment can be stimulated to immobilize a wide range of metals in highly insoluble sulfides. This approach is considered an efficient way for removing toxic metals from surface and underground waters (Tabak et al. 2005).

Both bioleaching and bioimmobilization can represent alternative biotechnological environmental friendly techniques for treating contaminated sediments. Their application is still to be considered as potential, and many aspects of their use need to be further investigated.

A new approach based on biosurfactant-producing microorganisms can be applied for the remediation of sediments contaminated with metals (Zouboulis et al. 2003; Aşçi, Nurbaş, and Açıkel 2007).

The desorption mechanism of heavy metals by biosurfactants occurs through complexation with free metals, according to the principles of Chatellier (according to which a system at equilibrium subjected to a change readjusts itself to counteract the effect of the applied change to establish a new equilibrium), and also with the linkage of metals bound to the solid matrix, and the bio-surfactant which consequently accumulates at the solid solution interface (Singh and Cameotra 2004).

Mulligan, Yong, and Gibbs, (2001) suggested that the metals present in the solid matrix can be seized by surfactants because these are initially absorbed in the matrix surface layer after which they are complexed with metals, promoting their detachment.

The decontamination of the solid matrix is complicated because of the strong bonds between metals and soil which depends on sediment composition, particle size, soil pH, cation exchange capacity (CEC), type and time of contamination. At the same time a prolonged contact between metals and soil determines a strengthening of the links between components (Singh and Cameotra 2004).

The biosurfactants most commonly used in heavy metal bioremediation include molecules with an electric charge, *i.e.* cationic and anionic biosurfactants, that bind metals having opposite charge and removing them through desorption (Ławniczak, Marecik, and Chrzanowski 2013). Such molecules bind the metals through the polar heads, which, as described by Satpute et al. (2010), point to outside of the micelles; whereas the hydrophobic residues are oriented toward the micelle core.

The most well characterized anionic biosurfactants are the rhamnolipids which are able to form micellar- and lamella-like structures or lipid aggregates, exhibiting negative charges at low pH, even if their highest surface activity is at near neutral pH (ca. 7.0-7.5; (Mulligan and Wang 2006)).

Due to these characteristics, few studies have demonstrated the ability of rhamnolipids to desorb heavy metals such as cadmium, copper, lanthanum, lead, zinc and nickel from contaminated sediments (Mulligan 2005). As demonstrated by Herman, Artiola, and Miller (1995) and by Frazer (2000), rhamnolipids preferentially complex with metals

that, due to a higher affinity, are toxic such as cadmium and lead, rather than sediment or soil metal cations such as calcium and magnesium. For example, Dahrazma and Mulligan (2007) have reported that the sediment removal rate of Cu, Zn, Ni, was respectively 37%, 13%, and 27%. Another study by Juwarkar et al. (2008) shows the efficacy of using di-rhamnolipids in remediation of soil contaminated by metals. These authors observed a significant soil bioremediation equal to 92%, 88%, 92%, 78%, 88% for Cr, Pb, Cd, Ni and Cu, respectively.

Studies conducted on *Pseudomonas aeruginosa*, a bio-surfactant producer bacterial strain, have shown that it is able to selectively bind the cationic metals Pb, Zn and Cd. In particular, the *P. aeruginosa* ATCC9027 strain is able to produce and release rhamnolipids with a removal capacity of Cd equal to 92% (Tan et al. 1994). A comparative study conducted by Mulligan, Yong, and Gibbs (2001) has analyzed the removal rates of Cu and Zn from sediment by three different bio-surfactants. In particular, the authors found that a single washing step with sophorolipids was able to remove 25% of copper and 60% of zinc, while single washing with rhamnolipids removed 65% of copper and 18% of zinc. Surfactin, a lipopeptide, was the least effective because the removal of Cu and Zn from the sediment was 15% and 6%, respectively. These data confirm previous studies by Mulligan, Yong, and Gibbs (1999) showing that surfactin obtained from *Bacillus subtilis*, achieved removal rates of Cu and Zn of around 25% and 6%. Massara, Mulligan, and Hadjinicolaou (2007) have shown the possibility to employ biosurfactants in [Cr(III)], [Cr(VI)] soil remediation. These authors investigated the effects of rhamnolipids in kaolinite contaminated with chromium. Data showed the ability of biosurfactants to remove 25% of the stable form of Cr(III), to enhance the removal of Cr

(VI) by two-fold, and to reduce up to 100% of extracted Cr(VI) to Cr(III) over a period of 24 days. Another study conducted by Ara and Mulligan (2008), has evaluated the effectiveness of the use of rhamnolipids for the removal and reduction of Cr(VI) from contaminated soil and water. Rhamnolipids were able to reduce the initial Cr(VI) in water by 100% when present at low concentration (10 ppm) and under optimum conditions (pH 6, 2% rhamnolipid and 25°C). At higher initial Cr(VI) concentrations (400 ppm), 24 hours were required to reduce Cr by 24.4%. In soil, rhamnolipids were only capable of removing the soluble fraction of Cr. Data further supported that the extraction of metals was enhanced by increasing the initial concentration in the soil, but diminished slightly with temperatures above 30°C. Other indications on chromium removal have been provided by Gnanamani et al. (2010) who studied the bioremediation of Cr(VI) using a lipopeptide biosurfactant produced by *Bacillus sp.* MTCC 5514. Remediation involved two processes: the reduction of Cr(VI) to Cr(III) through extracellular chromoreductase and the entrapment of Cr(III) by the biosurfactant. The first process transformed the toxic state of chromium into a less toxic state and the second avoided the exposure of the bacterial cells to Cr(III). Both reactions maintained the bacterial cells active throughout the entire experiment and promoted tolerance and resistance to high concentrations of both forms of chromium. Further information on the efficacy of rhamnolipids has been provided by Slizovskiy, Kelsey, and Hatzinger (2011) comparing the ionic rhamnolipid biosurfactant (JBR-425) with cationic surfactant (DPC) and a non-ionic surfactant (mmonyxKP). Results indicated the best removal rate for the ionic rhamnolipid biosurfactant (JBR-425), with a removal of about (Zn) 39%, (Cu) 56%, Pb 68% and (Cd) 43%. A study conducted by Okoro (2007)

highlighted that also saponin, a particular biosurfactant, can be efficient for heavy metal removal from soil and sediments. In their experiments, the soil was contaminated with 890 mg/Kg of zinc, 260 mg/Kg of copper, 170 mg/Kg of nickel and 230 mg/Kg of total petroleum hydrocarbons. The highest removal rates (88% for zinc at pH 3 and 76% for nickel at pH 5) were obtained after five washings with a saponin concentration of 30 g/L. The sediment, containing 4440 mg/Kg of zinc, 94 mg/Kg of copper and 474 mg/Kg of lead, after treatment with saponin (30 g/L) led to zinc and lead removal rates of 33% and 24%, respectively. Chen, Hsiao, and Chen (2008) found that 2000 mg/L of saponin was able to remove 83% and 85% of copper and nickel, respectively, from soil. Song, Zhu, and Zhou (2008) observed the suitability of saponin in removal treatment of soils contaminated with both organic and inorganic contaminants such as phenanthrene and cadmium. The removal rates for phenanthrene and cadmium were 87.7% and 76.2%, respectively, demonstrating the possibility of organic and inorganics pollutants removal by the biological tensioactive saponin, which may be an additional tool for bioremediation processes.

1.4) Towards an Omics bioremediation approach

The development of Next Generation Sequencing (NGS) techniques and *in silico* analyses have allowed improvements in the field of taxonomy leading to the identification of many novel microbes capable of degrading or reducing the damaging effects of several environmental hazardous compounds (Czaplicki and Gunsch 2016a). This high throughput technology has been very useful to better understand the composition of microbial communities that were not accessible using traditional culture dependent approaches. However, the identification of new microorganisms is not sufficient to have a complete knowledge of the dynamics of indigenous microbial consortia (Yang et al. 2016).

To this extent, economically feasible studies relying on metagenomics, metatranscriptomics, metaproteomics, metabolomics, and fluxomics along with bioinformatics analysis are providing massive information to really understand the molecular mechanisms underlying the bioremediation processes of contaminants and how bacteria influence each other's metabolic processes (Malla et al. 2018). Among the Omics tools, metagenomics has revolutionized the field of microbiology as it has allowed, avoiding the need to culture these organisms, concurrent analysis of thousands of microorganisms directly from polluted environments enabling the investigation of uncultured organisms in order to understand microbial community composition, functions and interactions, and finally their evolution under different stress conditions (Tripathi et al. 2018).

Metagenomic analysis can be divided between function-based or sequence-based approaches.

More specifically, sequence-based metagenomics involves sequencing and analysis of DNA from environmental samples providing microbial information for gene identification, genome assemblages, and the identification of complete metabolic pathways and comparison of organisms from different communities (Loman et al. 2013). In contrast, function-based metagenomics is widely used to search for a particular function or activity. It is a powerful tool to identify antibiotic compounds as well as proteins involved in metabolic pollutant degradation pathways. In order to study protein function, function-based metagenomics involves DNA isolation from the environment and, after preliminary analysis necessary to identify enzymes of interest, DNA fragments may be cloned and expressed in the most suitable host to test the effective enzymatic activities. Metagenomics is a very promising tool applied to bioremediation since many metagenomic databases are now available, thus providing a rich stock of genes for the construction of novel microbial strains for targeted use in bioremediation efforts (Ngara and Zhang 2018).

Although metagenomics is a powerful tool to describe microorganism community structure inhabiting polluted sites, it exhibits several limitations concerning gene expression and protein activity. To this extent, transcriptomics as well as metatranscriptomics, a RNA-based approach, represents a valid tool to assess the expression of potential bioremediative genes and thus enzymes, under stressful conditions. Indeed, RNA-level expression analyses provide an indirect measure of microbial activity, representing a better target than DNA to assess the degradation

ability of potential pollutants of a given microbial assemblage. Indeed, metatranscriptomic approaches provide information about which genes are up-regulated under different environmental stressors and might even help in identifying novel degrading genes (Bashiardes, Zilberman-Schapira, and Elinav 2016). Thus, such an approach is very useful since it allows for the identification of key enzymes regulating microbial interactions in the environment. The principal limitation of metatranscriptomic analyses is the inability to quantify the abundance of genes since the genes of interest transcript number are small compared to housekeeping genes. However, the missing information can be supplied by carrying out a RT-qPCR analysis (Czaplicki and Gunsch 2016a).

Other very promising tools often associated with transcriptomics are environmental proteomics and metabolomics. Proteomics as well as metaproteomics, is based on protein extraction (from culture media or environmental samples), followed by a separation phase on liquid chromatography and identification of the product by Mass Spectrometry (LC-MS)(Arsène-Ploetze et al 2015; Bargiela et al, 2015). These approaches have been widely used to investigate the proteins expressed by microorganisms under extreme conditions, such as hyperthermophilic conditions, since it allows for the investigation of the molecular basis of protein enabling enzyme stability at high temperatures (Malla et al. 2018). Moreover, despite metatranscriptomics represents a useful tool to monitor the physiological changes occurring in microorganisms in response to xenobiotics, the metaproteomic approach has some advantages since proteins are more stable than RNAs (especially those originating from prokaryotes). Thus, the metaproteome is likely to provide a better snapshot of biological mechanisms

expressed *in situ*, since this technique is supposedly less affected by extraction procedures compared to transcriptomics. Additionally, the proteomics approach can be very useful in bioremediation procedures, even without metagenomic sequences since as reported by Wilmes and Bond (2004) and Lacerda, Choe, and Reardon (2007), it has allowed, coupled with MALDI-TOF analysis, for the characterization of proteins involved in phosphorus removal and cadmium uptake, respectively.

Another Omics tool capable of better elucidating the complex mechanisms occurring in microorganisms under stress condition is metabolomics, a technique based on Gas Chromatography and Mass Spectroscopy to, respectively, separate and identify molecules. This approach, differently from proteomics which provides information about the total protein pattern expressed, aims to characterize the end product of enzyme activity *e.g.* the metabolites produced under a given condition (Singh 2006). To this extent, Keum et al. (2008) and Wharfe et al. (2010) have been able to monitor biochemical and phenotypic changes in *Sinorhizobium* sp. and in bacterial consortia under the effect of aromatic compounds. In general, application of metabolome-based approaches, including metabolism-based wide fluxes (fluxomes), to polluted environmental samples provide further knowledge on how to optimize bioremediation strategies, since it is possible to deeply analyze the effect and the response of microorganisms to toxic substances as well as molecules guiding the complex interactions in consortia degrading pollutants.

Even though results from the different Omics tools are providing unprecedented knowledge about survival mechanism and metabolism of microorganisms, a culture dependent approach, using a pure colony is still required since the physiological,

biochemical and phylogenetic characterization of the single colony allows us to more accurately predict the activity of microbes under different bioremediation strategies (Gutleben et al. 2018).

1.5) Aims of the thesis

My PhD project involves the study of a dismissed industrial site, the Bagnoli-Coroglio Bay situated North of the Gulf of Naples, where a large steel plant operated from 1906-1992. My PhD project was conducted within the framework of the ABBACO project, a nationally-funded project that aims at the restoration of this highly polluted site. The results of my thesis are a separate workpackage of the ABBACO project and will provide information on one of the most polluted areas of Bagnoli-Coroglio, the site where most of the loading and unloading operations of the steel plant were conducted. My thesis also involves the study of samples collected in another polluted site, the mouth of the Sarno River in the south-west part of the Gulf of Naples, which is the most polluted river in Italy due to the agricultural waste and waste water from the tanning factories located along the river.

The thesis is structured as follows:

Chapter 1 with an introduction on bioremediation strategies in general.

Chapter 2 describes the Bagnoli-Caroglio sampling site and investigates the biodiversity of the microbial assemblages inhabiting this polluted marine ecosystem, using a culture independent approach. The aim was to determine whether there were specific microbial taxa that were characterized by their high capacity for the degradation of organic

pollutants and / or resistance to PAHs and metal contamination, and understand the influence that environmental factors exerted on the degrading capacities of microorganisms.

Chapter 3 describes the most interesting species isolated from the Bagnoli-Caroglio and Sarno sediments. Preliminary tests were conducted to evaluate their ability to tolerate high concentrations of heavy metals and PAHs. The most promising species were further tested in microcosm experiments using contaminated sediments to evaluate their potential to degrade PAHs (through HPLC) and reduce the harmful effects of heavy metals such as As, Cd, Cu, Pb, Zn (through Selective Sequential Extraction and Atomic Absorption).

Chapter 4 involves the sequencing of the most interesting species identified in Chapter 3 in order to obtain whole genomes and characterize potential candidate enzymes involved in hydrocarbon degradation pathways and leading to reduced toxicity of heavy metals.

Chapter 5 including general conclusions and further perspectives.

The three main research topics may be summarized as follows:

- 1- Microbial characterization of the study area and evaluation of drivers involved in shaping microbial assemblages
- 2- Evaluation of bioremediation potential of the most promising isolated strains
- 3- Genome mining analysis to understand pathways activated by bacteria to survive in polluted sediments

Chapter 2

Effects of multiple pollution stressors on microbial diversity:

The case study of the Bagnoli-Coroglio area (Gulf of Naples, South Tyrrhenian Sea)

In this chapter prokaryotic diversity and assemblage composition were investigated for the first time after almost a century of pollution due to the activity of the Ilva steel plant in the Bagnoli-Coroglio area. Analysing the response of prokaryotic diversity of this coastal ecosystem following massive heavy metals and hydrocarbons contamination is of fundamental importance since benthic prokaryotes are known to be involved in key ecological and biogeochemical processes and knowledge concerning the long-term impact of chronic multiple pollution on prokaryotic component is still far from being fully elucidated.

Sediments from four areas were collected in order to characterize prokaryotic abundance and metabarcoding of community structure using Illumina sequencing of amplicons generated from the 16s rRNA gene. Bacterial abundances were fairly constant around 10^7 cells mL⁻¹. Similarly, Amplicon Sequence Variant (ASV) richness did not vary significantly among sediments affected by different levels of pollution. Taxonomic composition showed the prevalence of the phyla Proteobacteria, (36.7%), Planctomycetes (20.5%) and Bacteroidetes (9.6%) and highlighted the presence of a core microbiome suggesting that pollutants and other abiotic factors can contribute to shape benthic prokaryotic community.

1) Introduction

An example of contamination driven by multiple factors is the area of Bagnoli-Coroglio (Gulf of Naples, Tyrrhenian Sea, IT) that is a highly polluted post-industrial site due to the activity of the former ILVA steel plant, which operated from 1905 to 1992 (Sharp and Nardi 1987; De Vivo and Lima 2008). Chemical characterization of this area reported by Romano et al. (2004) revealed concentrations above the legal limits for heavy metals such as Cu, Fe, Hg, Mn, Ni, Pb, Zn, as well as polychlorobiphenyls (PCBs), polycyclic aromatic hydrocarbons (PAHs), and dichlorodiphenyl-trichloroethane (DDT). Very high levels of most heavy metals (Fe, Pb, Zn, Hg, Ag, As, Co, Cr, Cd) and Total Organic Concentration (TOC) were found at the "Colmata a Mare", an area between the two piers where all of the loading/unloading operations took place, and on the beach of Nisida (Arienzo et al. 2015). Analysis of the macrobenthic community (Fasciglione et al. 2016), on the other hand, surprisingly highlighted the presence of seagrasses, multicellular green algae and 280 species of benthic invertebrates, although there was a marked decline in species diversity from north to south, probably due to a decrease in hydrodynamic rates and the concomitant presence of higher levels of pollutants in the southern area.

In 2000, the area was declared a site of national interest (SIN) and thus subject to ministerial policies aimed at the reclamation of polluted areas. In order to plan the most accurate remediation and restoration strategy of this site, in May 2017 the Italian government funded the ABBACO project, the aim of which was to re-sample and further characterise, both chemically and biologically, the Bagnoli-Coroglio area. As part of this project, this thesis examined the bacterial assemblages colonizing the upper ten

centimeters of sediments sampled in front of four sewage discharges which as described by Bertocci et al. (2019) represent a major source of organic matter. This thesis provides new insights on the microbial community composition of sediments contaminated by both sewage and heavy metals. Moreover, it provides new information for a possible bioremediation-based approach to restore the site using bacteria isolated from the polluted sediments. Such a strategy may represent an interesting alternative to conventional chemical and physical remediation techniques due to lower costs and reduced environmental impact (Dell'Anno et al. 2012).

To date, most studies have focused on the bacterial communities of the uppermost centimeters, usually dominated by Proteobacteria (Catania et al. 2018), and only few studies have investigated the role played by multiple stressors, such as heavy metals and PAHs, on shaping sediment microbial communities (Quero et al. 2015). For this reason, determining the composition of dominant and rare taxa within prokaryotic assemblages through a high throughput sequencing (HTS) approach, can lead to a better understanding of the dynamics involved in determining the composition of autochthonous microbial populations and eventually to exploit their metabolic potential in bioremediation strategies.

This Chapter characterised the prokaryotic community of the upper 10 cm of sediments sampled at four stations polluted by sewage, hydrocarbons and heavy metals, within the Bagnoli-Coroglio area.

2) Material and Methods

2.1) Study area

Figure 1.1 shows the area previously sampled (2004-2005) by Romano et al. (2009) and the 4 sampling sites examined in the current study. Values for arsenic, cadmium, chromium, iron, mercury, magnesium, nickel, lead, zinc, and total PAH levels are reported in Romano et al. (2009). In order to assess the impact of multiple stressors, the sampling in this thesis was carried out in front of four different sewer drains. Samples were collected in April 2017 using a manual Core soil sampler operated by SZN scuba divers. For every sampling station pH, Eh, and T were monitored using a portable pH/EC/TDS meter HI9813-5, Hanna Instruments (Tab. 2.1). The sampling operations led to the collection of three cores for each of the four selected sites shown in Figure 1. Each core, collected by a scuba diver using sterile Plexiglas® tubes, was divided into three layers named A (0-3 cm), B (3-6 cm) and C (6-9 cm), which were processed separately for Illumina sequencing, to determine prokaryotic abundance and biomass, and for the analysis of Particulate organic matter (POM) according to the method described by Pusceddu, Bianchelli, and Danovaro (2015). POM analysis measured the concentration of total phytopigments, proteins, carbohydrates, lipids, and biopolymeric organic C. Each layer was stored in a 150 mL sterile box, and kept refrigerated at 4 C° until analysis.



Figure 1.1. Map of the four sampling sites analysed in the current study: 1) Impianto Sollevamento Dazio, 2) Scarico Conca di Agnano; 3) Canale Bianchettaro; 4) Galleria scarico Impianto Coroglio

Table 2.1. Coordinates, pH, Eh and T° of the four sampled stations

Id.	Name	WGS84 GSM		pH	Eh	T (C°)	Depth (m)
		Long.	Lat.				
1	Impianto sollevamento Dazio	14° 9'31.20"E	40°48'59.30"N	7,41	178	17,3	1
2	Scarico Conca di Agnano	14° 9'43.10"E	40°48'54.10"N	6,79	264	19,5	1
3	Canale Bianchettaro	14° 9'59.60"E	40°48'33.10"N	8,02	197	20	1,5
4	Galleria Scarico Impianto Coroglio	14°10'36.61"E	40°47'48.20"N	8,03	167	17,3	2,8

2.2) Prokaryotic abundance and biomass

Prokaryotic cells were extracted from the sediments, stained with SYBR Green I, and counted with an epifluorescence microscope to determine cell abundance according to the methods described in (Danovaro et al. 2009). In order to determine prokaryotic biomass, cell biovolumes were converted into carbon content assuming an average carbon content of 310 fg C μm^{-3} (Danovaro et al. 2010; Danovaro et al. 2015).

2.3) Illumina sequencing and bioinformatic procedures for sediment microbiome analyses

Microbial genomic DNA was extracted from sediments by using the DNeasy PowerSoil Kit (MO BIO) in Università Politecnica delle Marche facilities. Sequence library preparation of the gDNA was performed using the Nextera DNA Flex kit (Illumina, Hayward, USA) with 1 ng DNA according to the manufacturer's instructions. Sequencing was performed on an Illumina MiSeq platform by LGC Genomics GmbH using paired end read (Berlin, Germany).

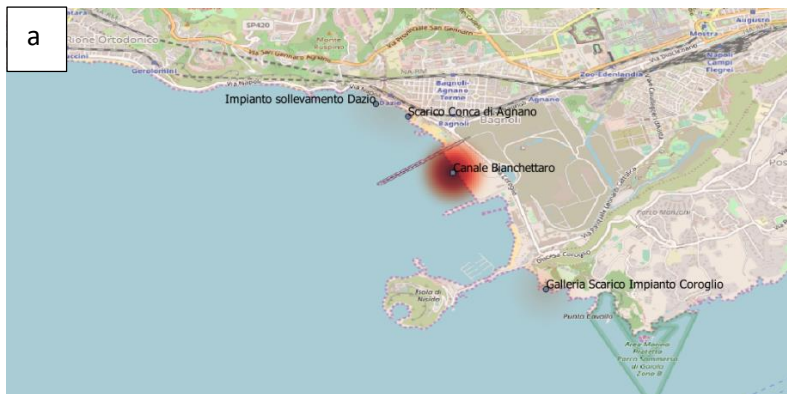
Raw sequencing paired-end reads were first joined using the *bbmerge* tool from the BBDMap suite (Bushnell, Rood, and Singer 2017) in a two-step process: reads that did not merge in a first step were quality-trimmed to remove low-quality bases ($Q < 10$) prior to re-joining to increase the number of merged sequences. Subsequently, joined sequences were analysed using the QIIME2 pipeline (<https://qiime2.org>) following a previously published pipeline (Bolyen et al. 2019). Amplicon sequence variants (ASVs) were identified using the DADA2 strategy (Callahan, McMurdie, and Holmes 2017). The SILVA database v132 (Quast et al. 2013) was used as a reference database for taxonomic affiliation of sequences; briefly, reference 16S sequences contained in the database were trimmed within QIIME2 to the region amplified by sequencing primers and representative ASVs were analyzed using the classify-consensus-vsearch approach (consensus over 51% of at most 5 best hits) for taxonomic affiliation (Rognes et al. 2016). The ASV abundance table was randomly subsampled to 50000 sequences per sample and used, together with the rooted phylogenetic tree, to carry out statistical analyses to compare samples according to the method described by Corinaldesi et al. (2019).

2.4) Statistical analyses

In order to evaluate whether differences in prokaryotic abundance, biomass, ASV richness and effective number of species (ENS, Cao and Hawkins 2019) observed were statistically significant, a 2-sample T testing using Welch's test (Welch 1947) was carried out. For β -diversity, Bray-Curtis dissimilarities (Bray and Curtis 1957) were calculated between different samples based on their ASV distribution. Dissimilarities were investigated using the Unweighted Pair Group Method with Arithmetic mean (UPGMA) dendrograms using the R package `vegan` (www.cran.r-project.org/web/packages/vegan/index.html).

3) Results and discussion

3.1) Chemical characterization



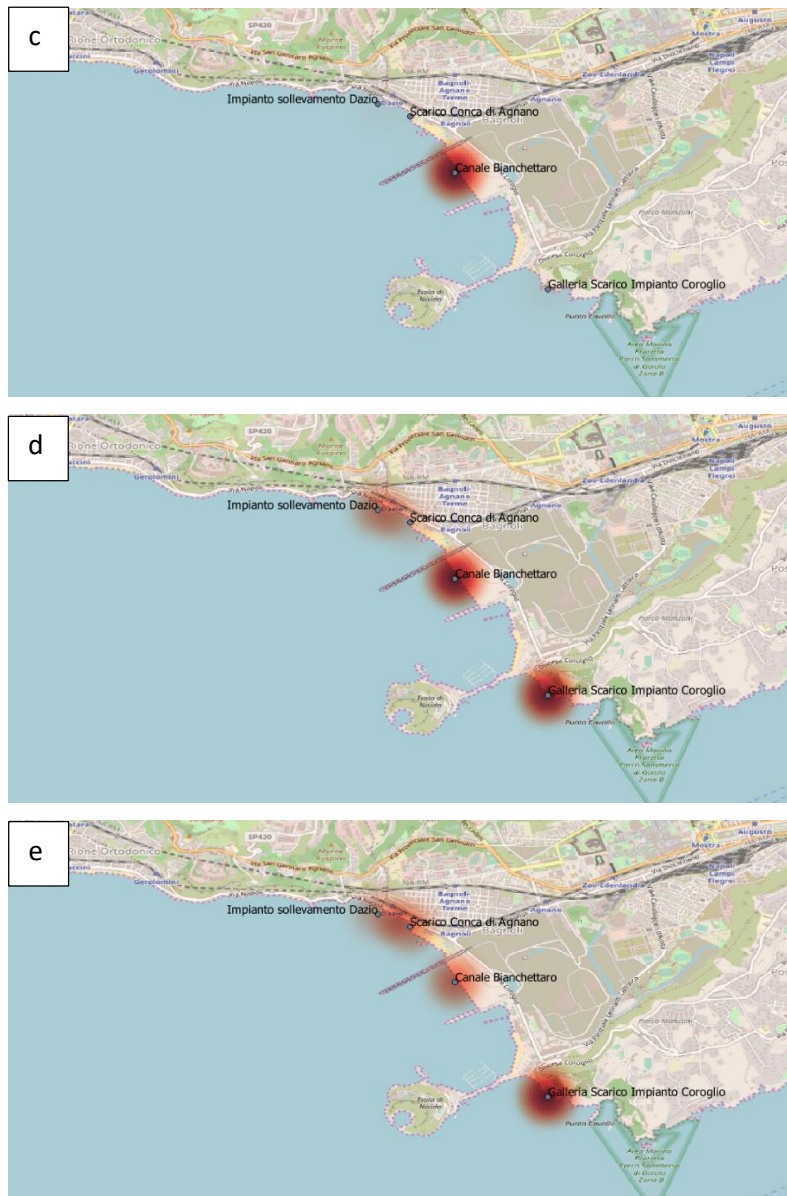


Figure 1.2. Heat-maps showing the concentrations reported of Biopolymeric organic C (a), Carbohydrates (b), lipids (c), phytopigments (d) and protein (e) along the littoral area of Bagnoli-Coroglio

The region investigated is highly affected by pollution from both heavy metals and PAHs (Romano et al. 2004; 2009). Specifically, sediments from Canale Bianchettaro exhibited the highest concentrations of arsenic ($13 \pm 10 \text{ mg kg}^{-1}$), cadmium (0.71 ± 1.16), copper (40 ± 35), lead (261 ± 281), zinc (539 ± 538), and PAHs (172 ± 506). Lower concentrations

of both PAHs and heavy metals were present in Conca di Agnano, Dazio, and Scarico Coroglio (Romano et al. 2009).

Although arsenic is the most widely distributed contaminant in the entire area, it has been suggested that it is released from nearby geothermal springs (Aiuppa et al. 2006). The pollutants present in the highest concentration were Zn, PAHs and Pb, reaching the values of 1110 ppm, 800 ppm and 540 ppm, respectively. The concentrations of Cu, As, and Cd ranged from 1 to 70 ppm and were also above the permitted limits (US EPA 2017), although they were lower than those for Zn, Pb, and PAH. The high concentrations of these heavy metals as well as PAHs might have contributed to shape the microbial assemblages (Ahmed et al. 2018).

In this thesis the concentrations of the different organic matter fractions in the Bagnoli-Coroglio area were investigated (Fig 1.2 and Tab 2.2). The lipid and Biopolymer C fractions were far more abundant in the Canale Bianchettaro compared to the other stations.

Tab 2.2: Distribution of the different fractions of organic matter in Bagnoli-Coroglio sediments

	Total phytopigment s	Proteins	Carbohydrate s	Lipids	Biopolymeri c organic C
	µg g⁻¹	mg g⁻¹	mg g⁻¹	mg g⁻¹	mg g⁻¹
<i>Impianto sollev. Dazio</i>	2,1 ± 0,06	0,3 ± 0,04	0,6 ± 0,09	0,4± 0,18	0,7 ± 0,17
<i>Scarico Conca Agnano</i>	1,1 ± 0,15	0,5 ± 0,03	0,6 ± 0,07	0,2± 0,03	0,6 ± 0,04
<i>Canale Bianchettaro</i>	4,5 ± 1,7	0,6 ± 0,1	1,1 ± 0,1	7,5± 4,2	6,3 ± 3,2
<i>Gall. scarico imp. Coroglio</i>	4,4 ± 0,6	1,0 ± 0,2	0,6 ± 0,0	0,6± 0,2	1,1 ± 0,2

3.2) Prokaryotic Abundance

No significant differences were observed in the prokaryotic abundances in the surface layers (0-3 cm) (Figure 1.3a) among the four analysed stations. The same trends were observed for prokaryotic biomass (Figure 1.3b). Such prokaryotic standing stocks differed from those previously reported in other benthic coastal ecosystems (Zhang et al. 2017; Sun et al. 2013). For example, the prokaryotic abundance in coastal contaminated sediments of Manfredonia Gulf (Southern Adriatic Sea) (Molari et al. 2012) and Mediterranean Sea (Luna et al. 2013) were over one order of magnitude higher than the values found here (10^8 vs 10^7). Prokaryotic abundances found here were, at least, one order of magnitude lower than those observed in sediments from the Medway Estuary (UK) even though these sites were contaminated by zinc, nickel, lead, and copper (Quillet et al. 2012).

Conversely the values found here are comparable to abundances typically found in deep-sea sediments (Danovaro et al. 2009).

From the data presented, it is not possible to assess a direct correlation between the different pollution patterns recorded throughout the entire area and the number of prokaryotic cells among the different sites analysed since abundances were fairly constant, around 2×10^7 even in the most polluted station (Canale Bianchettaro). Although Molari et al. (2012), have reported the importance of local trophic conditions in shaping prokaryotic abundances, the present study did not find any correlation between the organic matter content and prokaryotic abundances, despite Canale Bianchettaro exhibited the highest concentrations of Biopolymer C and lipids, while Conca di Agnano contained lower amounts of organic matter.

Additionally, bacterial abundances were not affected by other environmental variables (Tab 2.1) such as pH and Eh that differed by 1.5 and 90 mV, respectively, between Bianchettaro and Conca di Agnano.

Temperature is generally considered as an important factor influencing bacterial abundances and biomasses (e.g. Castro et al. 2010). However, temperature did not seem to play a role in determining bacterial abundances between the four stations. Indeed, bacterial abundances were constant in the area even if Bianchettaro and Conca di Agnano exhibited higher temperatures (> 2 °C) compared to the other stations.

Also no significant correlation was found between sediment grain size (analysed by Bertocci et al. (2019), in the same stations) and prokaryotic abundances. Moreover, the significant higher prokaryotic abundance (p-value 0,004) found in the deepest sediment layer of Dazio (6-9 cm) contrasts with previous findings, which showed a decrease in prokaryotic abundances with depth in the sediment (Rissanen et al. 2019).

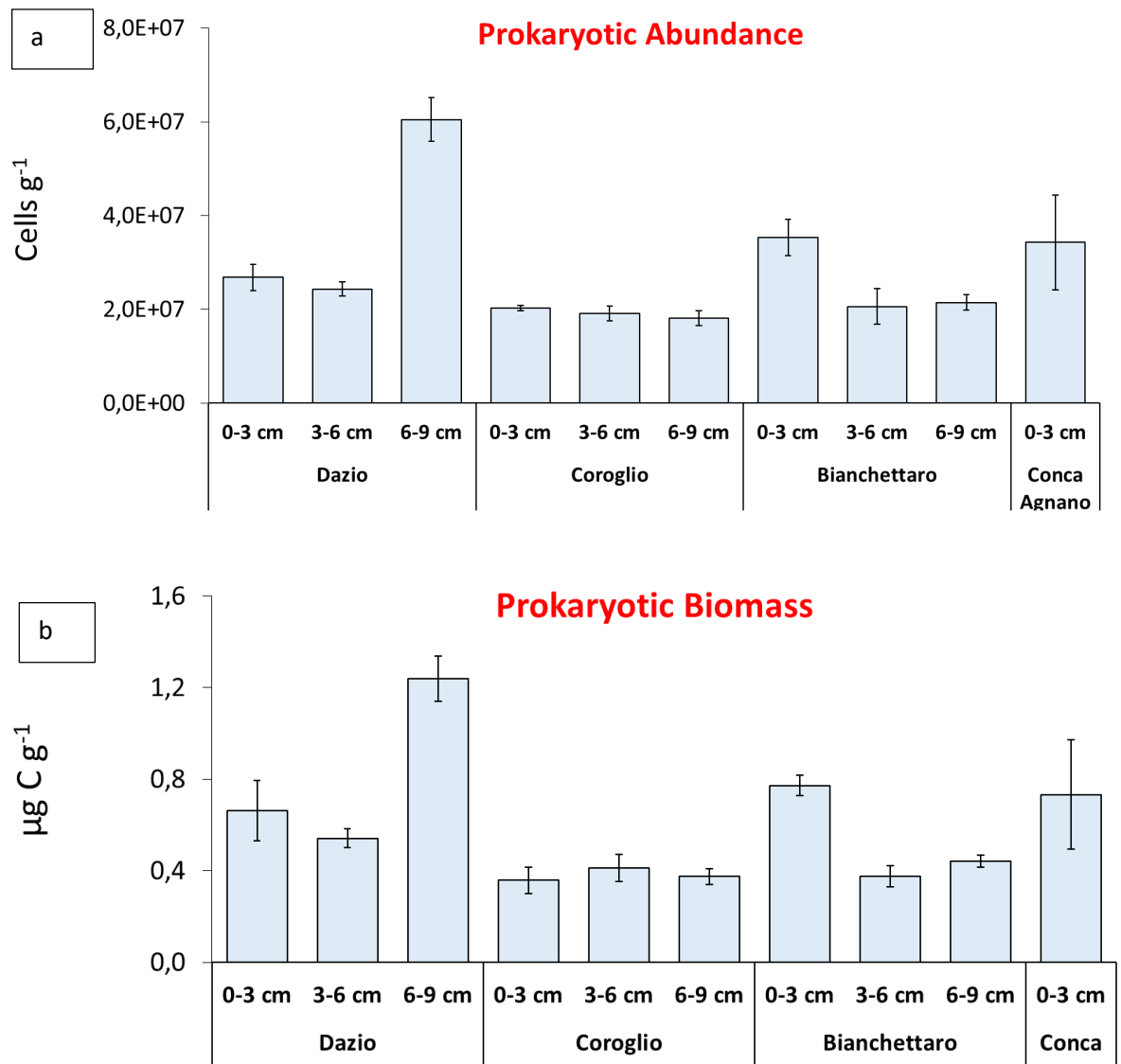


Figure 1.3. Prokaryotic Abundance (a) and Biomass (b) counting in epifluorescence bacterial cells labelled with SYBR Green according to Danovaro et al. 2009. Bacterial cells have been collected at three different depths (0-3 cm, 3-6 cm, 6-9 cm) at four different sites as indicated in the map. Biomass has been calculated basing on the different prokaryotic size.

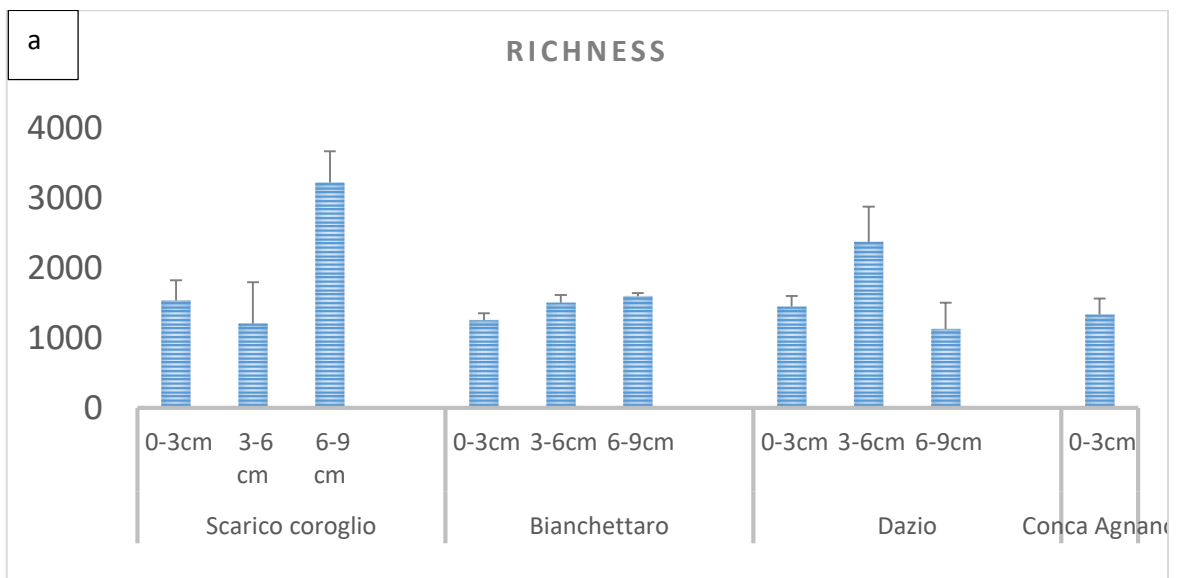
3.3) Alpha diversity

The analyses of α -diversity carried out across all samples highlight that the deepest sediment layer of Coroglio and the subsurface layer of Dazio exhibited the greatest ASV richness (Fig. 1.4 a). A similar pattern of higher ASV richness in subsurface sediment layers was already described in previous works (Luna et al. 2013), and can be due to a variety of factors such as a reduced energy-stress conditions, and/or predatory pressure and competition as well as to the effect of the pollutants (Molari et al. 2012). Shannon index, converted in Effective Species Number (ESN) (Fig 1.4 b) (Leinster and Cobbold 2012) was correlated to ASV richness. The highest values were found in the deepest sediment layers (31250 predicted species) and sub surface layer (20517 predicted species) of Scarico Coroglio and Dazio with an average value of 13248 predicted taxa per site.

Although (Quero et al. 2015) observed that the long term contamination of heavy metals and hydrocarbons in Taranto Gulf led to a selection of bacterial communities more tolerant to pollutants and Korlević et al. (2015) highlighted a negative correlation between OTU richness and the presence of pollutants, the metal concentrations found in the upper layer of sediments in the present study were not found to be related to ASV richness and ESN. Indeed, both indices did not present significant variations among the four stations characterized by different levels of contamination. Such observations are likely to depend not only on the role played by contaminants over almost a century but also on environmental and biological factors.

Conversely, although the Evenness index (Fig 1.4 c) showed an overall uniformity of species distribution in the different layers of the analyzed sites with an average value of

0.88, species evenness in the 0-3 cm and 3-6 cm layers from Canale Bianchettaro (0.85 ± 0.02) were significantly lower than those calculated for Scarico Coroglio (0.89 ± 0.01 , p-value of 0.026) and Dazio (0.88 ± 0.01 , p-value 0.0135). Thus, these data suggest the influence of toxic compounds on microbial assemblages since the Bianchettaro station contains greater concentrations of both heavy metals and hydrocarbons compared to the other stations (as reported by Romano et al. 2004). Environmental drivers such as pH, Eh, T° granulometry and organic matter did not explain the evenness distribution found here.



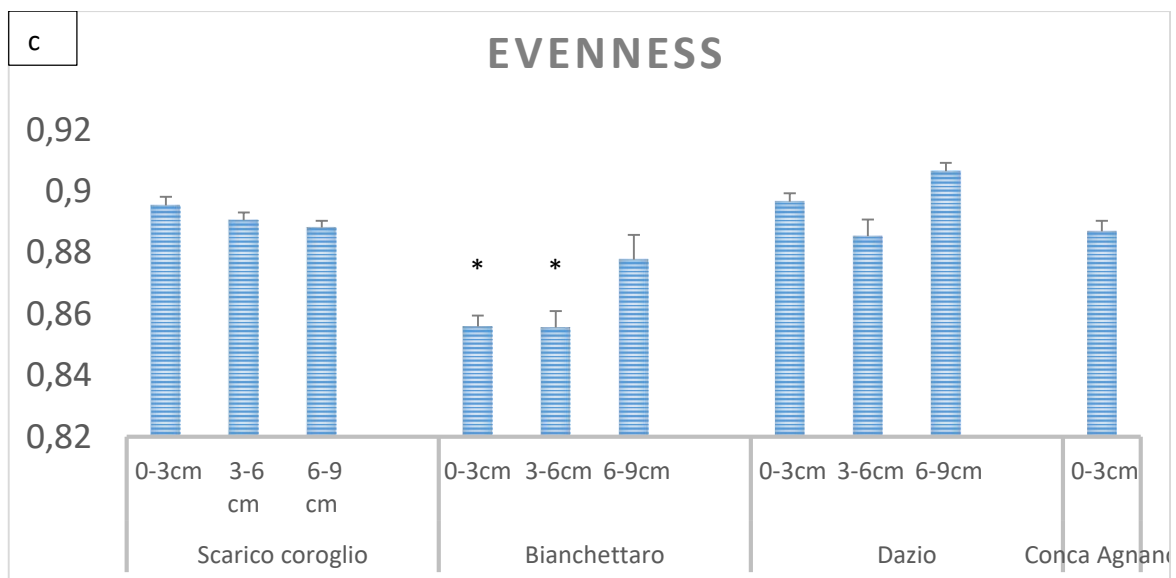
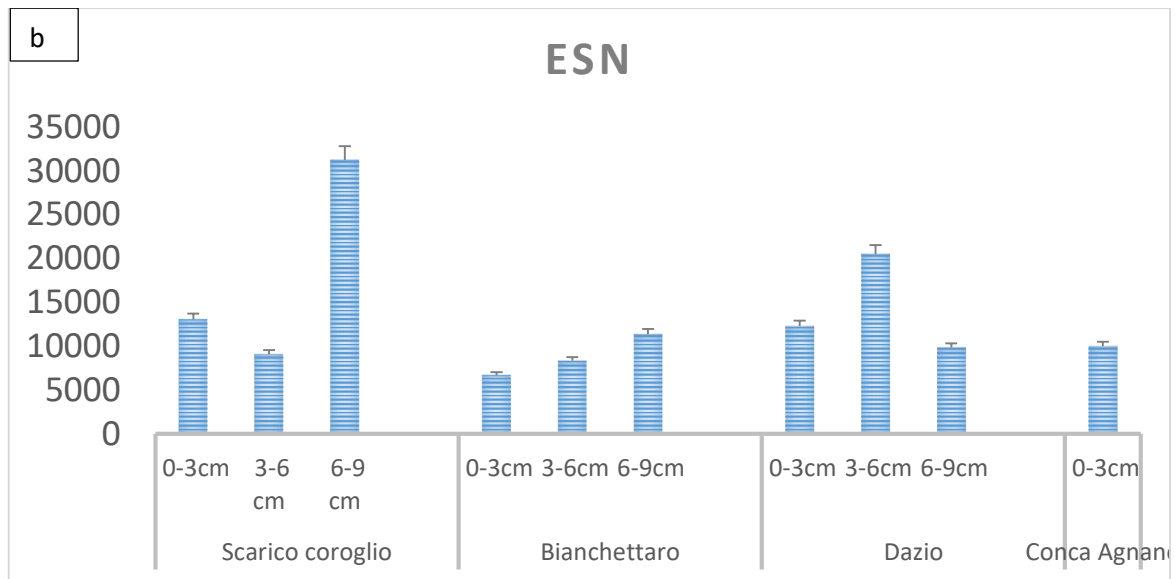


Figure 1.4. Amplicon Sequence Variance richness (a), effective species number (b) and Evenness values (c) calculated for samples collected at three different depths (0-3 cm, 3-6 cm, 6-9 cm) in the four analysed stations of Bagnoli-Coroglio area.

3.4) Taxonomic composition

The analysis of the prokaryotic assemblage assigns the ASVs found here to 53 Phyla and 156 Classes. As shown in Fig. 1.5, after removing phyla exhibiting low abundances (<1000 sequences), the most represented phyla at the various stations were Proteobacteria (36 % ASV richness; 45% read abundance), Planctomycetes (20% richness, 15% abundance), Bacteroidetes (9% richness, 13% abundance), Acidobacteria (6% ASVs; 5% sequences) and Actinobacteria (3% ASVs; 6% sequences). Specifically, observing the Class distribution at all stations (fig. 1.6), the most abundant Classes were Gamma-, Delta- and Alphaproteobacteria as well as Planctomycetacia, represented by 22%, 11%, 9.1%, 8% read abundances and 13%, 12.9%, 9.3%, 9.2% ASV richness, respectively. Overall, the results support findings from previous studies from New South Wales (Australia; Sun et al. 2013), Adriatic Sea (Italy; Quero et al. 2015), Northern Zhejiang Sea (China; Wang et al. 2016) and Basque coast (Spain; Aylagas et al. 2017).

At the Class level (fig. 1.7), the prokaryotic assemblage associated with the surface layers in the 4 stations was dominated by Gammaproteobacteria (~24.5%), although their contribution was lower for the Scarico Coroglio site (~18.1%). The dominance of this class has already been described previously (Franco et al. 2017; Chiellini et al. 2013; Danovaro et al. 2010; Edlund et al. 2008) and suggests an important ecological function for Gammaproteobacteria. Gammaproteobacteria have been shown to play a primary role in catalysing sulfur oxidation and carbon fixation in coastal sediments (Lenk et al. 2011; Dykema et al. 2016). Gammaproteobacteria were dominated by representatives from the order Xanthomonadales (fig. 1.8), in particular in Dazio (surface and deep layers) as well as in the surface layers of Conca di Agnano, Bianchettaro, and Coroglio;

Xanthomonadales were particularly abundant in areas polluted by metals and PAHs (Patel et al. 2012; Sun et al. 2013). These findings could provide a partial explanation for the high abundances of Xanthomonadales since the area in front of the steel plant has been polluted with PAHs for many years.

Most ASVs associated with Xanthomonadales (fig.1.9) were either uncultured or belong to the widespread marine benthic group JTB255 (Bienhold et al. 2016). Specifically, the abundance of JTB255 representatives was higher in Dazio (ca 4000 reads) than Scarico Coroglio (2000 reads). The presence of the JTB255 marine benthic group in heavily polluted sites could be attributed to the ability of this group to adapt to various biogeochemical conditions. The JTB255 group shows a wide metabolic versatility covering a broad physiological spectrum ranging from facultative sulfur- and hydrogen-based chemolithoautotrophy to obligate chemorganoheterotrophy (Mußmann et al. 2017).

Other 3 classes with abundant distribution in the surface layers of Scarico Coroglio and Bianchettaro were Flavobacteria, Planctomycetacia and Alphaprotobacteria, the abundance of which was 2 fold higher than that of the other two stations. The class Flavobacteria has been shown to be involved in organic matter degradation (Telling et al. 2012) and this capability may partially explain its presence in Bianchettaro site where TOC (Total Organic Carbon) concentrations were 10 times higher (Table 2.2) compared to the other stations. A number of Alphaproteobacteria representatives are known to be able to degrade aromatic compounds (Kim and Kwon 2010) and their high abundance in Bagnoli-Coroglio area might be attributed to the ubiquitous presence of PAH in this area (Romano et al. 2004). The lower abundances of Acidomicrobia,

Sphingobacteria and Delta proteobacteria in Scarico Coroglio and Bianchettaro stations does not agree with previous findings, since these classes have been found (Oregaard and Sørensen 2007; Dell'Anno et al. 2012) in contaminated sediments. Moreover, Coroglio and Bianchettaro sites differ from the others due to the presence of the Verrucomicrobia class that, according to Genovese et al. (2014) is considered capable of coping with hazardous compounds.

The deltaprotobacteria Classes especially from the order Desulfobacterales, are able to degrade hydrocarbons by methanogenesis and sulfate reduction (Stagars et al. 2017). These Classes are mostly represented in Dazio and Conca di Agnano. Compared to other sites, Dazio and Conca di Agnano also included Classes such as Holophage, Anaerollinae, Nitrospirae and Ignavibacteria. The presence of these latter Classes has already been described in contaminated areas probably due to their ability to survive the toxic effects of metals (Ni, Cu, Cd), and to degrade Polychlorinated biphenyls (PCB) as well as polycyclic aromatic hydrocarbons (Zanaroli et al. 2012; Wang et al. 2016).

The taxonomic composition of the sub-surface (3-6 cm) and deep (6-9 cm) layers differs only slightly from that of the surface layer. Indeed, the two deeper layers of Canale Bianchettaro were comparable to the surface layer in terms of number of classes with the only exception given by the presence of the Class Phycisphaerae belonging to the phylum Planctomycetes.

The bacterial composition of Scarico Coroglio sediments did not differ significantly between the surface and the sub-surface layers; in contrast the deep layer exhibited greater abundances of species belonging to the Classes Phycisphaerae and Nitrospirae. Finally, the 3-6 cm and 6-9 cm layers of the Dazio site showed a similar taxonomic

composition with the presence of Ignavibacteria that were not found in the surface layer.

In general, we observed a greater number of bacterial Classes in the sub-surface and deep layers compared to the surface layer only in Canale Bianchettaro; this might be due to the toxic activity of hazardous compounds in surface layers as suggested by the evenness index. However, comparing the layers at different depths from the 4 stations it is evident that Classes which have been shown to survive in polluted environments (Gillan et al. 2005; Yin et al. 2015), such as Nitrospirae, Chloroflexy were not detected in the most polluted station (Canale Bianchettaro) described in this study, but were present in less contaminated stations (Impianto Sollevamento Dazio and Conca di Agnano). Heavy metal and PAH pollution in the Bagnoli-Coroglio area might thus not be the only drivers shaping the microbial diversity.

Additionally, the analysis of OTU distribution between the different stations and layers led to the identification of a core microbiome composed by 57 ASVs (Table 2.3) belonging to the Classes Gamma, Delta, Alphaproteobacteria, Planctomycetacia, Phycisphaerae OM190, Nitrospira, PAUC43f marine benthic group, B2-11 terrestrial group, Sphingobacteriia, Flavobacteria, Thermoleophilia, Acidimicrobiia, Blastocatellia and Holophagae. This core microbiome comprised some of the more abundant OTUs, such as OTUs within the Flavobacteriales and Xanthomonadales Orders. The remaining core microbiome OTUs belong to 20 bacterial Orders.

A similar core microbiome has been found in a previous study by Sun et al. (2013), who reported the presence of Gamma, alpha, Deltaproteobacteria and Acidobacteria. However, Quero et al. (2015) reported a core microbiome consisting of OTUs belonging

to Beta, Epsilonbacteria, Clostridia, Cytophagia, and Archea. The reason why these differences in core OTUs were observed may depend on the different pollution patterns found in the various studies, the seasons in which the samplings took place (Gilbert et al. 2009) and also the different physico/chemical factors of the study site. In fact, as reported by Sun et al. (2013) the comparison of OTUs from contaminated and uncontaminated sites revealed that the drivers significantly influencing OTU abundance were related to other environmental conditions rather than the presence of contaminants.

In general, our data suggest that the presence of different levels of pollutants does not affect the composition of the microbial diversity along the investigated area since Scarico Coroglio and Canale Bianchettaro stations, showing a similar taxa composition, lie in areas exhibiting very different contamination levels in terms of PAHs as well as heavy metals. Moreover, even other environmental variables do not seem to act as drivers influencing taxonomic composition since values of pH, eH, T° did not change significantly between the four stations. The variables that may represent drivers capable of shaping bacterial community structure are organic matter concentration and grain size distribution: all samples from Bianchettaro and Coroglio group together in our Bray-Curtis dissimilarity matrix based dendrogram (fig. 1.10), exhibiting significantly higher concentrations of organic matter (p-value = 0.012) and contained coarser sediment grains (>0.5 mm, Bertocci et al. 2019) compared to samples from the other stations.

Finally, it is not excluded that the chronic contamination of metals and hydrocarbons over decades has selected for a microbial community tolerant to such pollutants since many classes shown here have been widely described as capable of adapting to both

PAH and heavy metals, but the ecological differences, shown here, are shaped by the presence of different levels of POM, related to sewage discharges and grain size.

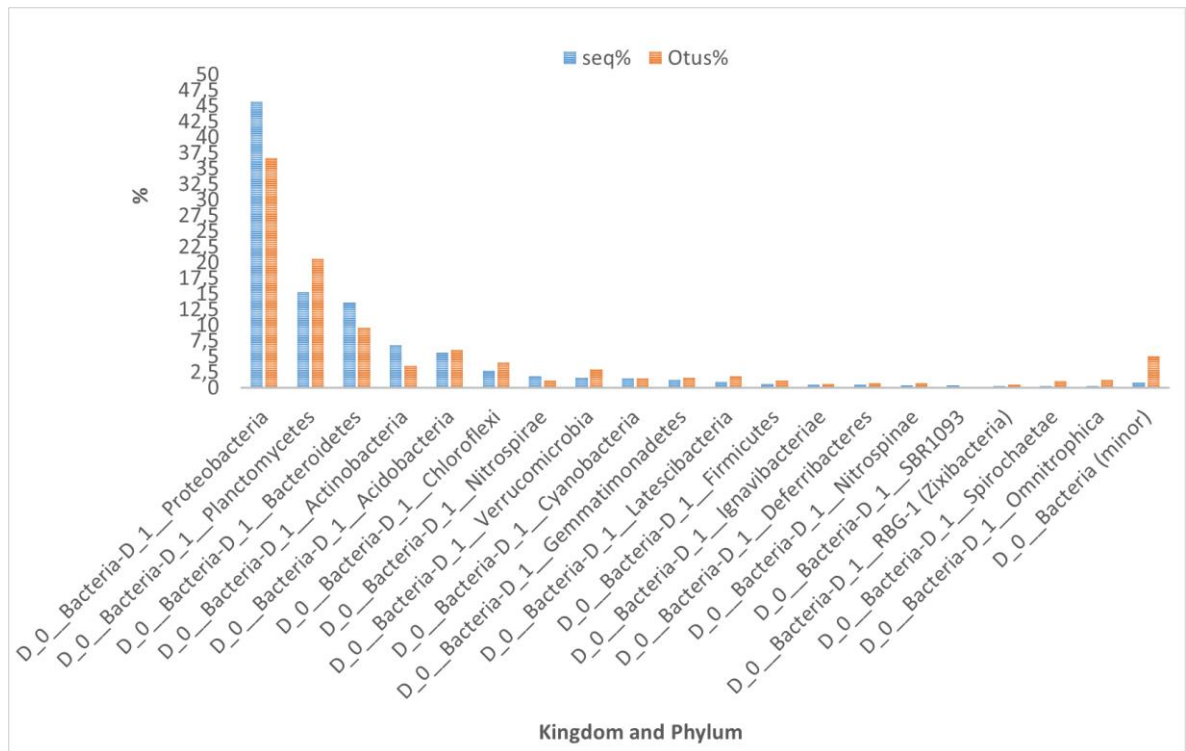


Figure 1.5. Abundances of the most represented Phylum in the study area of Bagnoli-Coroglio. Blue bars refer to percentage of sequences while red bars refer to percentage Otus observed.

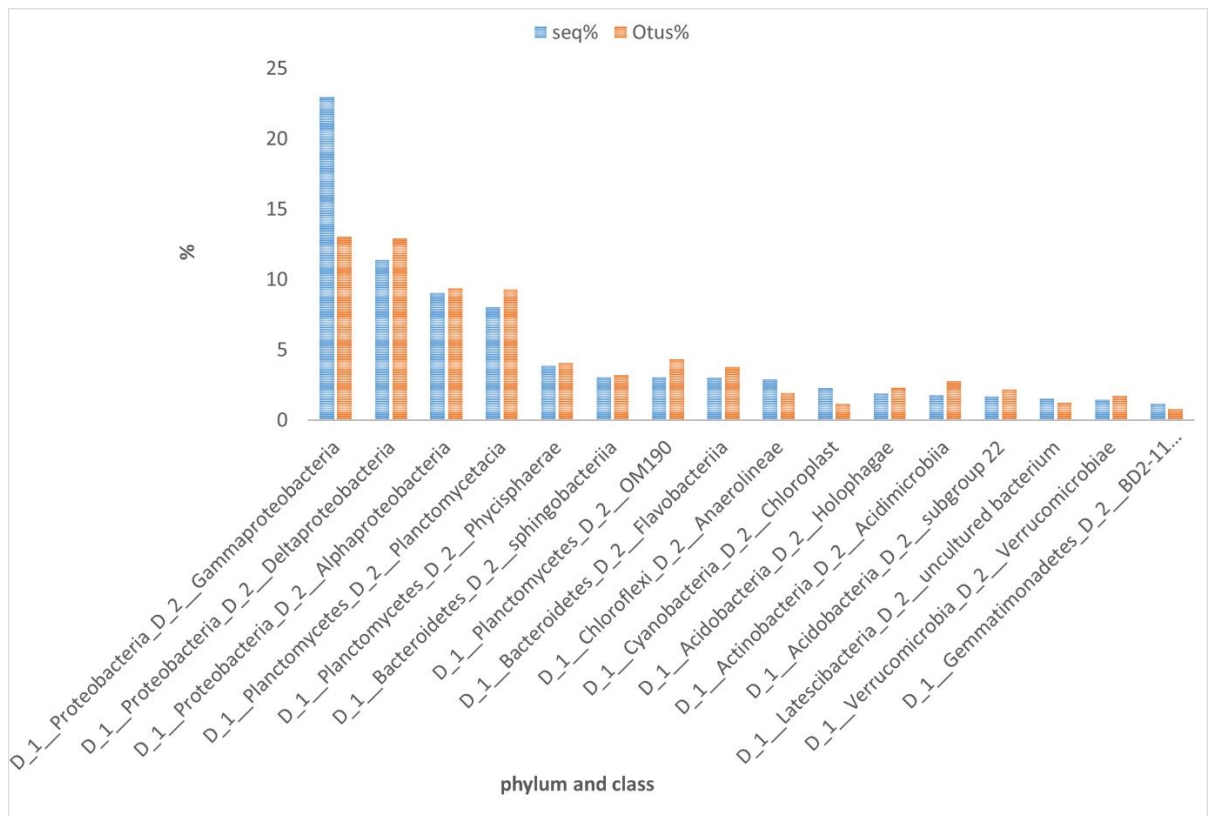


Figure 1.6. Abundances of the most represented phylum and classes in the study area of Bagnoli-Coroglio. Blue bars refer to percentage of sequences while red bars refer to percentage Otus observed.

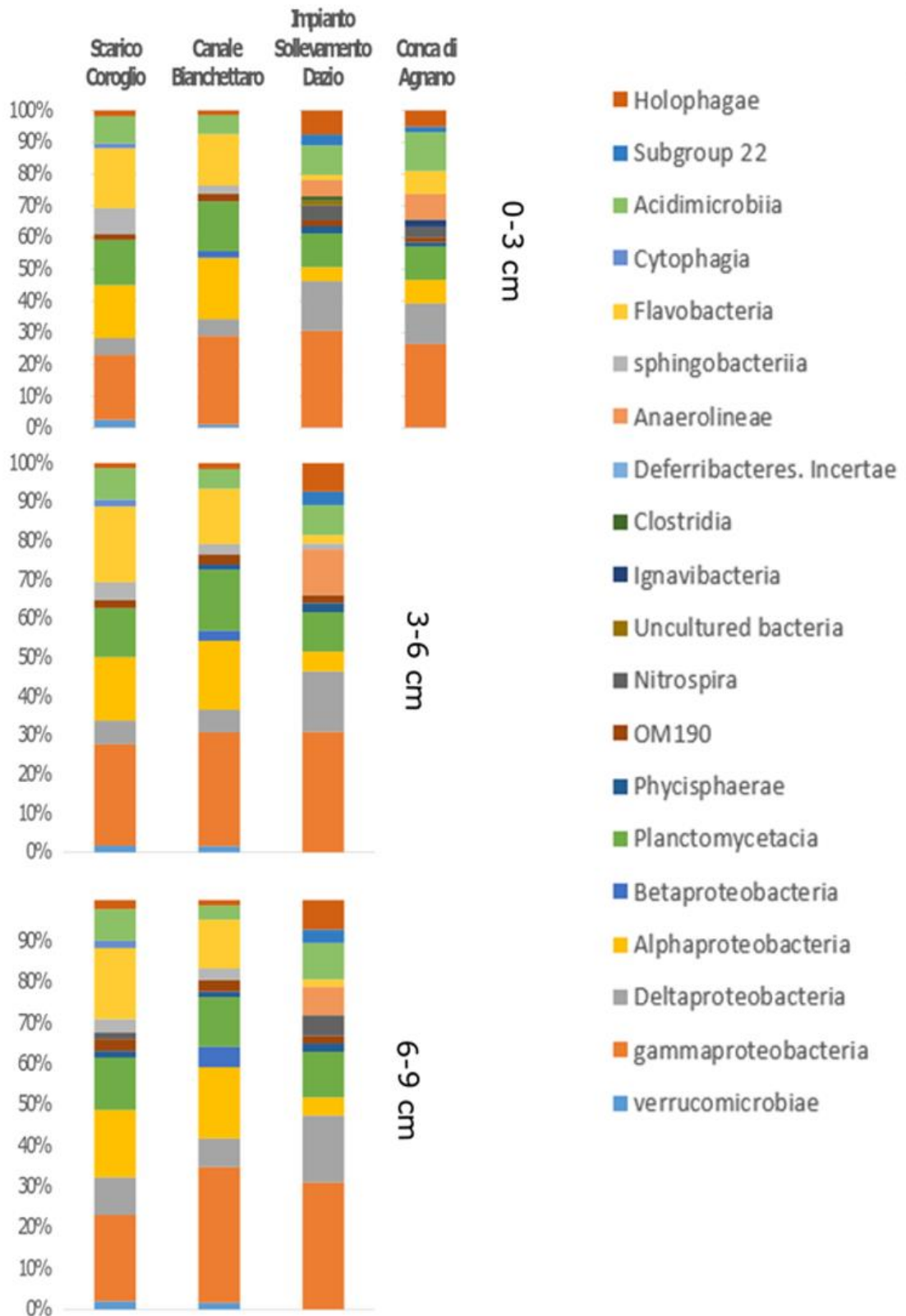


Figure 1.7. Percentage of distribution of bacterial Classes at different four stations and layers (0-3 cm, 3-6 cm, 6-9 cm) studied in Bagnoli Coroglio area

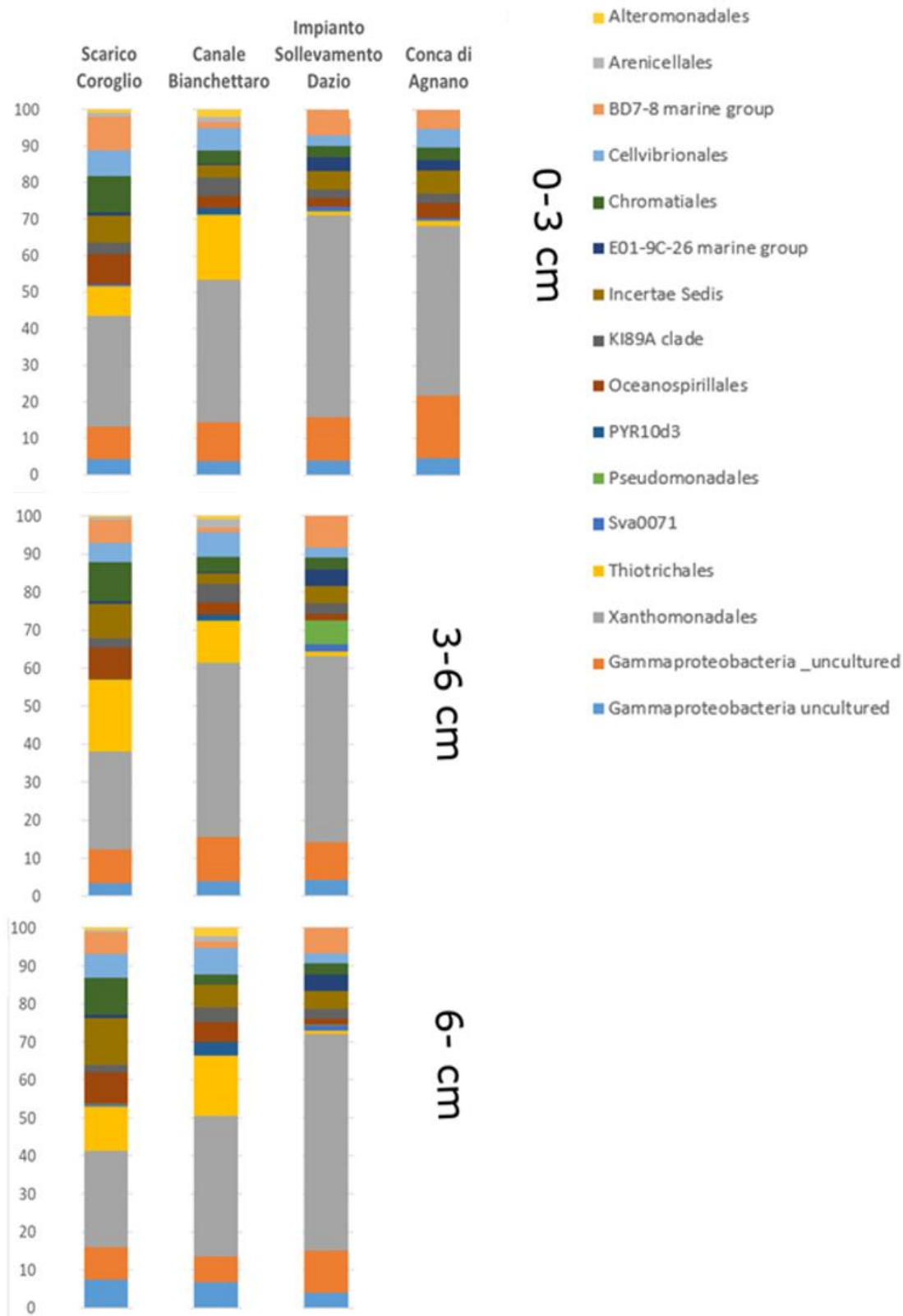


Figure 1.8. Percentage of distribution of Orders belonging to the Gamma Proteobacteria at four different station and layers (0-3 cm, 3-6 cm, 6-9 cm) analysed in Bagnoli-Coroglio area.

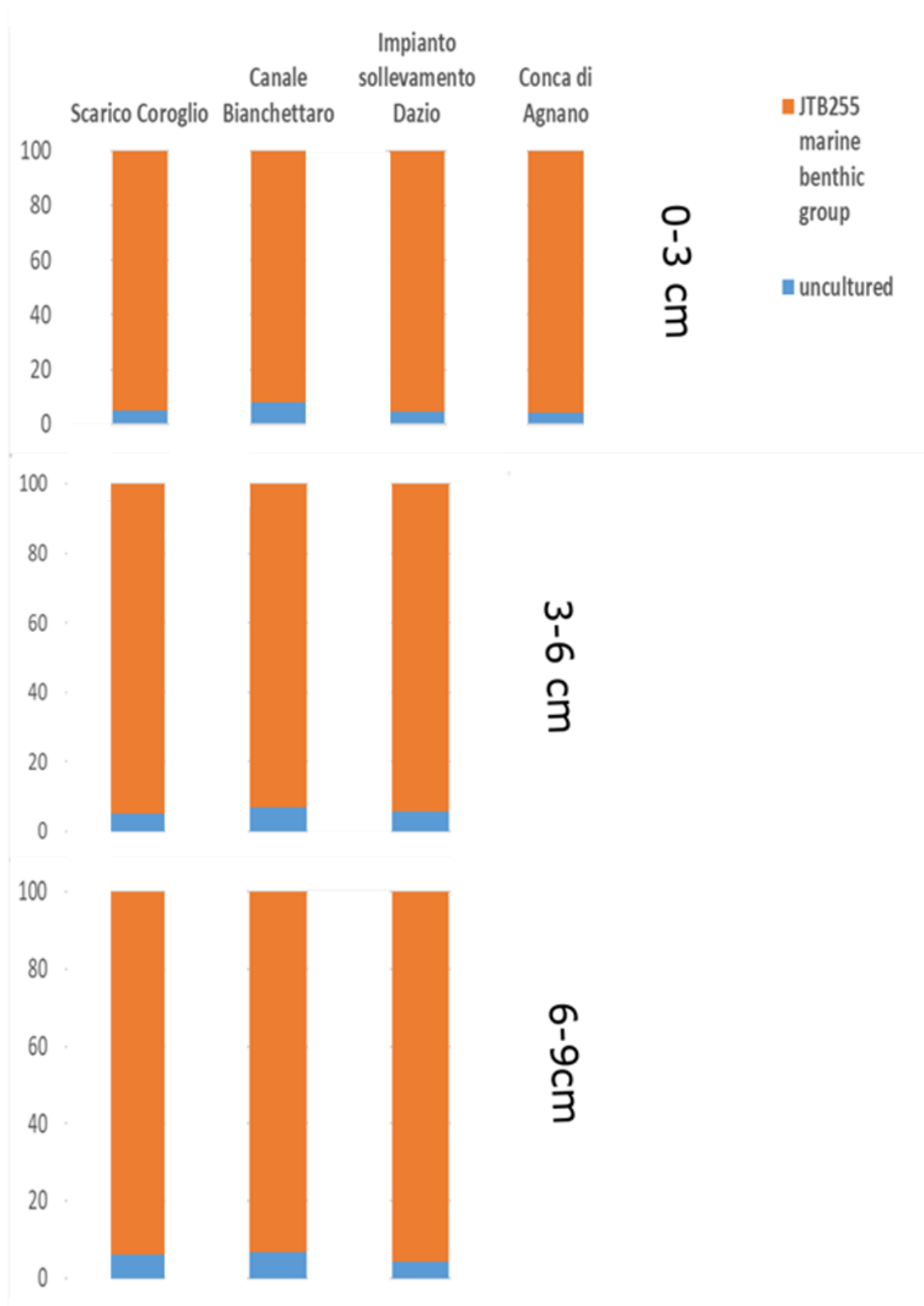


Figure 1.9. Distribution of the most abundant families belonging to the Order Xanthomonadales at different stations and layers (0-3 cm, 3-6 cm, 6-9 cm) analysed in Bagnoli-Coroglio area.

Table. 2.3: List of ASVs present in all samples at all sites.

Phylum	Class	Order	OTUs reads frequency
Acidobacteria	Blastocatellia	Blastocatellales	0.05
	Holophagae	Subgroup 10	0.02
	Subgroup 22	uncultured bacterium	0.03
Actinobacteria	Acidimicrobiia	Acidimicrobiales	0.91
	Thermoleophilia	Gaiellales	0.03
Bacteroidetes	Flavobacteriia	Flavobacteriales	3.08
	Sphingobacteriia	Sphingobacteriales	0.07
Gemmatimonadetes	B2-11 terrestrial group	uncultured bacterium	0.13
	PAUC43f marine benthic group	uncultured bacterium	0.06
Nitrospirae	Nitrospira	Nitrospirales	0.16
Planctomycetes	OM190	uncultured bacterium	0.08
	Phycisphaerae	Phycisphaerales	0.05
	Planctomycetacia	Planctomycetales	1.60
Proteobacteria	Alphaproteobacteria	Rhizobiales	0.29
		Rhodobacterales	0.13
		Rhodospirillales	0.29
		Sphingomonadales	0.15
	Betaproteobacteria	Nitrosomonadales	0.09
	Gammaproteobacteria	B7-8 marine group	0.74
		Oceanospirillales	0.16
		uncultured	0.99
Xanthomonadales		2.98	

Data refer to the proportion of total reads

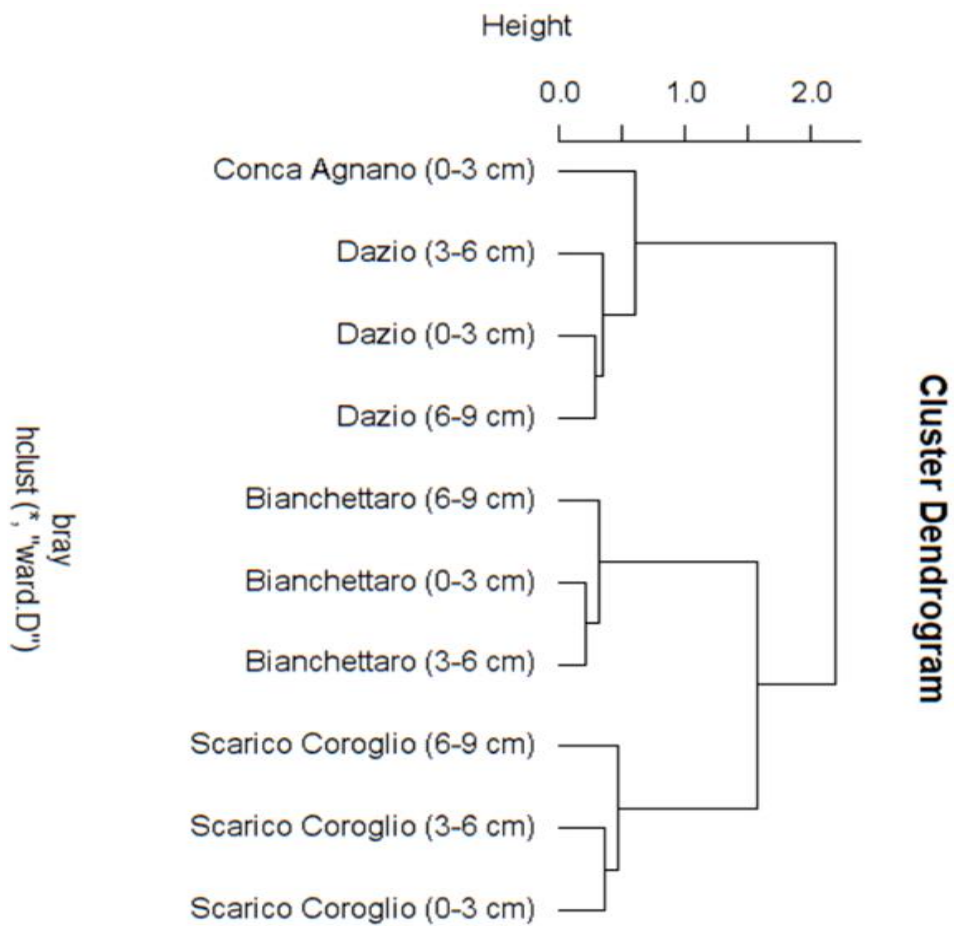


Figure. 1.10. Cluster Dendrogram (d) built using Bray-Curtis distances matrix, using R package Vegan. The dendrogram clustered the different layers belonging to the four analysed station relying on their similarity,

4) Conclusion

This study shows that contamination by multiple chemical stressors does not produce appreciable variations on alpha diversity and taxonomic composition at the four analysed stations. Such observations do not exclude that chemical pollution has selected a pool of resistant taxa over a century of contamination given by the activity of ILVA steel plant but, rather, they suggest that the different distribution of toxic compounds do not affect the microbial composition along the studied area. Conversely, the concentration of POM released by sewage discharge and the sediment grain size are likely to have played a major role in shaping the microbial assemblages since only these two variables are correlated with the clusterization of the four stations. Further studies are required to better understand the combined role of pollutants and environmental conditions in shaping microbial community composition.

Chapter 3

Biotechnological potential of bacteria isolated from two highly anthropic-impacted coastal areas from the Gulf of Naples

Abstract

In this chapter, I isolated bacteria from sediments of two highly polluted sites, the Bagnoli-Coroglio area and the mouth of the Sarno River, both located in the Gulf of Naples. Bacterial isolates, once identified on the basis of Sanger sequencing of 16S rRNA genes were tested for their ability to cope with heavy metal pollution (As, Cd, Cu, Pb, and Zn) and/or Polycyclic Aromatic Hydrocarbon (PAHs, Naphtalen, Phenantrene and Pyrene) pollution. Capacity to grow under different concentrations (100, 1000, and 10000 ppm) of these elements, separated or mixed together, was recorded over time together with the estimation of the removal rate of heavy metals and the PAH degradation rate ability.

This study aimed to investigate, select and propose efficient bacterial taxa – monospecific or consortium - for bioremediation purposes. Four mixed cultures composed by *Halomonas* sp., *Alcanivorax* sp., *Epibacterium* sp., *Pseudoalteromonas* sp., and *Virgibacillus* sp. were selected (one from the Sarno River and three from Bagnoli-Coroglio) because these were the ones that grew best in laboratory conditions. Both mixed cultures and single taxon exhibited a PAHs degradation rate ranging from 60 to 100%. They were also able to precipitate heavy metals from culture media, especially

Pb, with the highest removal rate reaching ~ 100%. Of the two, single taxon was less effective than mixed cultures. Results of Sequential Selective Extraction (SSE) analysis highlighted the ability of mixed strains in reducing the bioavailability and - thus the associated toxicity - of As, Cd and Zn by changing their partitioning in the geochemical fraction. These data indicate the strong potential interest of these mixed strains in effective bioremediation of polluted sediments. An interesting result from this study was the identification of the same species, *Holomonas* sp. and *Alcanivorax* sp., at both sites.

1) Introduction

The release and accumulation of inorganic (e.g., heavy metals) and/or organic (e.g., petroleum derivatives) compounds in coastal environments are an important threat affecting the ecological and economic quality of these areas, in term of biodiversity, human health and quality of the provisioned goods (Islam and Tanaka 2004). Contaminants of major concern include organic pollutants and heavy metals (Tashla et al. 2018) whose persistence in the environment is enhanced by accumulation affecting different levels of biological organization, from cells, tissues, organisms to communities. Bioaccumulation and biomagnification of these compounds occur along the entire food web representing a threat for human health (Fuentes-Gandara et al. 2018; Loflen et al. 2018; Buah-Kwofie, Humphries, and Pillay 2018).

Polycyclic aromatic hydrocarbons (PAHs) and heavy metals like arsenic (Yedjou and Tchounwou 2007a), cadmium (Tchounwou, Ishaque, and Schneider 2001), chromium (Patlolla et al. 2009), lead (Yedjou and Tchounwou 2007b) and mercury (Sutton et al. 2002) have been reported to affect biological systems such as cell membrane or organelles to enzymes involved in metabolism, detoxification and DNA damage repair (S. Wang and Shi 2001), thus causing cell cycle modulation, carcinogenesis or apoptosis (Beyersmann and Hartwig 2008; Kim, Kim, and Seo 2015).

The persistence, bioavailability and toxicity of heavy metals is modulated by microorganisms' activities that, through a great variety of resistance like chromosomal, transposon and, mostly, plasmid-mediated systems, modify their mineral forms and geochemical phases (Alomary and Belhadj 2007; Dziewit et al. 2015).

The present chapter aims to investigate the potential bioremediation activity of heavy metal and PAH resistant bacterial strains isolated from the marine sediments of two highly impacted coastal areas: The Bagnoli-Coroglio site (Gulf of Naples, Tyrrhenian Sea) described in the previous chapter and the Sarno river mouth (Gulf of Naples, Tyrrhenian Sea). The idea is to understand if differently polluted sites have selected similar taxa showing similar bioremediation abilities and if such taxa can be used for the decontamination of both the polluted sites. The Sarno River is one of the most polluted rivers in the world (Cicchella et al. 2014; Montuori et al. 2013; Pepi et al. 2016). In this area, multiple sources of pollution make it difficult to trace back the origin of the contamination (Lofrano et al. 2015). The high population density (Cicchella et al. 2014), the massive use of fertilizers/pesticides in agriculture and the industrial development of the area (Baldantoni et al. 2018) are among the main causes of pollution. The main pollutants affecting quality of water and sediments are heavy metals that originate mainly from the industrial activities along the river path (Montuori et al. 2013). Surface marine sediments at the mouth of the Sarno River present high levels of contamination by lead (Pb), arsenic (As), chromium (Cr), copper (Cu) and zinc (Zn) and moderate contamination by cadmium (Cd) and mercury (Hg) (Pepi et al. 2016). The objectives of this chapter was to isolate, select and characterize the most adapted bacterial strains growing in the Sarno site and to compare the bacterial communities with those isolated from the Bagnoli-Coroglio site. The final aim was to select the best strains from both sites able to survive in the presence of high concentrations of heavy metals and/or PAHs, and to evaluate their potential degradation of Polycyclic Aromatic Hydrocarbons (PAHs).

2) Material and Methods

2.1) Sediment sampling

The sampling was performed in April 2014 at one station at the mouth of the Sarno River (40.728156 N, 14.463472 E, Fig. 2.1), collecting the top (0–20 cm) sediment with a grab sampler. Duplicate samples were immediately placed into sterile sacks (Whirl-Pak, Nasco) and stored at 4 °C in the dark, until their processing in laboratory. Samples were collected by Dr. Milva Pepi of the Stazione Zoologica Anton Dohrn who kindly gave me the samples when I first started my PhD.

The Bagnoli-Coroglio Sediment sampling (Fig. 2.2) was carried out in November 2017 in the framework of the ABBACo research project, led to the harvesting of 127 sediment samples. Of the total sampled stations, 95 were sampled with a box corer which provided deeper cores of about 1 to 4 meters' length. The sediment samples that led to the isolation of the bacteria used in this study were taken with a grab sampler from the 3 sampled stations located as follow: 40.81555 N, 14.16075 E; 40.80834 N, 14.15966 E; and 40.79644 N, 14.17293 E.



Figure 2.1. Map of the study area with the position of the sampling site of Sarno River Mouth

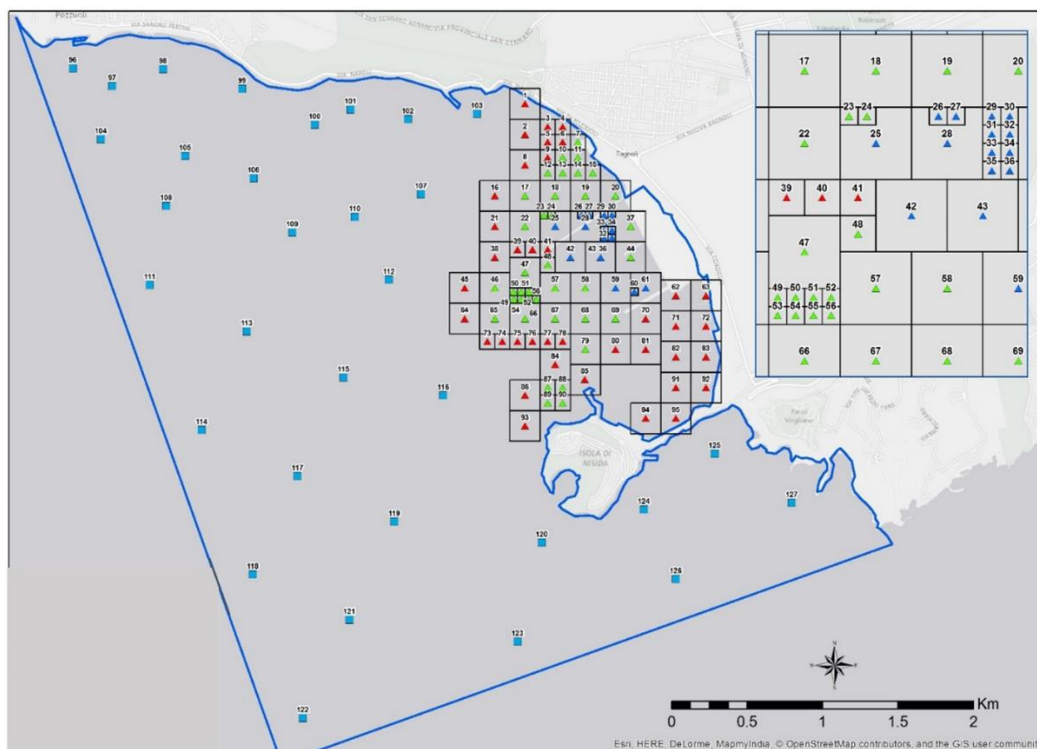


Figure 2.2. The Bagnoli-Coroglio Sediment sampling strategy (ABBaco research project). The blue dots outside the inner grid represents superficial sampling points. The triangles inside the grid represents sampling points where coring activity has been carried on

2.2) Bacteria isolation from sediments from both sites

The sediment was plate into Petri dishes containing Marine Agar (MA) (Bacto-Agar, Difco) in the presence of three different heavy metal concentrations: Pb^{2+} ($500 \mu\text{g}.\text{ml}^{-1}$), As^{3+} ($500 \mu\text{g}.\text{ml}^{-1}$), Cd^{2+} ($10 \mu\text{g}.\text{ml}^{-1}$), and incubated at 28°C for 48 hours. I selected such metals for the initial screening since As and Cd (Anetor, Wanibuchi, and Fukushima 2007; Jaishankar et al. 2014) are among the most toxic compounds while Pb is the most abundant element in the studied area.

At the end of the incubation time, growth of mixed strains in the plate was noted, and genomic sequencing (described in the Chapter 4 of the thesis) by Illumina Miseq identified all the strains present within the mixed cultures. To isolate the culturable strains, the mixed cultures were re-plated on Marine Agar for 15 days. At the end of the incubation period, 5 different types of colonies were noted, which were taken with a sterile loop and plated again on Marine Agar for another 15 days. In order to have mono specific strain colonies with specific colours, margins and shape, it was necessary to repeat the isolation operations 2 more times for a total of 30 days of incubation. Once isolated, the colonies were suspended in 30% sterile glycerol and stored at -80°C .

2.3) Bacteria characterization and identification

Strain DNA extraction was performed according colony PCR protocols as described by Bergkessel and Guthrie, (2013). Amplification of 16S rRNA gene was performed adding $1 \mu\text{L}$ ($10 \text{ ng}.\mu\text{L}^{-1}$) of genomic DNA to $24 \mu\text{l}$ of PCR mix composed by $2.5 \mu\text{L}$ of 10X

'Amplitaq' buffer (10 mmol.L⁻¹ Tris-HCl; 50 mmol.L⁻¹ KCl; 1.5 mmol.L⁻¹ MgCl₂; 0.001% gelatin), 2.5 µL of dNTPs (2 Mm), 1 µL each of E9F (5'- GAGTTTGATCCTGGCTCAG-3') and U10510 R (5'- GGTTACCTTGTTACGACTT-3') (0.5 µm), 16.875 µL of steril double distilled water and 0.125 µL of 'Taq Gold' (Applied Biosystem). The reaction mixtures were incubated at 95°C for 5 minutes and then cycled 30 times through the following temperature profile: 95°C for 30 s, 55°C for 30 s and 72°C for 90 s. Lastly, the mixtures were incubated at 72°C for 5 min; 2 µl of each amplification mixture was analyzed by agarose gel (1.2% w/v) electrophoresis in TAE buffer (0.04 M Tris-acetate, 0.001 M EDTA) containing 0.5 µg ml⁻¹ (w/v) ethidium bromide.

2.4) Analysis of sequenced data

The consensus sequences of the isolates were compared with those deposited in GenBank using the BLAST program. The 16S partial sequences strains were compared to the prokaryotic small subunit rDNA on the Ribosomal Database Project II website and the NCBI website using the BLAST program. The 16S rRNA gene sequences retrieved from the databases were aligned using CLUSTALW included in the MEGA software, version 7. The phylogenetic tree was inferred by NCBI website.

2.5) Bacteria growth *versus* metal and PAH concentrations

In order to assess the capability of the mixtures and/or isolated strains to cope with the pollutants, I evaluated their growth in the presence of five single heavy metals (As³⁺, Pb²⁺, Cd²⁺, Cu²⁺, Zn²⁺) and PAHs mix (Naphthalen, Pyren and Phenanthrene; ratio of 1:1;

previously solubilized in pure Exan). For each type of pollutant, three concentrations (100, 1000, 10000 ppm) were tested.

Growth curves were analyzed in triplicate in a 96 Multiwell plate using a UV spectrophotometer (TECAN, Infinite 1000) setup at 600 nm. Strains were diluted to a concentration of 1×10^6 cells/ml in a total volume solution of 200 μ l. The total volume of 200 μ l was distributed as follows: 100 μ l of metals / PAHs solution and the remaining 100 μ l divided between strain solution and Marine Broth (Pronadisa –Conda) MB medium to reach the desired volume. Optical Density (OD) measured in the presence of bacteria and metals/PAHs mix were normalized by subtracting the blank signal, *i.e.* the OD of the solution (200 μ l) containing metals, PAHs mix and MB. Also, a negative control, containing only MB and a positive control containing only MB and strains was set up. Multiwell plates were incubated in Tecan Microplate Readers Infinite 1000 at a constant temperature of 28 °C for 48 hours.

2.6) Evaluation of Polycyclic Aromatic Hydrocarbon (PAH) degradation and removal rate of heavy metals in liquid solution

In addition to assessing the ability of bacteria strains – in mixture or alone - to grow in culture conditions enriched with single metal contaminants, I evaluated the ability of the strains:

- to promote the precipitation of several metals simultaneously dissolved in the culture media (MB),
- and to degrade a hydrocarbon mix composed of Naphthalene, Phenanthrene and Pyren suspended in MB.

The concentrations of the toxic compounds added to the growth medium were selected from the data reported by Romano et al. (2009) from a sampling campaign carried out in the area of Bagnoli Coroglio.

The experiments were carried out in Marine Broth since the selected strains were not able to grow in seawater even when enriched with organic compounds and contaminants.

For this purpose, in flask T175 (TPP tissue culture flasks), an experimental system was set up in triplicate both for the consortium and for the single isolates. The different conditions were: three flasks with marine broth, bacteria (8×10^7 cells ml^{-1}) and As^{3+} (14 ppm), Pb^{2+} (331 ppm), Cd^{2+} (1 ppm), Cu^{2+} (74 ppm), Zn^{2+} (899 ppm), three flasks with the same metals as previously described and marine broth, three flasks with bacteria and Naphtalen, Pyren and Phenanthrene (ratio of 1: 1: 1 with a total concentration of 242 ppm) and three flasks with hydrocarbons and marine broth.

The flasks were incubated for 27 days at 28°C. Biomass growth and pH were monitored at day 0, 3, 9 and 27. The amount of precipitated metals and degraded hydrocarbons were analysed by the company Ambiente Spa (Massa-Carrara, Italy) using method EPA35108270 using GC-MS technique for the determination of the breakdown products of aromatic compounds and method EPA6010 for the determination of heavy metals using ICP-OES technique.

2.7) Evaluation of Polycyclic Aromatic Hydrocarbon (PAH) degradation and removal rate of heavy metals during coupled water-sediment experiments

20 ml of Marine Broth containing bacteria at a concentration of about 8×10^7 cells ml⁻¹ were incubated in TPP tissue culture flasks (50ml volume), together with 20 grams of sediment sampled in the area of Bagnoli Coroglio (14,16381 E; 40,80791 N). All experiments were carried out in triplicate.

Each experimental set was composed by six flasks. Three were filled with sediment, MB and bacteria, while the other three were used as control for metal and hydrocarbon analyses; controls were filled with sediment and marine broth. Flasks were incubated for 27 days at 28 °C and 10 ml samples were taken at day 0 and day 27. Analyses for the determination of heavy metal bioleaching and hydrocarbon degradation were carried out by the company Ambiente spa (Massa-Carrara, Italy) using, respectively, method EPA 30516020 based on ICP-MS and method EPA 35458270 based on GC-MS. In order to determine the solubilization of heavy metals from the sediment each sample was treated under sequential selective extraction following the protocol described by Tessier et al. (1979).

3) Results and Discussion

3.1) Bioremediation of Bacteria Isolated from the Sarno River Site

3.1.1) Identification of bacterial isolates and bacterial growth in the presence of contaminants

After several isolation procedures it was possible to isolate two different colonies from the initial mixed culture (Fig. 2. 3, a, b, c). Following extraction of the gDNA, amplification of the 16s rRNA gene (Fig. 2. 3, d) and subsequent Sanger sequencing it was possible to assign the two colonies to the genus *Halomonas* and *Alcanivorax*. The concomitant presence of *Halomonas* sp. and *Alcanivorax* sp. within a microbial community from sediments contaminated with hydrocarbons had already been described by Zhao et al. (2009), due to their hydrocarboclastic activity (Fathepure 2014). However, the phylogenetic tree (Fig. 2.4) created with 20 best matches after blasting both sequences against the NCBI database showed a significant difference compared to the other sequences suggesting a reduced conservation of this sequence. The percentage of similarity shown here is, for both strains below 95%, the threshold used as a cut off to distinguish microorganisms belonging to different genera (Stackebrandt and Goebel 1994). However, recent studies have shown that the use of this threshold is not anymore appropriate to distinguish different genera since as shown by Donovan et al. (2018) bacterial taxonomy have to be carried out using concatenated protein phylogeny. In any case data, relying on genomic analysis shown in chapter 4, allowed me to clearly identify the two isolated strains as belonging to genus *Halomonas* and *Alcanivorax*, from hereafter named *Halomonas* sp. SZN1 and *Alcanivorax* sp. SZN2

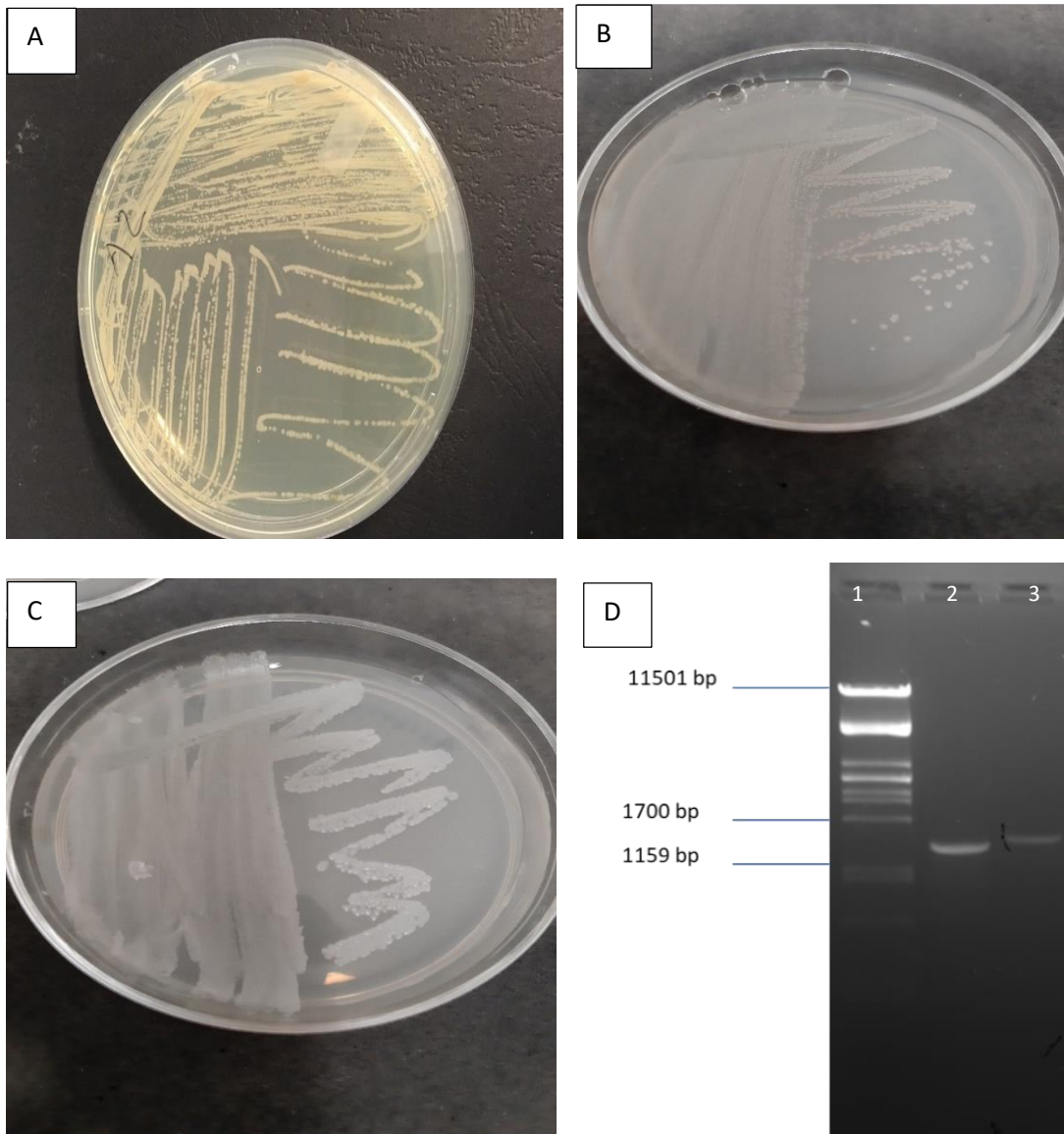


Figure 2.3. Agar plates with Mix culture (A), the two isolates *Halomonas* sp. (B), *Alcanivorax* sp. (C) and the agarose gel after 16s RNA amplicon (D) (Lanes 1, 2, 3, respectively contain DNA ladder, *Halomonas* SZN1 16s rRNA, *Alcanivorax* SZN2 16s rRNA)

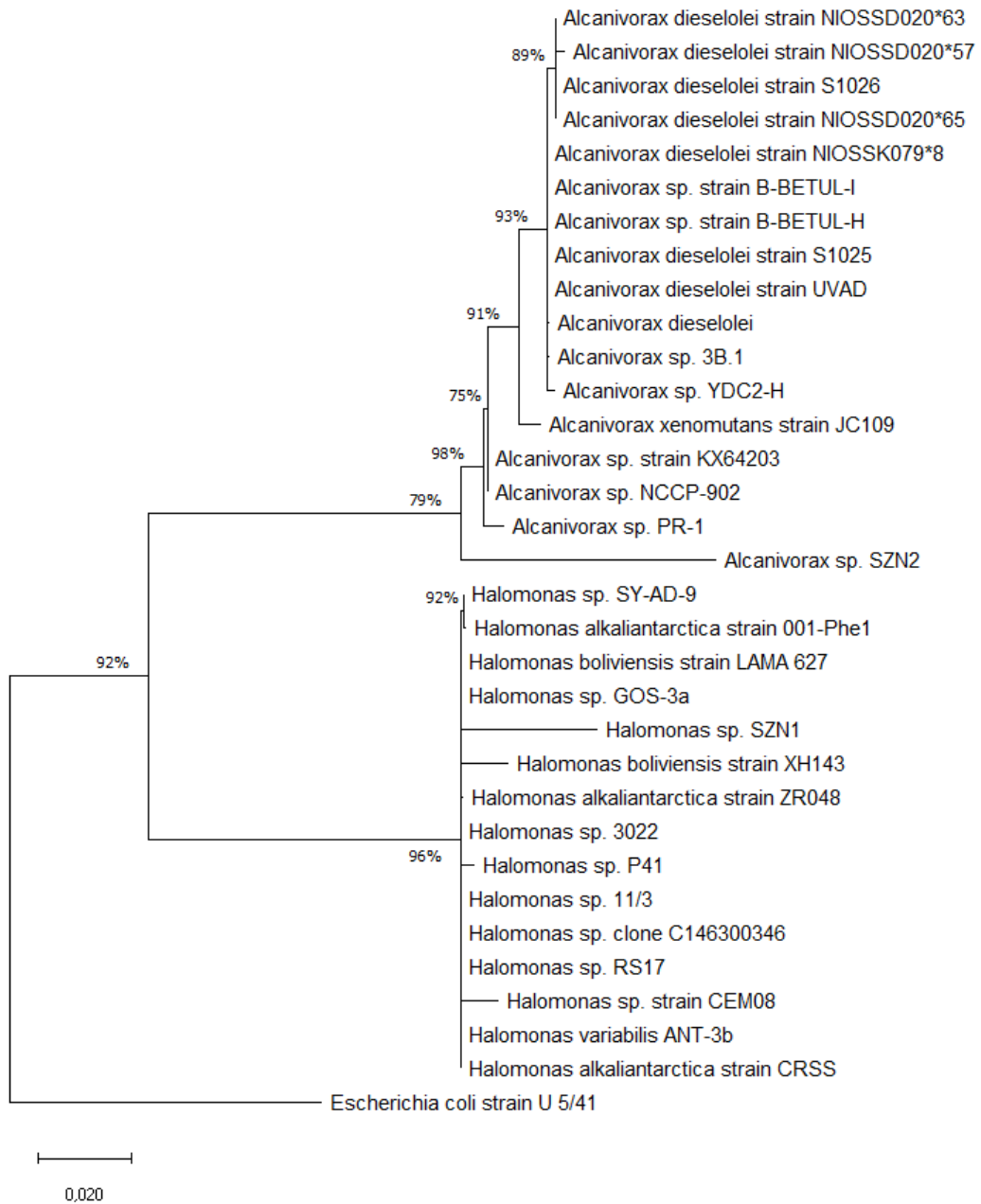


Figure 2.4. 16s RNA tree of *Halomonas* sp. SZN1 and *Alcanivorax* sp. SZN2 built using the best twenty 16s RNA sequences retrieved from NCBI database. Tree has been created with the Maximum Likelihood Method using MEGA 7 software after alignment conducted with Muscle algorithm.

Preliminary analyses of the mixed culture, from hereafter referred as Consortium A2, and the two relative isolates showed their ability to tolerate the presence of a mix of hydrocarbons and the majority of the metals tested.

Consortium A2, composed of *Halomonas* sp. SZN1 and *Alcanivorax* sp. SZN2 isolated from the sediment at the mouth of the Sarno River was able to grow in the presence of PAHs, As, Pb, Cd, Cu and Zn, with, however a reduced growth in the presence of Cd, Cu and Zn (Figures 2.5, 2.6, 2.7, 2.8, 2.9, 2.10).

More specifically, Consortium A2 showed a greater tolerance toward Pb (Fig. 2.5 A) since, after 24 h, it reached, in the presence of 100 and 1000 ppm, the same values as the control. In the presence of 10,000 ppm the curve reached optical density values lower than those observed for the other two concentrations. Nonetheless, the data denote the ability of these microorganisms to grow in a severely contaminated environment.

The growth of *Halomonas* sp. SZN1 and *Alcanivorax* sp. SZN2 in the presence of Pb (Fig. 2.5 B and C), showed differences compared to the treatment with the mixed culture since a growth similar to the control was observed only in the treatment with 100 ppm while the other two concentrations tested displayed a marked toxicity.

Consortium A2 also demonstrated an excellent adaptation to the presence of PAHs (Fig. 2.6 A) since at 100 and 1000 ppm the curves reached growth values equal to those of the control although concentrations of 10000 ppm lead to a growth inhibition.

Tests performed on *Halomonas* sp. SZN1 as well as *Alcanivorax* sp. SZN2 (Fig. 2.6 B and C) in the presence of PAHs showed, in some cases, a trend similar to those observed for

mixed cultures. In particular, *Halomonas* sp. SZN1 showed a growth curve similar to Consortium A2 as both curves, at 100 and 1000 ppm, reaching values of optical density one unit higher if compared with the control (3.5 OD vs 2.5 OD). Analyzing *Alcanivorax* sp. SZN2 only the curve at 100 ppm reached values similar to the control only at 38 h, highlighting a possible metabolic switch able to allow a better growth. For both isolated strains, as well as the consortium, a concentration of 10,000 ppm of PAHs was highly toxic inducing a growth inhibition.

In the presence of As, Consortium A2 (Fig. 2.7 A) reached values close to the control only in presence of 100 ppm concentration, while, surprisingly, concentrations of 10,000 ppm inhibited the growth of the culture less than 1000 ppm. This phenomenon is in contrast with the hormesis phenomenon described in the literature by Shi et al. (2016) as, generally, a low dose concentration leads to growth stimulation while a higher dose leads to a growth inhibition. A possible explanation for this phenomenon has been hypothesized by Torres-Barceló et al. (2016) who, studying the dose-effect response of antibiotics on *Pseudomonas aeruginosa*, noticed that this microorganism was capable to accelerate its growth by activating an SOS metabolic pathway, a response to DNA damage, when subjected to high stress.

The same phenomenon was also noted when studying the effects of pesticides on higher organisms such as arthropods, whose viability rate increased when treated with sublethal dose of pyrethroid permethrin (Guedes, Magalhães, and Cosme 2009). It is also interesting to understand why some compounds belonging to metals, antibiotics or pesticides lead to a dose-effect inverse response as well as conventional responses. In

the presence of As, both *Halomonas* sp. SZN1 and *Alcanivorax* sp. SZN2 (Fig 2.7 B and C) showed an overlapping trend with Consortium A2 as a marked growth was observed only in the presence of 100 ppm, although only *Halomonas* reached values of optical density of 3.5; a higher unit than the mix and *Alcanivorax* sp. SZN2.

Furthermore, Consortium A2 showed a kind of inverse hormesis, similar to the response with As, in the presence of Zn 10,000 ppm since the growth was higher than treatment with Zn 100 and 1000 (Fig. 2.8 A). Conversely, differences were noted by comparing the curves of Consortium A2 with *Halomonas* sp. SZN1 and *Alcanivorax* sp. SZN2 in the presence of Zn (Fig. 2.8 B and C). Indeed, *Halomonas* sp. SZN1 was inhibited in the presence of all three Zn concentrations while *Alcanivorax* sp. SZN2 when treated with 100 ppm, was able to achieve growth rates comparable to the control at the end of incubation period.

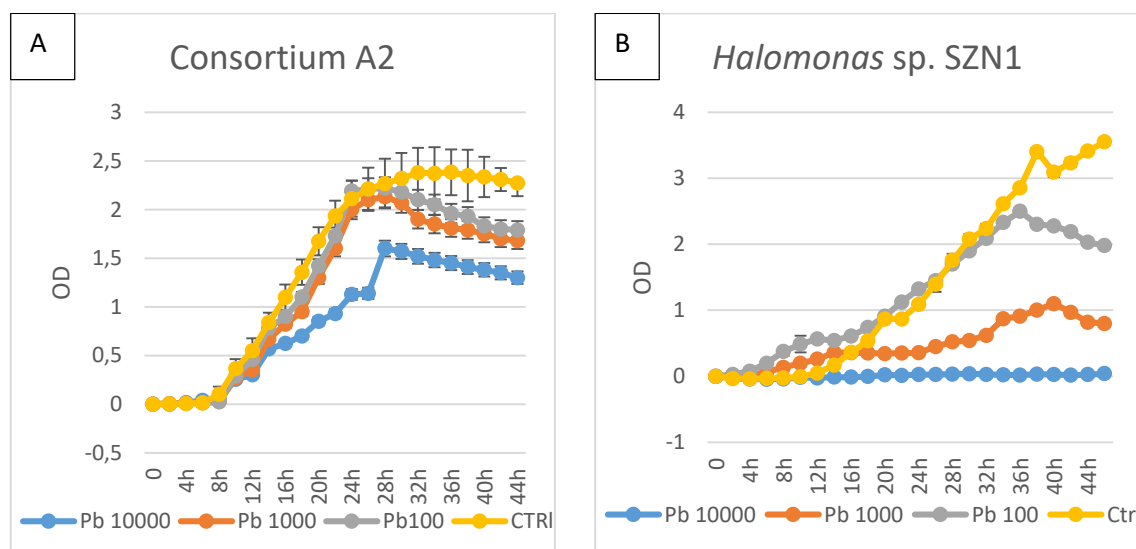
Consortium A2 response to Cd and Cu was almost similar, with strong toxicity at all three concentrations tested (Fig. 2.9 A and 2.10 A).

Differently from what was observed for Consortium A2, *Alcanivorax* sp. SZN2 was able to grow slowly in the presence of 100 ppm of Cd (Fig. 2.9 C). Surprisingly, under the stress of 100 Cu ppm, both *Halomonas* sp. SZN1 and *Alcanivorax* sp. SZN2 grew well, differently from what was observed in the treatment with Consortium A2 (Fig. 2.10 B and C).

MIC analysis of the two isolated strains indicated that *Alcanivorax* sp. SZN2 displayed the highest resilience as it was capable of growing with all the tested pollutants even if *Halomonas* sp., SZN1 according to Nanca et al. (2018), Dong et al. (2015), Dastgheib et al. (2012) is reported to have the highest tolerance towards PAHs. Moreover, despite

some strains of *Alcanivorax* sp. SZN2 have been isolated from polluted sediments with PAHs, heavy metals and PCBs (Gorovtsov, Sazykin, and Sazykina 2018), this is the first time that an isolated *Alcanivorax* strain exhibits a resistance pattern as shown here.

The results indicate that the two isolated strains act synergistically when present in the mixed culture thereby increasing their ability to resist the toxicity of a metal (e.g. Pb treatment). In other cases, this capacity is reduced as in the presence of Cu. As shown by Geesink et al. (2018) such different kinds of interactions depend on the secondary metabolites produced under different treatment conditions. In order to understand the dynamics driving the community response to toxic compound treatments, analyses detecting the production of growth promoting molecules such as nonribosomal peptide synthetases (NRPs), lipopeptides, polyketide synthases (PKSs) (Pawlowski et al. 2018; Shen et al. 2017) or inhibiting molecules (Antimicrobial agents), are required.



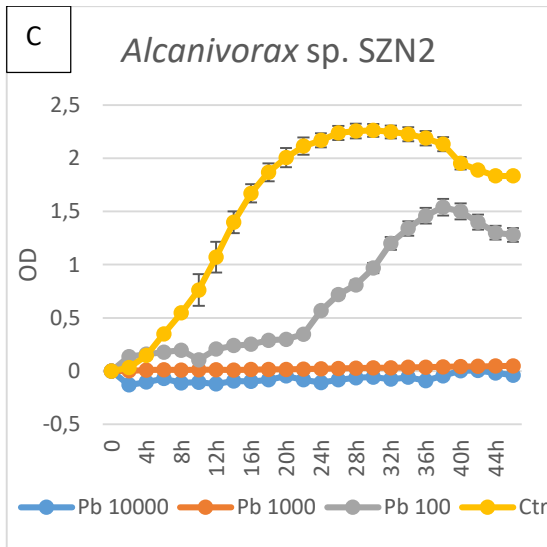
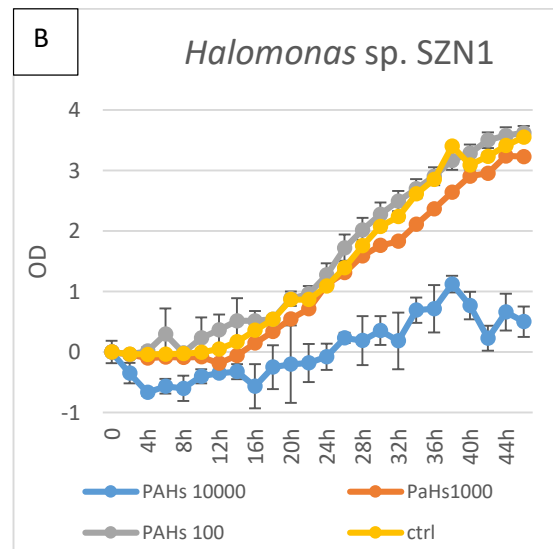
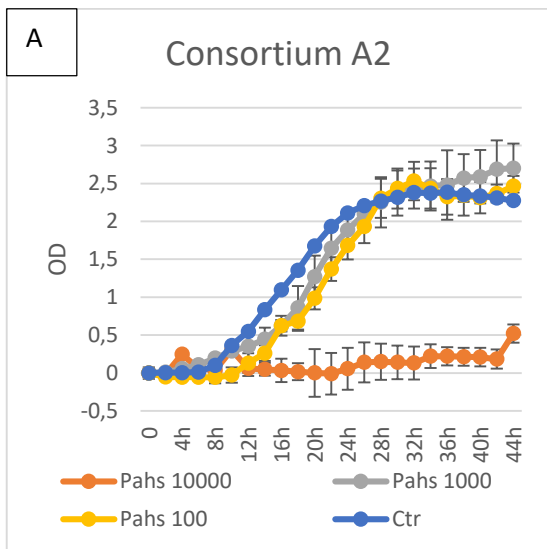


Figure 2.5. Minimum Inhibition Concentrations (MIC) testing Pb at concentrations of 100, 1000 and 10000 ppm on Consortium A2 (A), *Halomonas sp. SZN1* (B), and *Alcanivorax sp. SZN2* (C) expressed as Optical density (OD) values with time



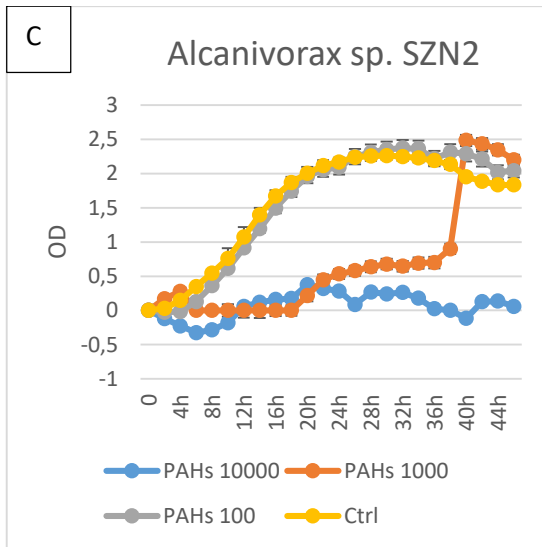


Figure 2.6. Minimum Inhibition Concentrations (MIC) testing PAHs at concentrations of 100, 1000 and 10000 ppm on Consortium A2 (A), *Halomonas* sp. SZN1 (B), and *Alcanivorax* sp. SZN2 (C) expressed as Optical density (OD) values with time



Figure 2.7. Minimum Inhibition Concentrations (MIC) testing As at concentrations of 100, 1000 and 10000 ppm on Consortium A2 (A), *Halomonas* sp. SZN1 (B), and *Alcanivorax* sp. SZN2 (C) expressed as Optical density (OD) values with time

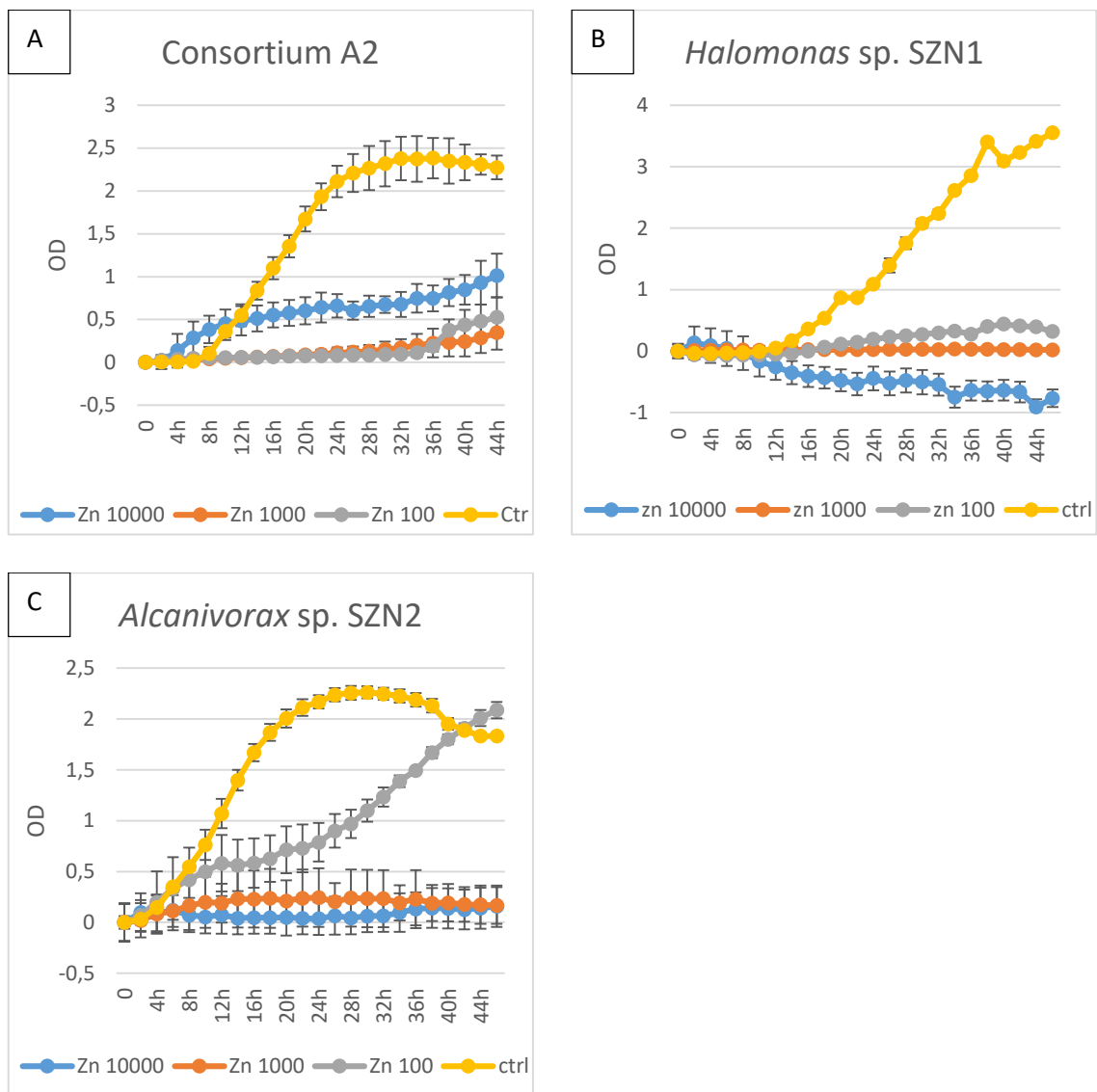


Figure 2.8. Minimum Inhibition Concentrations (MIC) testing Zn at concentrations of 100, 1000 and 10000 ppm on Consortium A2 (A), *Halomonas* sp. SZN1 (B), and *Alcanivorax* sp. SZN2 (C) expressed as Optical density (OD) values with time

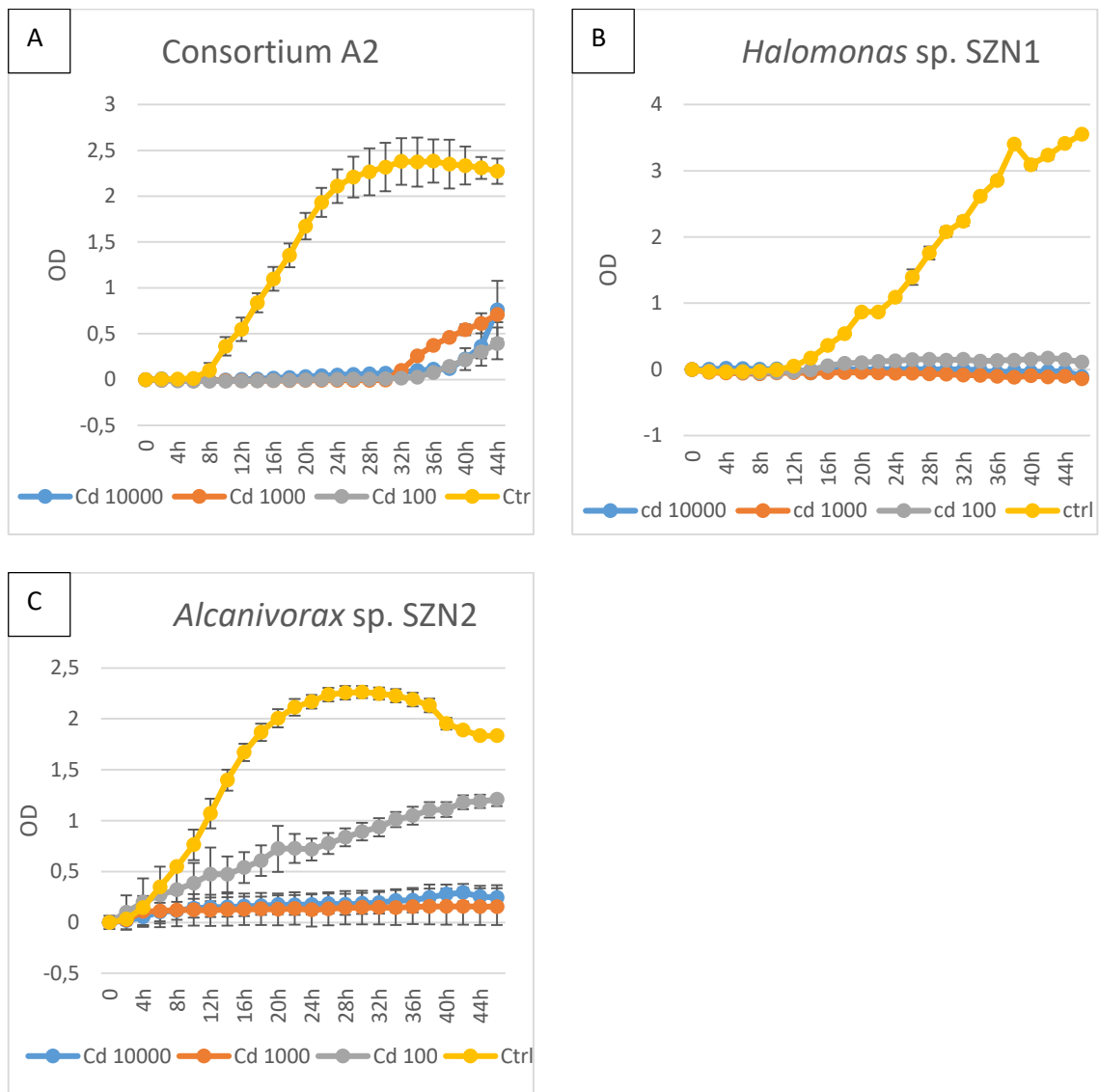


Figure 2.9. Minimum Inhibition Concentrations (MIC) testing Cd at concentrations of 100, 1000 and 10000 ppm on Consortium A2 (A), *Halomonas* sp. SZN1 (B), and *Alcanivorax* sp. SZN2 (C) expressed as Optical density (OD) values with time

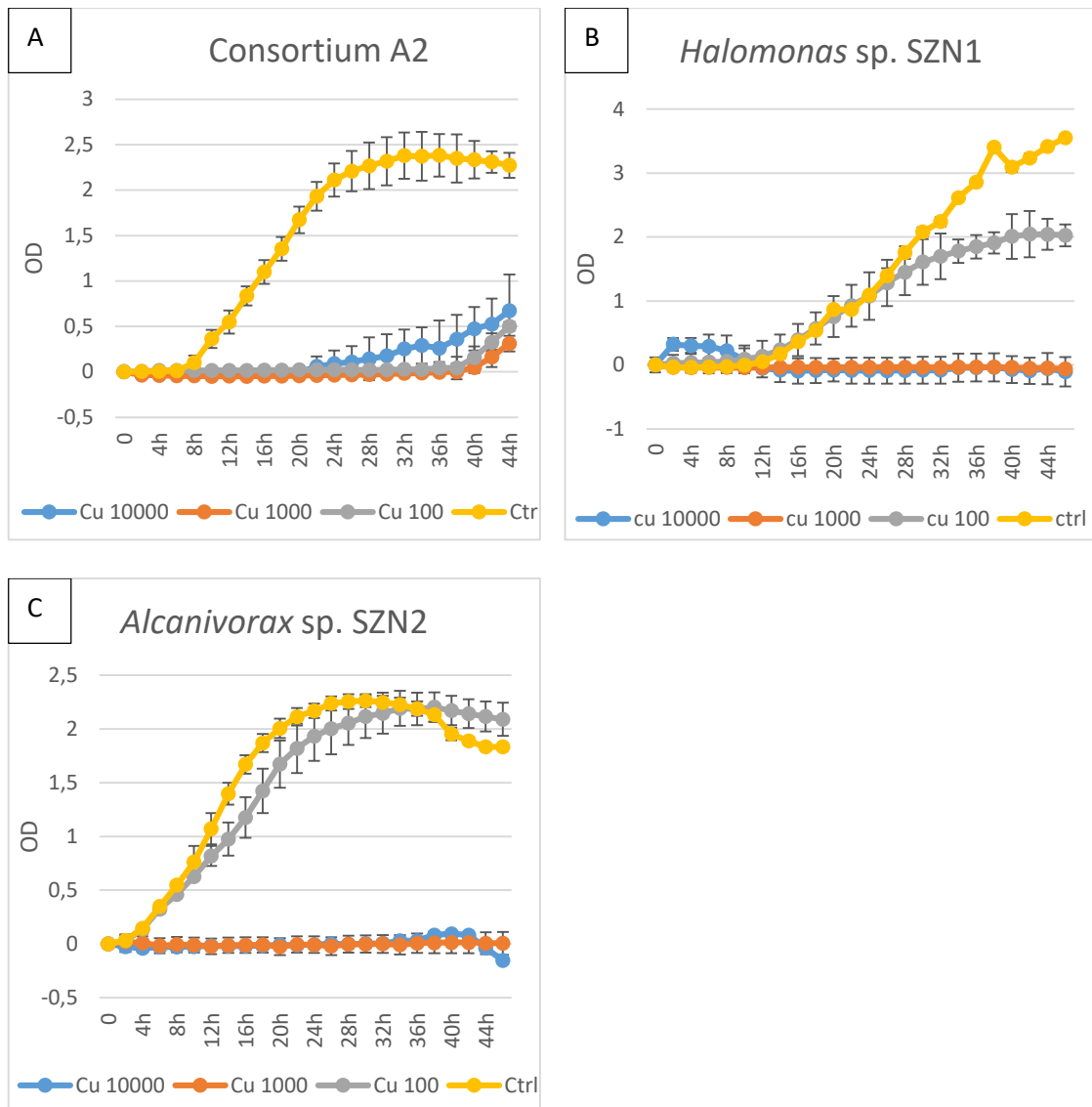


Figure 2.10. Minimum Inhibition Concentrations (MIC) testing Cu at concentrations of 100, 1000 and 10000 ppm on Consortium A2 (A), *Halomonas* sp. SZN1 (B), and *Alcanivorax* sp. SZN2 (C) expressed as Optical density (OD) values with time

3.1.2) Evaluation of PAH degradation and heavy metal precipitation of bacterial cultures (as single isolate and in mixtures)

Incubation experiments of bacterial cultures with the mix of hydrocarbons and heavy metals in Marine Broth showed the ability of microorganisms to effectively degrade hydrocarbons and precipitate heavy metals, especially Pb.

Atomic Absorption Spectroscopy to determine heavy metal content were performed on 3 cultures (Consortium A2, *Alcarivorax* sp. SZN2 and *Halomonas* sp. SZN1) on aliquots sampled at 0 and 27days since biomass growth and pH showed that at 27 days the overall culture conditions were the best to obtain an optimal bioremediation rate (in terms of resistance to heavy metals with respect to controls). Indeed, the three cultures reached maximum growth rates at the end of the incubation period when treated with heavy metals and hydrocarbons (Fig. 2.11 A, B, C). Furthermore, the number of cells at the end of the incubation with the hydrocarbon mix was found to be about 1.5 fold higher, suggesting a reduced toxicity of organic contaminants.

The pH variation data showed a different trend depending on the type of contamination used for the incubation. As shown in Figure 2.12 A, the pH of the cultures in the presence of metals showed an increase during the incubation period with the maximum values reached at the end of the incubation. This pH increase may be attributed to the growth of bacterial biomass as both *Halomonas* sp. SZN1, and *Alcanivorax* sp. SZN2, being moderately alkaliphilic microorganisms (B. Cheng et al. 2016; Kadri et al. 2018), tend to alkalize the medium. Ratzke and Gore (2018) have in fact shown that bacteria modify environmental pH with feedback systems in order to reach the optimal conditions for

growth. Additionally, a similar phenomenon was noted by Boechat et al. (2018) who, after adding metals to a culture containing moderate alkaliphilic bacteria, noticed an increase in pH, from 5 to 6.5 in time. Conversely the pH of the cultures incubated with the hydrocarbon mix (Figure 2.12 B), being apolar structures, showed a neutral initial pH followed by a reduction of about one unit. The pH decrease is due to the presence of weak acid intermediates such as benzoic acid derivatives and phenolic compounds following the activation of bacteria degradation pathway (Ghosal et al. 2016a).

In any case, the results of the 3 culture incubations with the hydrocarbons showed the ability of the microorganisms to effectively biodegrade all three compounds in the mix (Fig. 2.13 A). Both Pyrene and Naphthalene showed a rate of degradation close to 100% while Phenanthrene reached values around 60%. Although results confirmed the ability of *Halomonas* sp. SZN1, and *Alcanivorax* sp. SZN2 to degrade PAHs as described by Budiyanoto et al. (2018) and Kadri et al. (2018), no significant differences were noted in the degradation rates among the 3 different treatments suggesting that the concomitant presence of the two isolated strains does not lead to a synergistic effect in terms of degradation. Furthermore, the data shown here show a correlation between the PAHs degradation rate and the pH change as the acidification of the medium, present only in treatments with bacteria, corresponds to a high rate of degradation. Although Kim et al. (2005) and Liu et al. (2019) have described that a pH lowering corresponds to an increase in the degradation of aromatic compounds, this is the first time that a reduction of pH through the activity of *Halomonas* sp. SZN1, and *Alcanivorax* sp. SZN2 is observed.

The effect of the bacterial cultures on metal dynamics in Marine broth is described in Figure 2.13 B, which shows that Pb is the element that undergoes the greatest solubility reduction (i.e. by precipitation), reaching values above 80%. Furthermore, *Halomonas* sp. SZN1 and *Alcanivorax* sp. SZN2 showed a greater reduction of metal solubility when present as isolated rather than in mixed cultures as both significantly increased the precipitation of Cd (over 40% of the total fraction). Moreover, *Halomonas* sp. SZN1 was a valid candidate to reduce Zn solubility with a two-fold increase in precipitation rate compared to control and *Alcanivorax* sp. SZN1. The reduced solubility of As increased only with *Halomonas* sp. SZN1, although the increase was not statistically significant. Similarly, Cu was not influenced by the presence of microorganisms as its concentration in solution remained similar to the control. These observations suggest that the precipitation of As and Cu is to be attributed only to the saline component present in the culture medium. In general, the capacity of *Halomonas* sp. SZN1 of precipitating Pb and Cd confirms what has already been observed by Amoozegar, Ghazanfari, and Didari (2012) who, following incubation of *Halomonas elongata*, observed a precipitation rate of about 80% and 50% for Pb and Cd, respectively. Zinc removal through an *Halomonas* strain (*Halomonas halophila*), as well as Pb and Cd, has already been observed by Rothenstein et al. (2012), even though they used Zinc concentrations that were considerably lower than mine (32.5 ppm vs 899 ppm). In any case, this is the first time that a *Halomonas* strain is reported to co-precipitate Pb, Cd and Zn in the same treatment. Equally, although *Alcanivorax* sp. SZN2 has already been described as capable to survive in polluted environments (Ranawat and Rawat 2018), its capability to co-precipitate Pb and Cd has not been described so far. The mechanism by which

precipitation occurs is mainly due to the production of exopolysaccharides (EPS) widely produced by *Halomonas* sp. SZN1 (Gutierrez et al. 2013) and *Alcanivorax* sp. SZN2 (Suja, Summers, and Gutierrez 2017), able to complex the cations in solution (Morillo Pérez et al. 2008). Further studies are required to understand which molecular mechanism take place when the two cultures are mixed, since the treatment with both strains has highlighted a reduced metal precipitation capacity.

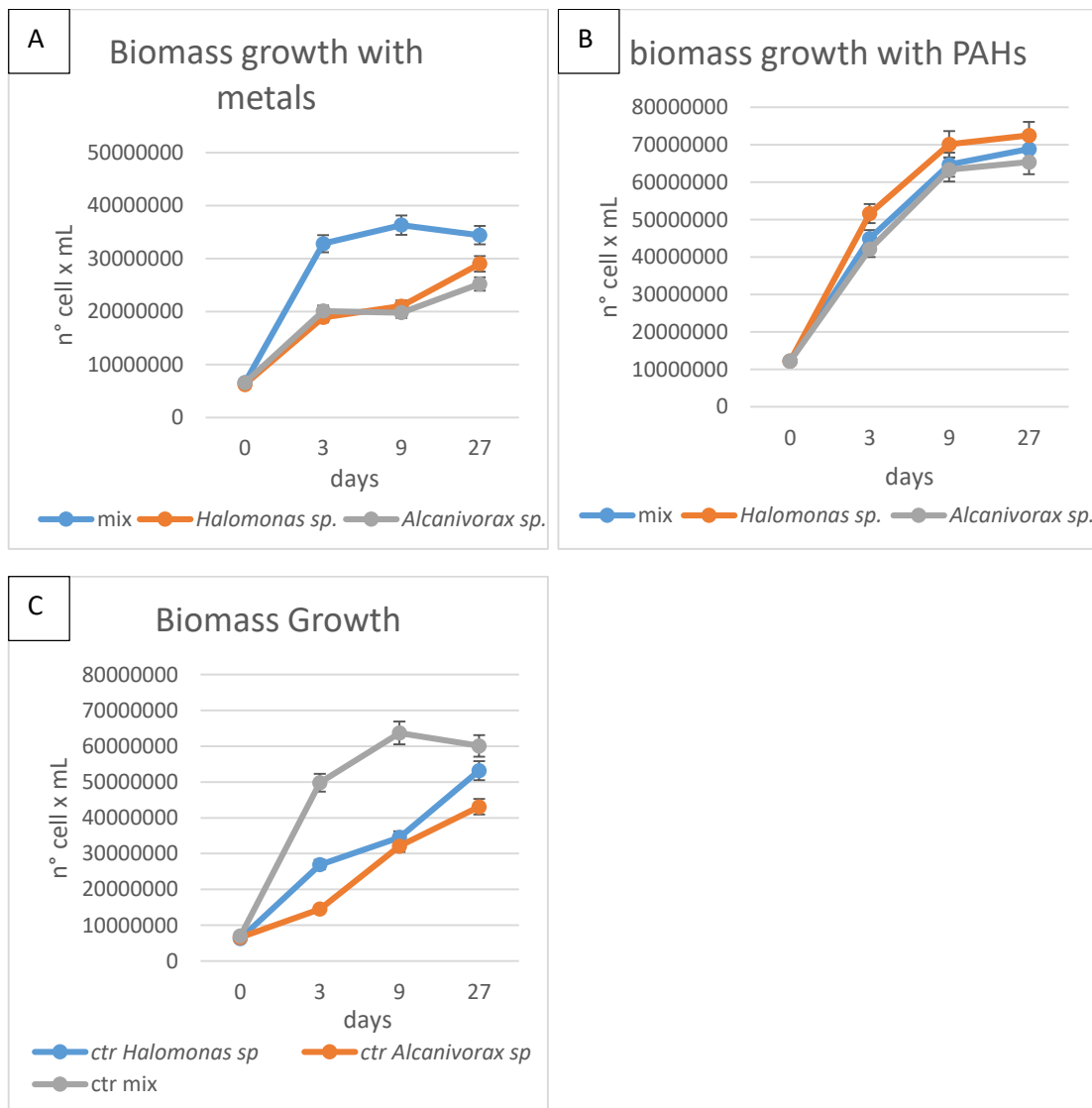


Figure 2.11: Biomass growth measurements at four different time, of the MIX culture (Consortium A2), *Halomonas* sp. SZN1 and *Alcanivorax* sp. SZN2 incubated with a mix of heavy metals (A), PAHs (B) and no amendments (C)

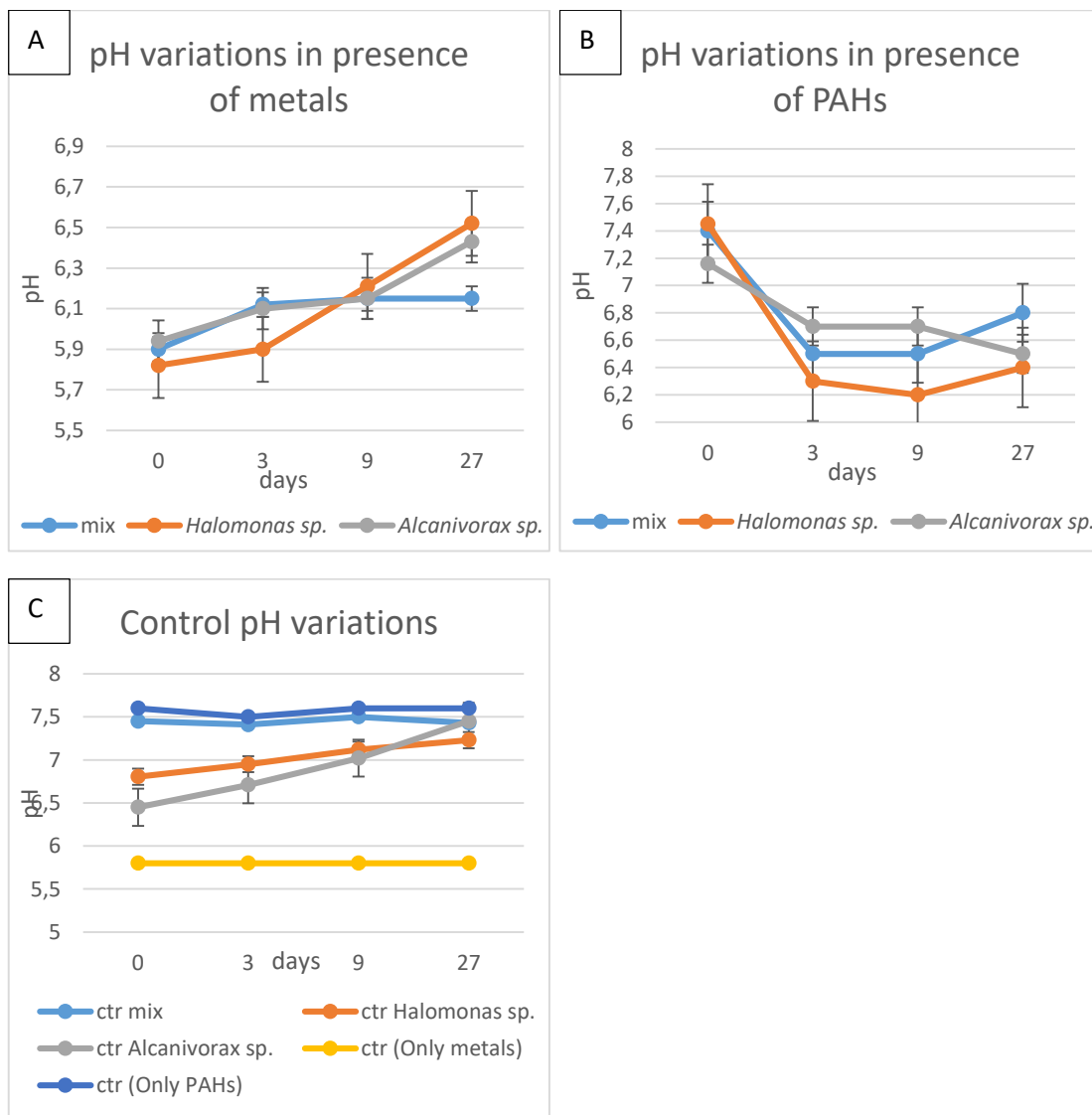


Figure 2.12: pH variations at four different hours, of the mix culture (Consortium A2), *Halomonas sp.* SZN1, and *Alcanivorax sp.* SZN2 incubated with a mix of Heavy metals(A), PAHs (B) and no amendments (C)

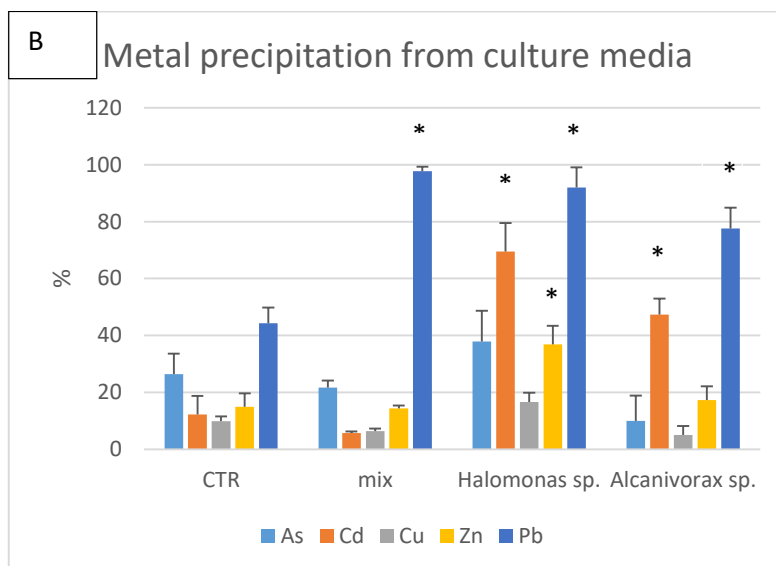
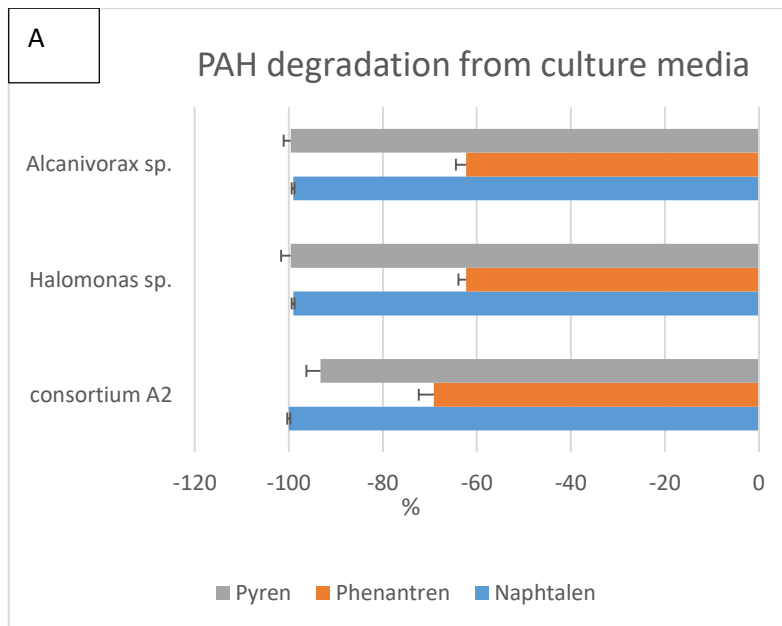


Figure 2.13: (A) Percentage of PAHs degradation after the incubation time (27 days) with *Halomonas* sp. SZN1 and *Alcanivorax* sp. SZN2 and its mixture. (B) Heavy metal precipitation after the incubation time (27 days) with *Halomonas* sp. SZN1 and *Alcanivorax* sp. SZN2 and its mixture

3.1.3) Effects of bacterial cultures addition (as isolates and as mixtures) on hydrocarbon degradation and heavy metal partitioning in contaminated sediments from Bagnoli-Coroglio

New experiments were performed by adding single bacterial taxon and mixed cultures to the contaminated sediment from Bagnoli-Coroglio to evaluate their effects on metal partitioning and on hydrocarbon degradation cultures directly.

The results of hydrocarbon degradation are shown in Figure 2.14. Hydrocarbon degradation ranged from 30% for benzo (k) fluorantrene by *Alcanivorax* sp. SZN2 to 90% for benzo (a) anthracene by Consortium A2. The addition of *Alcanivorax* sp. SZN2 was always less efficient in the degradation of hydrocarbons when compared to *Halomonas* sp. SZN1 and Consortium A2. Although Consortium A2 promoted degradation rates of Indeno (1,2,3, cd) pyrene (63.6%), benzo (a) anthracene (86.9%), and Benzo (a) pyrene (70%) significantly higher than those obtained using single taxon, *Halomonas* sp. SZN1 showed higher degradation rates for Pyrene (64%), benzo (k) fluoranthene (46%) and benzo b fluorantrene (68%) than Consortium A2 indicating that , depending on the molecule under examination, metabolic processes in the culture mix may have been inhibited or reduced by the presence of *Alcanivorax* sp. SZN2.

In general, PAH degrading activity of *Alcanivorax* sp. SZN2 and *Halomonas* sp. SZN1 in polluted sediments is described in association with other bacteria (Fodelianakis et al. 2015), and few studies describing the activity of single isolates on polluted sediments are reported in the literature (Kadri et al. 2018). The data reported here, therefore,

confirm that the strains *Alcanivorax* sp. SZN2 and *Halomonas* sp. SZN1 are effective in reducing the PAHs concentrations of contaminated sediment even when they do not act in consortia formed by multiple bacteria. Interestingly these data indicate that the consortium, even if composed by two highly specialized bacteria, do not always exhibit a better activity compared to the single isolates. These observations contrast with what is generally described in the literature (Bradáčová et al. 2019; Ding et al. 2017; Markiewicz et al. 2014), and therefore requires further studies to identify potential metabolites capable of reducing overall microbial PAHs degrading activity.

In this study, the addition of mixed cultures determined major changes in the repartition of metals among the different geochemical phases. In particular, such treatments significantly reduced the percentage of As, Cd and Pb (fig. 2.15 A, B, C) associated with the carbonate / exchangeable fraction, partitioning them in the Fe/Mn oxidizable and Organic matter fraction. Conversely, the treatments with *Halomonas* sp. SZN1 and *Alcanivorax* sp. SZN2 did not show significant differences compared to controls (i.e. without bacterial addition). The mixed cultures ability to reduce the fraction of metal associated with the exchangeable / carbonate is of significant interest in a bioremediation approach, as it is known (Sungur, Soylak, and Ozcan 2014) that the metals associated with the oxidizable and reducible fraction have a lower mobility, and thus a minor toxicity, than those associated with the exchangeable/carbonate fraction. The ability to reduce mobility of metals by changing their repartition in a less mobile sediment fraction has been described for sulfate reducing bacteria (Peng et al. 2018), which are able through their metabolism to form insoluble sulfur-metal complexes (Kramer, Bell, and Smith 2007). Conversely, *Halomonas* sp. SZN1 (Gupta and Diwan

2017) and, *Alcanivorax* sp. SZN2 are expected to stabilize heavy metals mainly by complexation with exopolysaccharides. However, Achal, Pan, and Zhang (2012), described the ability of *Halomonas* sp. SZN1 to immobilize metals through the formation of carbonate complexes and this may suggest that similar mechanism might take place during metals immobilization. More detailed analysis on geochemical changes and metabolites production are required in order to better understand the processes leading to metals immobilization.

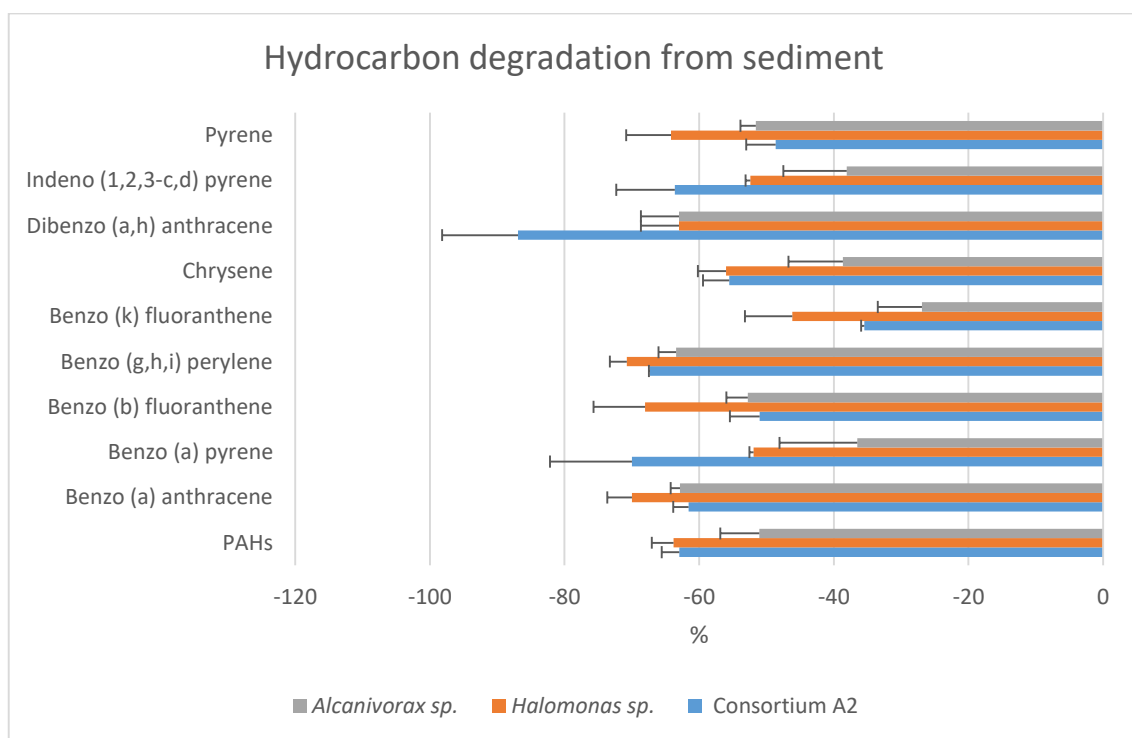


Figure 2.14. Percentage of PAHs removal rates in sediments after inoculation with *Halomonas* sp. SZN1 and *Alcanivorax* sp. SZN2 and a mixture of both strains (Consortium A2)

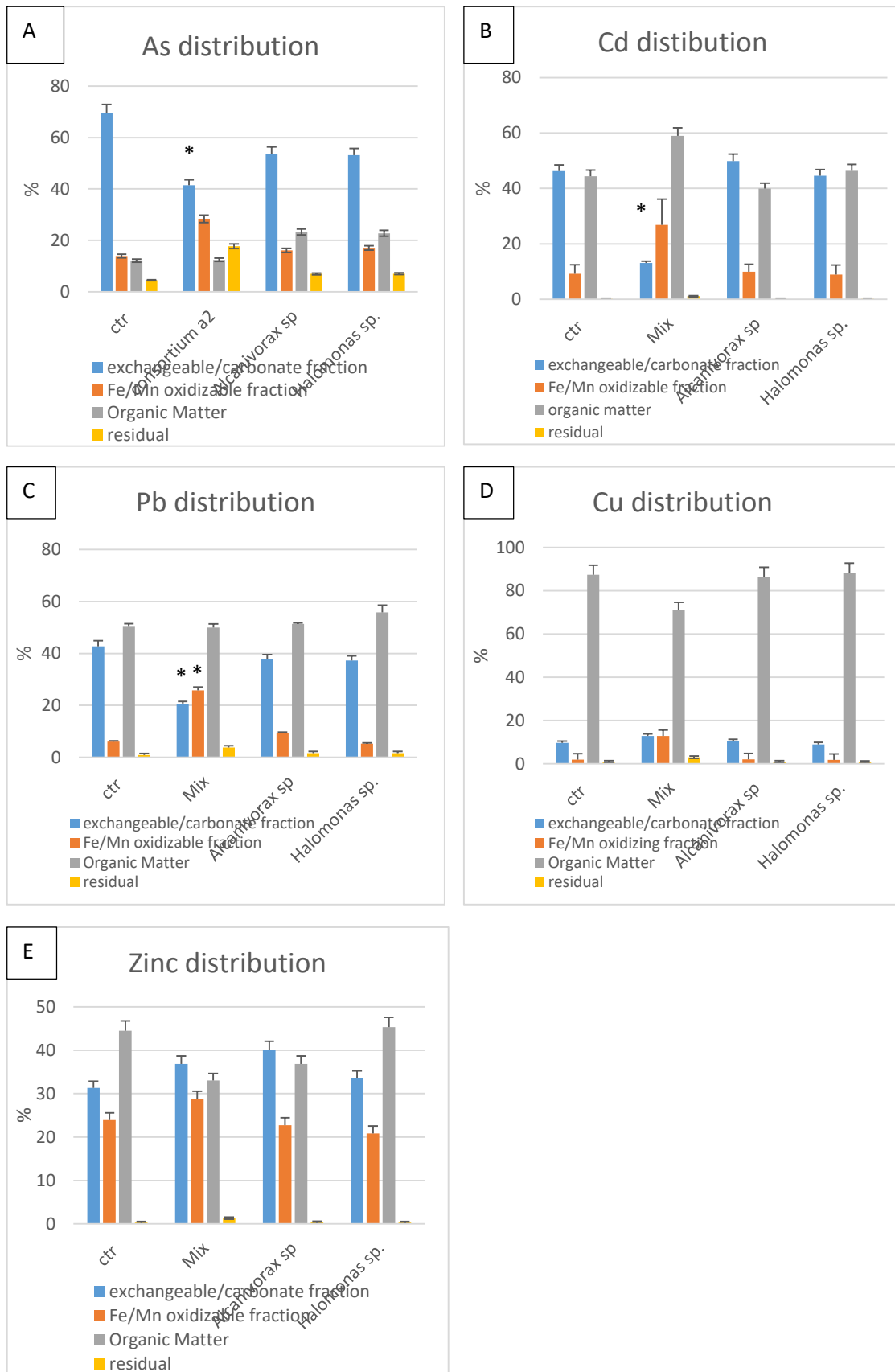


Figure 2.15. As (A), Cd (B), Pb (C), Cu (D) and Zn (E) distribution in the four sediment fractions following Selective Sequential Extraction

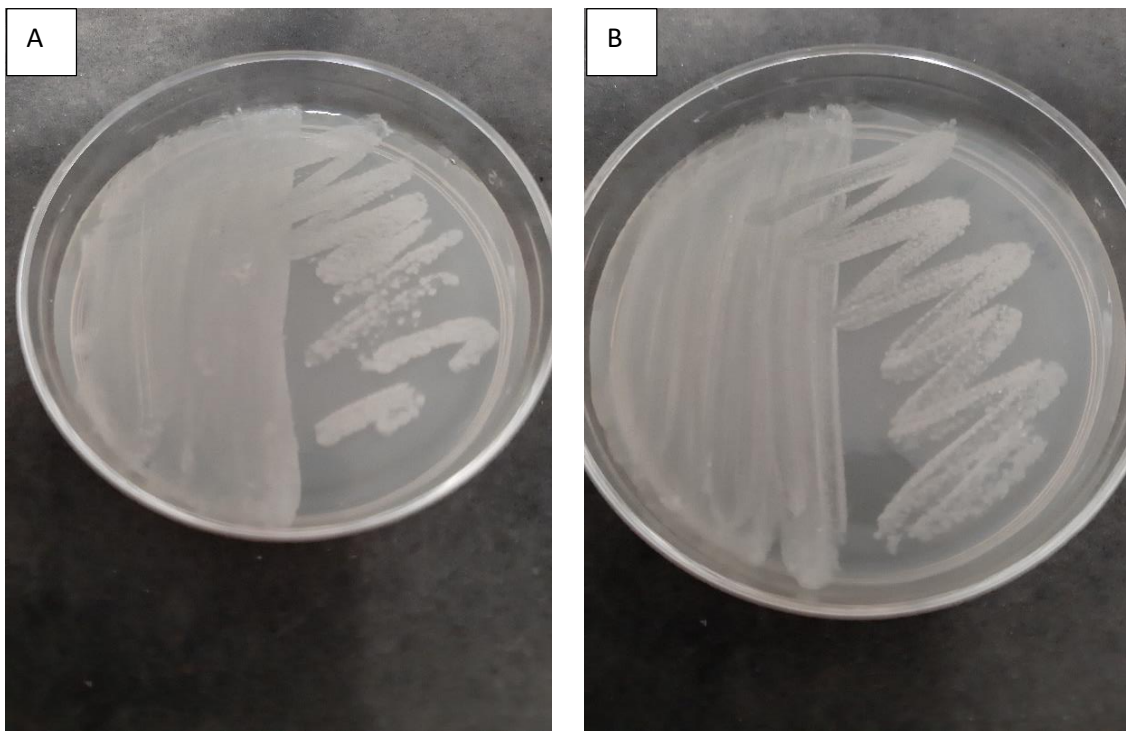
3.2) Microcosm simulation of Bacteria isolated from the Bagnoli-Coroglio site

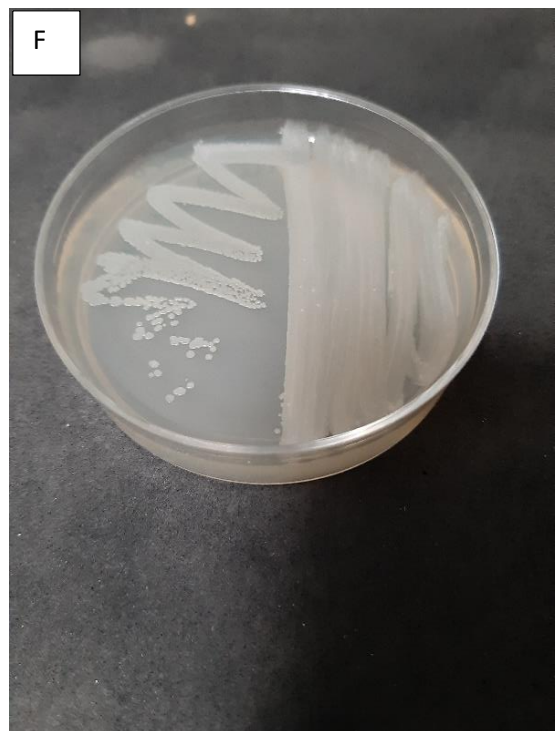
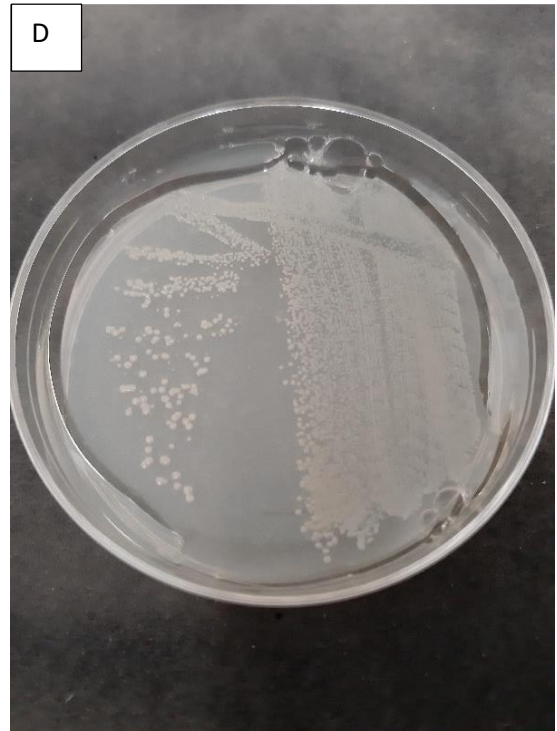
3.2.1) Identification of bacterial isolates and bacterial growth in the presence of contaminants

Following isolation procedures, it was possible to isolate 5 species belonging to 3 consortia (Fig. 2.16, a, f), 2 species of which were already isolated from the Sarno river Mouth (Consortium A2). The three consortia are referred to as Consortium 2b, Consortium 4, and Consortium 41. Following extraction of the gDNA, amplification of the 16s rRNA gene (Fig. 2.16 G) and subsequent Sanger sequencing, it was possible to assign the colonies to the genera *Epibacterium* sp., *Pseudolateromonas* sp., *Virgibacillus* sp., (Fig. 2.16 D, F and Fig. 2.17), and *Halomonas* sp. and *Alcanivorax* sp. In particular, *Halomonas* sp., *Pseudolateromonas* sp., and *Virgibacillus* sp. were isolated from Consortium 2b, *Pseudoalteromonas* sp. and *Alcanivorax* sp., from Consortium 41, *Epibacterium* sp., and *Halomonas* sp. from Consortium 4. Interestingly the 2 species *Halomonas* sp. and *Alcanivorax* sp. were present also at this site, as shown by the further genomic analysis (Chapter 4).

The isolation of a *Pseudoalteromonas* strain from such polluted sediments is consistent with data reported by Izzo et al. (2019), Liu et al. (2019), and Iohara et al. (2001) who showed that this strain plays a predominant role in the degradation of hydrocarbons and in the reduction of metal toxicity, for example through the presence of mercury-resistant operons whose presence has been described in *Pseudoalteromonas haloplanktis*. Few studies report the presence of *Epibacterium* sp. in contaminated

sediments because many of these strains are usually identified as belonging to the clade of *Reuveria*. Indeed, Ganesh Kumar et al. (2019), Kumar and Gopal (2015) and Horel, Mortazavi, and Sobecky (2015) highlighted how *Roseobacter* and specifically *Ruegeria* sp. were able to favor the degradation of hydrocarbons. Interestingly *Virgibacillus* sp. has been described as being associated with polluted sediments in a few studies (Besaury et al. 2013) but despite the limited literature information, it represents a promising bacteria for bioremediation purposes since it is able to produce bioflocculating compounds able to enhance hydrocarbon biodegradation and metal ion removal (Ugbenyen, Simonis, and Basson 2018; Cosa et al. 2011).





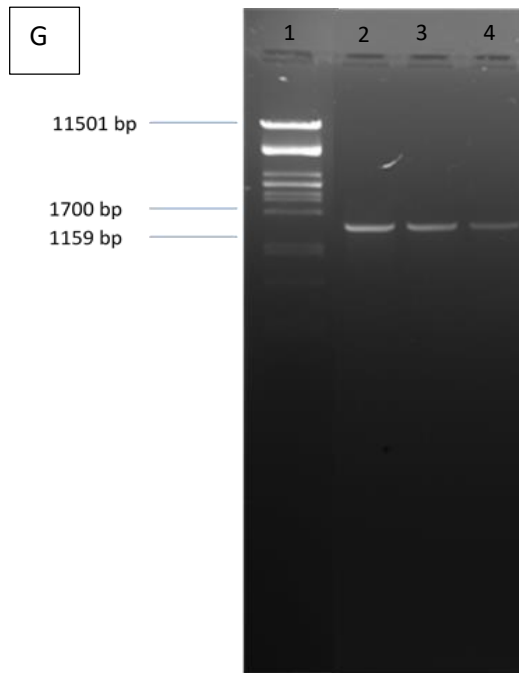


Figure 2.16. Agar plates with Mix cultures: Consortium 2B (A), Consortium 4 (B), Consortium 41 (C); the three isolates *Epibacterium* sp. SZN4 (D), *Pseudoalteromonas* sp. SZN3 (E), and *Virgibacillus* sp. SZN7 (F) and the agarose gel after 16s RNA amplification (G) (Lanes 1, 2, 3, 4, respectively contain DNA ladder, *Epibacterium* 16s rRNA, *Pseudoalteromonas* 16s rRNA, and *Virgibacillus* 16s)

Preliminary analyses on cultures grown in metal and hydrocarbon contaminated broth indicated that all Consortia and single cultures isolated from Bagnolo-Coroglio are promising microorganisms for bioremediation purposes.

The 3 mixed cultures (Consortia 2B, 4 and 41) showed the best growth capacity in the presence of As and hydrocarbons. In particular, Consortium 2B (Fig. 2.18 A) was able to grow at all three concentrations of As tested, although in the presence of 1000 and 100 ppm growth was reduced after 40 h and 36 h, respectively. Consortium 4 (Fig. 2.19 A) grew well at 100 ppm of As reaching the highest levels of optical density, equal to controls. However, growth diminished at 1000 and 10000 ppm. Similarly, to what has already been described for the curves of the A2 consortium (previous chapter), the growth of Consortium 41 at 100 and 10000 ppm of As (Fig. 2.20 A) were equivalent at 46 hours, while the growth at 1000 ppm was significantly reduced.

In the presence of PAHs, all three consortia (Fig. 2.18 B, 2.19 B and 2.20 B) reached optical density levels comparable to controls in the presence of 100 and 1000 ppm, but only consortium 41 was able to grow even at 10000 ppm. The high capacity of this consortium to tolerate hydrocarbons was also highlighted by the number of cells reached in the presence of the different concentrations of PAHs, since although at different times, all curves significantly exceeded the controls.

Consortium 4 was the most tolerant to the presence of Pb since growth in presence of 100 and 1000 ppm was superimposable to the controls (Fig. 2.19 C). Although 10,000 ppm of Pb exhibited high toxicity for consortium 4, this was the only concentration allowing growth of the 2b and 41 consortia.

The presence of 1000 and 10000 ppm of Cd and Cu was highly toxic for all three consortia as none showed an appreciable increase in biomass. Consortium 2b was able to grow in the presence of 100 ppm of Cd as well as Cu, reaching comparable optical density values in both treatments (Fig. 2.18 D and E). In contrast, consortia 4 and 41 showed biomass growth only in the presence of 100 ppm of Cu (Fig. 2.19 E and 2.20 E), with cell concentrations comparable to controls. Finally, although Zn proved to be highly toxic for consortia 2b and 4, consortium 41 showed, in presence of 10,000 ppm, an increase in the number of cells, albeit reduced compared to controls (Fig. 2.20 F).

The capacity of certain pollutants to stimulate bacterial growth at high concentrations is consistent with what has been confirmed by Pearce et al. (2014), who noted an increase in tumor mass following treatment with high doses of N-glycolylneuraminic acid. A cellular response of this type is called inverse hormesis and could therefore be a cellular survival mechanism used also in prokaryotes where environmental conditions become too hostile. Further studies are needed to understand the molecular basis of this phenomenon.

Epibacterium sp. SZN4 showed the highest tolerance to As since it was able to grow as well as controls even at concentrations of 10,000 ppm (Fig. 2.21 A). Conversely, *Pseudoalteromonas* sp. showed tolerance to As only at 100 ppm (Fig. 2.22 A), while *Virgibacillus* sp. was unable to grow at any of the concentrations tested (Fig. 2.23 A). The tests carried out in the presence of Cd confirmed the high toxicity of this heavy metal since only *Epibacterium* sp. SZN4 was able to reach growth rates close to the control at 100 ppm (Fig 2.21 B). Similarly, Cu, Pb and Zn exerted toxic effects on the 3 isolates since none of the 3 bacteria was able to grow at concentrations above 100 ppm. More

specifically, *Pseudoalteromonas* sp. SZN3 and *Virgibacillus* sp. SZN7 reached and exceeded control OD values only when treated with 100 ppm of Cu and Pb (Fig 2.22 C, D and 2.23 C, D).

On the other hand, *Epibacterium* sp. SZN4 exhibited reduced growth compared to the other two strains since its growth, on Cu and Pb, did not reach the control values (Fig 2.21 C, D). In contrast, *Epibacterium* sp. SZN4 had the best growth capability when exposed to Zn since it was able to reach values equal to about half of those reached by the controls in the presence of 100 ppm of Zn (Fig 2.21 E). The other two strains were more sensitivity to this metal although *Virgibacillus* sp. SZN7 showed an increase in cell numbers starting from 36 h (Fig. 2.23 E). These observations may suggest that Zn induces the activation of metabolic resistance mechanisms over time allowing survival in *Virgibacillus* sp. SZN7.

Finally, despite *Virgibacillus* sp. SZN7 was the most tolerant to hydrocarbons, exhibiting an appreciable growth also at 10,000 ppm (Fig 2.23 F), both *Epibacterium* sp. SZN4 and *Pseudoalteromonas* sp. SZN3 reached a biomass growth equal to the control at 100 and 1000 ppm (Fig 2.21 F and 2.22 F), suggesting that the three isolates are potential candidates for PAHs bioremediation.

In general, although many studies, mainly metagenomics (Chauhan, Nain, and Sharma 2017; Keren, Lavy, and Ilan 2016; Zhou et al. 2013; Nithya and Pandian 2010) describe the ability of *Epibacterium* sp. SZN4, *Pseudoalteromonas* sp. SZN3 and *Virgibacillus* sp. SZN7 to survive in environments contaminated by heavy metals this is the first study that investigates the real tolerance capacity of these isolates at different concentrations of heavy metals.

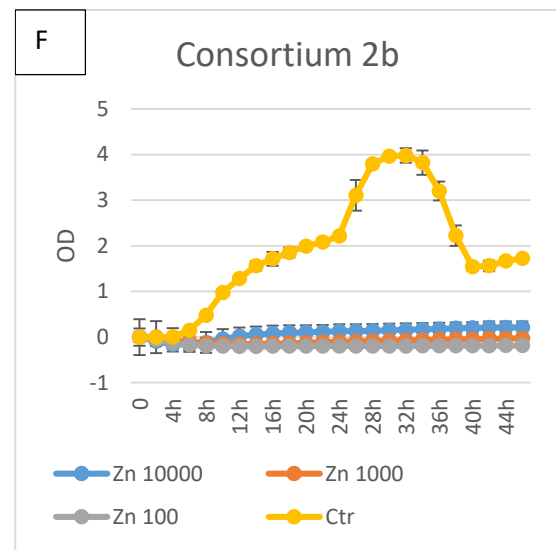
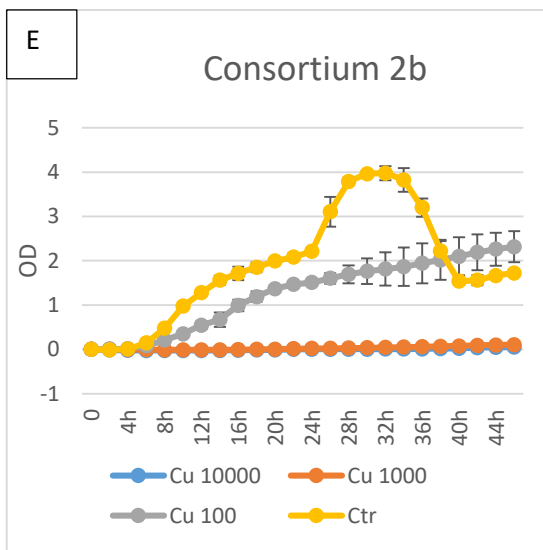
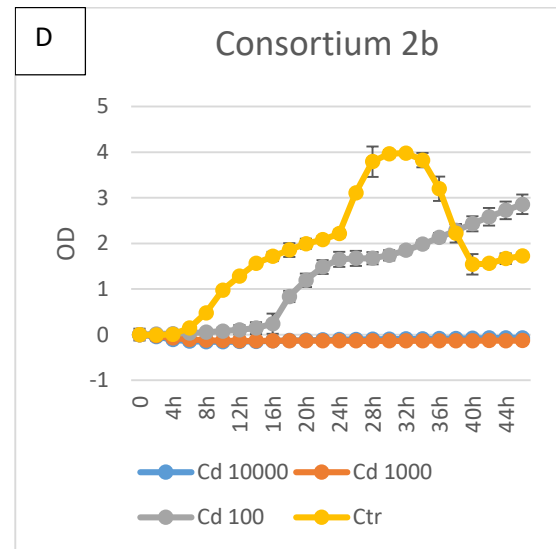
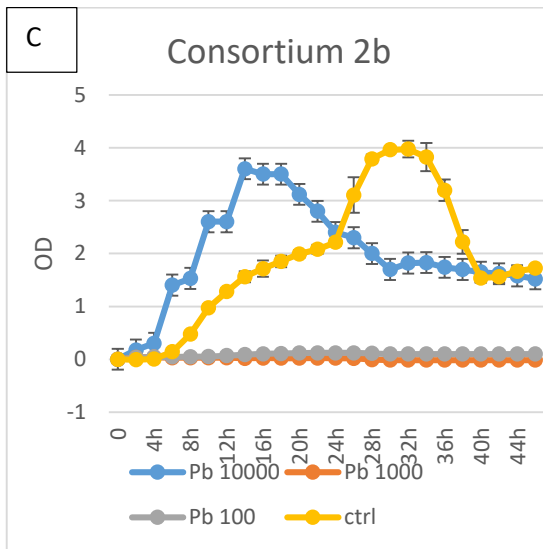
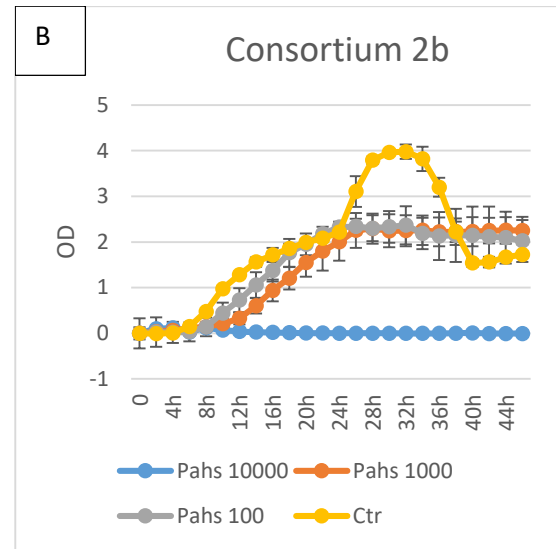
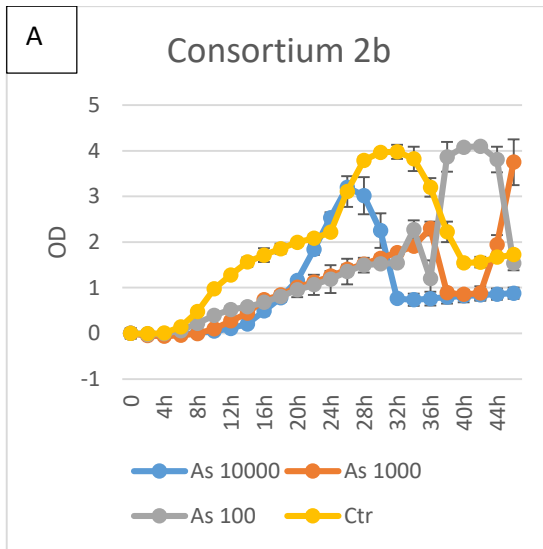
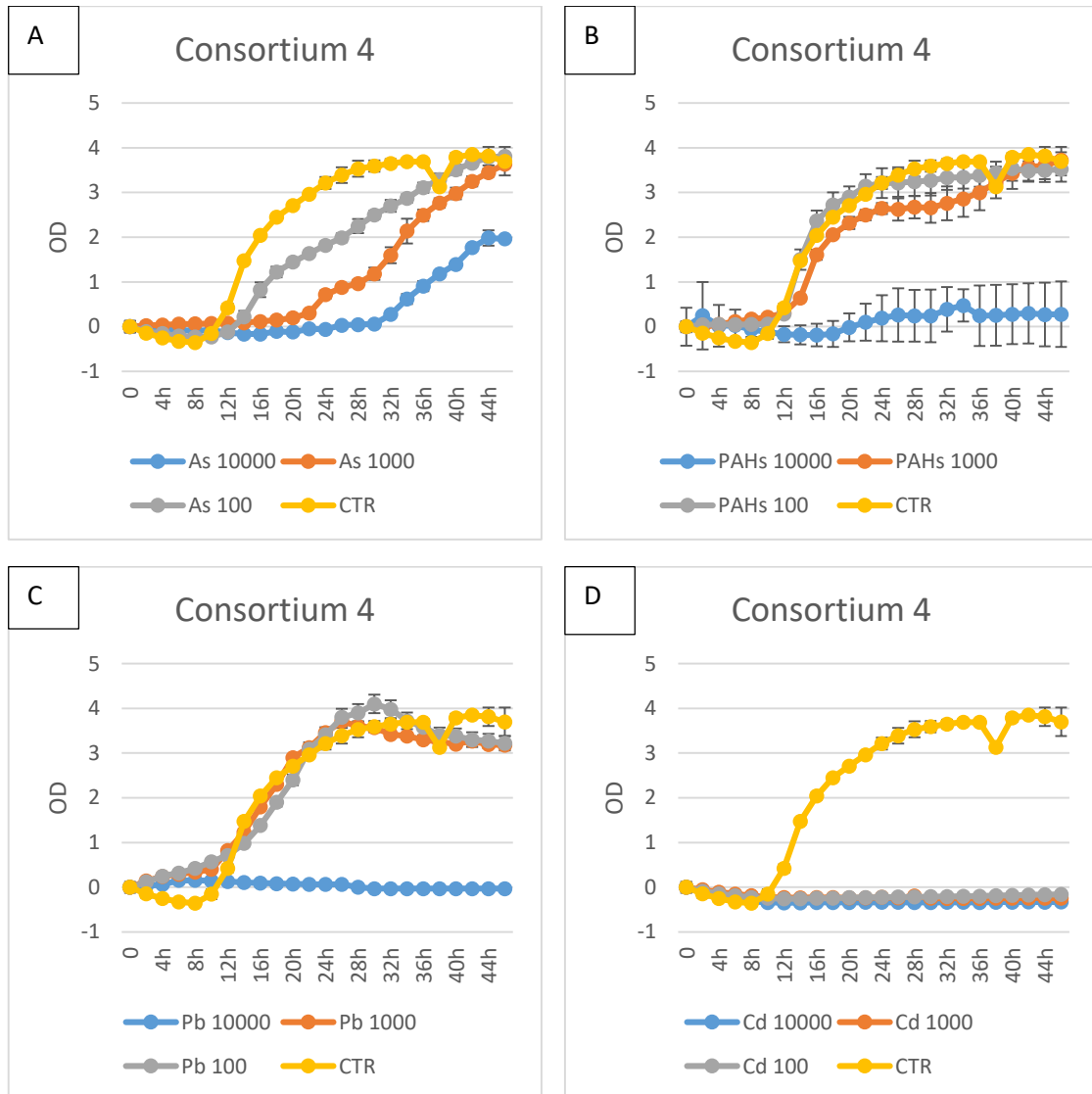


Figure 2.18: Minimum Inhibition Concentrations (MIC) testing As (A), PAHs (B), Pb (C), Cd (D), Cu (E), and Zn (F), on Consortium 2B at concentrations of 100, 1000 and 10000 ppm, expressed as Optical density (OD) values with time



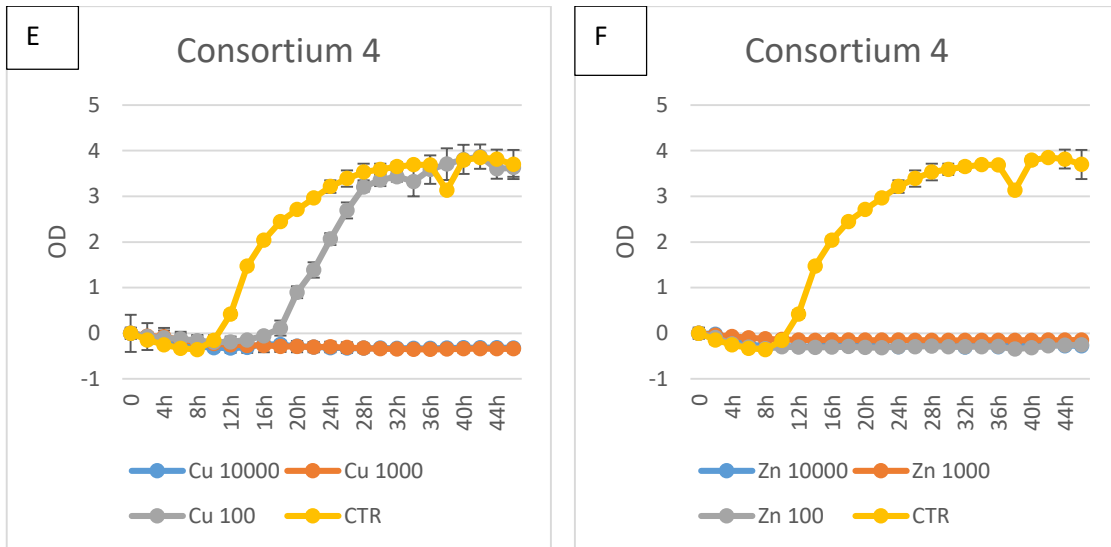
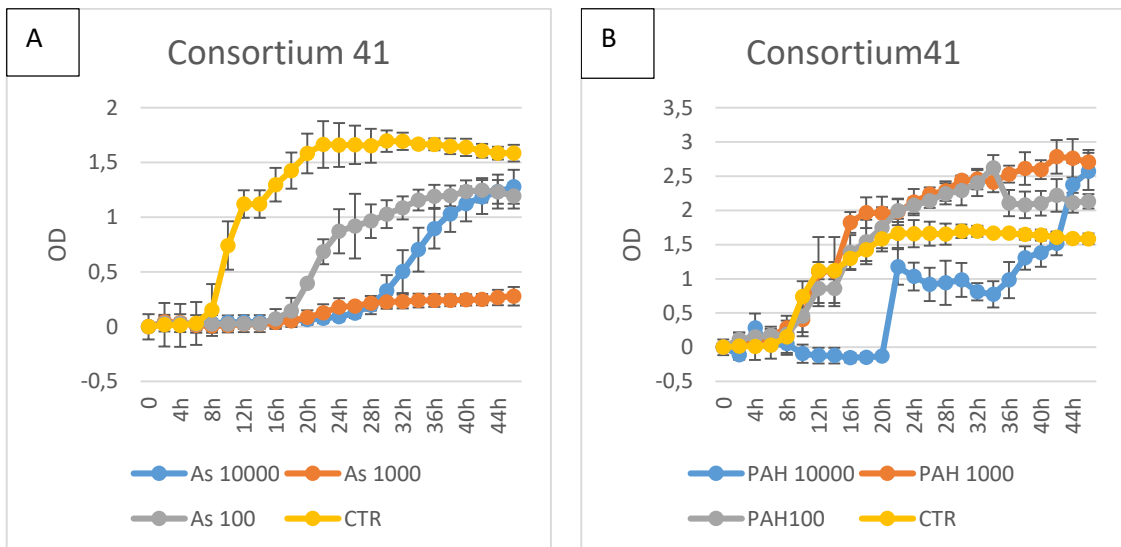


Figure 2.19: Minimum Inhibition Concentrations (MICs) testing As (A), PAHs (B), Pb (C), Cd (D), Cu (E), and Zn (F), on Consortium 4 at concentrations of 100, 1000 and 10000 ppm, expressed as Optical density (OD) values with time



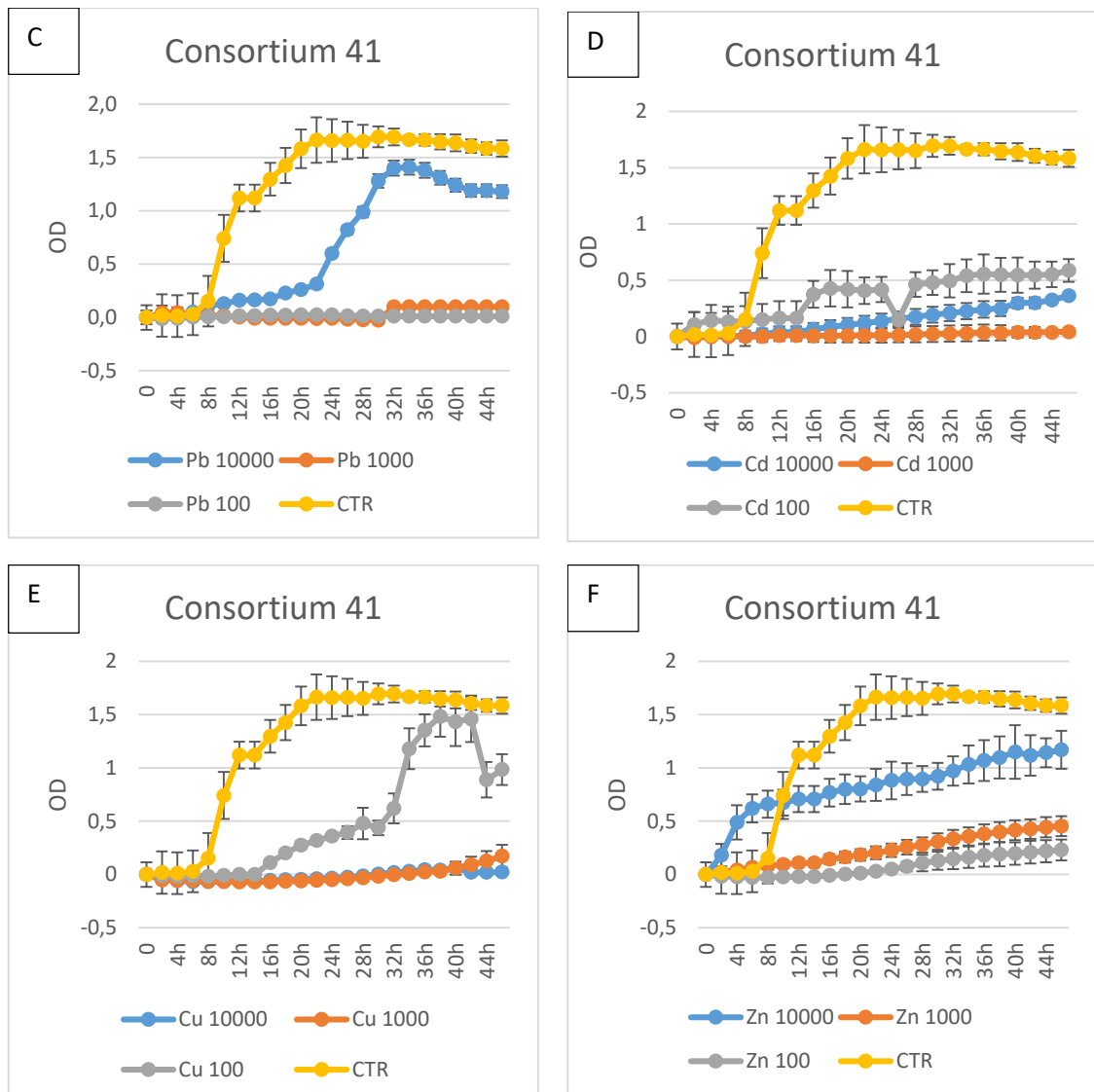


Figure 2.20: Minimum Inhibition Concentrations (MIC) testing As (A), PAHs (B), Pb (C), Cd (D), Cu (E), and Zn (F), on Consortium 41 at concentrations of 100, 1000 and 10000 ppm, expressed as Optical density (OD) values with time

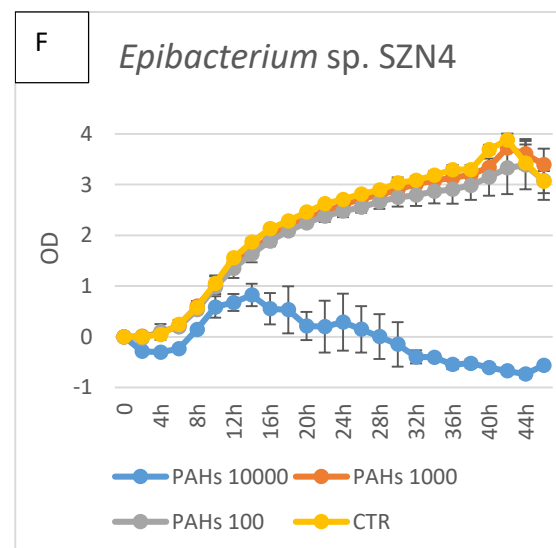
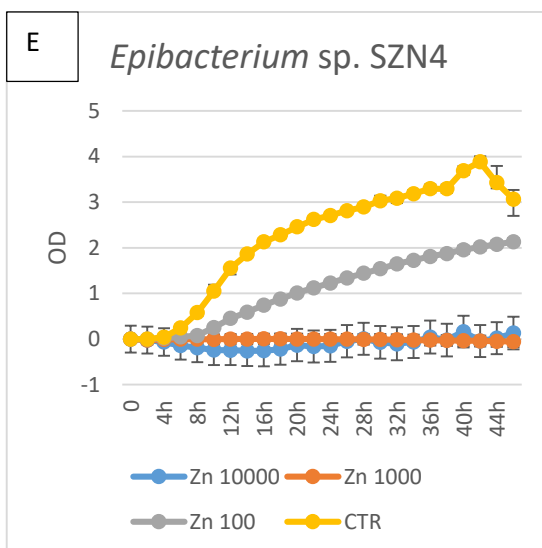
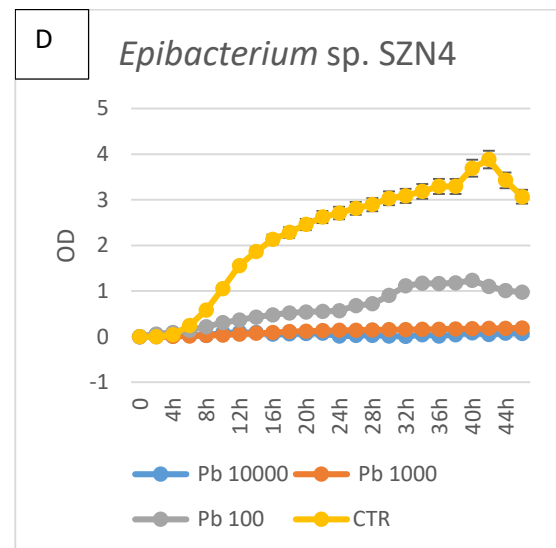
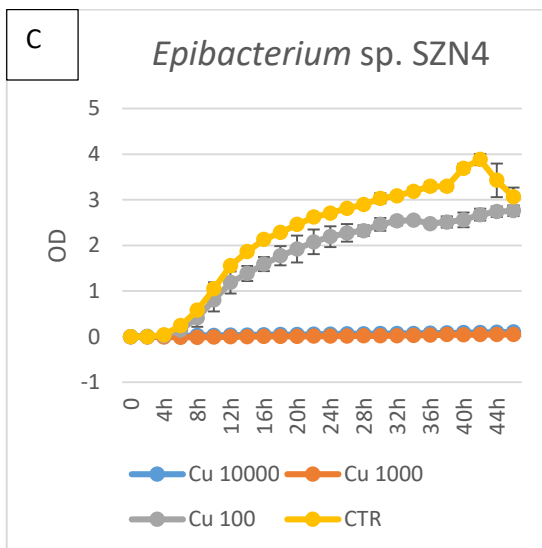
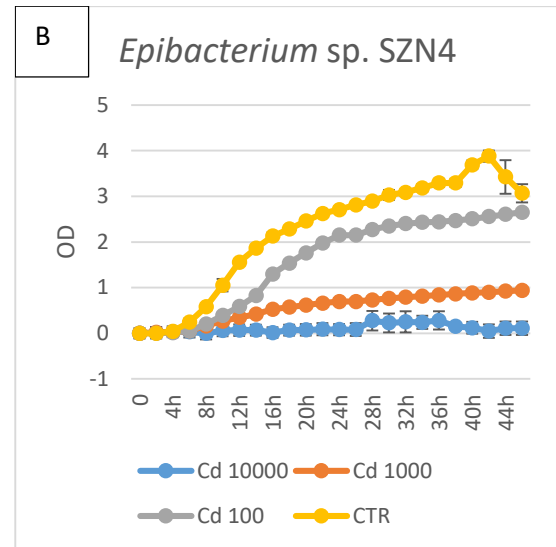
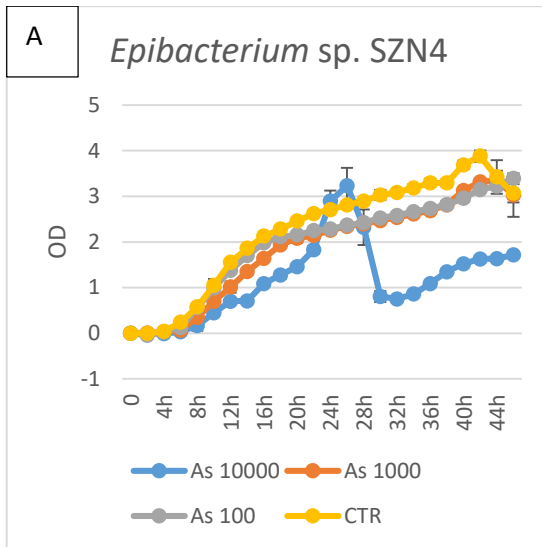
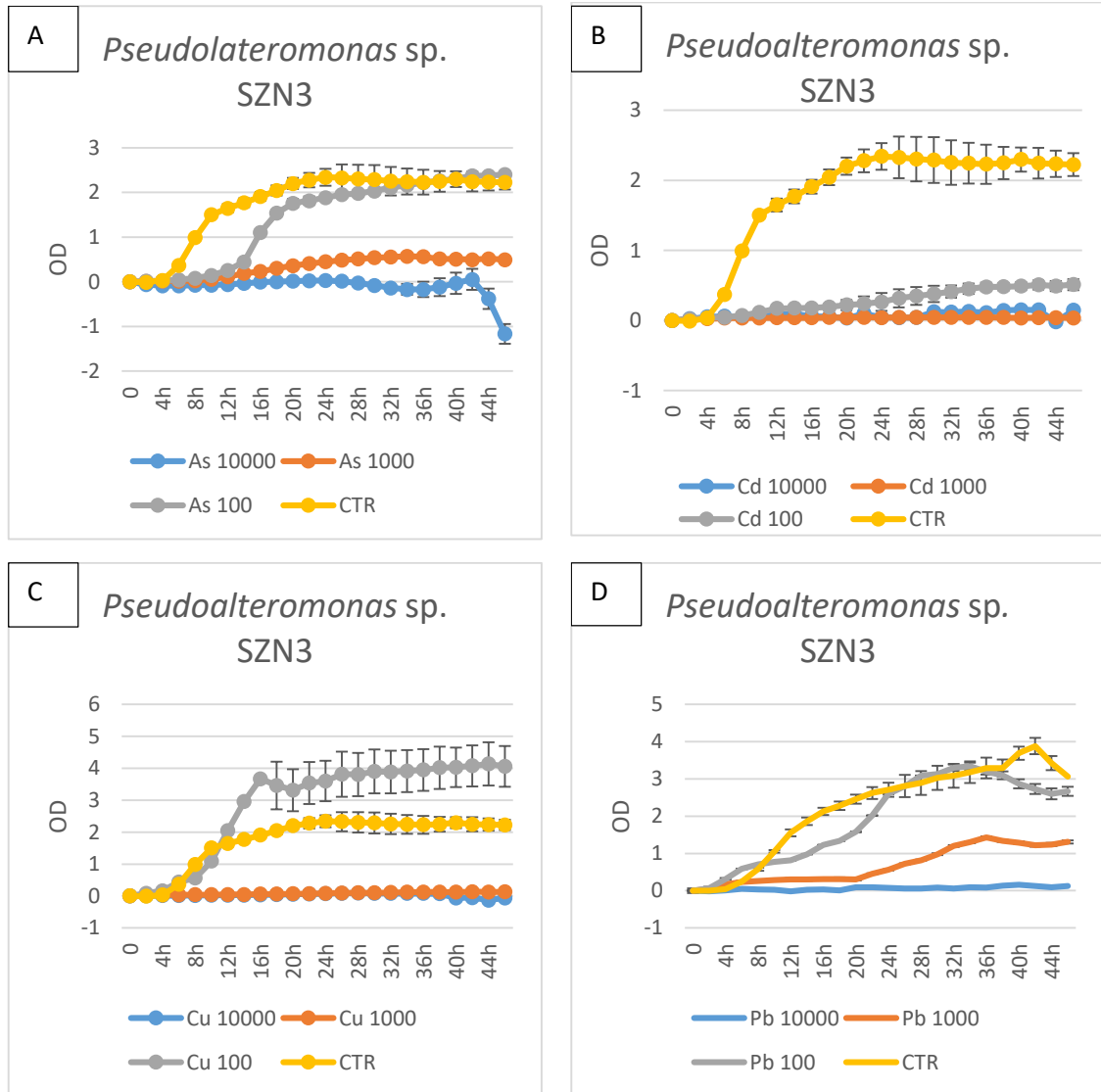


Figure 2.21: Minimum Inhibition Concentrations (MIC) testing As (A), PAHs (B), Pb (C), Cd (D), Cu (E), and Zn (F), on *Epibacterium* sp. SZN4 at concentrations of 100, 1000 and 10000 ppm, expressed as Optical density (OD) values with time



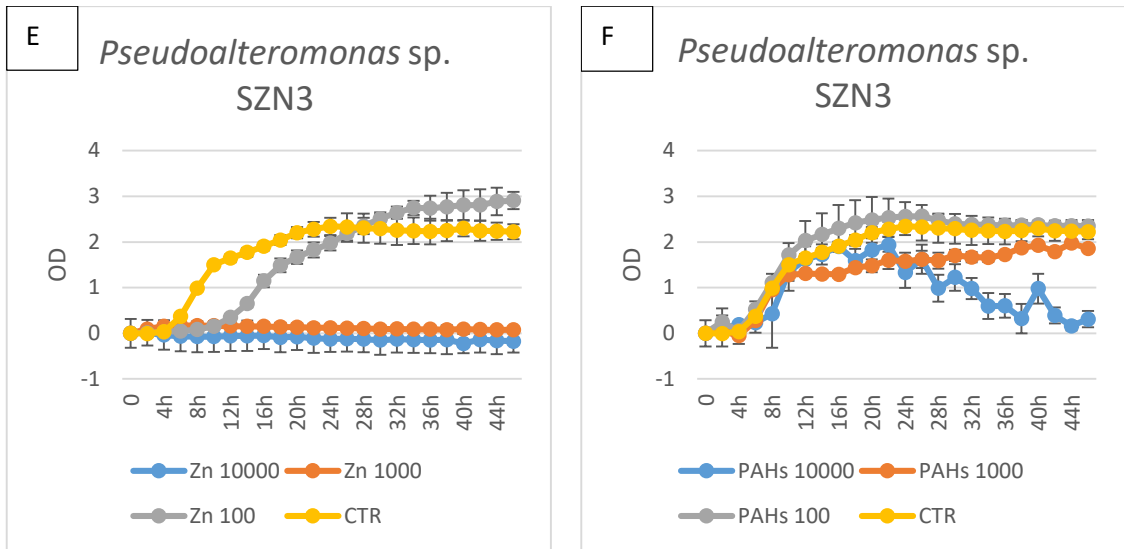
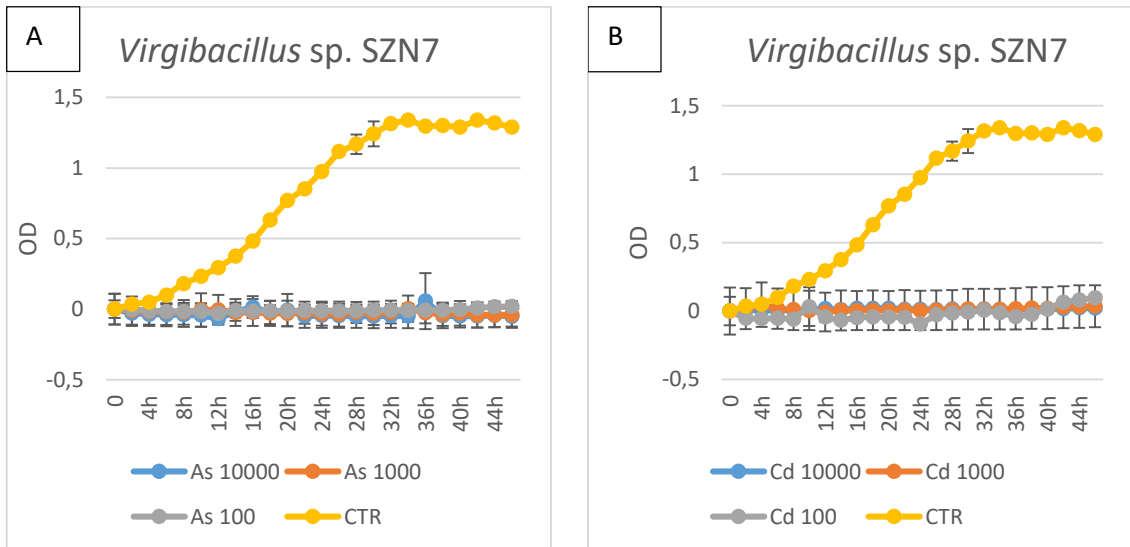


Figure 2.22: Minimum Inhibition Concentrations (MIC) testing As (A), PAHs (B), Pb (C), Cd (D), Cu (E), and Zn (F), on *Pseudoalteromonas sp.* SZN3 at concentrations of 100, 1000 and 10000 ppm, expressed as Optical density (OD) values with time



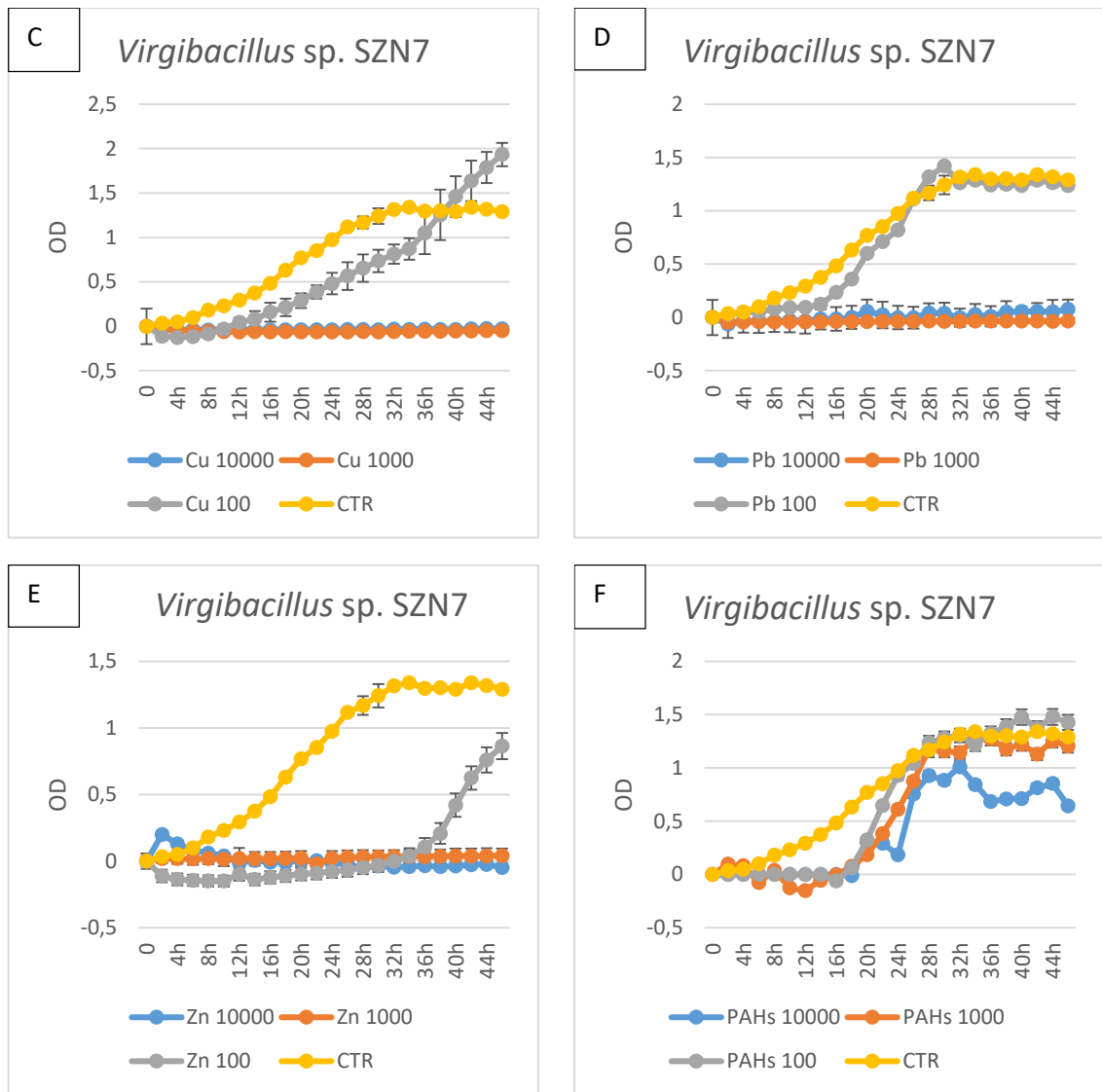


Figure 2.23: Minimum Inhibition Concentrations (MIC) testing As (A), PAHs (B), Pb (C), Cd (D), Cu (E), and Zn (F), on *Virgibacillus sp. SZN7* at concentrations of 100, 1000 and 10000 ppm, expressed as Optical density (OD) values with time

3.2.2) Evaluation of PAHs degradation and heavy metal precipitation capacity of bacterial cultures (as isolates and in mixtures)

In order to evaluate the possible bioremediation applications of these cultures, I investigated the ability to degrade hydrocarbons and precipitate heavy metals after 27 days of incubation in contaminated broth. As shown in Figure 2.24, culture growth decreased in the presence of metals and hydrocarbons, reaching a maximum growth only after 27 days. Conversely, controls reached the end of the exponential phase already after 3 days of incubation. Moreover, as already described in the previous chapter, the incubation with hydrocarbons led to a significantly higher number of cells than incubation with heavy metals, indicating that the latter compounds exerted a more toxic effect than the organic contaminants. pH changes (Fig. 2.25) were monitored during the incubation period to determine if 27 days of incubation led to optimal conditions for the evaluation of bioremediation activity. pH variations followed an opposite trend depending on the type of pollutant used (organic vs inorganic). Indeed, as observed for the cultures isolated from the Sarno river, an increase in pH was noted after treatment with metals, confirming the moderately alkaliphilic nature of bacterial taxa under examination (Senghor et al. 2017; Collins et al. 2015; Ali, Habib, and Riaz 2009) *vice versa*, a lowering of pH was recorded during incubation with hydrocarbons, suggesting the production of weak acids by bacterial metabolism.

Analyses concerning metal precipitation ability carried on samples collected at the end of the experiments showed a higher capability of the 3 consortia to precipitate Pb (c.a. .50%) compared to controls (Figure 2.26 B).

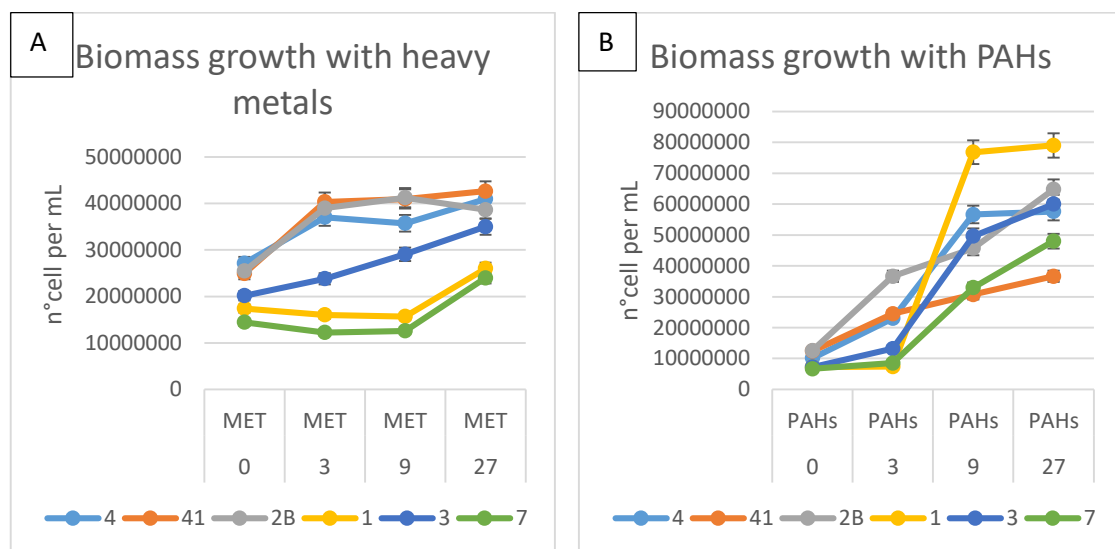
Differently, Pb precipitation did not change compared to controls in single strain treatments. The effect of single strains was appreciable in terms of Cd and Cu removal, as all three taxa led to the precipitation, respectively, of about 60% and 80% of metals under examination.

These data confirm what has already been described by Caruso et al. (2018), Vela-Cano et al. (2014), Zhou et al. (2013), who described the capacity of *Virgibacillus* sp., *Pseudoalteromonas* sp. MER144 and *Pseudolateromonas* sp. SCSE709-6 to effectively remove heavy metals (Cd and Hg) from the medium through the production of extracellular polysaccharides.

Conversely, metal precipitation from solution via *Epibacterium* sp. SZN4 had not yet been reported in the literature and suggests that this microorganism may be a promising new candidate for bioremediation processes. In general, the data here reported show the absence of a direct correlation between cell growth and metal removal as the metal removal efficiency of *Pseudolateromonas* sp. SZN3 did not differ significantly from the other two isolates, although it exhibits a higher biomass at the end of the incubation period. Thus, these data may suggest, in agreement with Zhou et al. (2013), that the removal of contaminants occurs by exopolysaccharide adsorption rather than intracellular accumulation.

Similarly to what has been described for the bacterial isolated from the mouth of the Sarno River, all cultures shown here were able to degrade the 3 PAHs analysed (Figure 2.26 A). Degradation rates on naphthalene were close to 100% in all investigated systems.

With the exception of *Epibacterium* sp. SZN4 which allowed a decrease of about 50% of Pyrene, the concentration of this hydrocarbon was significantly reduced in a range between 75% and 95% by Consortium 4, 41, 2B and *Pseudoalteromonas* sp. SZN3 and *Virgibacillus* sp. SZN7. Phenanthrene has been the most recalcitrant pollutant to bacterial degradation, as degradation has never exceeded 65% and the 2B consortium was not able to degrade more than 30%. The degradation observed here suggest, unlike the cultures of the Sarno River, that in certain situations, the single bacterial isolates may have a better degradation performance than the original consortium since both *Halomonas* sp. SZN1 and *Pseudoalteromonas* sp. SZN3 exhibited better phenanthrene degradation than when present together in the same culture (consortium 2B). This phenomenon is consistent with results reported by Piakong and Zaida Z (2018), and it is likely due to the antagonistic interaction among members of the consortium which may lead to a reduced degradation efficiency.



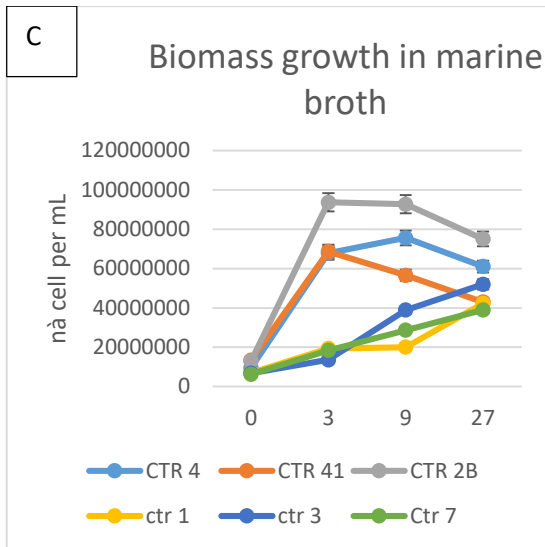
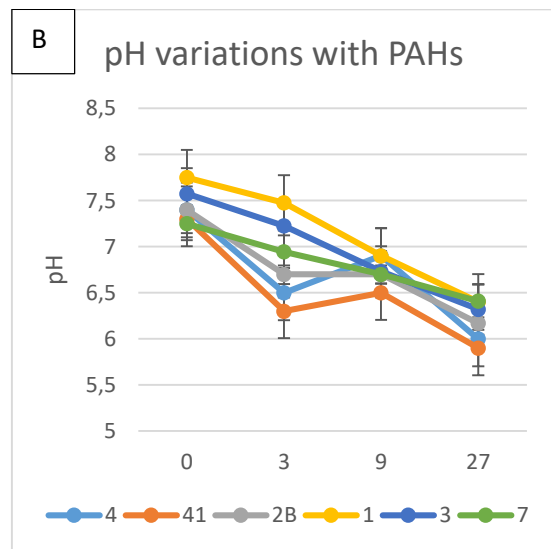
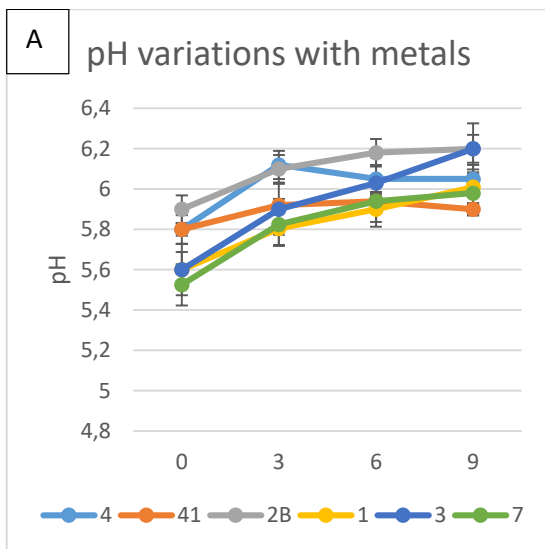


Figure 2.24: Biomass growth measurements, at four different timings, of Consortium 4 (4), Consortium 41 (41), Consortium 2B (2B), *Epibacterium* sp. SZN4, (1), *Pseudoalteromonas* sp. SZN3, (3), *Virgibacillus* sp. SZN7(7) incubated with a mix of heavy metals (A), PAHs (B) and no amendements (C)



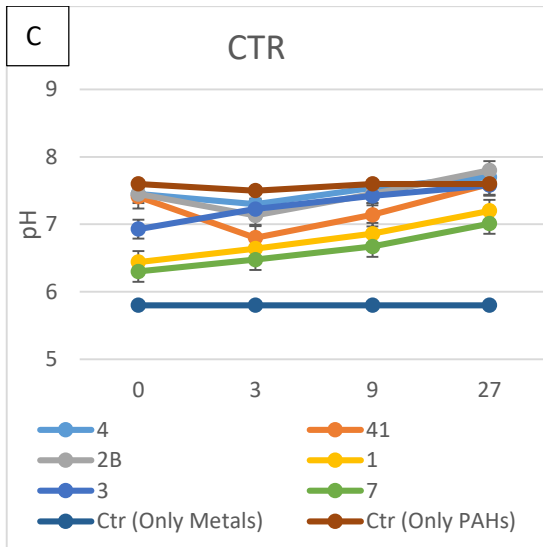
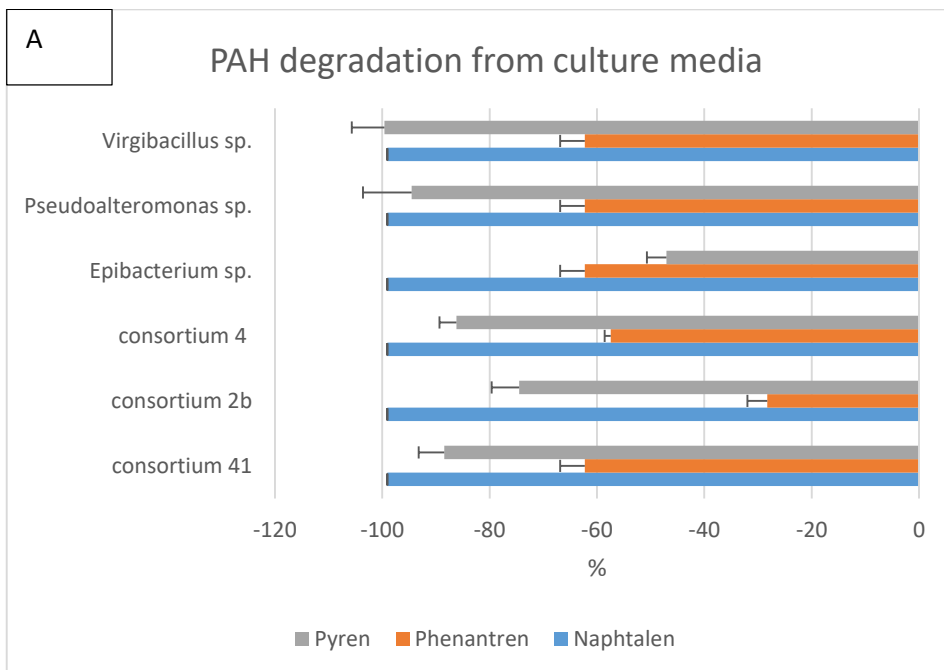


Figure 2.25: pH measurements, at four different hours, of Consortium 4 (4), Consortium 41 (41), Consortium 2B (2B), *Epibacterium* sp. SZN4, (1), *Pseudoalteromonas* sp. SZN3, (3), *Virgibacillus* sp. SZN7 (7) incubated with a mix of heavy metals (A), PAHs (B) and no amendments (C)



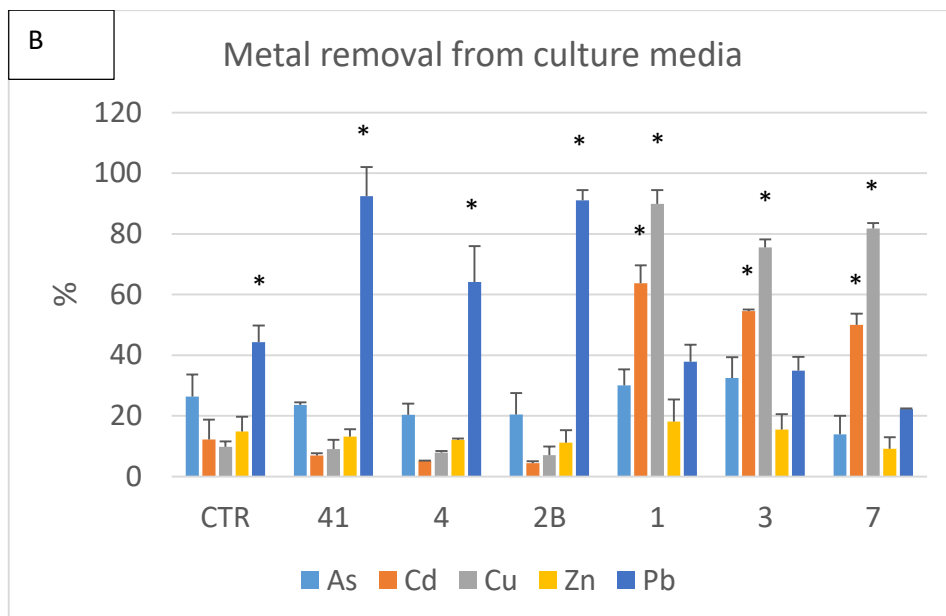


Figure 2.26: PAH degradation rates (A) and heavy metals removals (B) of Consortium 4 (4), Consortium 41 (41), Consortium 2B (2B), *Epibacterium* sp. SZN1, (1), *Pseudoalteromonas* sp. SZN3, (3), *Virgibacillus* sp. SZN7, (7) at the end of incubation time (27 days)

3.2.3) Effects of bacterial culture addition (as isolates and as mixtures) on hydrocarbon degradation and heavy metal partitioning in contaminated sediments from Bagnoli-Coroglio

After verifying the performance of consortia and isolates in contaminated liquid solutions I proceeded to inoculate bacteria into flasks containing polluted sediment samples collected from Bagnoli-Coroglio.

Data regarding the degradation of hydrocarbons (Fig. 2.27) from sediments showed that the cultures were generally capable of degrading hydrocarbons (about 40% on average), although each culture had a specific degradation rate for each substrate. For example, Consortium 41 showed a degradation capacity of around 90% for Dibenzo (a, h) Anthracene, and 50% for PAHs, Benzo (a) Pyrene, Benzo (g, h, i) Perylene and Indeno (1, 2, 3) Pyrene while the degradation of Pyrene, Chrysene, Benzo Fluoranthrene and Benzo (a) Anthracene was almost null. Similarly, *Pseudolateromonas* sp. SZN3 exhibited a degradation below 10% for Benzo (a) pyrene and Pyrene; Benzo (g, h, i) Perylene, Indeno (1, 2, 3) Pyrene were also not significantly degraded by Consortium 2B.

Only Consortium 4, had an overall degrading ability of around 40% even if it showed lower degradation yield for Benzo (g, h, i) perylene and Pyrene. These data are also in agreement with what described by Nuñal et al. (2017) who, using an artificial consortium composed of *Pseudomonas aeruginosa*, *Marinobacter mobilis*, *Gaetbulibacter* sp. and *Halomonas* sp. observed a degradation rate of about 50 % of hydrocarbons added to the sediment.

Of the pure isolates, *Virgibacillus* sp. SZN7 showed the best biodegradation capacity since the least degraded compound (Benzo (g, h, i) Perylene) reached degradation values of above 20%. Finally, *Epibacterium* sp. showed an effective degradation between 30% and 50% for the majority of the analyzed compounds except for Benzo (a) pyrene and Chrysene whose degradation did not exceed 20%. The data shown here, thus, highlight the possibility of using such consortia as effective tools capable of degrading most of the pollutants present in the area of Bagnoli-Coroglio.

Likewise, the results here reported indicate that even single isolates may be valid candidates in the degradation of hydrocarbons. Indeed, although the ability of *Pseudolateromonas* sp. SZN3 to degrade hydrocarbons in association with other bacteria and within artificial systems was already known (Hochstein et al. 2019; Morenulloa et al. 2019; Hedlund and Staley 2006) its real ability to degrade hydrocarbons following a bioaugmentation directly into the polluted sediment had never been evaluated. Similarly, this is the first study where *Epibacterium* sp. SZN4 and *Virgibacillus* sp. SZN7 are proposed as new potential candidates for hydrocarbon bioremediation in polluted environments and the results shown below suggest that they can also be applied in heavy metal bioremediation.

To this aim, the results of the selective sequential extraction (SSE) analysis indicated that the addition of bacteria significantly reduced the mobility (and thus bioavailability and toxicity) of As as the percentage of such metalloid associated with the exchangeable carbonate fraction decreased in favor of a more stable fraction (Fig 2.28 A).

Consortium 4 was the culture that highly reduced the mobility of As, since it partitioned the metal into a Fe / Mn oxidizing fraction and into the residual fraction, considered the

least bioavailable fraction of all. Moreover, this consortium was the only one to exert an effect on Cd (Fig. 2.28 B), reducing the component associated with the exchangeable carbonate fraction to about 15%.

Similarly, the mobility of Pb (Fig. 2.28 C) also decreased following treatment with bacterial cultures. The effects were significant for all microorganisms except for *Virgibacillus* sp. SZN7 which did not generally affect the repartition of any metal.

Finally, none of the microorganisms significantly partitioned Cu and Zn (Fig. 2.28 D and E) in the other fractions, compared to controls. This observation suggests that the proposed bacteria are not optimal for the biostabilisation (*i.e.* reduction of metal mobility) of these elements in the analyzed sediments.

In general, data regarding the changes in metal partitioning after treatment with isolated cultures from Bagnoli-Coroglio, agree with results obtained following treatment with the consortium isolated from the Sarno River, as in both cases the mobility of As, Cd and Pb significantly decreased.

Additionally, the reduced mobility of these metals can be superimposed on the activity of the sulfur reducing bacteria described by Li et al. (2016) which led to the metals Cu, Cd, Zn and Pb in a more stable mineral phase. Interestingly, in my study Cu and Zn metals were not affected by the bacterial treatment. According to Zhang et al. (2014), this difference could be attributed to a different composition of the sediment used.

However, my study indicates that other bacteria that do not belong to the class Deltaproteobacteria, that are widely recognized as comprising most of the sulfur-reducing bacteria (Barton and Fauque 2009), are able to lower the toxicity of metals by

increasing their immobilization. Further studies based on genome mining are needed to confirm if the same molecular mechanisms employed in these processes by sulphur reducing bacteria occur even in bacteria here investigated

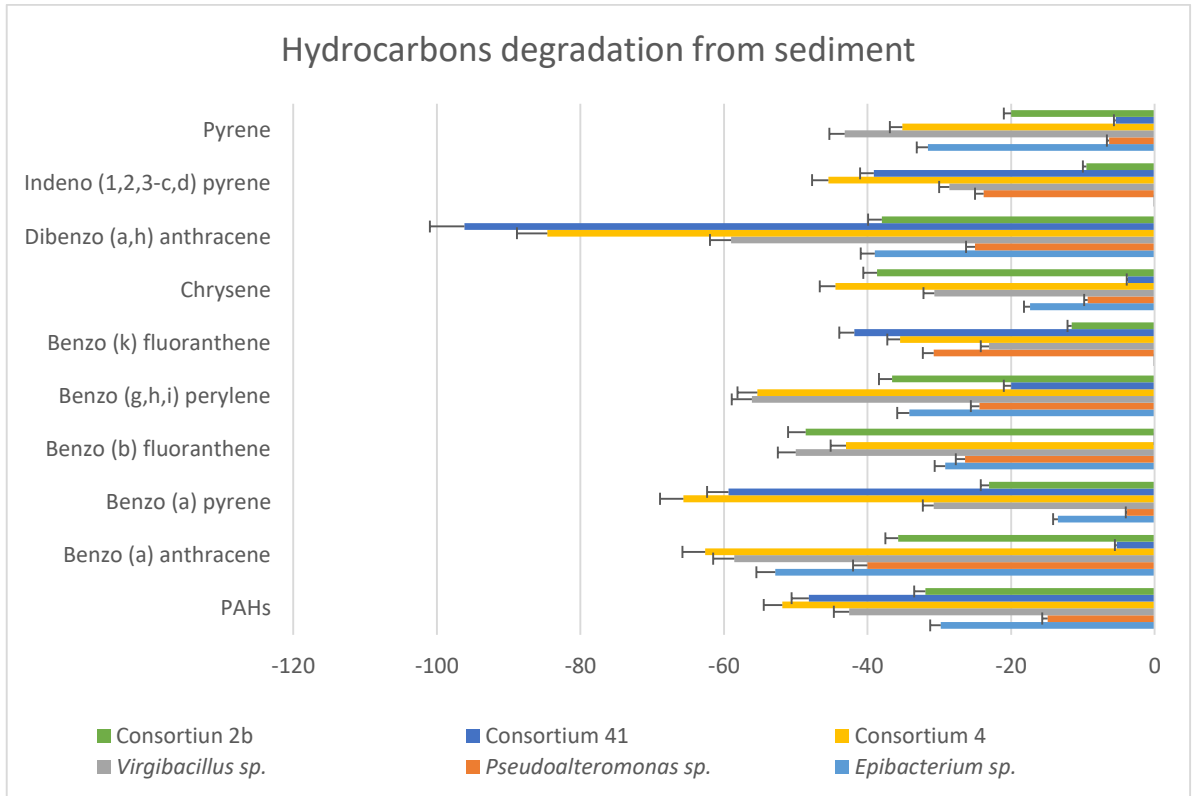
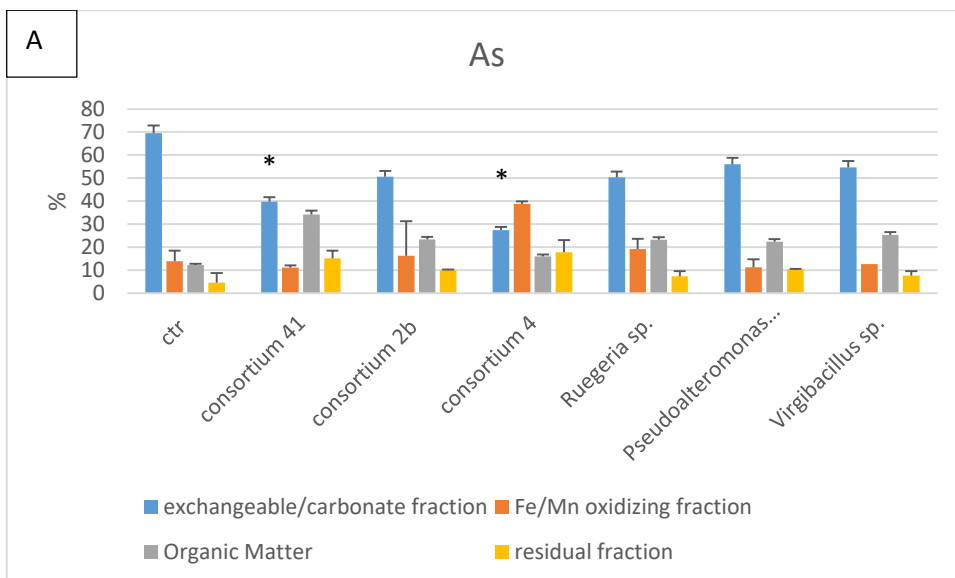
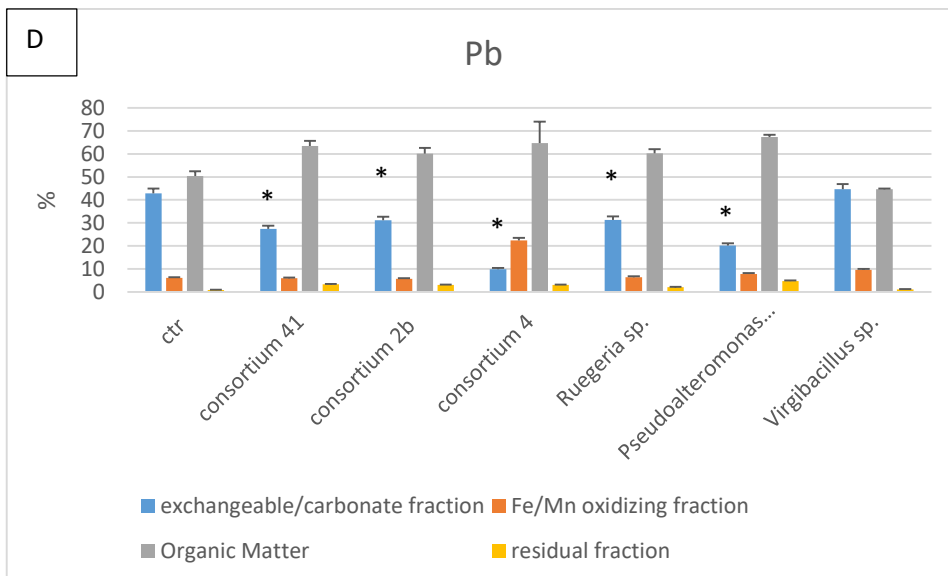
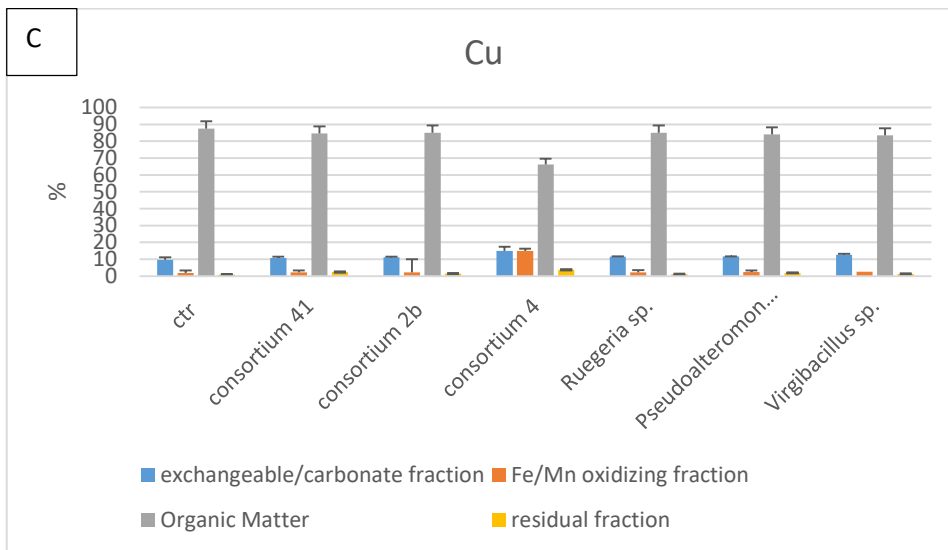
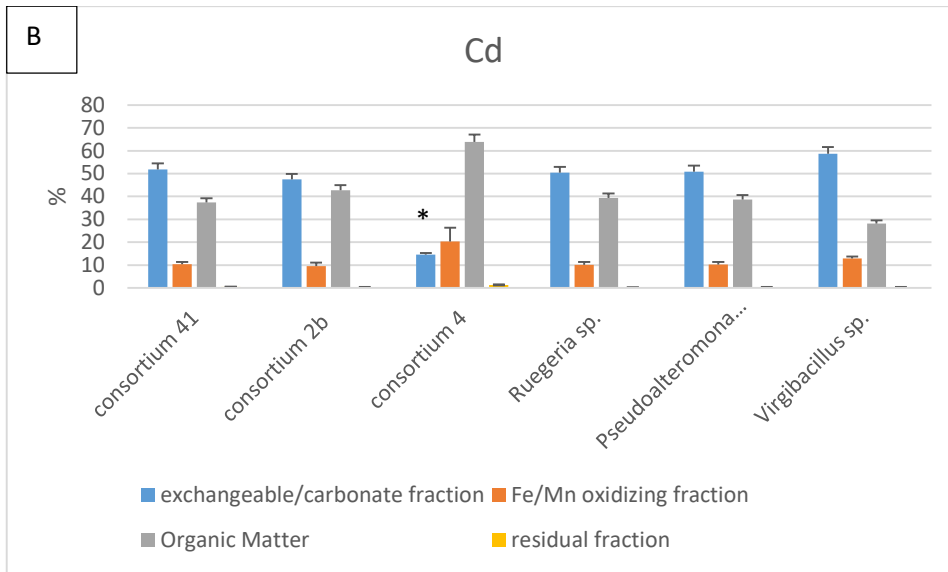


Figure 2.27. Percentage PAH degradation rates in sediments at the end of the incubation time (27 days) compared to controls





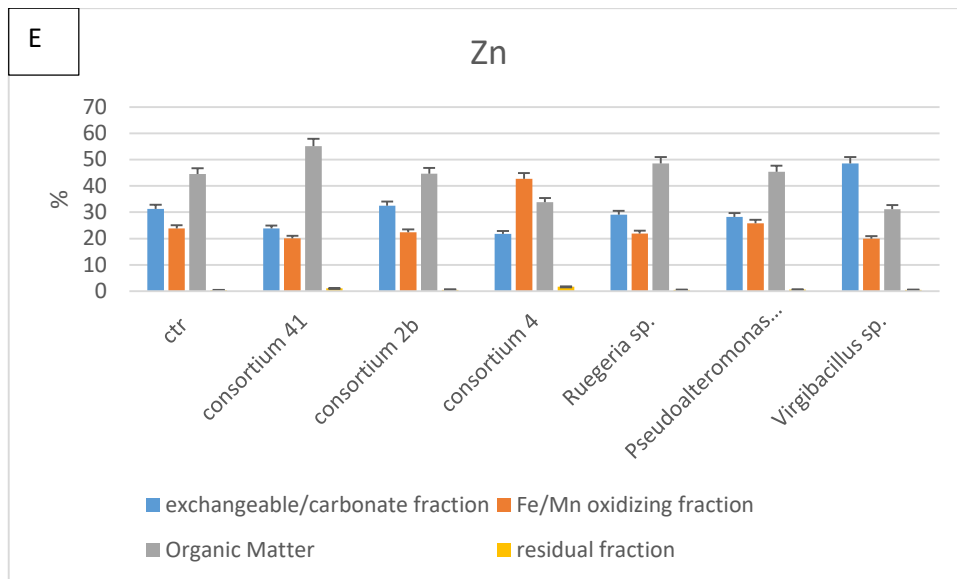


Figure 2.28. As (A), Cd (B), Pb (C), Cu (D) and Zn (E) distribution in the four sediment fractions following Selective Sequential Extraction at the end of incubation time (27 days)

4) Conclusion

The data here reported show the capability of the four consortia and the isolated strains to grow under heavy metal and hydrocarbon stress as well as to degrade PAH mixtures and effectively precipitate lead, cadmium and copper from solutions. Moreover, the ability of all cultures, both consortia and pure colonies, to degrade PAHs directly in the contaminated sediments, suggest their possible employment as an effective solution for the bioremediation of hydrocarbon derivatives polluting Bagnoli-Coroglio sediments. Additionally, the ability of Consortium A2 and Consortium 4 to reduce the bioavailability and thus the toxicity of three of the tested metals (As, Cd and Pb) suggests that these Consortia may be suitable for in situ bioremediation since these heavy metals would not be resuspended into the water column.

This study opens new insights into marine bioremediation strategies since it highlights that a similar pattern of pollution characterized by high concentrations of heavy metals and hydrocarbons, found in the two different study areas (Sarno River and Bagnoli-Coroglio), has selected the same strains with bioremediation potential in the two investigated areas.

Further studies are required to better understand chemical interactions among strains comprising the Consortia since, under different treatments, different responses were observed between the single isolates and mixtures containing the same taxa.

Furthemore, the mechanism used by these bacteria, leading to a different heavy metal partitioning in the sediments, need to be better investigated since, for the isolated colonies described in this study, this has not yet been described in the literature.

Chapter 4

Genomic characterization and functional analysis of bacterial isolates

Abstract

Marine bacteria have long been known as potentially employable in bioremediation strategies (Dash et al. 2013). In order to fully exploit their potential, genome characterization appears to be desirable as it allows for in depth studies of the genetic and molecular mechanisms underlying processes of degradation and detoxification of xenobiotics. This chapter reports the genomic sequencing results of bacteria isolated during the sampling activities that took place in the former industrial area of Bagnoli Coroglio (Naples, IT). The investigation has allowed me to identify 6 different genomes belonging to the genera *Alcanivorax*, *Alkaliphilus*, *Epibacterium*, *Halomonas*, *Pseudoaltromonas* and *Oceanicaulis*. The results of the Average Nucleotide alignment demonstrated the presence of 4 new taxa belonging to *Alkaliphilus* sp., *Halomonas* sp, *Oceanicaulis* and *Pseudoalteromonas* since the scores with closest related strains were under the cutoff of 95%. Automatic and manual annotation confirmed the possibility of employing these bacteria in bioremediation processes since many genes are involved in hydrocarbon degradation pathways and in heavy metal detoxification systems, the sequences and organization of which are described below.

1) Introduction

Environmental pollution is of global concern since mutagenic and toxic effects of compounds such as polycyclic aromatic hydrocarbons, metals and chlorinated / nitro aromatic hydrocarbons pose a serious threat to the entire ecosystem (Fulekar and Sharma 2008).

Despite the existence of many chemical-physical methods, microbial bioremediation has been demonstrated to be one of the most effective sustainable and cost competitive approaches to remove anthropogenic compounds from polluted environments. In order to optimise this strategy, a thorough understanding of features driving the removal of pollutants and of degradation processes is required (Desai, Pathak, and Madamwar 2010). Microorganisms have colonized almost all extreme environments due to their ability to activate a myriad of different metabolic pathways. For this reason they harbour a reservoir of genes with high biotechnological potential that has yet to be fully exploited (Plewniak et al. 2018).

In order to investigate this potential, the use of molecular biology associated with DNA sequencing techniques appears to be the preferred strategy as it allows to obtain an overall view of genes involved in pollution abatement. In particular, the technological achievements of the last twenty years in the field of high-throughput sequencing based on Next generation sequencing (NGS) and software assemblies have allowed the rapid sequencing at affordable costs of entire bacterial genomes, which according to the estimates of the Earth Microbiome Project, will allow for the full sequencing of 500,000 genomes (Thompson et al. 2017; Bharagava et al. 2019).

A very effective strategy for identifying the dynamics of communities and the distribution of non-cultivable microorganisms in highly polluted sites is metagenomic sequencing to obtain the overall microbial assemblage genomes from direct sequencing of metagenomic libraries or environmental DNA (Martín et al. 2006; Plewniak et al. 2018). However, the simple mapping and sequencing of genomes does not provide a complete explanation of ongoing processes unless associated with a functional study of genes that can lead to the identification of various promoters and genes involved in degradation pathways and the choice of optimal candidates to design high performance bioremediation treatments (Czaplicki and Gunsch 2016b). The advancement of Omics approaches based on functional genomics, considered as the set of techniques aimed at whole genome sequencing associated with bioinformatics analysis, has provided effective tools such as proteomics and transcriptomics able to clarify the biological function of genes and thus, to reveal the complex regulation of biochemical pathways activated under stress conditions (Deutschbauer, Chivian, and Arkin 2006).

Although culture independent methods such as metagenomic and metatranscriptomic techniques associated with bioinformatics and genome-mining analyses are useful tools to unveil the potential of bacterial communities (Machado and Gram 2017; Vallenet et al. 2017), a culture dependent approach still remains an important strategy to isolate microorganisms with high biotechnological potential directly usable in bioremediation strategies based on bioaugmentation (Overmann, Abt, and Sikorski 2017). In this chapter I describe the genomes obtained at the Institute for Microbial Biotechnology and Metagenomics (University of Western Cape, SA) through Next Generation Sequencing, after having assessed the capacity (described in chapter 1 and 3) of isolated

colonies to reduce metal mobility and degrade polycyclic aromatic hydrocarbons. In addition, following automatic and manual annotation, I describe the main genes involved in mechanisms of resistance and degradation of hazardous compounds.

2) Materials and Method

2.1) Bacterial culturing

The four cultures were isolated from sediments sampled from the Sarno River (Culture A2) and Bagnoli-Coroglio regions (Consortia 2B, 41, 4) as described in chapter 3. Each of these cultures represents a consortium of bacteria but for simplicity they are referred to in the text as A2, 2B, 41 and 4.

2.2) Genomic DNA preparation and Genome sequencing

Genomic DNA (gDNA) was extracted with the DNeasy Blood & Tissue kit, according to the manufacturer's instructions. DNA concentration was estimated by measuring the absorbance at 260 nm and purity by 260/230 nm and 260/280 nm ratios (Thermo Fisher, Waltan, US).

Sequence library preparation of gDNA was performed using the Nextera DNA Flex kit (Illumina, Hayward, USA) with 1 ng input DNA according to the manufacturer's instructions. The resultant libraries were sequenced with an Illumina MiSeq instrument at the University of Western Cape sequencing facility using a MiSeq Reagent kit V2 (500 cycle) with a 10% phiX v3 spike generating 2 × 250 bp reads per sample. The raw reads

were trimmed (bases with a Q-score less than 36 were trimmed from the 3' end) and demultiplexed at the sequencing facility.

2.3) Annotation and comparative genomics

To assemble the genomes, contigs generated with Illumina Miseq were up loaded on a binning tool called MyCC (Lin and Liao 2016). Subsequently I evaluated the degree of completeness of the genome by uploading them into CheckM (Parks et al. 2015). To identify the *de novo* assembled genomes I proceeded with phylogenetic identification using three housekeeping genes. More specifically I selected, as suggested by Chun et al. (2018), the genes *recA* (recombinase A), *gyrB* (DNA gyrase subunit B), and *rpoB* (RNA polymerase subunit beta) since such genes, in terms of phylogenetic resolution, can be comparable or even better than 16S rRNA (Větrovský and Baldrian 2013). In order to determine the species relatedness of the genomes I evaluated the average nucleotide identity (ANI) (Rodriguez-R and Konstantinidis 2016; Han, Qiang, and Zhang 2016) by comparing the *de novo* genomes with the genomes found following the analysis with the three marker genes and with the closest related genomes identified by loading the major contigs (> 100,000 bp) on BLAST (Madden 2013). The closest related genomes were chosen using a cut-off point of 90% nucleotide sequence identity. The obtained genomes were annotated by RAST (Overbeek et al. 2014) providing an automatic and hypothetical annotation for every gene of the genome. KEGG was used to predict the pathways in which the annotated protein could be involved (Kanehisa et al. 2017). After having identified the genes involved in metal resistances or hydrocarbon degradation, I

verified their identity by manual annotation. In order to manually annotate the sequences, the genomes were handled with CLC Genomic Workbench 11 (<https://www.qiagenbioinformatics.com/>) to detect all open reading frames (ORF) and translated into aminoacidic sequences. I also carried on synteny analysis through manual annotation of the sequences flanking the genes of interest to better understand the organisation of these areas and to compare them with homologous sequences of other phylogenetically similar strains. To graphically represent the comparison of the most interesting sequences with the closest homologous sequences I used the program Easyfig (Sullivan, Petty, and Beatson 2011). To verify the degree of correlation between the different dioxygenases, key enzymes in the hydrocarbon degradation pathways identified in the 6 different genomes, I used MEGA X (S. Kumar et al. 2018), a phylogenetic and molecular evolutionary software.

3) Results and discussion

The output (Fig. 3.1) generated, following sequencing by Illumina Miseq highlighted the presence of multiple clusters, in particular 59 clusters for culture 2B, 46 for culture A2, 15 for culture 41 and 7 for culture 4. The *de novo* assembly highlighted the presence of two different genomes for culture 2B, A2 and 41, while 3 different genomes were detected in culture 4 (table 3.1).

Phylogenetic investigations using three housekeeping genes (Table 3.2) identified three Gammaproteobacteria, two Alphaproteobacteria and one Clostridia. In particular housekeeping gene analysis (table 3.2) clearly indicated the presence of the following strains: *Alkaliphilus oremlandii* OhILAs, *Epibacterium scottomollicae* DSM 25328, *Halomonas alkaliantarctica* strain FS-N4, *Oceanicaulis alexandrii* HTCC2633, and *Pseudoalteromonas spiralis* DSM 16099 c4. Conversely, a double affiliation was found for *Alcanivorax* since *recA* and *rpoB* matching the sequences belonging to *Alcanivorax dieselolei* B5, while *gyrB* was affiliated to *Alcanivorax xenomutans* p 40.

The results of Average Nucleotide identity (Table 3.3) highlighted the presence of new species for *Alkaliphilus oremlandii* sp, *Halomonas alkaliantarctica* sp, *Oceanicaulis alexandrii* sp and *Pseudoalteromonas spiralis* sp, with highest ANI values of 77.47%, 87.63%, 82.53% and 93.99%, below the species similarity cutoff of 96% (Richter and Rosselló-Móra 2009; Kim et al. 2014). Conversely, the ANI alignment for *Alcanivorax* sp. and *Epibacterium* sp. led to the assignment of such taxa to the species *Alcanivorax xenomutans* p 40 and *Epibacterium scottomollicae* DSM 25328 since the values were respectively 97.53% and 98.82%.

Surprisingly, the alignment of the de novo *Pseudoalteromonas spiralis* sp. with *Pseudoalteromonas* sp. DL-6 showed an ANI value (93.99%) greater than the alignment with *Pseudoalteromonas spiralis* DSM 16099 c4 (88.78%) which was the closest species as indicated by the marker gene score.

The same was observed for the de novo *Halomonas alkaliantarctica* sp. with higher ANI values following alignment with *H. ventosae* NRS2Hap1 (87.20%), *H. sp.* R57-5 (87.18), *H.sp.* K0166 (85.67) and *H. olivaria* TYRC17 (87.63%) compared to *Halomonas alkaliantarctica* strain FS-N4 (78.68%). Although a negative correlation between marker gene and ANI values has been described by Kim et al. (2014) and Gomila et al. (2015), these findings are not very frequent compared to the inter-species concordance between marker genes and ANI values. A possible explanation for this uncoupling may be due to the presence of chemical pollutants which may force horizontal gene transfer and therefore the composition of genomes (Zhang et al. 2018). However, further investigations based on concatenated genes are required in order to fully assess the novelty of draft genomes here presented.

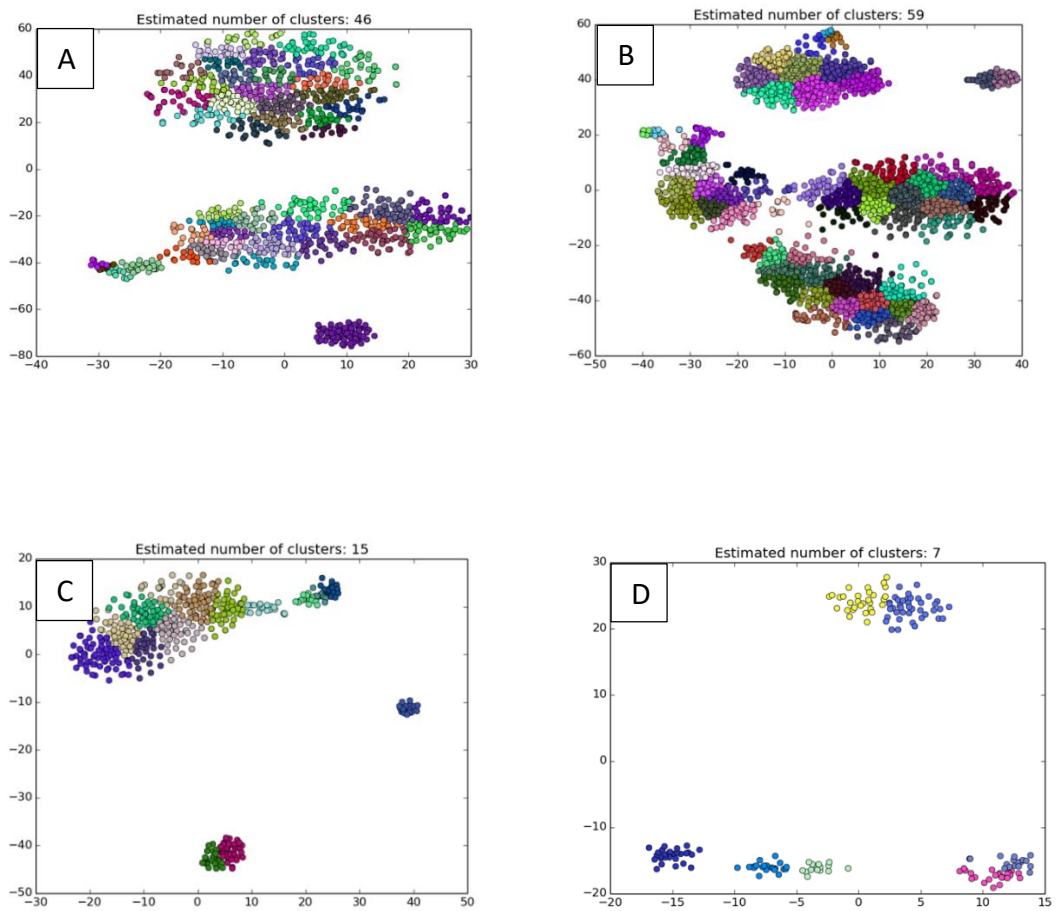


Figure 3.1. Illumina Miseq Output after sequencing. The different colours of the dots represent a different number of estimated clusters for consortia 2B (A), A2 (B), 41 (C) and 4 (D).

Table 3.1. List of identified strains per culture consortia (see text for explanation)

Original culture ID	Identified genomes
2B consortium	<i>Halomonas</i> sp. <i>Pseudoalteromonas</i> sp.
41 consortium	<i>Pseudoalteromonas</i> sp. <i>Alkaliphilus</i> sp. <i>Alcanivorax</i> sp.
4 consortium	<i>Epibacterium</i> sp., <i>Alkaliphilus</i> sp., <i>Glycoaulis</i> sp. <i>Halomonas</i> sp.
A2 consortium	<i>Halomonas</i> sp., <i>Alcanivorax</i> sp.

Table 3.2. Homology % of marker genes in recombinase A (*recA*), DNA gyrase subunit B (*gyrB*) and RNA polymerase subunit B (*rpoB*)

Identified taxa	Marker genes	% homology	E value	Taxa
<i>Alcanivorax</i> sp.	<i>recA</i>	97.97	0.0	<i>Alcanivorax dieselolei</i> B5
	<i>gyrB</i>	99.88	0.0	<i>Alcanivorax xenomutans</i> p 40
	<i>rpoB</i>	98.08	0.0	<i>Alcanivorax dieselolei</i> B5
<i>Alkaliphilus</i> sp.	<i>recA</i>	82.39	0.0	<i>Alkaliphilus oremlandii</i> OhILAs
	<i>gyrB</i>	79.30	0.0	<i>Alkaliphilus oremlandii</i> OhILAs
	<i>rpoB</i>	80.82	0.0	<i>Alkaliphilus oremlandii</i> OhILAs
<i>Epibacterium</i> sp	<i>recA</i>	100	0.0	<i>Epibacterium scottomollicae</i> DSM 25328
	<i>gyrB</i>	100	0.0	<i>Epibacterium scottomollicae</i> DSM 25328
	<i>rpoB</i>	100	0.0	<i>Epibacterium scottomollicae</i> DSM 25328
<i>Halomonas</i> sp.	<i>recA</i>	99.72	0.0	<i>Halomonas alkaliantarctica</i> strain FS-N4

	gyrB	100	0.0	<i>Halomonas alkaliantarctica</i> strain FS-N4
	rpoB	99.85	0.0	<i>Halomonas alkaliantarctica</i> strain FS-N4
<i>Oceanicaulis</i> sp.	recA	100	0.0	<i>Oceanicaulis alexandrii</i> HTCC2633
	gyrB	99.75	0.0	<i>Oceanicaulis alexandrii</i> HTCC2633
	fusA	99.06	0.0	<i>Oceanicaulis alexandrii</i> HTCC2633
<i>Pseudoalteromonas</i> sp.	recA	99.71	0.0	<i>Pseudoalteromonas spiralis</i> DSM 16099 c4
	gyrB	100	0.0	<i>Pseudoalteromonas spiralis</i> DSM 16099 c4
	rpoB	100	0.0	<i>Pseudoalteromonas spiralis</i> DSM 16099 c4

Table 3.3: Results of the average nucleotide alignment. Each reference genome was chosen following the output generated by blast of the 3 largest contigs for each genome, assembled with MYCC

Identified taxa	Reference strains used for the comparison	ANI Identity	SD	NCBI reference sequence
<i>Alcanivorax</i> sp..	<i>Alcanivorax borkumensis</i> SK2	77.99%	5.74%	NC_008260
	<i>alcanivorax dieselsoi</i> B5	93.41%	3.08%	NC_018691
	<i>Acanivorax</i> sp. N3-2°	80.84%	6.95%	CP022307.1
	<i>Alcanivorax xenomutans</i> strain P40	98.82%	2.12%	NZ_CP012331.1
	<i>Gottschalkia acidurici</i> 9°	73.62%	3.15%	CP003326.1
	<i>Alkaliphilus oremlandii</i> OhILAs	77.47%	4.80%	NC_009922.1

<i>Alkaliphilus</i> sp..	<i>Clostridium formicaceticum</i> strain DSM 92	73.55%	3.91%	NZ_CP020559.1
	<i>Alkaliphilus metalliredigens</i> QYMF,	74.50%	4.24%	NC_009633.1
<i>Epibacterium</i> sp.	<i>Ruegeria</i> sp.TM1040	81.86%	4.59%	NC_008044.1
	<i>Ruegeria mobilis</i> F1926	83.24%	5.38%	CP015230.1
	<i>Epibacterium mobile</i> EPIB1	83.09%	5.21%	NZ_LR027553.1
	<i>Epibacterium scottomollicae</i> strain DSM 25328	97.53%	1.60%	PVUF01000001.1
<i>Halomonas</i> sp.	<i>halomonas ventosae</i> NRS2Hap1	87.20%	4.37%	CP022737.1
	<i>halomonas</i> sp.R57-5.	87.18%	4.38%	NZ_LN813019.1
	<i>halomonas</i> sp.Ko166	85.67%	4.96%	NZ_CP011052.1
	<i>halomonas olivara</i> TYRC17	87.63%	4.23%	AP019416.1
	<i>Halomonas alkaliantarctica</i> strain FS-N4	78.68%	4.92%	JHQL01000001.1
<i>Oceanicaulis</i> sp.	<i>Parvibaculum lavamentivorans</i> DS-1	74.09%	3.66%	NC_009719.1
	<i>Maricaulis maris</i> MCS10	75.38%	3.78%	NC_008347.1
	<i>Glycocaulis alkaliphilus</i> strain 6B-8	76.23%	4.18%	CP018911.1
	<i>Brevundimonas naejangsanensis</i> strain FS1091	73.98%	3.77%	CP038027
	<i>Oceanicaulis alexandrii</i> HTCC2633	82.53%	4.56%	CH672428.1
<i>Pseudoalteromonas</i> sp.	<i>pseudoalteromonas tetradonis</i> strain GFC	89.49%	4.78%	CP011041.1
	<i>pseudoalteromonas</i> sp. DL-6	93.99%	3.67%	NZ_CP019770.1
	<i>pseudoalteromonas issachenkonii</i> strain KMM3549	89.41%	4.74%	CP011030
	<i>pseudoalteromonas issachenkonii</i> strain KCTC12958	89.33%	4.77%	CP013350.1
	<i>pseudoalteromonas</i> sp. SM9913	89.57%	4.77%	NC_014803.1
	<i>Pseudoalteromonas spiralis</i> strain DSM 16099 c4	88.78%	5.44%	LVCN01000034.1

3. 1) General features of Metagenome Assembled Genomes (MAGs)

3.1.1) *Halomonas* sp. SZN1

Complete genome sequencing (Fig. 3.2) of *Halomonas* sp. SZN1, a gammaproteobacteria belonging to the Order Oceanospirillales, was 4,673,840 bp long; CheckM analysis showed a 100% completeness with a contamination of 0.87% as two markers were duplicated (Tab. 3.4). *Halomonas* sp. SZN1 had a G+C content of 54.8% and contained 4217 predicted protein-coding sequences (CDSs) with an average length of 1006.73 with a protein coding density of 88.32% (Tab. 3.4). Of the total predicted CDSs, 3200 (75.9%) were assigned as functional, 1017 (24.11%) were classified as hypothetical and 74 (1.75%) as coding for RNAs (see Clusters of Orthologous Groups (COG) annotation in Fig. 3.2 and Tab. 3.4). Thirty-four Genomic Islands (GIs) (part of a genome that has evidence of horizontal origins) were predicted in the genome of *Halomonas* sp. SZN1 using the integration of IslandPath-DIMOB, SIGI-HMM and Island Pick provided by IslandViewer4 (Bertelli et al. 2017), comprising a total of 334,200 bp (7.15% of the genome) and 281 predicted CDSs of which 151 were classified as proteins of unknown function. The most interesting GC island (Fig. 3.3), relying on automatic annotation, was in the genome region between 1.96 Mb and 1.995 Mb that included genes involved in PAHs degradation. In addition, heavy metal cation efflux coding genes were found along the GIs, suggesting that horizontal gene transfer may have increased hydrocarbon degradation capacity.

Table 3.4: General genomic features of *Halomonas* sp. SZN 1

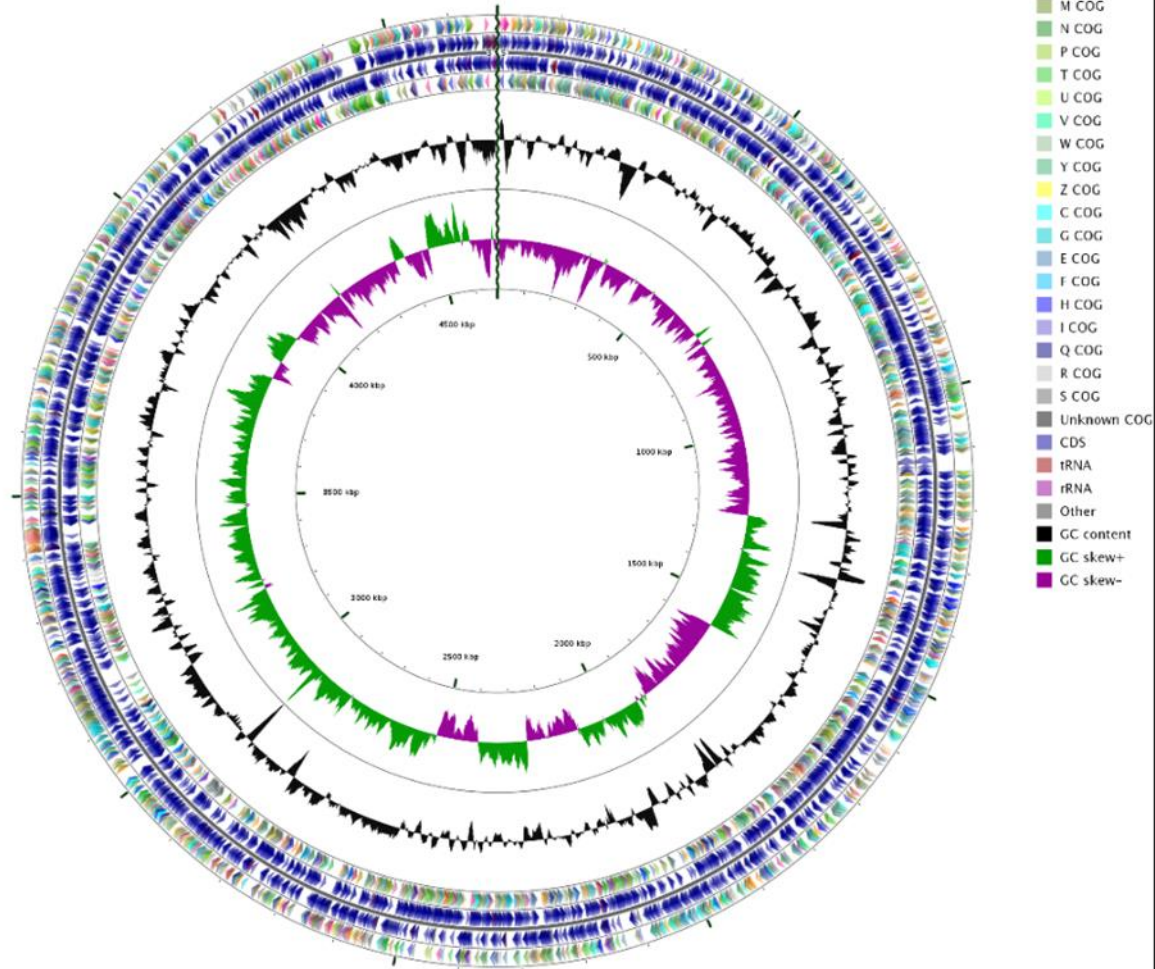
HALOMONAS SP. SZN 1

CHECKM COMPLETENESS	100%
CHECKM CONTAMINATION	0.87%
SIZE, BP	4,673,840
G+C CONTENT, %	54.8
N50	282492
L50	6
NUMBER OF CONTIGS (WITH PEGS)	41
NUMBER OF SUBSYSTEMS	498
NUMBER OF CODING SEQUENCES	4217
FUNCTION ASSIGNED	3200
HYPOTHETICAL	1017
NUMBER OF RNAS	74

Accession: HLOA2.1

Length: 4,677,840 bp

Topology: linear



Halomonas sp. SZN1

Figure 3.2. Circular representation of *Halomonas* sp. SZN1 genome. The different rings represent (from outer to inner) predicted protein-coding sequences (CDS) on the forward (outer wheel) and the reverse (inner wheel) strands (circle 2 and 3) colored according to the assigned COG classes (circle 1, 4), G+C content (circle 5), GC skew (circle 6), genomic position (circle 7). The COG colors represent functional groups (A, RNA processing and modification; B, chromatin structure and dynamics; J, Translation, ribosomal structure and biogenesis; K, Transcription; L, Replication, recombination and repair; D, Cell cycle control, cell division, chromosome partitioning; O, Posttranslational modification, protein turnover, chaperones; M, Cell wall/membrane/envelope biogenesis; N, Cell motility; P, Inorganic ion transport and metabolism; T, Signal transduction mechanisms; U, Intracellular trafficking, secretion, and vesicular transport; V, Defense mechanisms; W, Extracellular structures; Y, Nuclear structure; Z, Cytoskeleton; C, Energy production and conversion; G, Carbohydrate transport and metabolism; E, Amino acid transport and metabolism; F, Nucleotide transport and metabolism; H, Coenzyme transport and metabolism; I, Lipid transport and metabolism; Q, Secondary metabolites biosynthesis, transport and catabolism; R, General function prediction only; S, Function unknown)

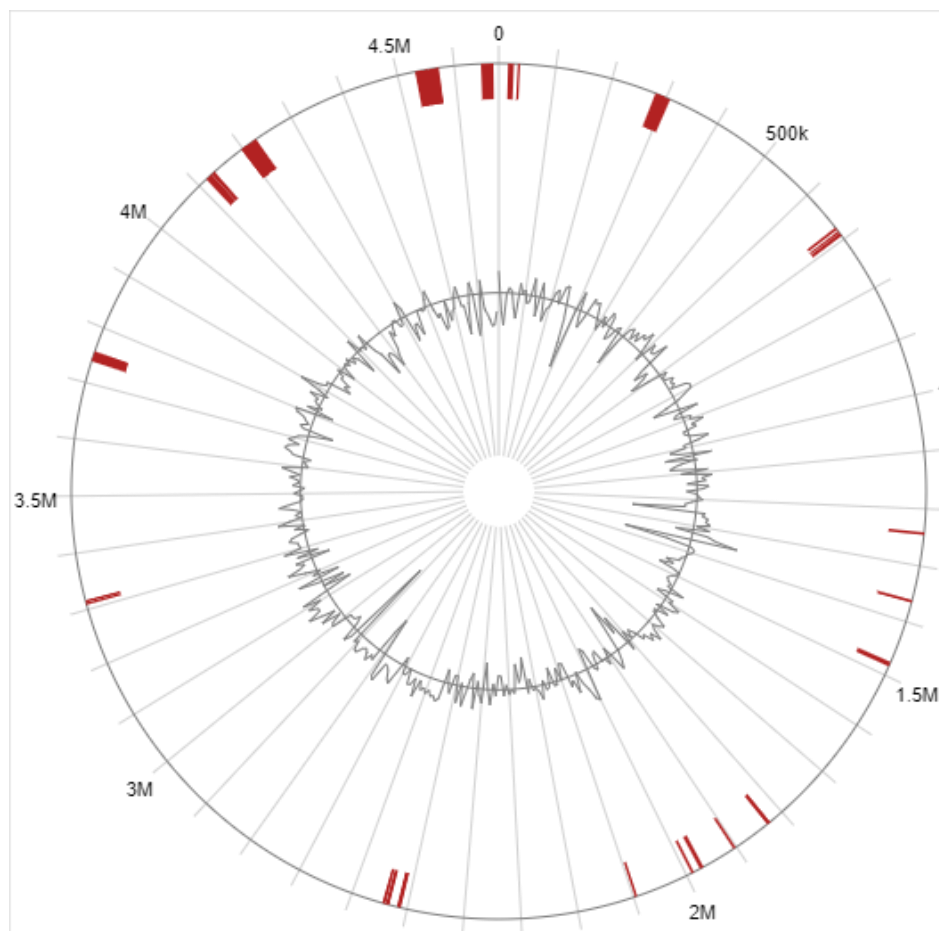


Figure 3.3. The red bars indicate the Genomic Islands found in *Halomonas* sp. SZN1. The most interesting GC island was in the genome region between 1.96 Mb and 1.995.

3.1.2) *Alcanivorax* sp. SZN2.

Alcanivorax sp. SZN2 complete genome (Fig. 3.4), a gammaproteobacteria belonging to the Order Oceanospirillales, presents 3,881,818 bases; CheckM analysis showed a completeness of 83.6% (70 markers missing) and a contamination of 0.5% (3 markers duplicated) (Tab. 3.5). *Alcanivorax* sp. SZN2 presents a GC content of 61.5% and 3528 predicted coding sequences with an average length of 956.77 bp having a protein coding density of 90.01% (Tab. 3.5). Of the total predicted CDSs, 2.641 (74.8%) were assigned a function. 887 (25.1%) were classified as hypothetical and 36 (1%) as coding for RNAs (see COG annotation in Fig. 3.4 and Tab. 3.5), Twenty four GIs were predicted for the *Alcanivorax* sp. SZN2 genome using the integration of IslandPath-DIMOB, SIGI-HMM and Island Pick provided IslandViewer4 (Bertelli et al. 2017), comprising a total of 181,712bp (4.68% of the genome) and 177 predicted CDSs of which 88 were classified as proteins of unknown function (Fig. 3.5).

From the automatic annotation provided by island viewer it was possible to identify only one gene (beta-ketoadipyl CoA thiolase) as 1673405-1674613, involved in the beta-ketoadipate pathway, a metabolic central pathway of hydrocarbon degradation (Song 2009).

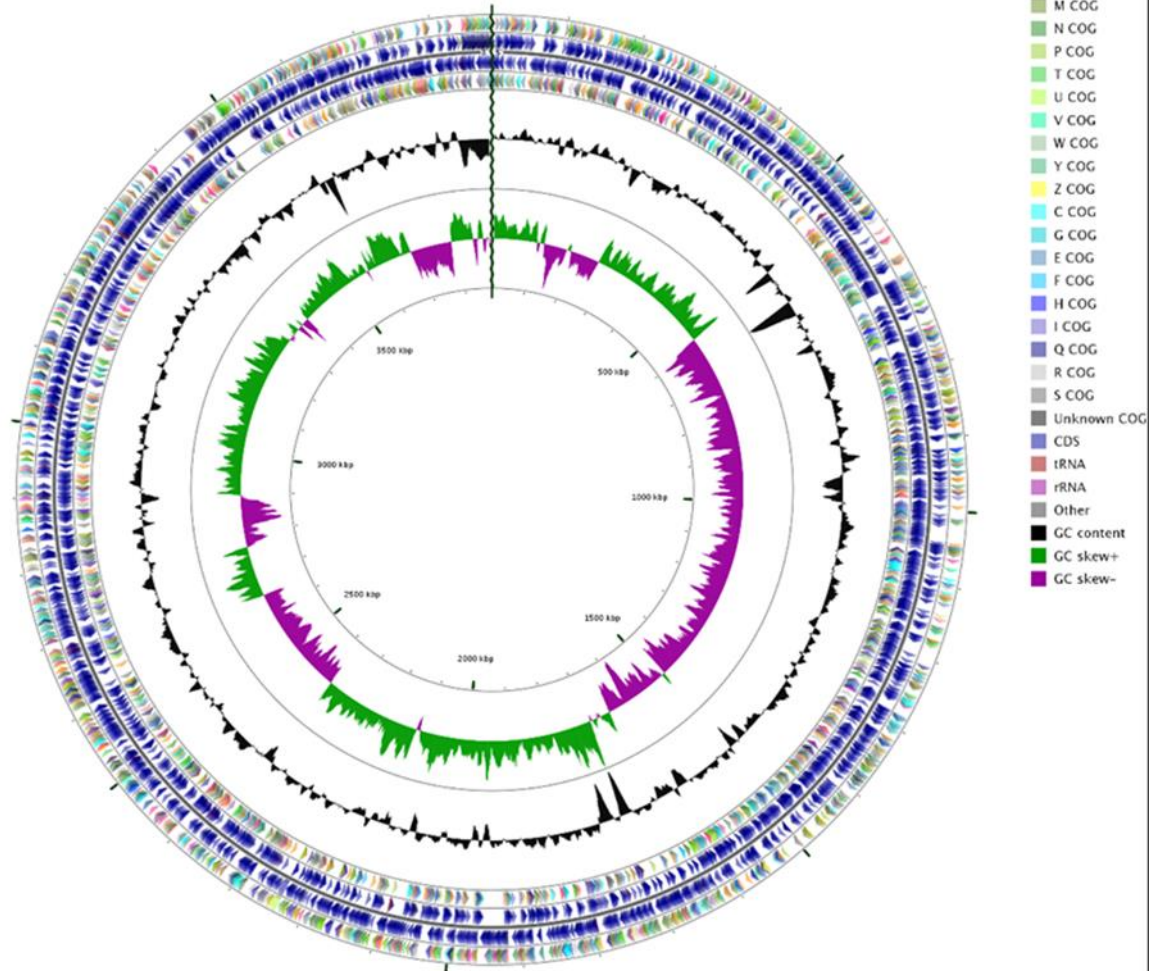
Table 3.5. General genomic features of *Alcanivorax* sp. SZN2.

ALCANIVORAX SP. SZN2	
CHECKM COMPLETENESS	83.6
CHECKM CONTAMINATION	0.47%
SIZE, BP	3,881,818
G+C CONTENT, %	61,5
N50	306,384
L50	5
NUMBER OF CONTIGS (WITH PEGS)	55
NUMBER OF SUBSYSTEMS	388
NUMBER OF CODING SEQUENCES	3528
FUNCTION ASSIGNED	2,641
HYPOTHETICAL	887
NUMBER OF RNAS	36

Accession: AVXA2.1

Length: 3,881,818 bp

Topology: linear



Alcanivorax sp. SZN2

Figure 3.4. Circular representation of *Alcanivorax* sp. SZN2 genome. The different rings represent (from outer to inner) predicted protein-coding sequences (CDS) on the forward (outer wheel) and the reverse (inner wheel) strands (circle 2 and 3) colored according to the assigned COG classes (circle 1, 4), G+C content (circle 5), GC skew (circle 6), genomic position (circle 7). The COG colors represent the functional groups (A, RNA processing and modification; B, chromatin structure and dynamics; J, Translation, ribosomal structure and biogenesis; K, Transcription; L, Replication, recombination and repair; D, Cell cycle control, cell division, chromosome partitioning; O, Posttranslational modification, protein turnover, chaperones; M, Cell wall/membrane/envelope biogenesis; N, Cell motility; P, Inorganic ion transport and metabolism; T, Signal transduction mechanisms; U, Intracellular trafficking, secretion, and vesicular transport; V, Defense mechanisms; W, Extracellular structures; Y, Nuclear structure; Z, Cytoskeleton; C, Energy production and conversion; G, Carbohydrate transport and metabolism; E, Amino acid transport and metabolism; F, Nucleotide transport and metabolism; H, Coenzyme transport and metabolism; I, Lipid transport and metabolism; Q, Secondary metabolites biosynthesis, transport and catabolism; R, General function prediction only; S, Function unknown)

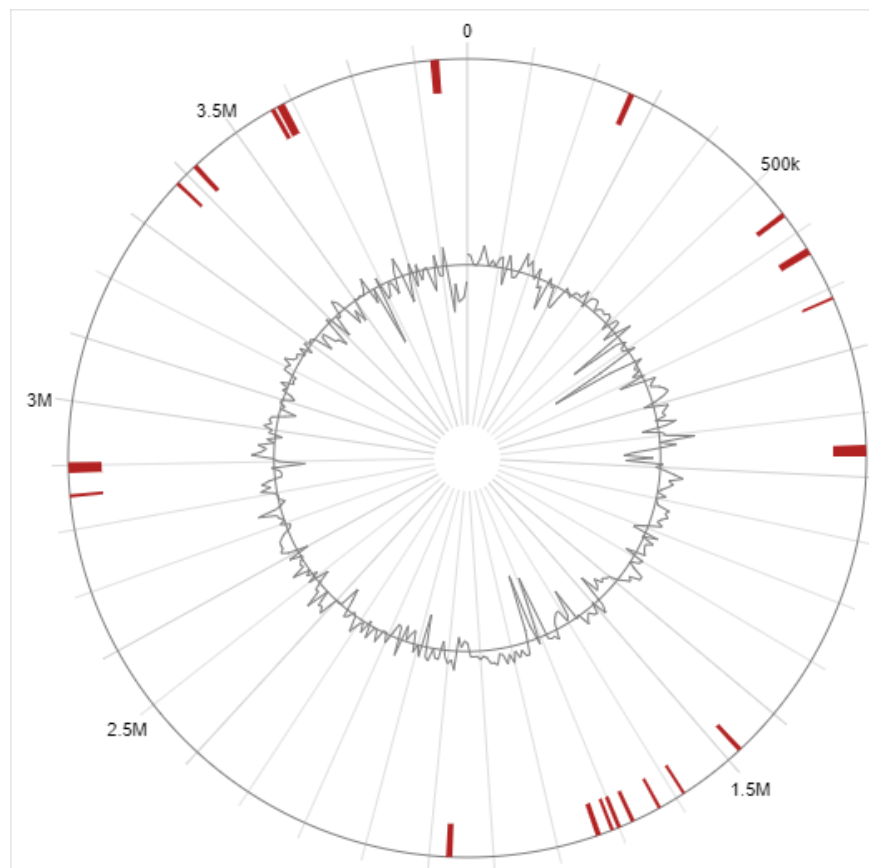


Figure 3.5. The red bars indicate the Genomic Islands found in *Alcanivorax* sp. SZN2. From the automatic annotation provided by island viewer only one gene (beta-ketoadipyl CoA thiolase; 1673405-1674613 bp), linked to central hydrocarbon degradation pathway has been identified

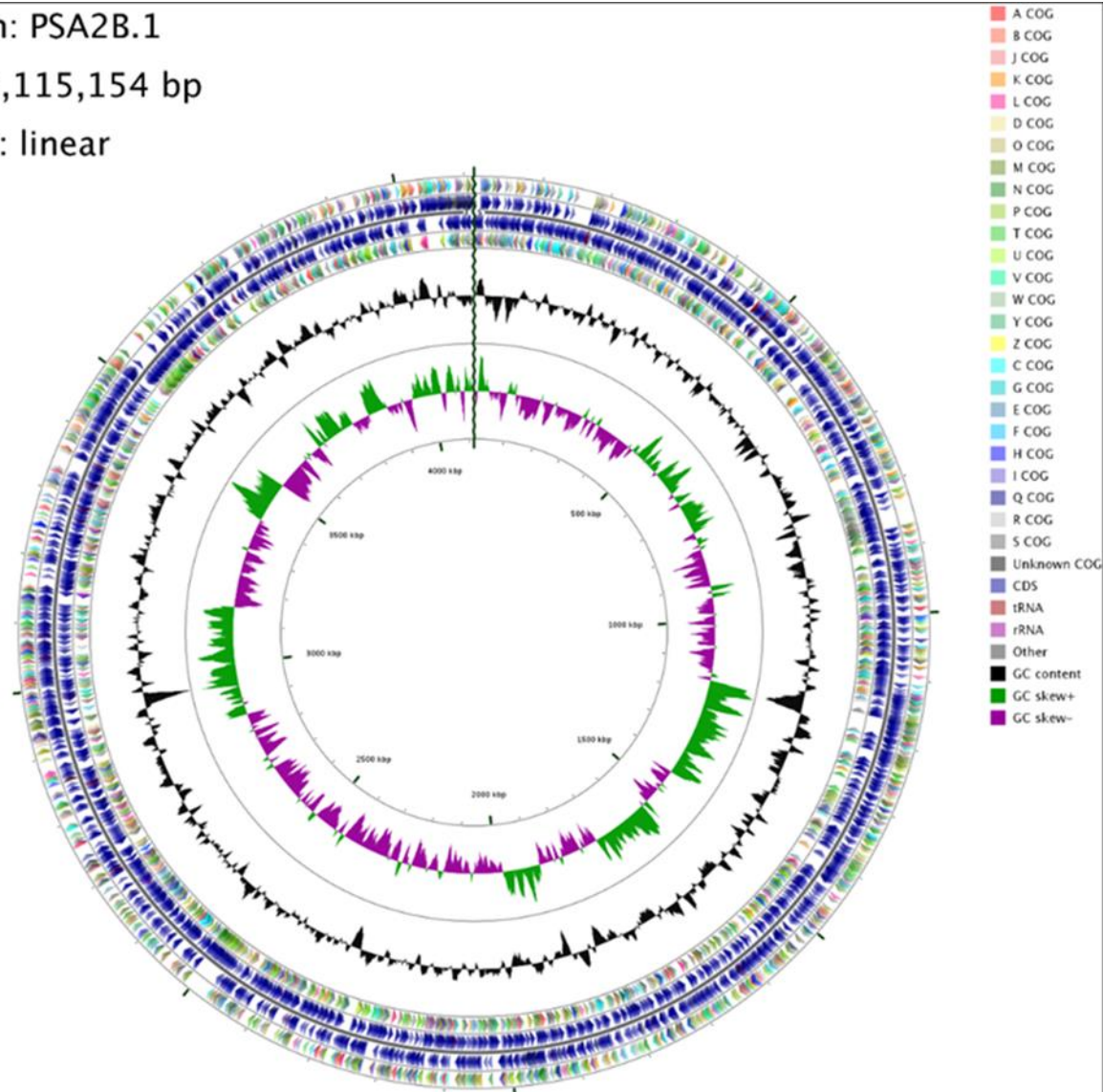
3.1.3) *Pseudoalteromonas* sp. SZN3

The *Pseudoalteromonas* sp. SN3 complete genome (Fig. 3.6), a Gammaproteobacteria belonging to the Order Alteromonadales, presents 4,115,154 bases; CheckM analysis showed a completeness of 100% and a contamination of 2.6 % (20 markers duplicated) (Tab. 3.6). *Pseudoalteromonas* sp. SZN3 had a GC content of 39.9 % and 3674 predicted coding sequences with an average length of 957.61 bp having a protein coding density of 89.01% (Tab. 3.6). Of the total predicted CDSs, 2.661 (72.4%) were assigned a function, 1013 (27.6%) were classified as hypothetical and 128 (3,5%) as coding for RNAs (see COG annotation in Fig. 3.6 and Tab. 3.6). Eighteen GIs were predicted (Fig. 3.7) for the *Pseudoalteromonas* sp. SZN3 genome using the integration of IslandPath-DIMOB, SIGI-HMM and Island Pick provided IslandViewer4 (Bertelli et al. 2017), with a total of 214,638 bp (5.2% of the genome) and 250 predicted CDSs of which 123 were classified as proteins of unknown function. No genes involved in metal tolerance and hydrocarbon degradation were detected in the identified genome islands.

Table 3.6. General genomic features of *Pseudoalteromonas* sp. SZN3

PSEUDOALTEROMONAS SP. SZN3	
CHECKM COMPLETENESS	100%
CHECKM CONTAMINATION	2,64%
SIZE, BP	4,115,154
G+C CONTENT, %	39.9
N50	267815
L50	6
NUMBER OF CONTIGS (WITH PEGS)	32
NUMBER OF SUBSYSTEMS	461
NUMBER OF CODING SEQUENCES	3674
FUNCTION ASSIGNED	2661
HYPOTHETICAL	1013
NUMBER OF RNAS	128

Accession: PSA2B.1
Length: 4,115,154 bp
Topology: linear



***Pseudoalteromonas* sp. SZN3**

Figure 3.6. Circular representation of *Pseudolateromonas* sp. SZN3 genome. The different rings represent (from outer to inner) predicted protein-coding sequences (CDS) on the forward (outer wheel) and the reverse (inner wheel) strands (circle 2 and 3) colored according to the assigned COG classes (circle 1, 4), G+C content (circle 5), GC skew (circle 6), genomic position (circle 7). The COG colors represent the functional groups (A, RNA processing and modification; B, chromatin structure and dynamics; J, Translation, ribosomal structure and biogenesis; K, Transcription; L, Replication, recombination and repair; D, Cell cycle control, cell division, chromosome partitioning; O, Posttranslational modification, protein turnover, chaperones; M, Cell wall/membrane/envelope biogenesis; N, Cell motility; P, Inorganic ion transport and metabolism; T, Signal transduction mechanisms; U, Intracellular trafficking, secretion, and vesicular transport; V, Defense mechanisms; W, Extracellular structures; Y, Nuclear structure; Z, Cytoskeleton; C, Energy production and conversion; G, Carbohydrate transport and metabolism; E, Amino acid transport and metabolism; F, Nucleotide transport and metabolism; H, Coenzyme transport and metabolism; I, Lipid transport and metabolism; Q, Secondary metabolites biosynthesis, transport and catabolism; R, General function prediction only; S, Function unknown)

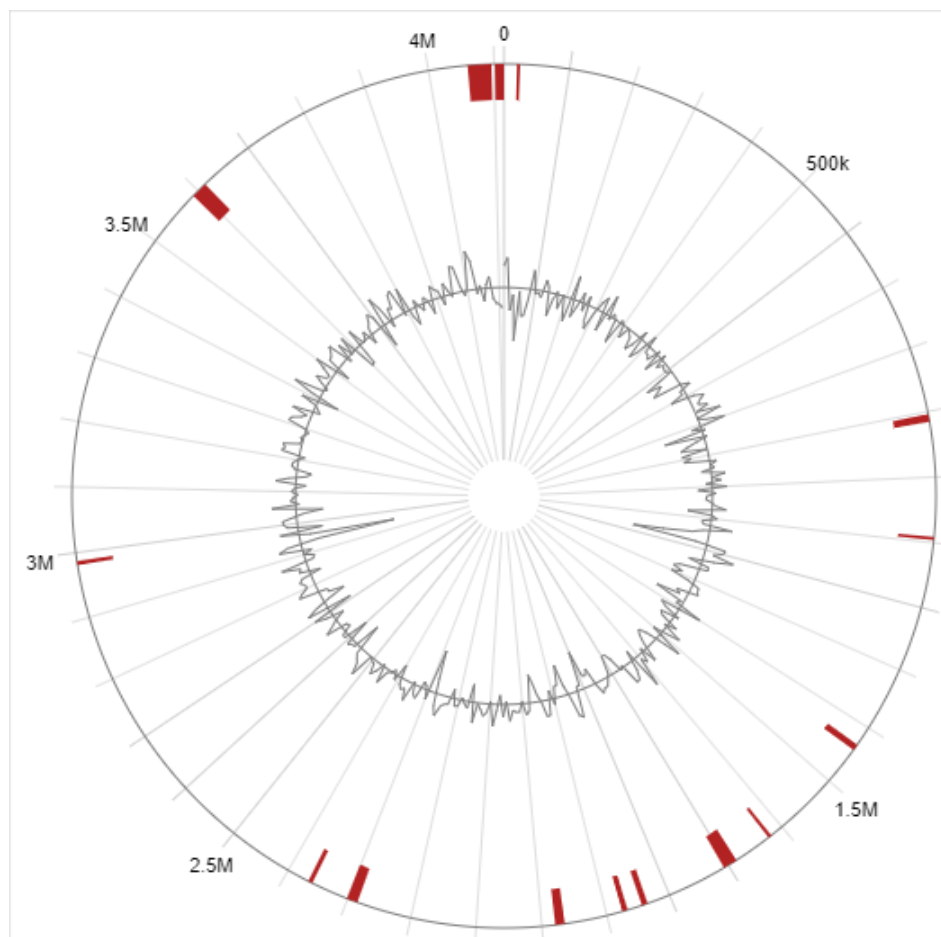


Figure 3.7. The red bars indicate the Genomic Islands found in *Pseudoalteromonas* sp. SZN3. No genes involved in metal tolerance and hydrocarbon degradation were detected in the identified genome islands.

3.1.4) *Epibacterium* sp. SZN4

The complete genome of *Epibacterium* sp. SZN4 (Fig. 3.8), an Alphaproteobacteria belonging to the Order Rhodobacterales, presents 4,702,605 bases; CheckM analysis showed a completeness of 99.9% (1 marker missing) and a contamination of 0.4 % (2 markers duplicated) (Tab. 3.7). *Epibacterium* sp. SZN4 had a GC content of 60.95 % and 4547 predicted coding sequences with an average length of 873.28 bp having a protein coding density of 89.32% (Tab. 3.7). Of the total predicted CDSs, 3295 (72.4%) were assigned a function, 1252 (27.5%) were classified as hypothetical and 46 (1%) as coding for RNAs (see COG annotation in Figure 3.8, and Table 3.7). Thirty five GIs were predicted for the *Pseudoalteromonas* sp. SZN4 genome using the integration of IslandPath-DIMOB, SIGI-HMM and Island Pick provided IslandViewer4 (Bertelli et al. 2017), with a total of 610,124bp (12.97% of the genome) and 776 predicted CDSs of which 494 were classified as proteins of unknown function.

Genes involved in mechanisms of resistance to Zinc, Cadmium Nickel, Copper (CzcA, czrB NccC, CopA, cueR) and Mercury (merR, merT, merA) were identified in the region between 4.25M and 4.65M (Fig. 3.9) which has numerous transposase and integrase sites suggesting that these genes may have been acquired through horizontal transfer.

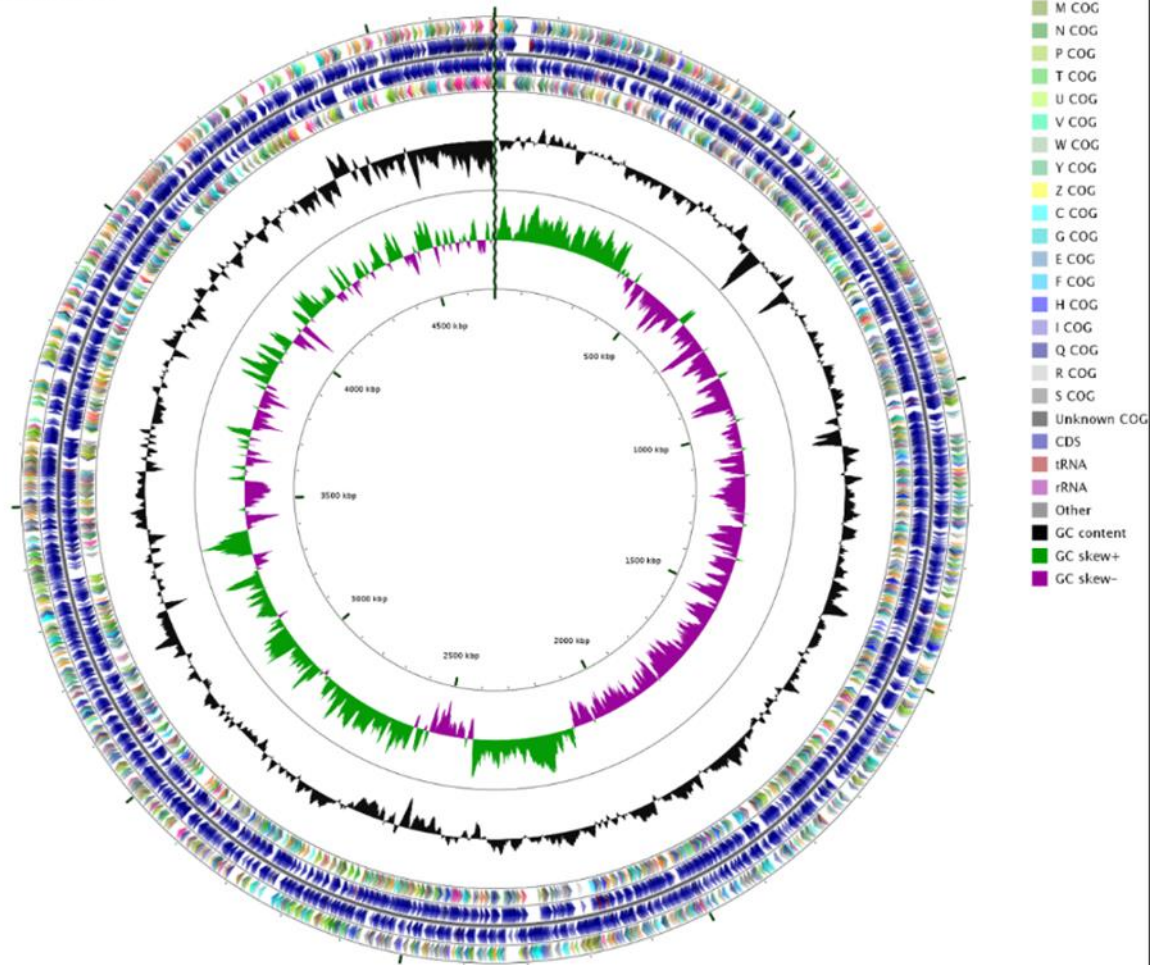
Table 3.7. General genomic features of *Epibacterium* sp. SZN 4

EPIBACTERIUM SP. SZN4	
CHECKM COMPLETENESS	99.1%
CHECKM CONTAMINATION	0.4%
SIZE, BP	4,702,605
G+C CONTENT, %	60.95%
N50	298271
L50	63
NUMBER OF CONTIGS (WITH PEGS)	73
NUMBER OF SUBSYSTEMS	465
NUMBER OF CODING SEQUENCES	4547
FUNCTION ASSIGNED	3295
HYPOTHETICAL	1252
NUMBER OF RNAS	46

Accession: RG4.1

Length: 4,702,605 bp

Topology: linear



Epibacterium sp. SZN4

Figure 3.8. Circular representation of *Epibacterium* sp. SZN4 genome. The different rings represent (from outer to inner) predicted protein-coding sequences (CDS) on the forward (outer wheel) and the reverse (inner wheel) strands (circle 2 and 3) colored according to the assigned COG classes (circle 1, 4), G+C content (circle 5), GC skew (circle 6), genomic position (circle 7). The COG colors represent functional groups (A, RNA processing and modification; B, chromatin structure and dynamics; J, Translation, ribosomal structure and biogenesis; K, Transcription; L, Replication, recombination and repair; D, Cell cycle control, cell division, chromosome partitioning; O, Posttranslational modification, protein turnover, chaperones; M, Cell wall/membrane/envelope biogenesis; N, Cell motility; P, Inorganic ion transport and metabolism; T, Signal transduction mechanisms; U, Intracellular trafficking, secretion, and vesicular transport; V, Defense mechanisms; W, Extracellular structures; Y, Nuclear structure; Z, Cytoskeleton; C, Energy production and conversion; G, Carbohydrate transport and metabolism; E, Amino acid transport and metabolism; F, Nucleotide transport and metabolism; H, Coenzyme transport and metabolism; I, Lipid transport and metabolism; Q, Secondary metabolites biosynthesis, transport and catabolism; R, General function prediction only; S, Function unknown)

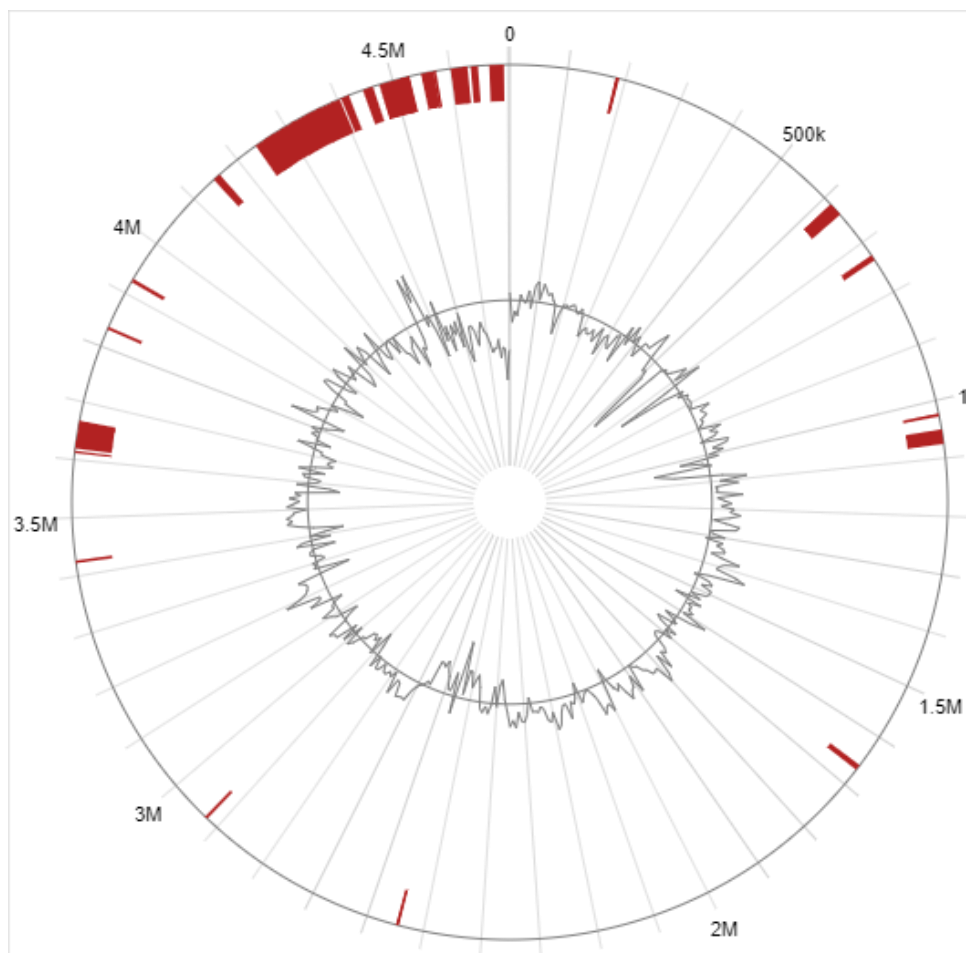


Figure 3.9. The red bars indicate the Genomic Islands found in *Epibacterium* sp. SZN4. The following genes *CzcA*, *czrB*, *NccC*, *CopA*, *cueR*, *merR*, *merT*, *merA* involved in mechanisms of resistance to Zinc, Cadmium Nickel, Copper and Mercury were identified in the region between 4.25M and 4.65M

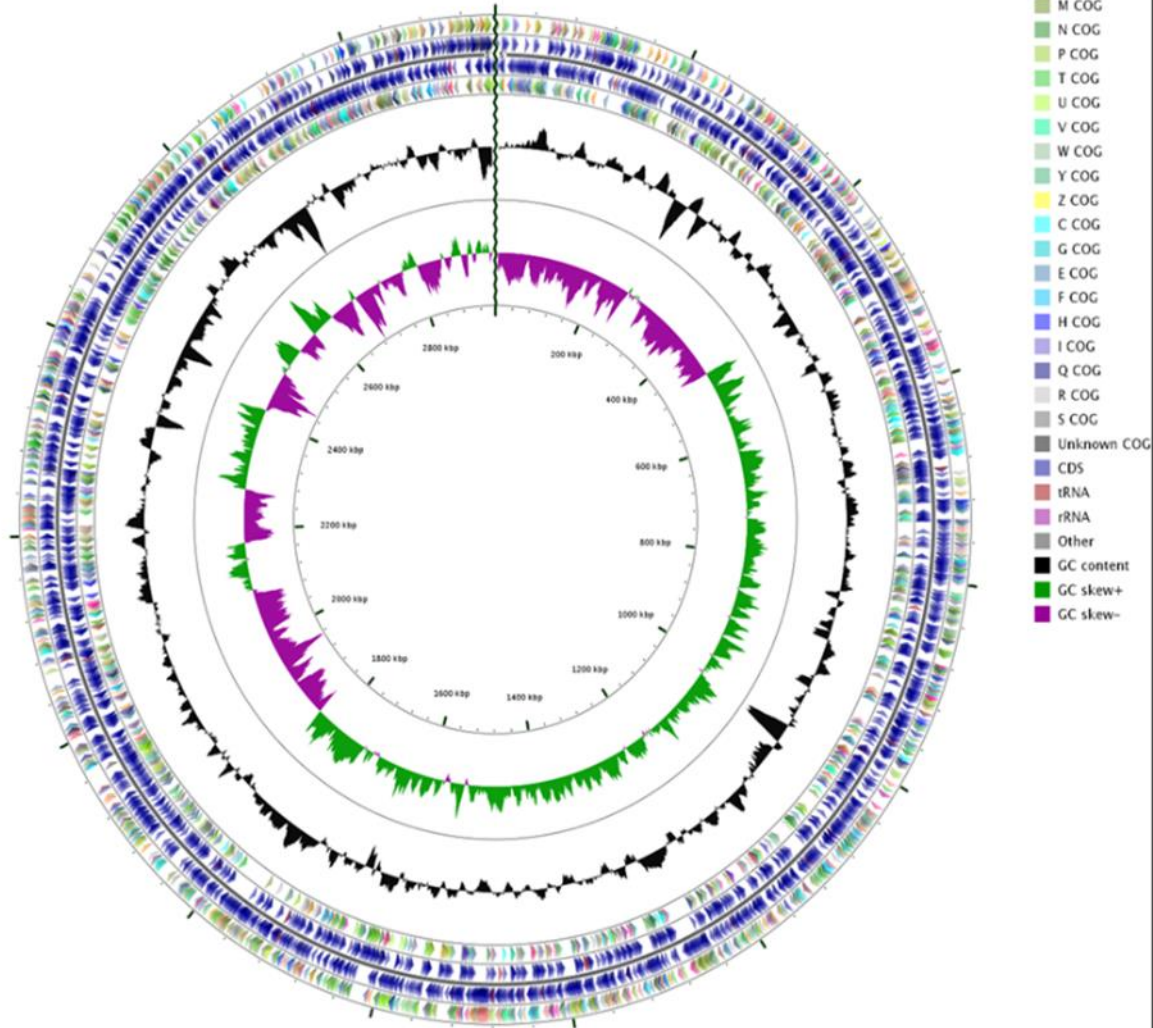
3.1.5) *Oceanicaulis* sp. SZN5

The complete genome of *Oceanicaulis* sp. SZN5 (Fig. 3.10), an Alphaproteoacteria belonging to the Order Rhodobacterales, presents 2,954,327 bases; CheckM analysis showed a completeness of 96.5 % (27 markers missing) and a contamination of 0.32 % (1 marker duplicated) (Tab. 3.8). *Oceanicaulis* sp. SZN5. had a GC content of 62.71 % and 2873 predicted coding sequences with an average length of 937.28 bp having a protein coding density of 91.51% (Tab. 3.8). Of the total predicted CDSs, 1995 (69.4%) were assigned a function, 842 (29.3%) were classified as hypothetical and 44 (1,5%) as coding for RNAs (see COG annotations in Fig. 3.10 and Tab. 3.8). Eleven GIs were predicted for the *Oceanicaulis* sp. SZN5 genome using the integration of IslandPath-DIMOB, SIGI-HMM and Island Pick provided IslandViewer4 (Bertelli et al. 2017), with a total of 129,287 bp (4.39% of the genome) and 151 predicted CDSs of which 42 were classified as proteins of unknown function. MATE multi-drug resistance genes possibly involved in mechanisms of resistance to metals (B. Dong et al. 2019) were identified in the region between 1.142 M and 1.154 M (Fig 3.11).

Table 3.8. General genomic features of *Oceanicaulis* sp. SZN5

OCEANICAULIS SP. SZN5	
CHECKM COMPLETENESS	96.5%
CHECKM CONTAMINATION	0.3%
SIZE, BP	2,954,327
G+C CONTENT, %	62.71%
N50	209292
L50	2
NUMBER OF CONTIGS (WITH PEGS)	40
NUMBER OF SUBSYSTEMS	383
NUMBER OF CODING SEQUENCES	2837
FUNCTION ASSIGNED	1995
HYPOTHETICAL	842
NUMBER OF RNAS	44

Accession: MRL4.1
Length: 2,954,327 bp
Topology: linear



***Oceanicaulis* sp. SZN5**

Figure 3.10. Circular representation of *Oceanicaulis* sp. SZN5 genome. The different rings represent (from outer to inner) predicted protein-coding sequences (CDS) on the forward (outer wheel) and the reverse (inner wheel) strands (circle 2 and 3) colored according to the assigned COG classes (circle 1, 4), G+C content (circle 5), GC skew (circle 6), genomic position (circle 7). The COG colors represent functional groups (A, RNA processing and modification; B, chromatin structure and dynamics; J, Translation, ribosomal structure and biogenesis; K, Transcription; L, Replication, recombination and repair; D, Cell cycle control, cell division, chromosome partitioning; O, Posttranslational modification, protein turnover, chaperones; M, Cell wall/membrane/envelope biogenesis; N, Cell motility; P, Inorganic ion transport and metabolism; T, Signal transduction mechanisms; U, Intracellular trafficking, secretion, and vesicular transport; V, Defense mechanisms; W, Extracellular structures; Y, Nuclear structure; Z, Cytoskeleton; C, Energy production and conversion; G, Carbohydrate transport and metabolism; E, Amino acid transport and metabolism; F, Nucleotide transport and metabolism; H, Coenzyme transport and metabolism; I, Lipid transport and metabolism; Q, Secondary metabolites biosynthesis, transport and catabolism; R, General function prediction only; S, Function unknown)

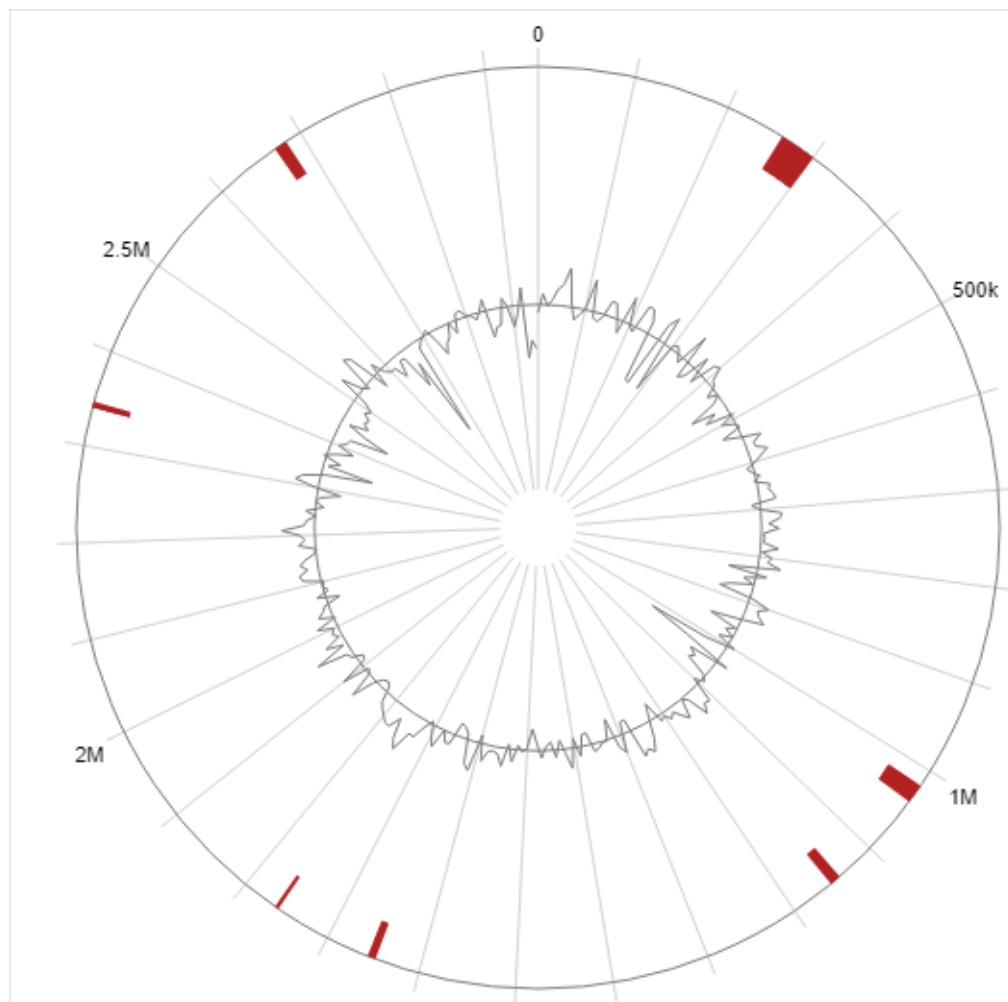


Figure 3.11. The red bars indicate the Genomic Islands found in *Oceanicaulis* sp. SZN5. MATE multi-drug resistance genes linked to metals resistance were identified in the region 1.142 M and 1.154 M

3.1.6) *Alkaliphilus* sp. SZN6

The complete genome of *Alkaliphilus* sp. SZN6 (Fig. 3.12), a Clostridium belonging to the Order Clostridiales, presents 2,581,546 bases; CheckM analysis showed a completeness of 98.6 % (2 markers missing) and a contamination of 0.23 % (1 marker duplicated). *Alkaliphilus* sp. SZN6 had a GC content of 29.1% and 2671 predicted coding sequences with an average length of 814.49 bp having a protein coding density of 86.22% (Tab. 3.9). Of the total predicted CDSs, 1827 (68.4%) were assigned a function, 844 (31.6%) were classified as hypothetical and 25 (0.93%) as coding for RNAs (see COG annotations in Fig. 3.12 and Tab. 3.9). Fifteen GIs were predicted for the *Alkaliphilus* sp. SZN6 genome using the integration of IslandPath-DIMOB, SIGI-HMM and Island Pick provided IslandViewer4 (Bertelli et al. 2017), with a total of 155.812 bp (6.1% of the genome) and 213 predicted CDSs of which 61 were classified as proteins of unknown function. MATE multi-drug resistance gene possibly involved in mechanisms of resistance to metals (B. Dong et al. 2019) was identified in the region between 429K and 448K (Fig. 3.13).

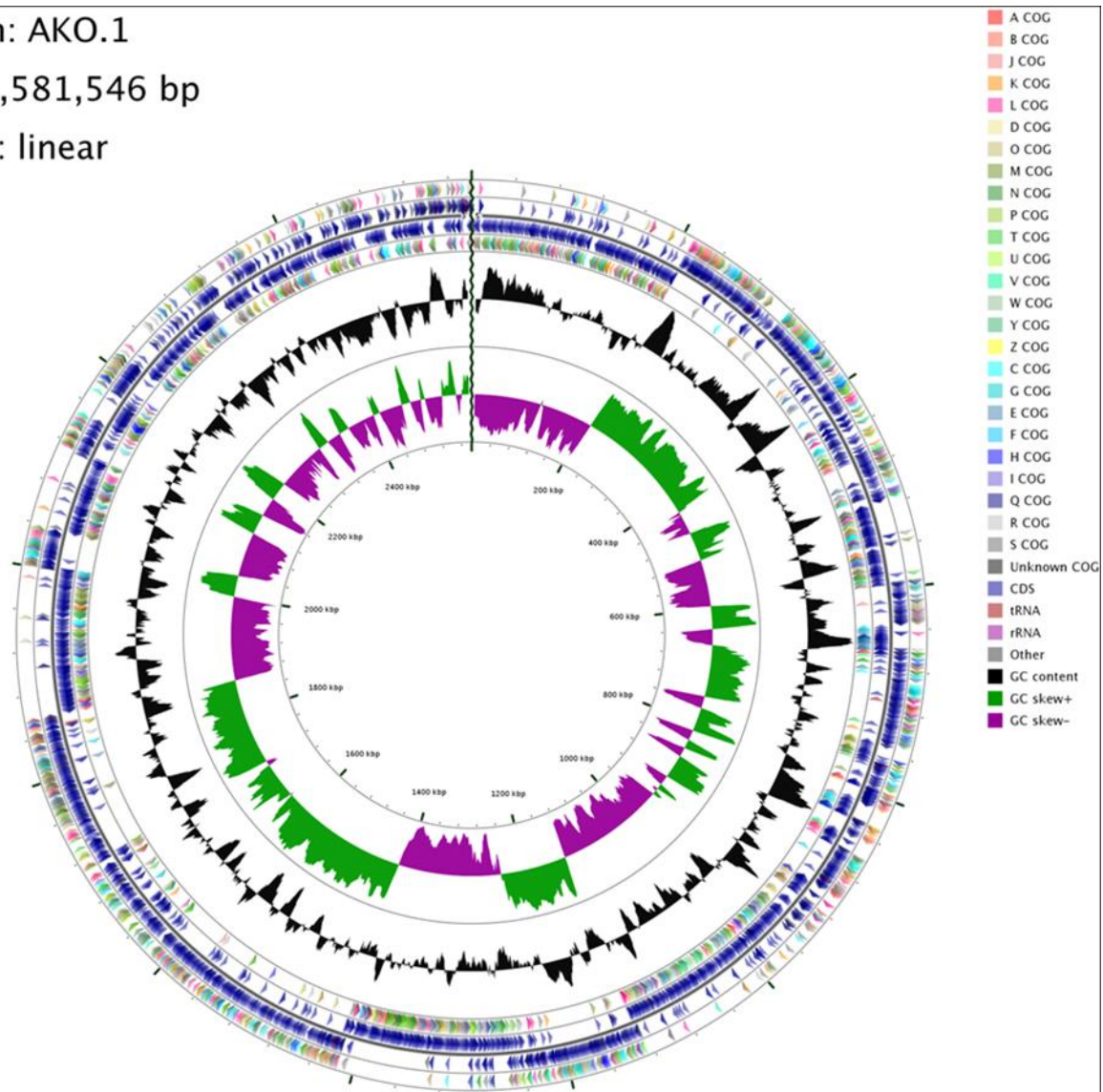
Table 3.9. General genomic features of *Alkaliphilus* sp. SZN6

ALKALIPHILUS SP. SZN6	
CHECKM COMPLETENESS	98.6%
CHECKM CONTAMINATION	0.23%
SIZE, BP	2,581,546
G+C CONTENT, %	29.1%
N50	65217
L50	12
NUMBER OF CONTIGS (WITH PEGS)	81
NUMBER OF SUBSYSTEMS	336
NUMBER OF CODING SEQUENCES	2671
FUNCTION ASSIGNED	1827
HYPOTHETICAL	844
NUMBER OF RNAS	25

Accession: AKO.1

Length: 2,581,546 bp

Topology: linear



Alkaliphilus sp. SZN6

Figure 3.12. Circular representation of *Alkaliphilus* sp. SZN 6 genome. The different rings represent (from outer to inner) predicted protein-coding sequences (CDS) on the forward (outer wheel) and the reverse (inner wheel) strands (circle 2 and 3) colored according to the assigned COG classes (circle 1, 4), G+C content (circle 5), GC skew (circle 6), genomic position (circle 7). The COG colors represent functional groups (A, RNA processing and modification; B, chromatin structure and dynamics; J, Translation, ribosomal structure and biogenesis; K, Transcription; L, Replication, recombination and repair; D, Cell cycle control, cell division, chromosome partitioning; O, Posttranslational modification, protein turnover, chaperones; M, Cell wall/membrane/envelope biogenesis; N, Cell motility; P, Inorganic ion transport and metabolism; T, Signal transduction mechanisms; U, Intracellular trafficking, secretion, and vesicular transport; V, Defense mechanisms; W, Extracellular structures; Y, Nuclear structure; Z, Cytoskeleton; C, Energy production and conversion; G, Carbohydrate transport and metabolism; E, Amino acid transport and metabolism; F, Nucleotide transport and metabolism; H, Coenzyme transport and metabolism; I, Lipid transport and metabolism; Q, Secondary metabolites biosynthesis, transport and catabolism; R, General function prediction only; S, Function unknown)

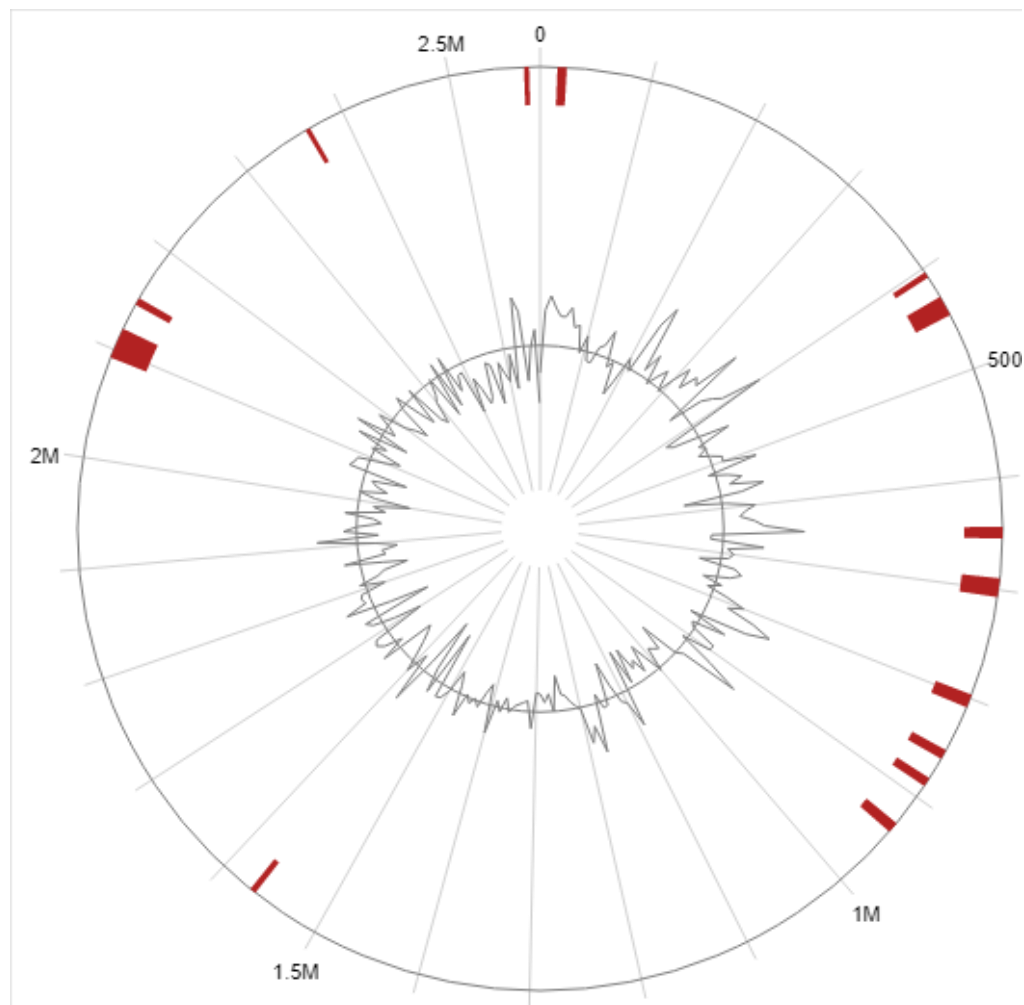


Figure 3.13. The red bars indicate the Genomic Islands found in *Alkaliphilus* sp. SZN6. MATE multi-drug resistance gene, involved in mechanisms of resistance to metals, was identified in the region comprised 429K and 448K.

3.2) Genetic basis of PAHs degradation

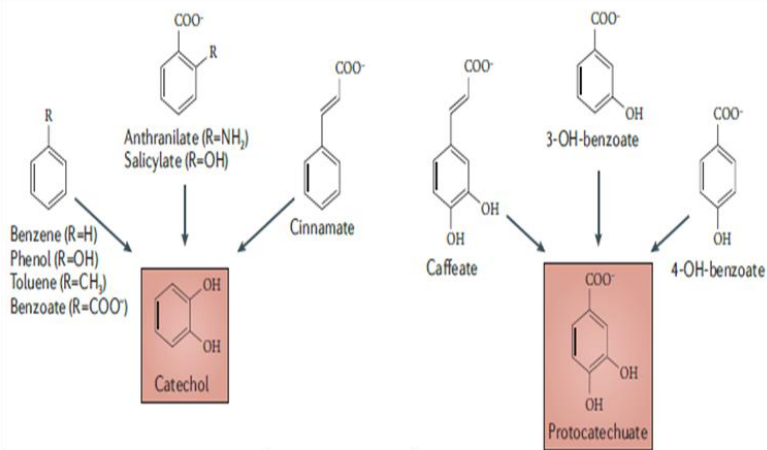
Rapid Annotation using Subsystem Technology (RAST) generated annotation allowed the identification of genes coding for proteins related to the metabolism of Aromatic Compounds (36, 61, 11, 52 and 15 genes for *Alcanivorax* sp. SZN2, *Halomonas* sp. SZN1, *Pseudoalteromonas* sp. SZN3, *Epibacterium* sp. SZN4, and *Oceanicaulis* sp. SZN5, respectively). Figure 3.14 reports the genes involved in the metabolism of Aromatic Compounds and their distribution and number of copies in the different taxa. *Halomonas* sp. SZN1, had the highest number of genes followed by *Epibacterium* sp. SZN4, and *Alcanivorax* sp. SZN2. Interestingly *Alkaliphilus* sp. SZN6 did not possess any gene possibly involved in the degradation of hydrocarbons. Conversely, the automatic annotation of the other five genomes allowed the identification of several genes involved (whose distribution among the draft genomes is reported in Fig. 3.15) in the central pathways of hydrocarbon degradation, including the catechol, protocatechuate, homoprotocatechuate, homogentisate and phenil acetic pathways. The only strain with almost all the enzymes involved in these metabolic pathways was *Halomonas* sp. SZN1 while the other strains possessed only some of the required enzymes. The heterogenous distribution of enzymes involved in pollution-resistance mechanisms found in the five draft genomes can be explained by the fact that they have been isolated in consortia and that therefore each strains may play a complementary role in the degradation of hydrocarbons by producing metabolites accessible for the other bacteria as described by Festa et al. (2017). In addition, it is possible that some enzymes have not been identified by automatic annotation since they may have sequences that are poorly

conserved and were not been found in the reference databases. An example is the absence of enzymes capable of the first oxidation of aromatic rings such as ring hydroxylating dioxygenase. Even if RAST did not provide annotations for such enzymes I proceeded to select enzymes described in the literature as capable of degrading molecules which I later manually blasted within the draft genomes. In this way, I succeeded in identifying two enzymes able to catalyze, through the addition of an oxygen atom in the aromatic ring (Fig 3.15), the initial step in the aerobic bacterial PAH degradation pathway: ring hydroxylating dioxygenase (RHD) subunit α (2Fe-2S) (Singleton, Hu, and Aitken 2012) and cytochrome P450 (Brezna et al. 2006). In particular I found these enzymes in the draft genome of *Alcanivorax* sp. SZN2, *Halomonas* sp. SZN1, *Pseudoalteromonas* sp. SZN3, and *Epibacterium* sp. SZN4.



Figure 3.14. Heat map of genes and relative copy numbers identified by RAST in the five draft genomes analyzed. On the left column are indicated genes involved in the metabolism of aromatic compounds. The different colour intensity is related to number of gene copies. (white: “no genes”; dark green “max. number of genes)

A



B

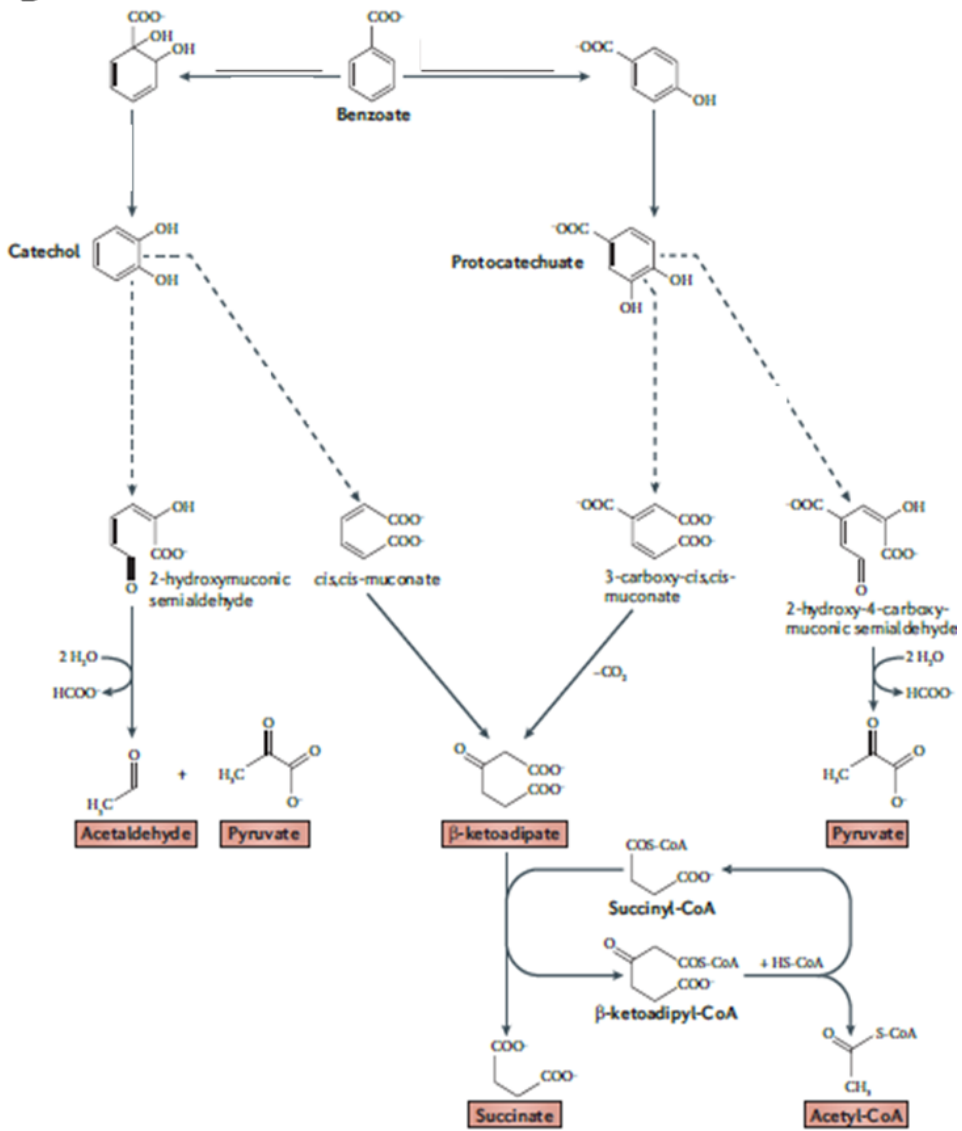


Figure 3.15. Aromatic hydrocarbon degradation pathway. A) catechol and protocatechuate produced as central intermediates of aerobic pathways. B) Degradation pathway of Benzoate. Benzoate can be degraded through a dioxygenase or a monooxygenase. Both the enzymes capable of such reactions (Ring Hydroxylating Dioxygenase and Cytochrome P 450 monooxygenase) have been identified in the draft genomes of *Halomonas* sp. SZN1, *Alcanivorax* sp. SZN2, *Pseudolateromonas* sp. SZN3, *Epibacterium* sp. SZN4. The cis hydroxylation via dioxygenase favours the formation of Salicylate and the subsequent Catechol formation through salicylate hydroxylase found in *Alcanivorax* sp. SZN2, *Halomonas* sp. SZN1, and *Epibacterium* sp. SZN4. The catechol became substrate of catechol 1,2 dioxygenase (only in *Halomonas* sp. SZN1) that led to formation of cis cis muconic acid and β ketoadipic acid. This compound enters the β -ketoadipate pathway that, through the β -ketoadipate succinyl CO-A transferase and β ketoadipyl thiolase (*Halomonas* sp. SZN1, *Epibacterium* sp. SZN4, *Pseudoalteromonas* sp. SZN3, and *Oceanicaulis* sp. SZN5), led to the formation of Acetyl CoA and succinyl CoA. The trans hydroxylation via monooxygenase led to the formation of protocatechuate intermediate. This pathway begins with a hydroxylation in position 3 of 4-Hydroxybenzoate by hydroxybenzoate hydroxylase, found only in the genomes of *Halomonas* sp. SZN1, and *Epibacterium* sp. SZN4, which leads to the formation of the compound 3,4 hydroxybenzoate. The next step is catalyzed by the protocatechuate enzyme 3, 4 dioxygenase able to convert 3, 4 hydroxybenzoate in β carboxy muconate which through the activity of 3 carboxy ci-cis muconolactone cycloisomerase is transformed in γ Carboxy muconolactone. The protocatechuate 3, 4 dioxygenase sequence found in *Halomonas* sp. SZN1, and *Epibacterium* sp. SZN4. The subsequent decarboxylation reaction catalyzed by the enzyme 4 carboxy muconolactone decarboxylase is described only in *Halomonas* sp. SZN1, *Epibacterium* sp. SZN4, and *Oceanicaulis* sp. SZN5. This leads to the formation of 3 oxoadipate enol lactonase which is transformed in 3 oxoadipate by the activity of β ketoadipate enol lactonase, an enzyme identified in the genomes of *Halomonas* sp. SZN1, *Alcanivorax* sp. SZN2, and *Epibacterium* sp. SZN4. The last two steps of the pathway are catalyzed by enzymes whose sequences have been reported only in *Alcanivorax* sp. SZN2, and *Halomonas* sp. SZN1; more specifically, the activity of 3 oxo adipate Co-A transferase promotes the formation of 3 oxoadipyl CoA which becomes a substrate of β ketoadipyl CoA thiolase catalysing the production of succinyl CoA, a compound involved in the citric acid cycle.

3.2.1) Ring Hydroxylating dioxygenase

Generally, *RHDs* need a reductase and a ferredoxin to be functional. In this system, the dioxygenase is composed of large α and small β subunits (Kauppi et al. 1998). The alpha subunit (*RHD α*) contains two conserved regions: the [Fe2-S2] Rieske centre and the mononuclear iron-containing catalytic domain which promotes the incorporation of molecular oxygen into the aromatic nucleus forming a cis-dihydrodiol.

Comparing the sequence (about 20 kb) of *Halomonas* sp. SZN1, including the gene encoding for *Ring Hydroxylating dioxygenase* and the sequences flanking the gene of interest with the closest related sequences corresponding to *Halomonas olivaria* TYR C 17, *Halomonas alkaliphila* X3 and *Halomonas campaniensis*, it was possible to identify about 10 genes in the same position in all four sequences (Fig. 3.15). From this comparative analysis it was possible to observe that in addition to *ring hydroxylating dioxygenase* and *ferredoxin*, both directly involved in the degradation of hydrocarbons, *serin hydroxy methyl transferase* genes, *sarcosine oxydase sub unit* (alpha, beta, gamma) and *formyl tetra hydrofolate deformylase* were also located in proximity of *ring hydroxylating dioxygenase*. The presence of these genes confirms observations by Yan and Wu (2017) that genes associated with the metabolism of glycine and serine are involved in the mechanisms of hydrocarbon degradation.

Conversely, the sequence of *Alcanivorax* sp. SZN2 showed a homology of 100% with the entire gene region of *Alcanivorax xenomutans* sp 40 even if *AraC* and *ThiJ* genes were absent, confirming the results obtained through the average nucleotide alignment (Fig 3.16). Comparison between *Alcanivorax* sp. and *A. dieselsoi* B5 showed a lower correlation than the previous comparison even if 11 Open Reading Frames (ORFs)

(including the *ring hydroxylating dioxygenase*) showed a homology of $\geq 70\%$. Other genes involved in hydrocarbon detoxification and degradation processes were found analyzing the flanking region of *ring hydroxylating dioxygenase* including *glutathione s-transferase*, *linear amide C-N hydrolase*, *aldo-keto reductase* and *nitrite reductase*. According to Cao et al. (2015), Al-Turki (2009) and Lloyd-Jones and Lau (1997), *glutathione s transferase* is often involved in PAH degradation processes due to its ability to render compounds less toxic. *Aldo keto reductase* is involved in PAHs degradation since it is capable of oxidating trans dihydrodiols and reducing PAHs or quinones to PAHs catechols (Zhang et al. 2012). According to Imperato et al. (2019) and Salam and Ishaq (2019), *amidase (C-N hydrolase)* and *nitrite reductase* are associated with the benzoate, styrene and pyrene degradation pathways. Similarly to *Alcanivorax* sp., comparison of the sequences of *Pseudoaltromonas* sp. SZN3 with *Pseudoalteromonas* sp. DL-6 showed a high conservation of the gene region under examination, with a homology close to 100% for enzyme ring hydroxylating dioxygenase and for the subsequent transporter (Fig. 3.17).

Comparison of the gene regions of *Pseudoalteromonas tetradonis* GFC and *Pseudoalteromonas* sp. SM9913 showed a reduced homology with the draft genome, highlighting the absence of dioxygenase and thus a different gene rearrangement. Analysis of the ring hydroxylating dioxygenase flanking region indicated the presence of 2 other genes involved in the degradation of hydrocarbons: a *rubredoxin reductase* and an *aldehyde dehydrogenase* (ORF 6, 7, 8) which according to Brooijmans, Pastink, and Siezen (2009) are involved in the degradation of alkanes and pyrene. Similarly to *Pseudoalteromonas* sp. SZN3, *Epibacterium* sp. SZN4 showed a different genetic

reorganization compared to the 3 genomes: *Epibacterium mobile* EPIB1, *Ruegeria mobilis* 1921, *Ruegeria* sp. TM1040 (Fig. 3.18). The only two conserved genes were *NADP dependent oxidoreductase* required for the functionality of dioxygenase and *ring hydroxylating dioxygenase*. In the region flanking the above mentioned enzymes, no genes involved in the degradation of hydrocarbons were found. Finally, a transposase was identified that could indicate a successful gene transfer, capable of explaining such a reduced conservation of the region.

Phylogenetic analysis of the four ring hydroxylating dioxygenases identified in the draft genomes of *Halomonas* sp. SZN1, *Alcanivorax* sp. SZN2., *Pseudoalteromonas* sp. SZN3., and *Epibacterium* sp. SZN4, showed an absence of correlation between the investigated enzyme, clustering the four ring hydroxylating dioxygenases with organisms of the same genus in the case of *Halomonas* sp. SZN1, *Epibacterium* sp. SZN4, and *Oceanicaulis* sp. SZN5 (Fig. 3.19). Interestingly, *Alcanivorax* sp. SZN2 and *Pseudoalteromonas* sp. SZN3 showed an homology with the sequences belonging respectively to *Tistrella mobilis* strain KA081020-065, an alpha protobacterium isolated from the Red Sea (Xu et al. 2012), and to *Vibrio nereis*, isolated from a shrimp intestine in Bangladesh (Mondal et al. 2016).

Halomonas sp. (Ring hydroxylating dioxygenase)

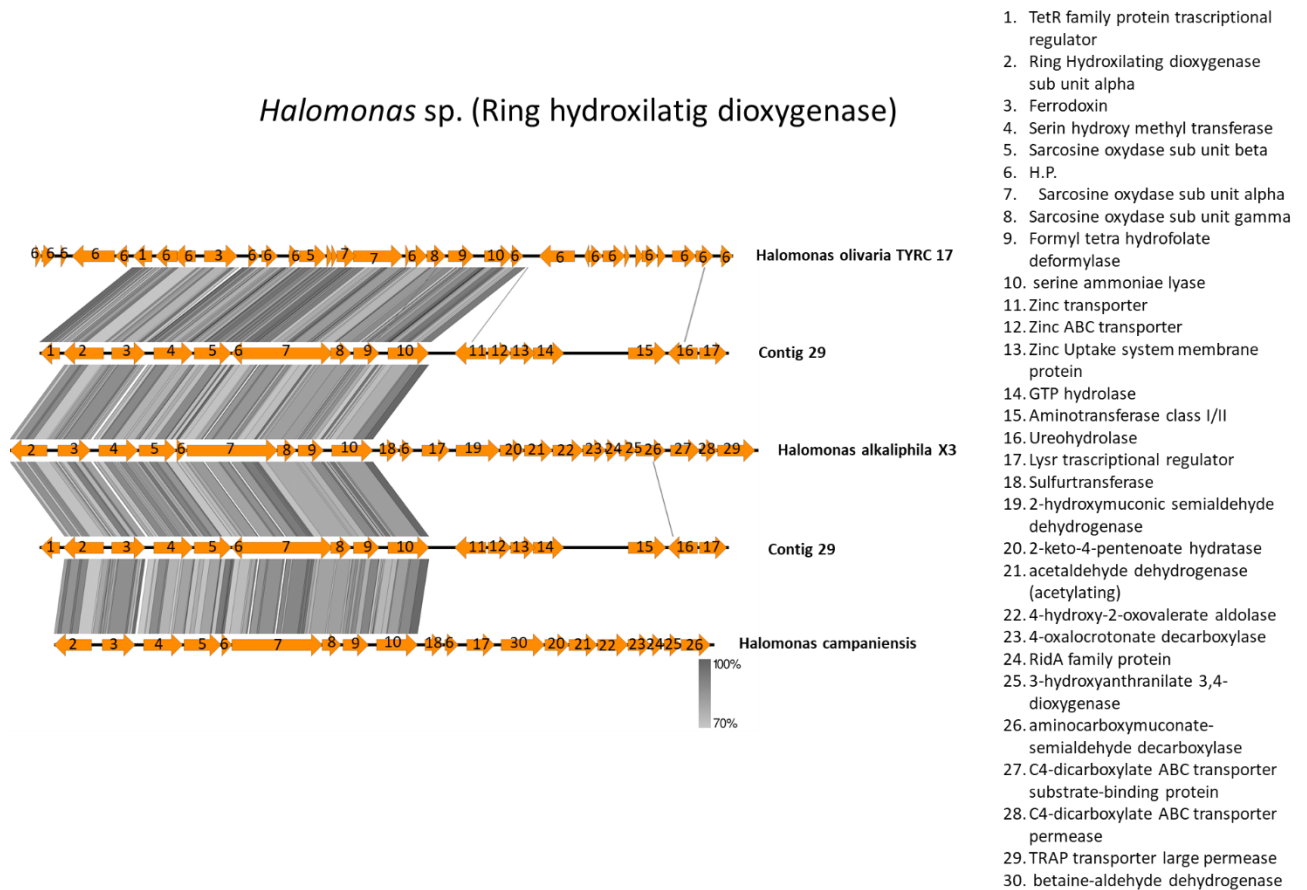
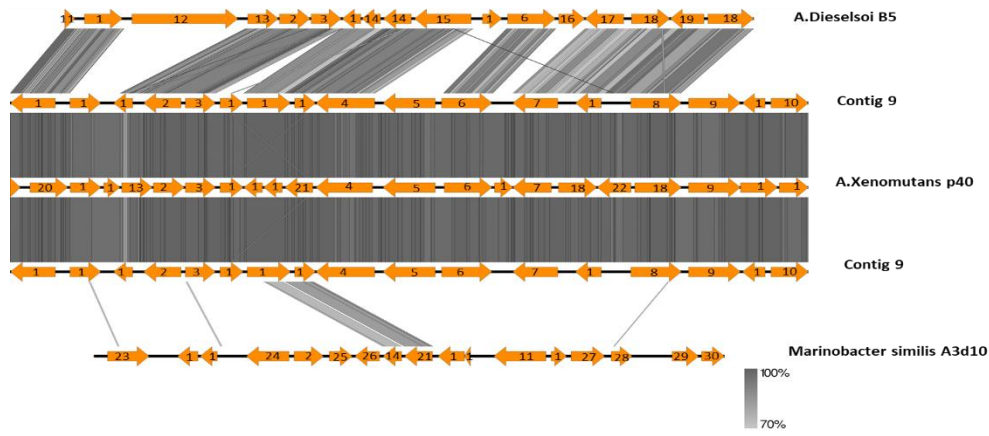


Figure 3.16. Comparison of strain sequences from my *Halomonas* sp. SZN1 draft genome and the three closest sequences identified in the National Centre for Biotechnology Information (NCBI) data bank. Ring hydroxylating dioxygenase (RHD) is indicated as ORF 2. Contig 29 is the genomic region where the gene encoding for RHD was identified in my draft genome. The right panel lists genes that are encoded by *Halomonas* sp. SZN1 (ORFs 1-10) and those that are encoded by reference genomes (ORFs 11-30)

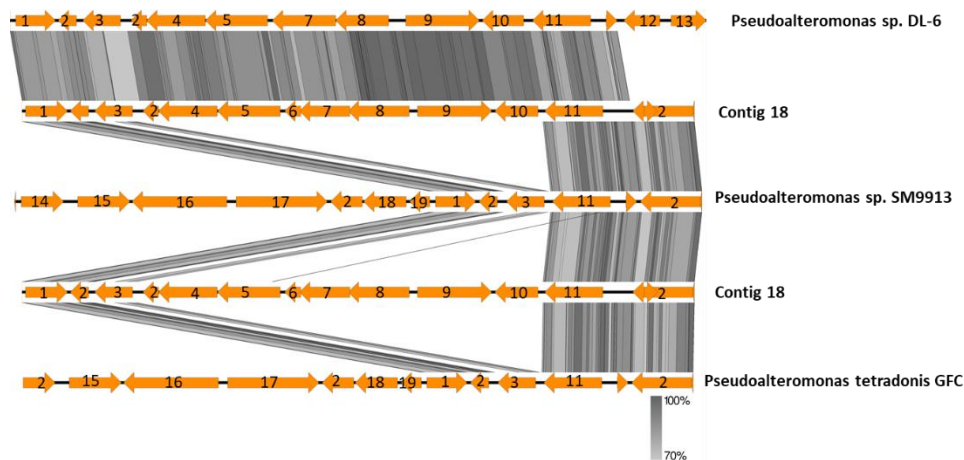
Alcanivorax sp. (Ring Hydroxylating dioxygenase)



1. Hypotetical protein
2. Lys E family translocator
3. Glutathione S transferase
4. Aromatic ring Hydroxylating protein
5. Linear amide C-N hydrolase
6. Aldo ket0 reductase
7. Sulfite exporter TAU/Saf E family protein
8. GLX A family trascriptional regulator
9. Nitrite reductase
10. SCO family protein
11. alpha/beta Hydrolase
12. TON B siderophor receptor
13. epimerase
14. proteinase
15. Protease
16. Phenilacetic acid degradation protein
17. Membrane protein
18. Ara C
19. Hydratase
20. Nucleotydil transferase
21. Glutamine amido tranferase
22. ThiJ
23. Enoil coA hydratase
24. Lys R trascriptional activator
25. EF P translational elongation factor P
26. Glycoside hydrolases
27. Short chain dehydrogenase
28. Organic hydroperoxide resistance protein
29. 2-5 RNA ligase
30. nitrilase/cyanide hydratase and apolipoprotein N- acyltransferase

Figure 3.17. Comparison of strain sequences from my *Alcanivorax* sp. SZN2 draft genome and the three closest sequences identified in the National Centre for Biotechnology Information (NCBI) data bank. Ring hydroxylating dioxygenase is indicated as ORF 4. Contig 9 is the genomic region where the gene encoding for RHD was identified in my draft genome. The right panel lists genes that are encoded by the draft genome of *Alcanivorax* sp. SZN2 (ORFs 1-10) and those that are encoded by reference genomes (ORFs 11-30)

Pseudoalteromonas sp. (Ring Hydroxylating dioxygenase)



1. Lys R family trascriptional regulator
2. Hipotethical protein
3. HDOD domain
4. FAD binding oxido reductase
5. Rubredoxin NAD reductase
6. aldehyde dehydrogenase family protein
7. aldehyde dehydrogenase family protein
8. Ring hydroxylating dioxygenase
9. BCC transporter family
10. Lys R family trascriptional regulator
11. Carbohydrate porin
12. alpha/beta hydrolase
13. exodeoxyribonuclease I
14. Permease
15. transport protein of the major facilitator
16. DNA helicase IV
17. methyl-accepting chemotaxis sensory transducer
18. putative glutathione S-transferase
19. putative membrane DoxD-like family protein

Figure 3.18. Comparison of strain sequences from my *Pseudoalteromonas* sp. SZN3 genome and the three closest sequences identified in the National Centre for Biotechnology Information (NCBI) data bank. Ring hydroxylating dioxygenase is indicated as ORF 8. Contig 18 is the genomic region where the gene encoding for RHD was identified in my draft genome. The right panel lists genes that are encoded by the draft genome of *Pseudoalteromonas* sp. SZN3 (ORFs 1-11) and those that are encoded by reference genomes (ORFs 12-19)

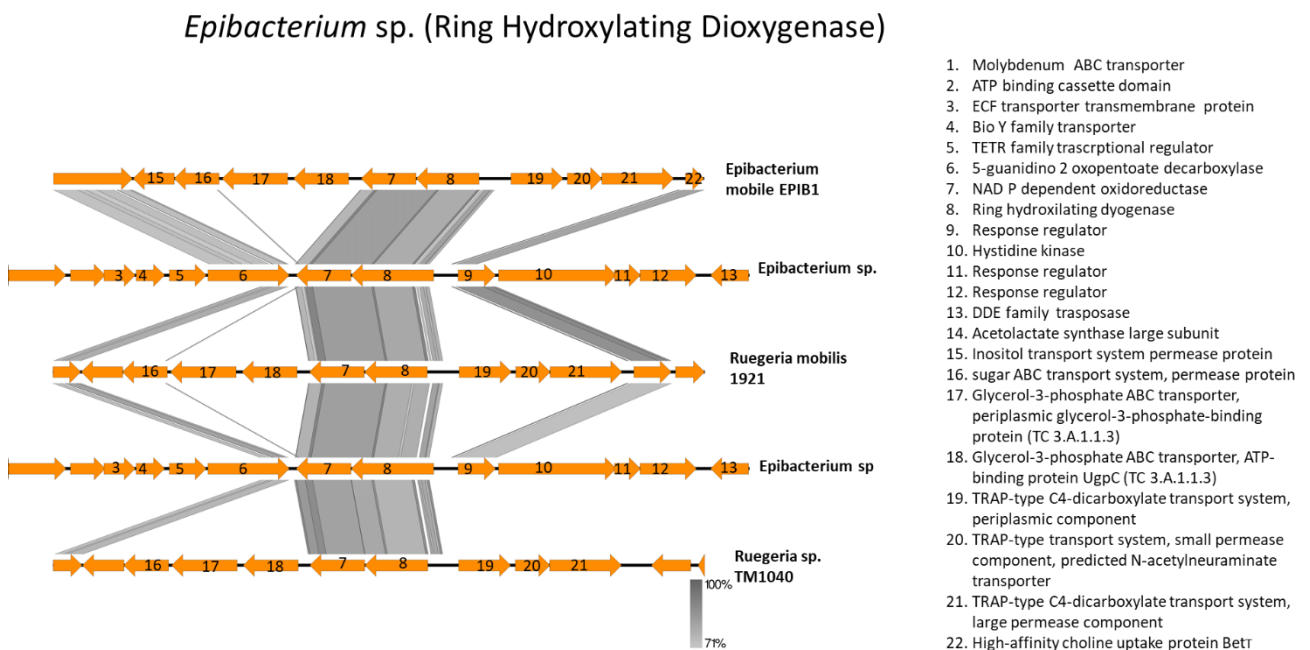


Figure 3.19. Comparison of strain sequences from my *Epibacterium* sp. SZN4 draft genome and the three closest sequences identified in the National Centre for Biotechnology Information (NCBI) data bank. Ring hydroxylating dioxygenase is indicated as ORF 8. The right panel lists genes that are encoded by the draft genome of *Epibacterium* sp. SZN4 (ORFs 1-13) and those that are encoded by reference genomes (ORFs 14-22)

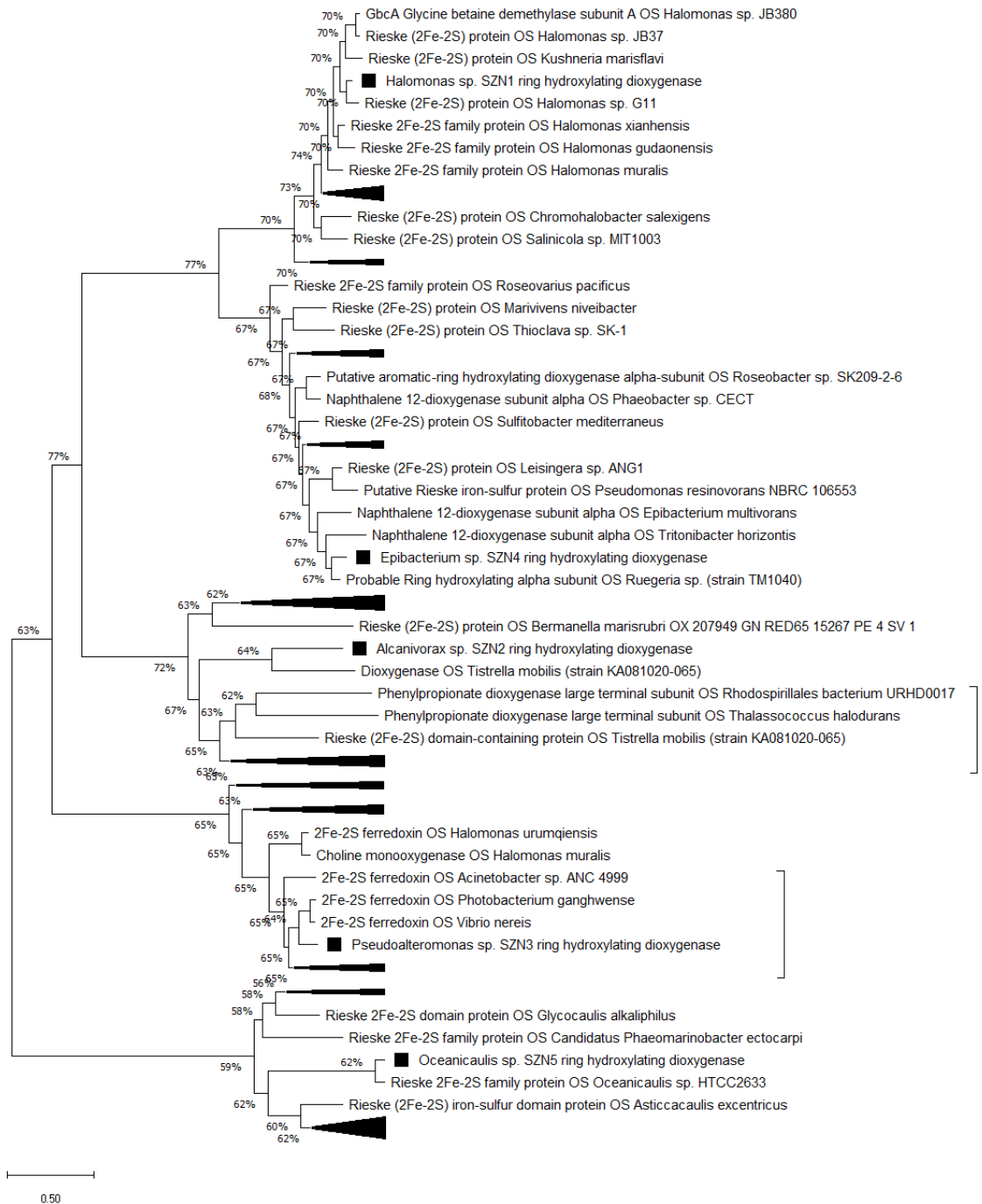


Figure 3.20. Phylogenetic tree built with MEGA 7 using the best twenty hits after blasting the ring hydroxylating dioxygenase belonging to *Halomonas* sp. SZN1, *Alcanivorax* sp. SZN2, *Epibacterium* sp. SZN4, *Pseudoalteromonas* sp. SZN3) and *Oceanicaulis* sp. SZN5 on Swiss Prot Data bank.

3.2.2) Cytochrome P450

Even though *Cytochrome P450 monooxygenase* is a very versatile superfamily protein, its role in degradation of hydrocarbons by microorganisms has already been documented (Moody, Freeman, and Cerniglia 2005). The CYP 450 system acts by catalyzing trans dihydrodiols formation by the epoxidation of the aromatic nucleus with enzymatic hydration by epoxide hydrolase. Depending on whether it occurs in cis or in trans form, the aromatic compound can then be degraded by the catechol or procatechuate degradation pathways.

Comparative analysis of cytochrome P450 and the related flanking sequence of *Halomonas* sp. SZN1 with the regions belonging to *Halomonas axialiensis* *Althf1*, *Halomonas olivaria* *TYRC17* and *Halomonas aestuari* *Hb3* highlighted the absence of this enzyme in the 3 reference sequences. This indicates a genetic rearrangement in the region, even if the subsequent nucleotide composition, corresponding to *cytochrome C genes*, nitrogen metabolism (*NosR*, *NosD*) and membrane transporters, is conserved in the other *Halomonas* species (Fig. 3.20). The presence of oxidizing nitrogen proteins close to Cytochrome P450 has been extensively described in fungal organisms (Shoun et al. 2012) and therefore this organization could be due to a horizontal passage from eukaryotic organisms. To validate this assumption other studies are necessary. Conversely, the sequence comparison containing cytochrome P450 of *Alcanivorax* sp. SZN2 with three sequences belonging to the genus *Alcanivorax*, highlighted an almost complete conservation of the entire analyzed region (Fig. 3.21). In particular the homology with the sequence of *Alcanivorax xenomutans* sp. 40 is equal to 100% and is

above 70% compared with *Alcanivorax* sp. N3-2A and *Alcanivorax dieselsoi* B5. Two other genes used in the detoxification and biodegradation of xenobiotics were found by analysing the region containing cytochrome P450: *glutathione disulfide reductase* (Moron, Depierre, and Mannervik 1979) and a rieske domain non heme oxygenase (Barry and Challis 2013). The presence of the gene encoding for a *Par A* family protein, responsible for segregating protein clusters through the spatial organization of DNA sequences (Roberts et al. 2012) suggests that it could play a role in the organization of this region.

Although the sequence related to *Epibacterium* sp. SZN4 showed a homology higher than 70% for the regions containing 6 ORFs (*Cytochrome P450*, *C-4 decarboxylate* and TRAPP transporters, a transcriptional regulator and a precursor for *Arylsulfatase B*) belonging to the genomes of *Epibacterium mobile* EPIB1, *Ruegeria mobilis* F1926 and *Ruegeria* sp. TM1040, the flanking regions did not have any relation to each other suggesting that the shared region could be due horizontal gene transfer (Fig. 3.22).

Phylogenetic analysis showed the absence of an evolutionary correlation between the sequences of the P450 cytochromes identified in the three draft genomes clustering them with proteins belonging to the genomes of *Halomonas subglaciescola*, *Alcanivorax dieselsoi* B5 and *Ruegeria* sp. TM1040 (Fig. 3.23). With the exception of *A. dieselsoi* B5, the other species *Halomonas subglaciescola* and *Ruegeria* sp. TM1040 have not been isolated from contaminated areas (Lai, Li, and Shao 2012; Moran et al. 2007). This observation may suggest that cytochrome P450, at least for *Halomonas* sp. SZN1 and *Epibacterium* sp. SZN4 could be evolutionary conserved in these microorganisms.

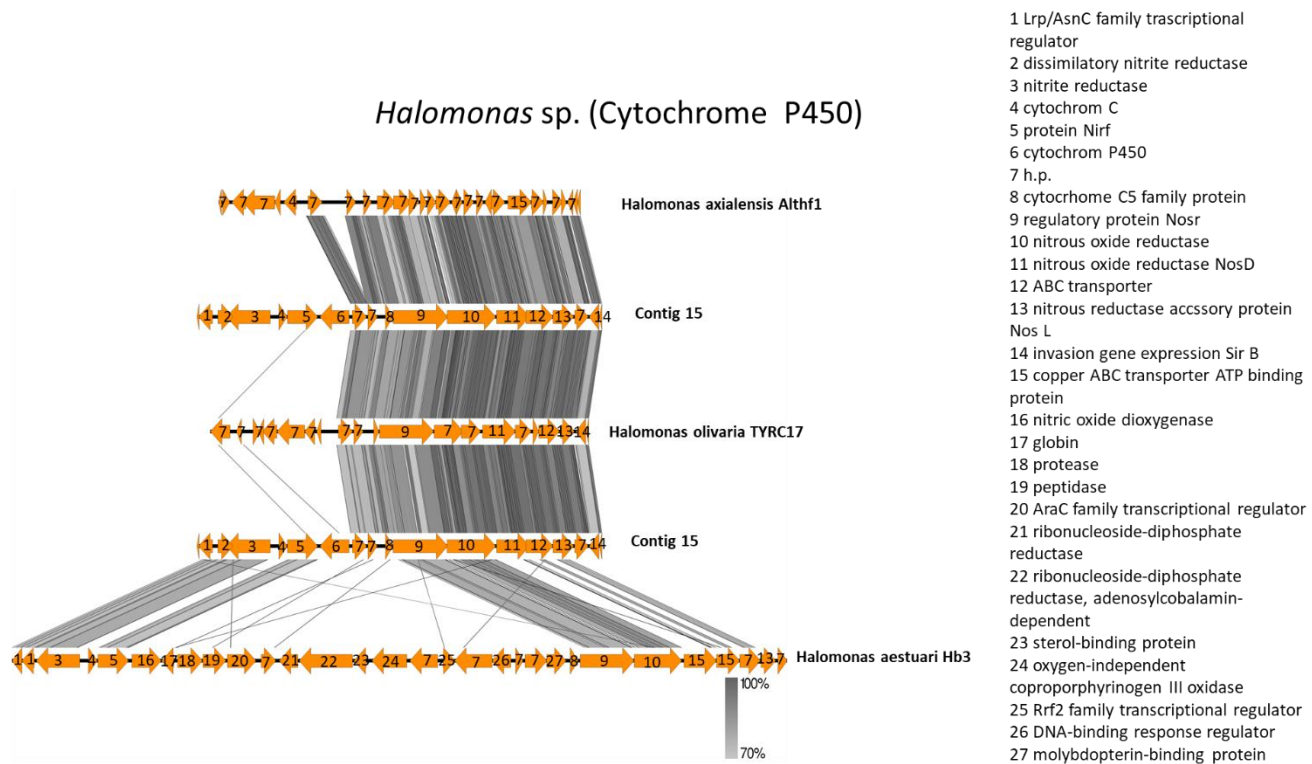


Figure 3.21. Comparison of strain sequences from my *Halomonas* sp. SZN1 draft genome and the three closest sequences identified in the National Centre for Biotechnology Information (NCBI) data bank. Cytochrome P450 is indicated as ORF 6. Contig 15 is the genomic region where the gene encoding for Cytochrome P450 was identified in my draft genome. The right panel lists genes that are encoded by the draft genome of *Halomonas* sp. SZN1 (ORFs 1-14) and those that are encoded by reference genomes (ORFs 15-27)

Alcanivorax sp. (Cytochrome P450)

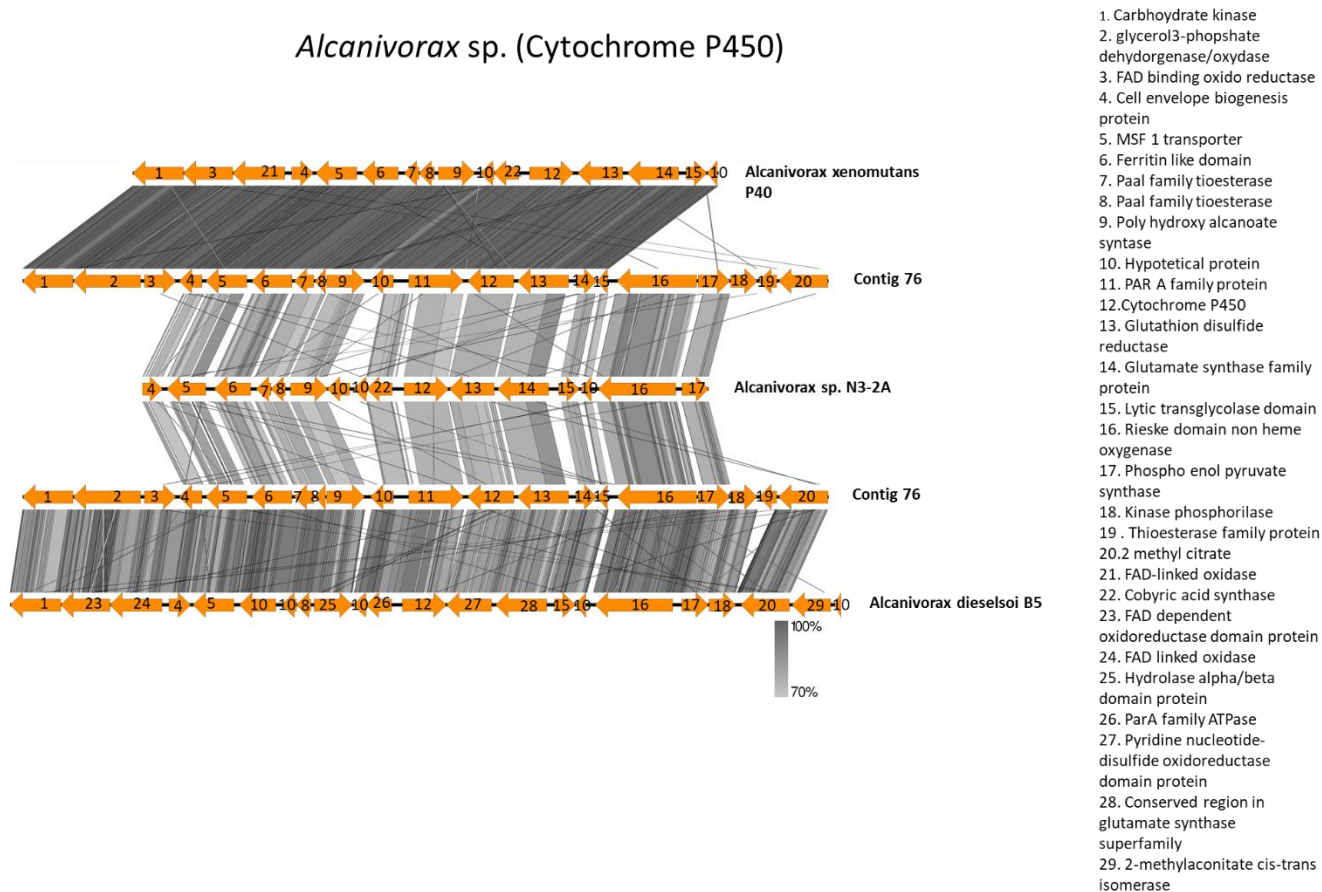


Figure 3.22. Comparison of strain sequences from my *Alcanivorax* sp. SZN2 draft genome and the three closest sequences identified in the National Centre for Biotechnology Information (NCBI) data bank. Cytochrome P450 is indicated as ORF 12. Contig 76 is the genomic region where the gene encoding for Cytochrome P450 was identified in my draft genome. The right panel lists genes that are encoded by the draft genome of *Alcanivorax* sp. SZN2 (ORFs 1-20) and those that are encoded by reference genomes (ORFs 21-29)

Epibacterium sp. (Cytochrome P450)

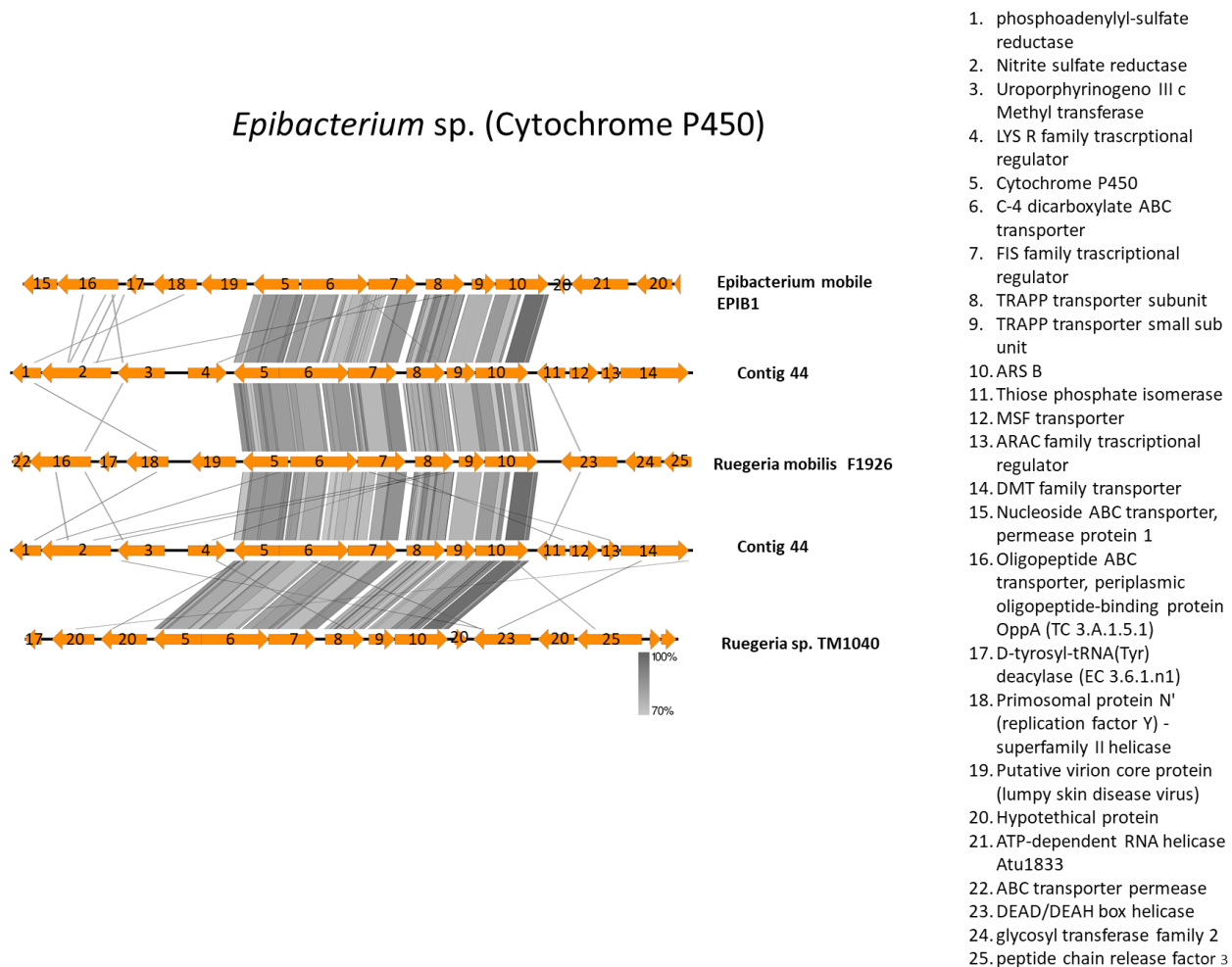


Figure 3.23. Comparison of strain sequences from my *Epibacterium* sp. SZN4 draft genome and the three closest sequences identified in the National Centre for Biotechnology Information (NCBI) data bank. Cytochrome P450 is indicated as ORF 5. Contig 44 is the genomic region where the gene encoding for Cytochrome P450 was identified in my draft genome. The right panel lists genes that are encoded by the draft genome of *Epibacterium* sp. SZN4 (ORFs 1-14) and those that are encoded by reference genomes (ORFs 15-25)

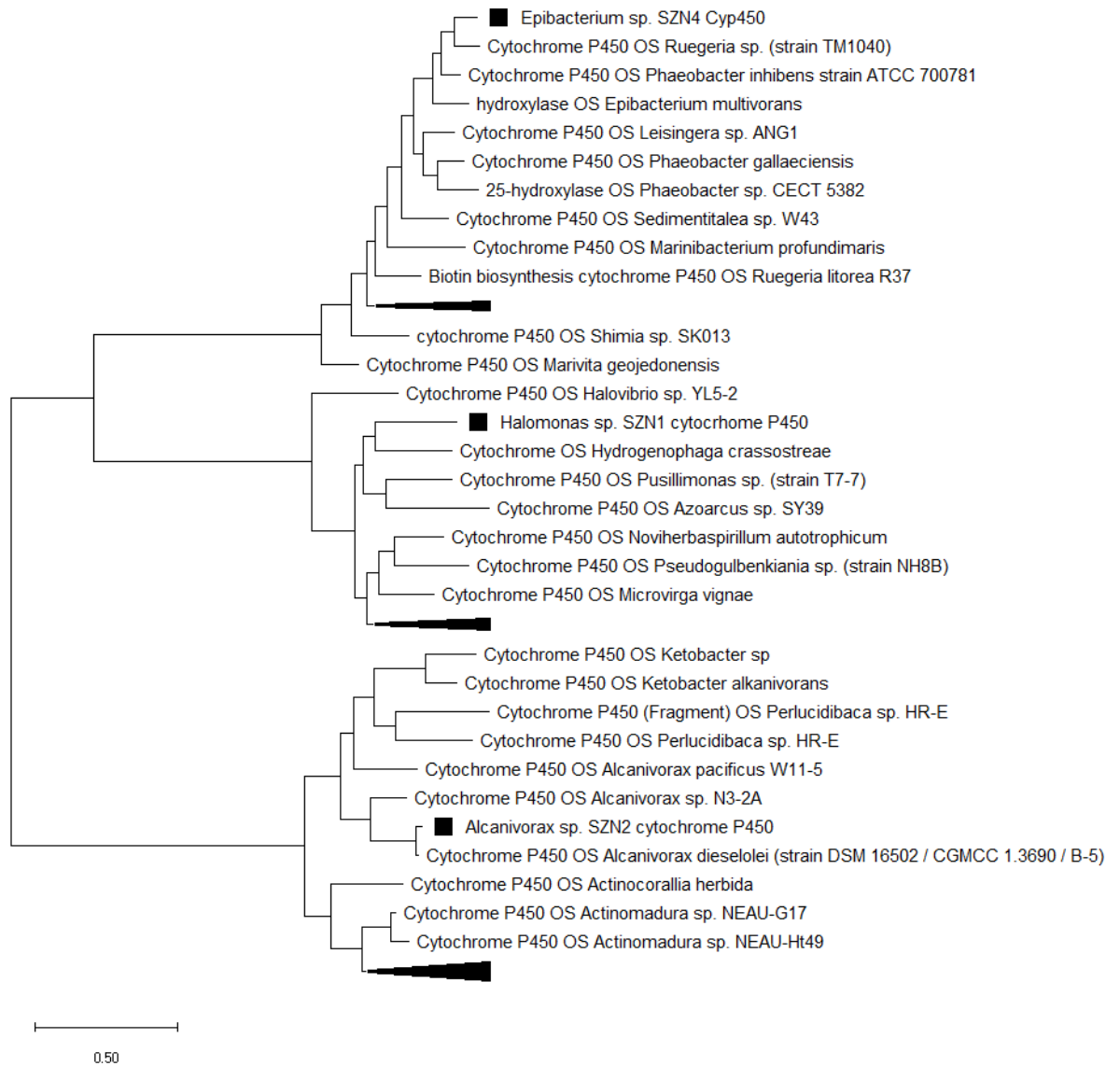


Figure 3.24. Phylogenetic tree of built with MEGA 7 using the best twenty hits after blasting the Cytochrome P450 belonging to *Halomonas* sp. SZN1, *Alcanivorax* sp. SZN2, and *Epibacterium* sp. SZN4 on SwissProt Databank.

3.2.3) Catechol pathway

In general, molecules having two cis diols lead to the formation of salicylate that enters the catechol pathway, a typical bacterial degradation pathway found mainly in proteobacteria and actinobacteria (Nešvera, Rucká, and Pátek 2015). Here I propose this pathway based on a previous description of Habe and Omori (2003) and the identification of the involved enzymes by automatic notation. The enzyme *salicylate hydroxylase* present in the draft genomes of *Alcanivorax* sp. SZN2, *Halomonas* sp. SZN1, and *Epibacterium* sp. SZN4, catalyzes the formation of catechol acid which becomes the substrate of the catechol 1-2 dioxygenase like enzyme. Only *Halomonas* sp. SZN1 showed a catechol 1, 2 dioxygenase like protein. More specifically, the protein I identified by blasting against the Swissprot database was *hydroxiquinol 1,2 dioxygenase*. Phylogenetic analysis clustered this protein with a dioxygenase belonging to the genome of GFAJ-1, a strain isolated in a hypersaline lake located in California (Fig 3.24). Ferraroni et al. (2005) suggested that *hydroxiquinol 1,2 dioxygenase*, as well as *Catechol 1-2 dioxygenase*, is able to promote the formation of cis cis muconic acid and, following a double oxygenation, the formation of β ketoadipic acid. This compound enters the β -*ketoadipate* pathway and through the addition of a CoA group by the β -*ketoadipate succinyl CO-A transferase*, forms β -*ketoadipyl-CoA* which, due to the action of β -*ketoadipyl thiolase*, leads to the formation of the terminal products Acetyl CoA and succinyl CoA able to enter the citric acid cycle (R. H. Peng et al. 2008). Interestingly, the enzyme catalysing the formation of β -*ketoadipyl-CoA* was found in the genome of *Halomonas* sp. SZN1, *Epibacterium* sp. SZN4, *Pseudoalteromonas* sp. SZN3, and *Oceanicaulis* sp. SZN5, while β -*ketoadipyl thiolase* has been identified only in *Alcanivorax*

sp. SZN2, and *Halomonas* sp. SZN1. The presence of a salicylate hydroxylase in the draft genome of *Epibacterium* sp. SZN4 is quite rare since Buchan, González, and Chua (2019), analyzing the overall metabolic pathways of strains belonging to the family *Rhodobacteraceae* did not include such enzymes and thus the catechol pathway in the list of prevalent routes involved in hydrocarbon breakdown. Further analyses are required in order to understand if the presence of *salicylate hydroxylase* in the *Rhodobacteraceae* genome is an exception or is due to limited data.

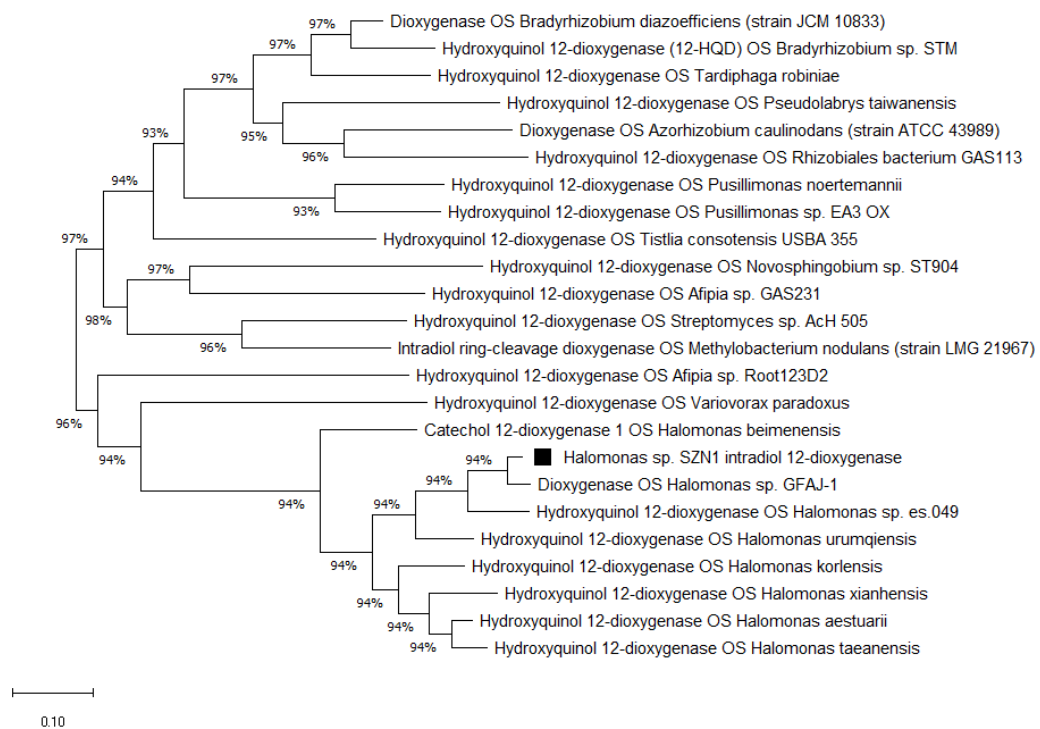


Figure 3.25. Phylogenetic tree built with MEGA 7 using the best twenty hits after blasting the Hydroxyquinol 1,2 dioxygenase belonging to *Halomonas* sp. SZN1 on Swiss Prot data bank.

3.2.4) Protocatechuate pathway

The degradation of hydrocarbons following trans-hydroxylation takes place via the Protocatechuated metabolic pathway (Fuchs, Boll, and Heider 2011). This pathway begins with a hydroxylation in position 3 of 4-Hydroxybenzoate by *hydroxybenzoate hydroxylase*, found only in the genomes of *Halomonas* sp. SZN1, and *Epibacterium* sp. SZN4, which leads to the formation of the compound 3,4 hydroxybenzoate. The formation of 3,4 hydroxybenzoate can also derive from the activity of the enzyme *vanillate o demethylase monooxygenase* starting from the monocyclic vanillate compound. This latter enzyme has been identified only in *Halomonas* sp. SZN1, after manual annotation (Fig 3.25, ORF 1). The next step is catalyzed by the *protocatechuate 3, 4 dioxygenase* able to convert 3, 4 hydroxybenzoate in β carboxy muconate which through the activity of *3 carboxy ci-cis muconolactone cycloisomerasi* is transformed in γ Carboxy muconolactone. The protocatechuate 3, 4 dioxygenase sequence found in *Halomonas* sp. SZN1, and *Epibacterium* sp. SZN4 was clustered, through phylogenetic analysis, with sequences belonging to *Halomonas* sp. G11 and *Ruegeria* strain TM1040, suggesting an absence of a close evolutionary relation between the two homologous enzymes (Fig. 3.27). The subsequent decarboxylation reaction catalyzed by the enzyme 4 carboxy muconolactone decarboxylase is described only in *Halomonas* sp. SZN1, *Ruegeria* sp. SZN4, and *Oceanicaulis* sp. SZN5. This leads to the formation of 3 oxoadipate enol lactonase which is transformed in 3 oxoadipate by the activity of β *keto adipate enol lactonase*, an enzyme identified in the genomes of *Halomonas* sp., SZN1 *Alcanivorax* sp., SZN2 and *Epibacterium* sp. SZN4. The last two steps of the pathway are catalyzed by enzymes whose sequences have been reported only in *Alcanivorax* sp.,

SZN2 and *Halomonas* sp. SZN1; more specifically, the activity of *3 oxo adipate Co-A transferase* promotes the formation of 3 oxoadipyl CoA which becomes a substrate of β *ketoadypil CoA thiolase* capable of catalysing the production of succinyl CoA, a compound involved in the citric acid cycle.

Comparison of the sequences belonging to *Halomonas* sp. SZN1 and *Epibacterium* sp. SZN4 with the homologous sequences has shown an overall conservation of all genes actively involved in this pathway (> 70%), with the only difference given by the absence of the PCA operon transcript factor PCAQ in the sequence belonging to the genome of *Halomonas Olivaria* TYRC 17 (Figs. 3.25 and 3.26). Moreover, as suggested by Kamimura and Masai (2013), by observing the *protocatechuate 4, 5* cleavage pathway, the structure of the analyzed sequences suggests that also the organization, not yet described in the literature, of the genes associated with the 3, 4 protocatechuate degradation pathway is operon like for both for *Halomonas* sp., and *Epibacterium* sp. Indeed, both genomes adjacently localized the genes coding for *3, 4 protocatechuate dioxygenase, 3 carboxy ci-cis muconolactone cycloisomerase, 4, carboxy muconolactone decarboxylase, β ketoadipate enol lactonase / thiolase*. Further analyses are needed to fully understand whether the organization in operon of the aforementioned pathway is a peculiarity of the two draft genomes or if this structure is widely diffused in other microorganisms.

Halomonas sp. (protocatechuate pathway)

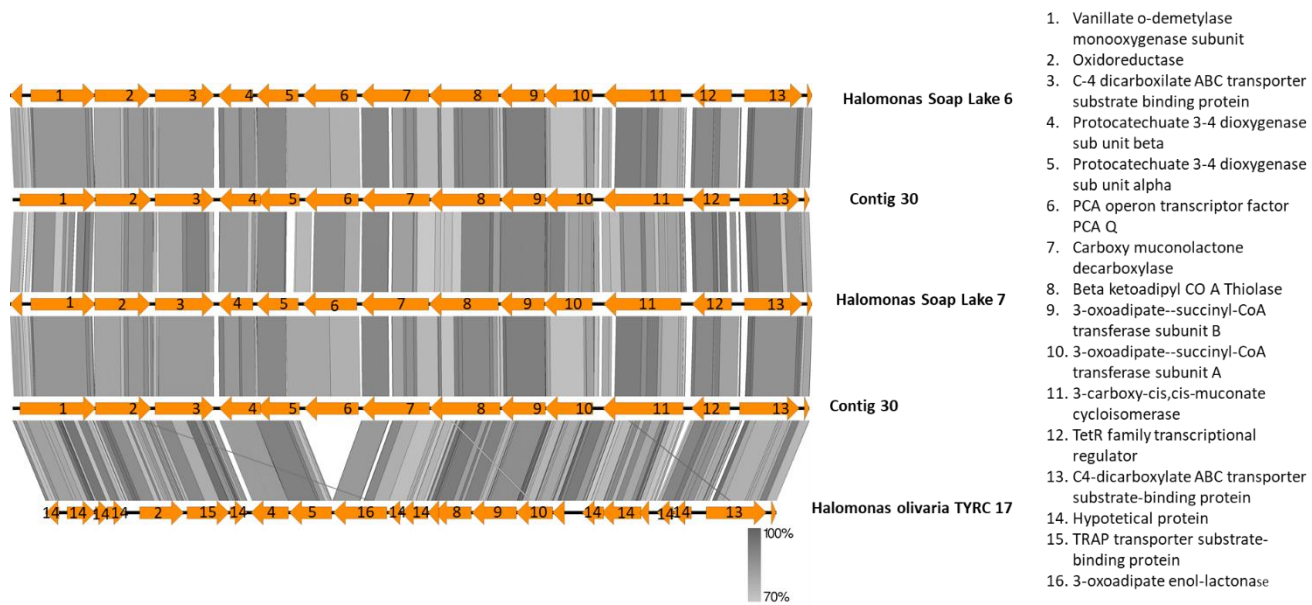


Figure 3.26. Comparison of strain sequences from my *Halomonas* sp. SZN1 draft genome and the three closest sequences identified in the National Centre for Biotechnology Information (NCBI) data bank. Protocatechuate 3-4 dioxygenase sun unit beta and alpha are indicated as ORF 4 and 5. Contig 30 is the genomic region where the genes encoding for Protocatechuate 3-4 dioxygenase sun unit beta and alpha were identified in my draft genome. The right panel lists genes that are encoded by the draft genome of *Halomonas* sp. SZN1 (ORFs 1-13) and those that are encoded by reference genomes (ORFs 14-16)

Epibacterium sp. (protocatechuate pathway)

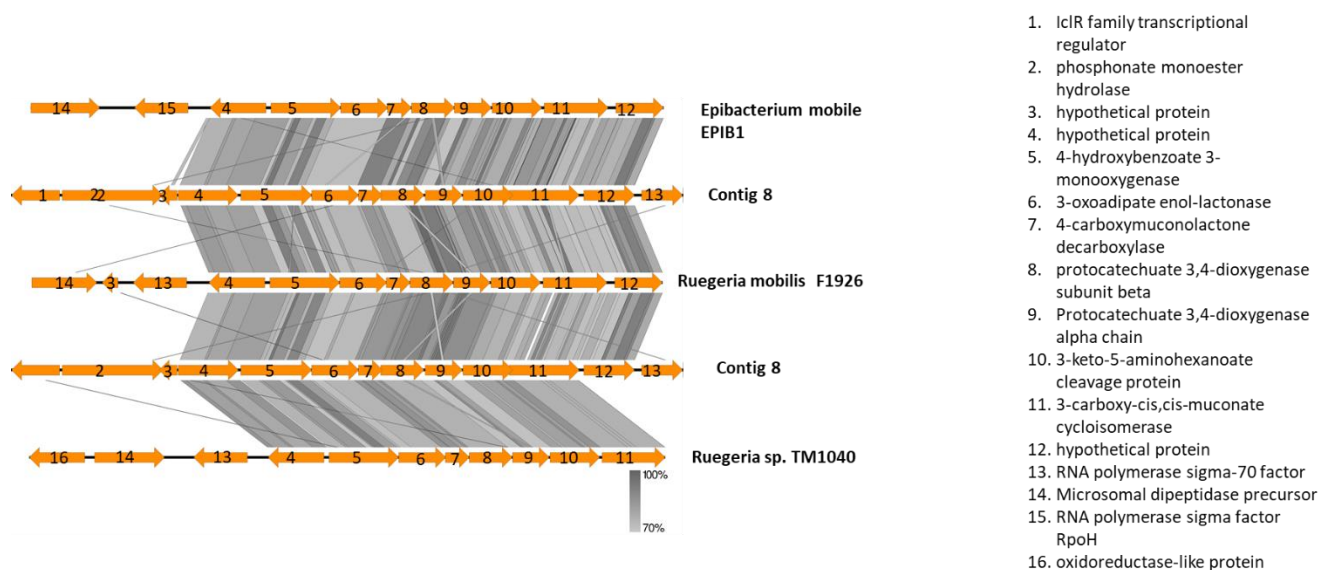


Figure 3.27. Comparison of strain sequences from my *Epibacterium* sp. SZN4 draft genome and the three closest sequences identified in the National Centre for Biotechnology Information (NCBI) data bank. Protocatechuate 3-4 dioxygenase subunit beta and alpha are indicated as ORF 8 and 9. Contig 8 is the genomic region where the genes encoding for Protocatechuate 3-4 dioxygenase subunit beta and alpha were identified in my draft genome. The right panel lists genes that are encoded by the draft genome of *Halomonas* sp. SZN4 (ORFs 1-13) and those that are encoded by reference genomes (ORFs 14-16)

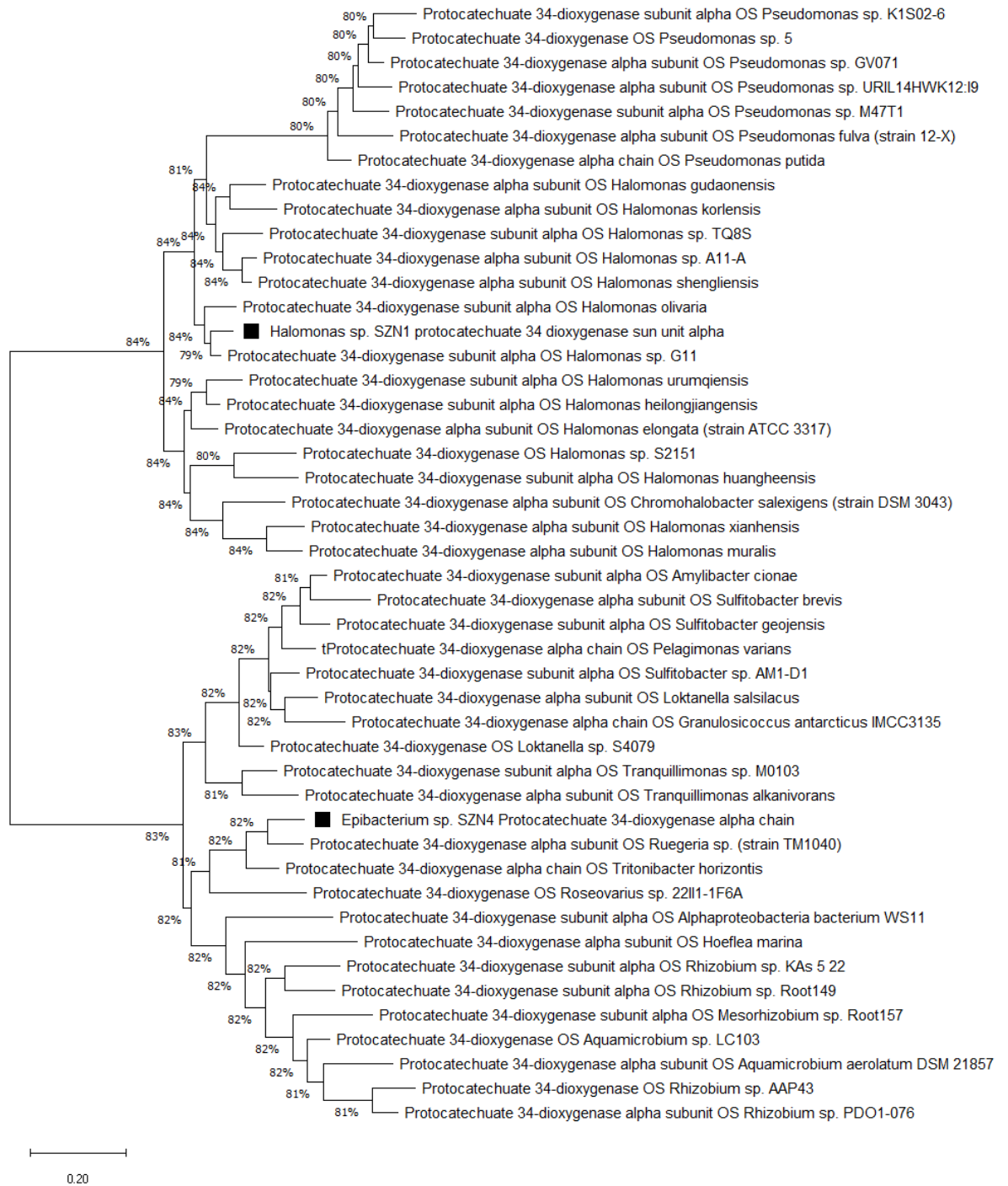


Figure 3.28. Phylogenetic tree built with MEGA 7 using the best twenty hits after blasting the *protocatechuete 3, 4 dioxygenase* belonging to *Halomonas* sp. SZN1 and *Epibacterium* sp. SZN4 on Swiss Prot data bank.

3.2.5) Homogentisate pathway

The homogentisate pathway, involved in the catabolism of the aromatic amino acids phenylalanine and tyrosine is also involved in the degradation of PAHs (Arias-Barrau et al. 2004). As suggested by Guazzaroni et al. (2013), Fuchs, Boll, and Heider (2011), hydroxylation by oxygenases can lead to the formation of various products including hydroxyphenylacetate which, following decarboxylation to hydroxyphenyl pyruvate, can be transformed in homogentisate via *4 hydroxy phenil pyruvate dioxygenase*. The sequences coding for this latter enzyme have been identified in the genomes of *Halomonas* sp. SZN1, *Pseudoalteromonas* sp. SZN3, and *Oceanicaulis* sp. SZN5. The activity of homogentisate 1,2 dioxygenase (HmgA), showed by *Halomonas* sp. SZN1, *Pseudoalteromonas* sp. SZN3, *Oceanicaulis* sp. SZN5, and *Epibacterium* sp. SZN4, promotes the conversion of homogentisate in 4 maleyloacetate. This is then converted in a second step into fumaryl aceto acetate by *maleyloacetate isomerase (HmgC)*, an enzyme found in all the genomes except for *Alkaliphilus* sp. SZN6. The pathway ends with the production of fumarate, which can thus enter the citric acid cycle. This last step is catalyzed by *fumaryl aceto acetate hydrolase (HmgB)* which is shared among all the genomes except for *Oceanicaulis* sp. SZN5 and *Alkaliphilus* sp. SZN6.

Although the aforementioned pathway has been described in the Roseobacters clade (Buchan, González, and Chua 2019), I describe its presence for the first time in *Oceanicaulis* and *Epibacterium* strains.

Interestingly, the only two genomes that showed genes involved in the pathway, organized in an operon-like structure, were *Pseudolateromonas* sp. SNZ3 and

Epibacterium sp. SZN4, whose sequences are reported and described below (Figs. 3. 28 and 3.29).

Comparison of the sequences of *Pseudolateromonas* sp. SZN4 containing the Homogentisate 1, 2 dioxygenase with *Pseudoalteromonas issachenkoni* KMM3549, *Pseudolateromonas* sp. SM9913 and *Pseudolateromonas tetradonis* GFC showed a sequence homology higher than 70% for the genes encoding for *maleylacetate isomerase* and *homogentisate 1, 2 dioxygenase* enzymes that are well known to be involved in PAHs degradation (Arias-Barrau et al. 2004), and for Mar transcriptional regulator and Ton B channels. Although the Mar family has been described in antibiotic response pathways, its conservation within the region suggests that it may play a role in the degradation of hydrocarbons, confirming what was observed by J. Cao et al. (2015). Similarly, the presence of Ton-B channels also appears to be related to hydrocarbon metabolism that act by mediating the uptake of chemical compounds through the outer membrane (Hua and Wang 2014).

Similarly to what observed for *Pseudoalteromonas* sp. SZN3 also the comparison of *Epibacterium* sp. SZN4 with the sequences belonging to *Epibacterium mobile* EPIB1, *Ruegeria mobilis* F1926 and *Ruegeria* sp. TM1040 showed a homology higher than 70% for the genes potentially involved in the homogentisate pathway, i.e. the Mer R family transcriptional regulator, *Homogentisate 1, 2 dioxygenase*, and *fumarylacetoacetate*. The rich homology suggests an evolutionary conservation of this region in the Roseobacter clade since the contiguous genes of the analyzed sequences (*metallophosphoesterase*, *histidine phosphatase* and *HprK kinase B*) did not show any homology with the

sequences of the other reference microorganisms and did not seem to have any relation with the Homogentisate pathway.

Phylogenetic analysis showed the absence of a relationship between the *Homogentisate 1, 2 dioxygenase* identified in 4 different draft genomes, excluding that the enzyme has been transferred from an organism to another by horizontal transfer (Fig. 3.30). Indeed, the homogentisate 1, 2 dioxygenase found in the genomes of *Pseudolateromonas* sp., *Halomonas* sp., *Epibacterium* sp. and *Oceanicaulis* sp. clustered respectively with *Pseudoalteromonas haoplanktis* TAC 125, *Halomonas olivaria*, *Ruegeria* sp. TM1040 and *Oceanicaulis* sp. HTCC2633.

Pseudoalteromonas sp. (homogentisate pathway)

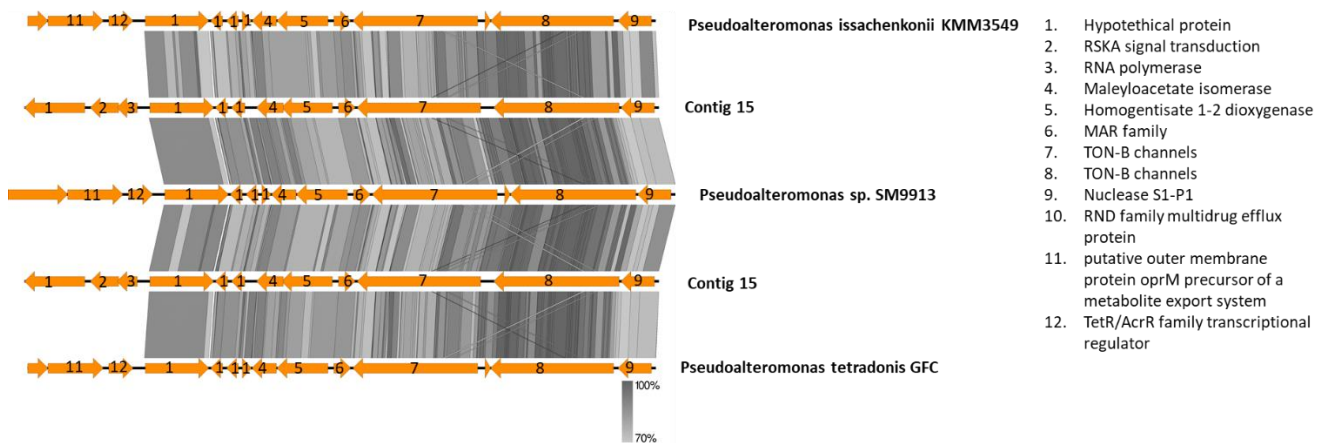


Figure 3.29. Comparison of strain sequences from my *Pseudoalteromonas* sp. SZN3 draft genome and the three closest sequences identified in the National Centre for Biotechnology Information (NCBI) data bank. Homogentisate 1-2 dioxygenase is indicated as ORF 5. Contig 15 is the genomic region where the genes encoding for Homogentisate 1-2 dioxygenase was identified in my draft genome. The right panel lists genes that are encoded by the draft genome of *Pseudoalteromonas* sp. SZN3 (ORFs 1-9) and those that are encoded by reference genomes (ORFs 10-12)

Epibacterium sp. (homogentisate pathway)

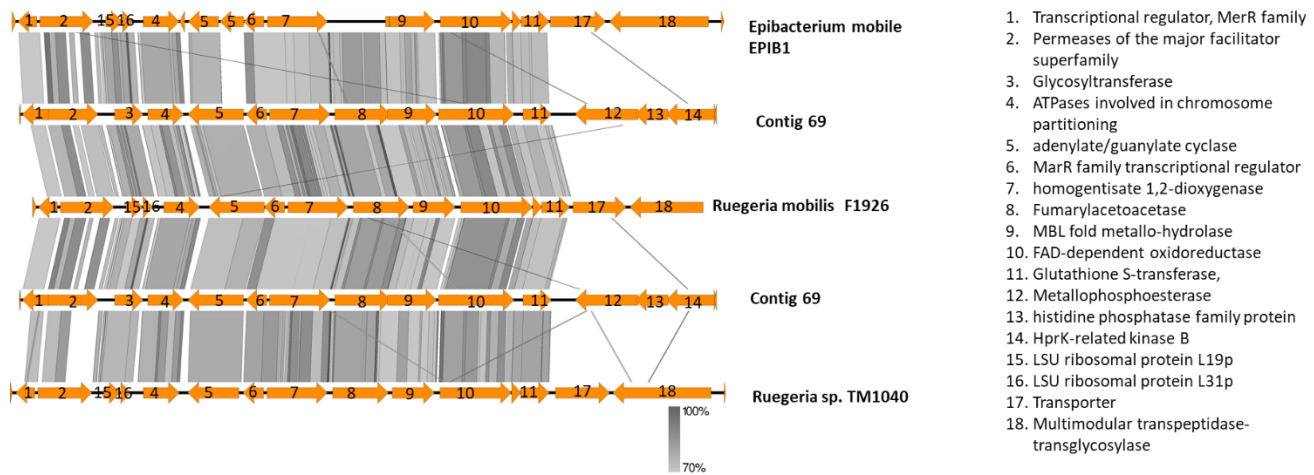
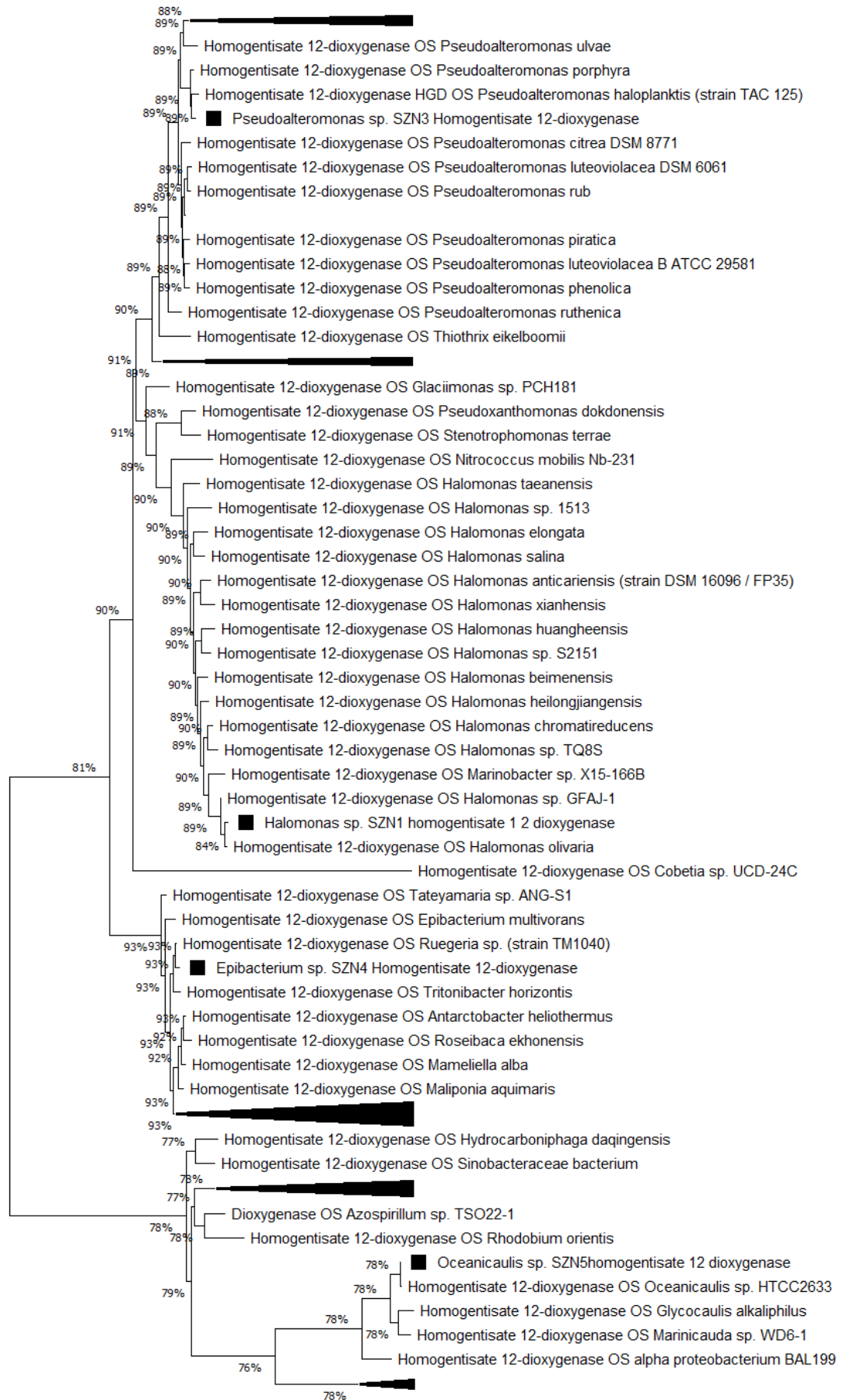


Figure 3.30. Comparison of strain sequences from my *Epibacterium* sp. SZN4 draft genome and the three closest sequences identified in the National Centre for Biotechnology Information (NCBI) data bank. Homogentisate 1-2 dioxygenase is indicated as ORF 7. Contig 69 is the genomic region where the genes encoding for Homogentisate 1-2 dioxygenase was identified in my draft genome. The right panel lists genes that are encoded by the draft genome of *Epibacterium* sp. SZN4 (ORFs 1-14) and those that are encoded by reference genomes (ORFs 15-18)



0.50

Figure 3.31. Phylogenetic tree built with MEGA 7 using the best twenty hits after blasting the Homogentisate 1, 2 dioxygenase belonging to *Halomonas* sp. SZN1, *Epibacterium* sp. SZN4, *Pseudoalteromonas* sp. SZN3 and *Oceanicaulis* sp. SZN5 on Swiss Prot databank.

3.2.6) Homoprocatechuate pathway

Another route associated with PAHs degradation is the homoprotocatechuate pathway, whose genes identified in *Halomonas* sp. SZN1 and *Alcanivorax* sp. SZN2, and the associated organization are described below. As suggested by (Méndez et al. 2011), this metabolic route involves the degradation of homoprotocatechuate, a compound generated from 4 hydroxyphenylacetate via *4 hydroxyphenyl acetate 3 monooxygenase reductase* and *4 hydroxyphenyl acetate 3 monooxygenase* (not identified in the draft genomes). The following reactions catalyzed by *3, 4 dihydroxy phenylacetate 2, 3 dioxygenase* led to the formation 2 hydroxy 5 carboxy methyl muconate semialdehyde converted to 5 carboxyl methyl 2 hydroxymuconate by the *enzyme 5 carboxymethyl 1,2 hydroxy muconic semialdehyde dehydrogenase*.

The latter mentioned compound is isomerated, through *5 carboxymethyl 2 hydroxy muconate delta isomerase*, into 5 carboxy 2 oxo hepta 3 enedioate which is converted to 2 hydroxyhepta 2-4 dienedioate by the enzyme *5-carboxymethyl-2-oxo-hex-3-ene-1,7-dioate decarboxylase* (not shown in the sequence comparison). The enzymes *2 hydroxy epta diene 1,7 dioate isomerase* and subsequently *the 2-oxo-hept-3-ene-1,7-dioate hydratase* catalyze the formation of 2 oxohepta 3 enedioate and 2, 4 dihydroxyhepta 2 enedioate respectively. These are in turn converted to succinate

semialdehyde by 2, 4 dihydroxy hepta diene 1, 7 dioic acid aldolase. Finally, succinate semialdehyde dehydrogenase leads to the formation of succinate and thus its availability for the citric acid cycle.

Although the comparison of the gene sequence coding for the Homoprotocatechuate pathway identified in *Alcanivorax* sp. SZN2, with the homologous sequences of *Alcanivorax xenomutans* p 40 and *Alcanivorax dieselsoi* B5 showed a high nucleotide conservation, the protein products associated with ORFs were, in some cases, different indicating therefore a different organization of the operon during the evolution of the organisms (Fig. 3.31). Indeed, the ORF 13 of *Alcanivorax* sp. SZN2 coding for 2 oxohepta 3 ene 1, 7 dioic acid hydratase found no match in the genome of *A. xenomutans* p40 as well as NAD dependent succinate semialdehyde dehydrogenase (ORF 16) that was not found in the sequence of *A. dieselsoi* B5. Finally, the comparison with the sequence of *Alcanivorax* sp. N3-2A demonstrated the absence of the Homoprotocatechuate pathway in the genome of this microorganism as the only two homologous ORFs code for sterol desaturase and aconitate hydratase.

Similar to what has just been described, the analysis of the region including the homoprotocatechuate pathway identified in *Halomonas* sp. SZN1 showed a very low homology among the reference genomes of *Halomonas hydrothermalis* Y2, *Halomonas* R 57-5 and *Halomonas ventosae* strain NRS2HaP1 (Fig. 3.32). Except for the GNTR family transcriptional regulator and cytochrome C oxidase with a homology greater than 70%, all other genes involved in the pathway did not have homologous sequences in the other organisms indicating a reduced conservation of the region probably due to horizontal gene transfer. The phylogenetic tree (Fig. 3.33) related to the sequence of 3, 4

dihydroxyphenylacetate 2, 3 dioxygenase of *Halomonas* sp. SZN1, and *Alcanivorax* sp. SZN2 clustered the sequence of *Halomonas* sp. with the dioxygenase belonging to the strain *Terasakiispira papahanaumokuakeensis*, a gram negative bacteria Oceanospirillaceae isolated in a volcanic hyper saline lake located in the Northwestern Hawaiian Islands (Zepeda et al. 2015). Furthermore *3, 4 dihydroxyphenylacetate 2, 3 dioxygenase* of *Halomonas* sp. SZN1 falls into the clade also comprising the dioxygenase identified in *Alcanivorax* sp. SZN2 confirming a high diversity with respect to the enzymes belonging to the genus *Halomonas*.

Alcanivorax sp. (homoprotocatechuate pathway)

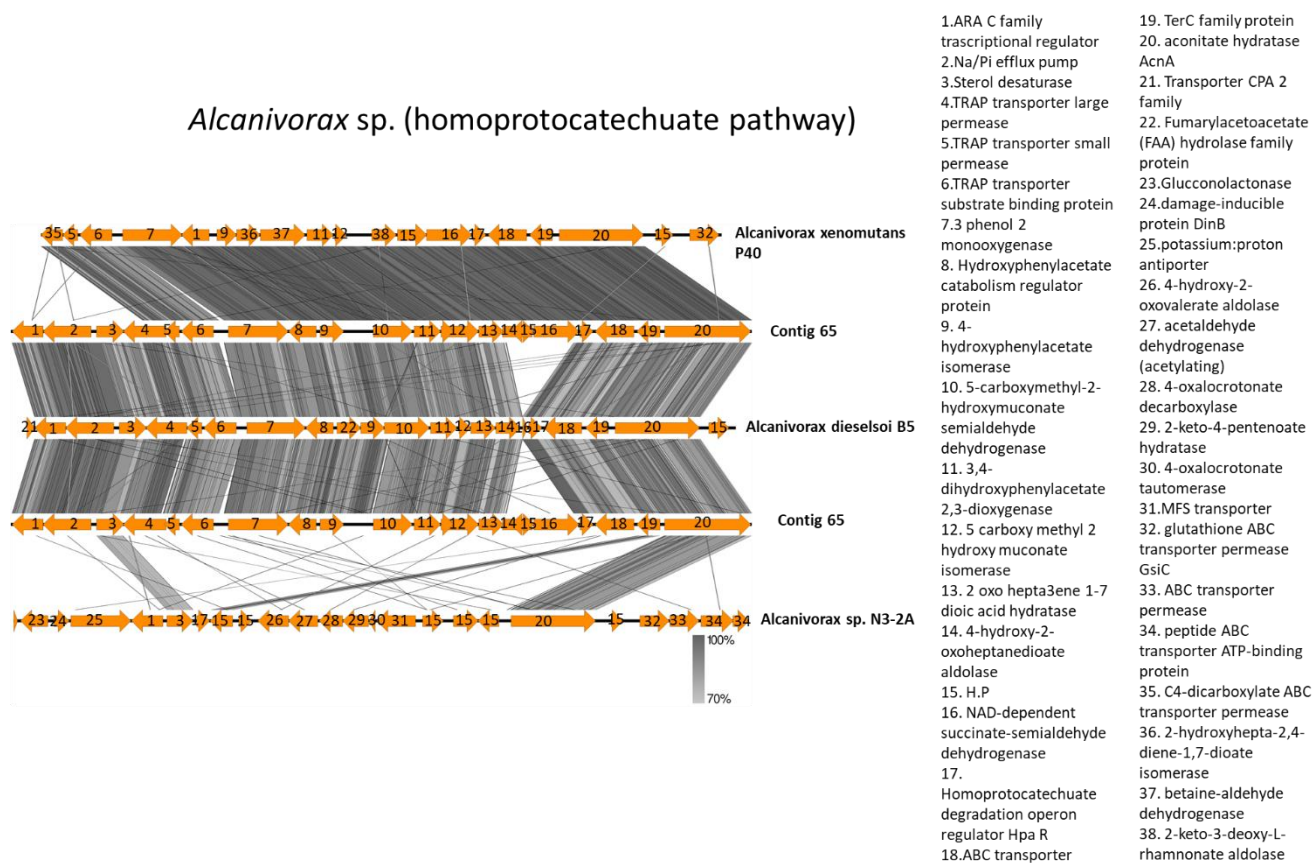


Figure 3.32. Comparison of strain sequences from my *Alcanivorax* sp. SZN2 draft genome and the three closest sequences identified in the National Centre for Biotechnology Information (NCBI) data bank. The genes involved in Homoprotocatechuate pathway are indicated from ORF 7 to ORF 19. Contig 65 is the genomic region where the genes encoding for Homoprotocatechuate pathway were identified in my draft genome. The right panel lists genes that are encoded by the draft genome of *Alcanivorax* sp. SZN2 (ORFs 1-20) and those that are encoded by reference genomes (ORFs 21-38)

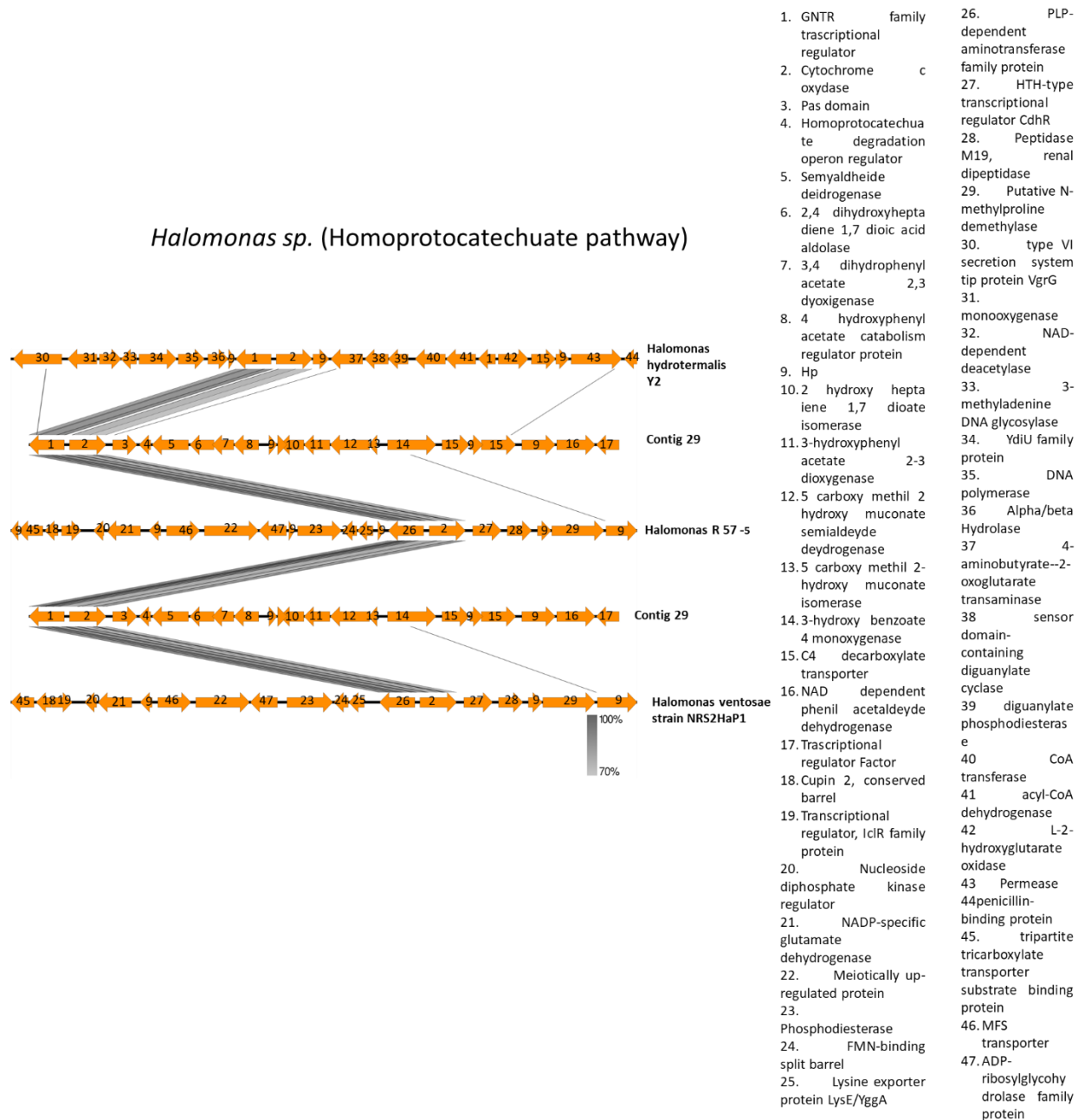


Figure 3.33. Comparison of strain sequences from my *Halomonas* sp. SZN1 genome and the three closest sequences identified in the National Centre for Biotechnology Information (NCBI) data bank. The genes involved in Homoprotocatechuate pathway are indicated from ORF 4 to ORF 14. Contig 29 is the genomic region where the genes encoding for Homoprotocatechuate pathway were identified in my draft genome. The right panel lists genes that are encoded by the draft genome of *Halomonas* sp. SZN1 (ORFs 1-17) and those that are encoded by reference genomes (ORFs 18-47)

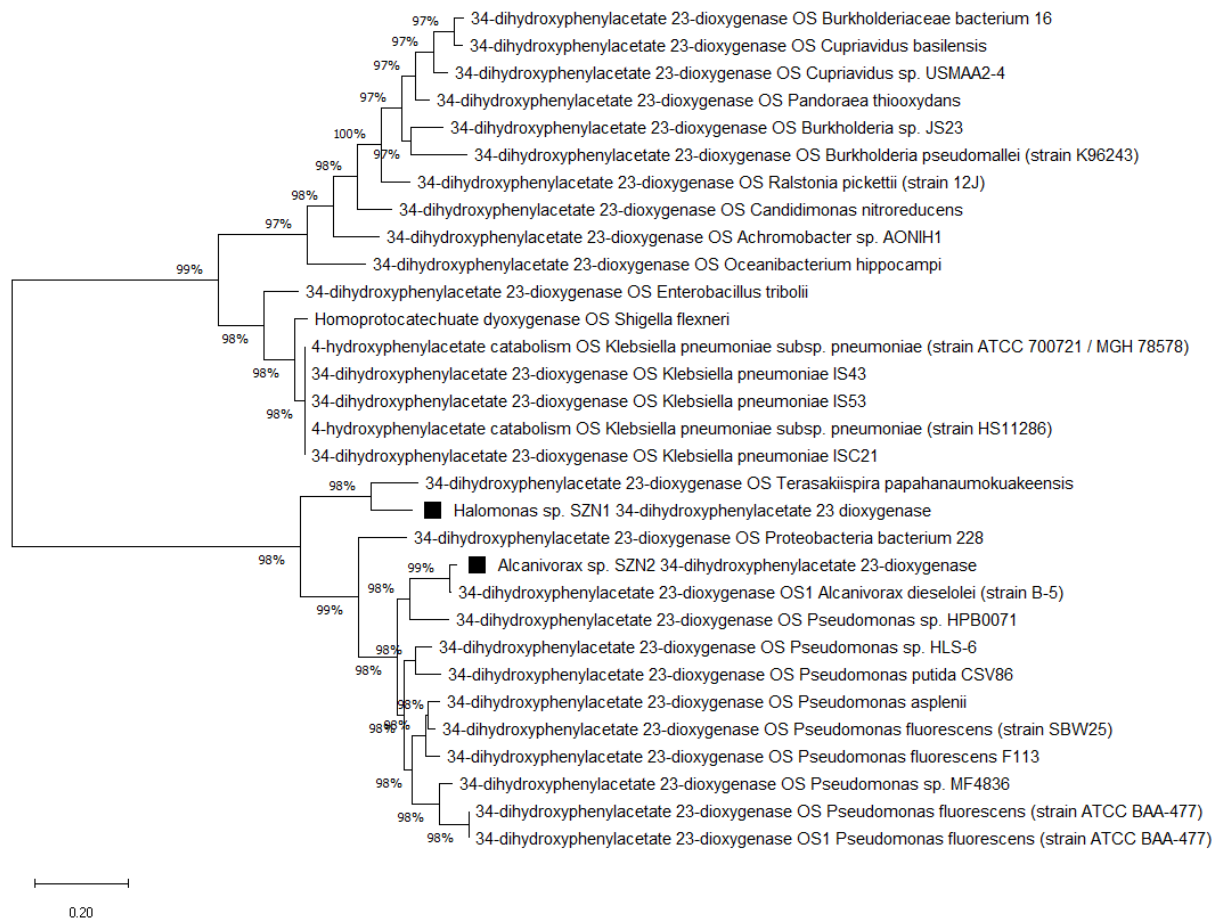


Figure 3.34. Phylogenetic tree built with MEGA 7 using the best twenty hits after blasting the 3, 4 dihydroxy phenylacetate 2, 3 dioxygenase belonging to *Halomonas* sp. SZN1 and *Alcanivorax* sp. SZN2 on Swiss Prot data Bank.

3.2.7) Phenilacetic pathway

A metabolic route to degrade aromatic compounds such as styrene and trans styrylacetic acid is represented by the phenilacetic pathway which involves the addition of Coenzyme A to a carboxylic residue through a *Phenil acetate CoA ligase*. This pathway has been described in about 16% of all bacterial species with sequenced genomes including gammaproteobacteria, actinobacteria, firmicutes and some bacteroidetes (Fuchs, Boll, and Heider 2011). Moreover, despite Liebgott et al. (2007) reported *Halomonas orgarivorans* and *Halomonas* sp. strain HTB24 as capable, respectively, to grown on phenilacetic acid and to degrade 3,4-dihydroxyphenylacetic acid, there are no previous descriptions in the literature of the phenilacetic degradation pathway in *Halomonas* sp. SZN1. Below I report the complete pathway based on the enzymes identified in the draft genome after manual annotation. More specifically, phenyl acetate degradation starts with the conjugation with a CoA group through the activity of *phenylacetate CoA ligase PaaK* (ORF15 and ORF 11) which then undergoes an epoxidation driven by *1, 2 phenyl acetate CoA epoxydase sub unit A PaaA*, *hydroxyphenyl acetate PaaD and PaaC* (ORF 14, 16, 12) leading to the formation of 2 (1, 2 epoxy 1-2 dihydro phenyl) acetyl- CoA. The activity of *2 (1, 2 epoxy 1, 2 dihydroxy phenyl acetyl CoA isomerase PaaG* (ORF 17) promotes the formation of 2 oxepin 2 (3H) ylideneacetyl-CoA, whose conversion into 3 oxo 5,6 dehydro suberyl CoA semialdehyde and 3 oxo 5-6 didehydrosuberyl CoA is catalyzed by *Oxepin-CoA hydrolase (PAAZ* (ORF 10)). The final conversion step in acetyl CoA and succinyl CoA is promoted, respectively, by *3-oxoadipyl-CoA thiolase (PAAJ* (ORF12)).

Comparing the sequence described above with homologous regions identified in *Halomonas* GFAJ-1, *Halomonas* sp. GT and *Halomonas campaniensis* LS21 C showed a high conservation of the genes coding for this pathway (Fig. 3.34). This observation is in contrast with what observed by Martin and McInerney (2009) who stated that this gene cluster was hardly seen to be complete of all the pathway components as it was supposed to be subjected to weak selective pressure. Since *Halomonas* GFAJ-1 isolated from Mono lake in California (Wolfe-Simon et al. 2011), and *Halomonas campaniensis* isolated from an algal mat from the Malvizza site in Italy (I. Romano et al. 2005) (the isolation site of *Halomonas* sp. GT is not well described), both coming from volcanic areas with a high presence of hydrocarbons (mainly methane), the data could suggest that the phenylacetic pathway is widespread in the *Halomonas* genus and represents an additional pathway capable of favoring its survival. In order to confirm this hypothesis, an in-depth study is needed to correlate the possible presence of genes for the phenylacetic pathway in the already sequenced genomes of *Halomonas* and the chemical characteristics of the isolation sites.

Finally, the *PaaJ* gene, coding for an enzyme capable of catalyzing the last step of the pathway, was also identified in the draft genomes of *Alcanivorax* sp. SZN2 and *Epibacterium* sp. SZN4. Although the presence of a single gene does not mean the presence of the entire pathway, it could however suggest that these two microorganisms can contribute to the detoxification of hydrocarbons, especially when they are associated in a microbial consortium exhibiting the entire route of degradation. The phylogenetic analysis of the *PaaJ* gene (Fig. 3.35) did not show the existence of a close evolutionary correlation between the three genes.

Halomonas sp. (Phenilacetic pathway)

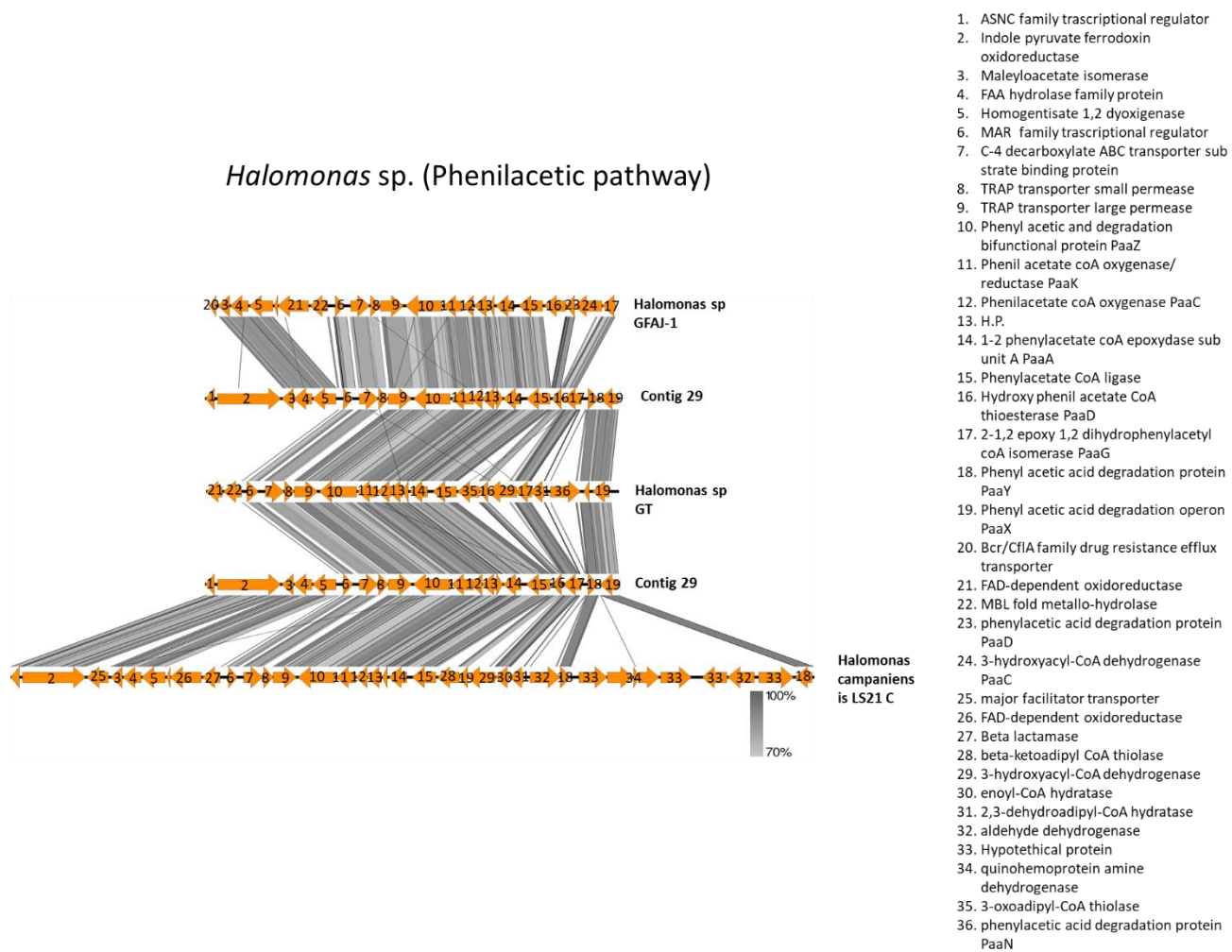


Figure 3.35. Comparison of strain sequences from my *Halomonas* sp. SZN1 genome and the three closest sequences identified in the National Centre for Biotechnology Information (NCBI) data bank. The genes involved in Phenilacetic pathway are indicated from ORF 10 to ORF 19. Contig 29 is the genomic region where the genes encoding for Phenilacetic pathway were identified in my draft genome. The right panel lists genes that are encoded by the draft genome of *Halomonas* sp. SZN1 (ORFs 1-19) and those that are encoded by reference genomes (ORFs 20-36)

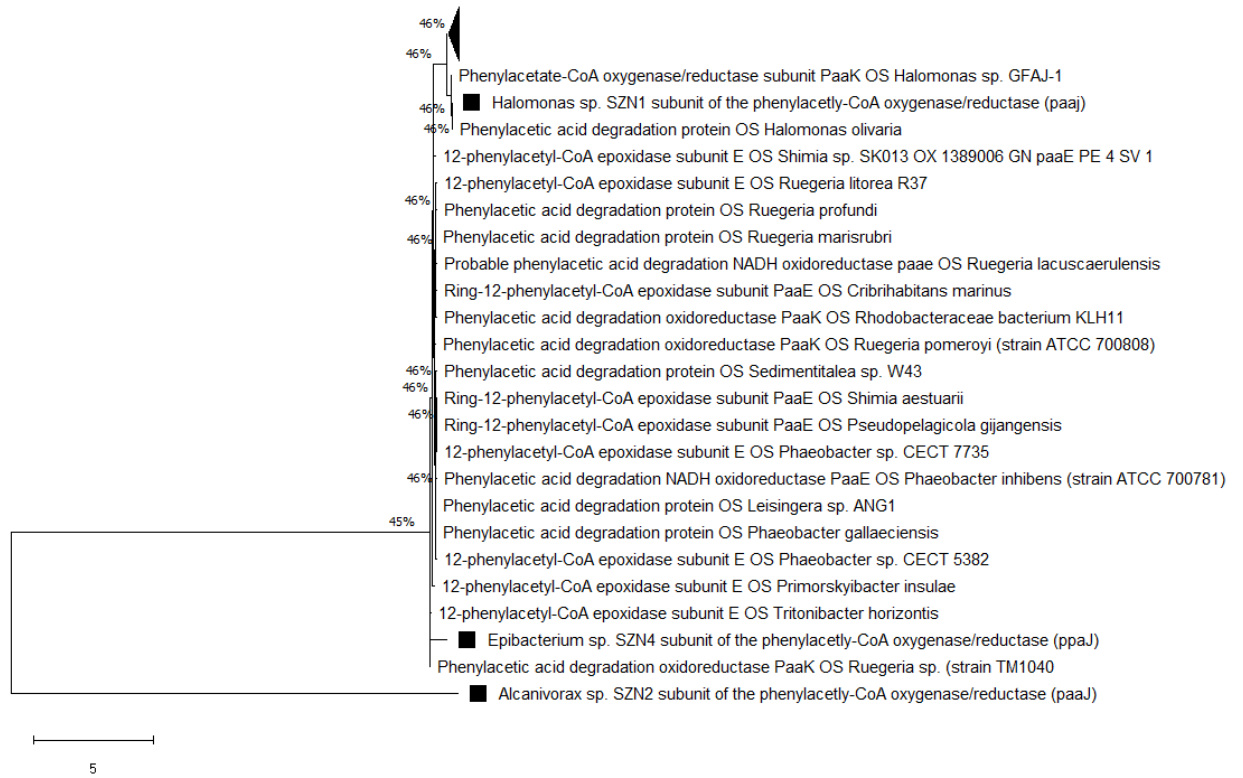


Figure 3.36. Phylogenetic tree built with MEGA 7 using the best twenty hits after blasting the phenylacetyl CoA oxygenase reductase belonging to *Halomonas* sp. SZN1, *Alcanivorax* sp. SZN2 and *Epibacterium* sp. SZN4 on Swiss Prot data bank.

3.3) Genetic bases for Metal detoxification

The automatic annotation generated by Rast allowed the identification of the draft genomes of *Alcanivorax* sp. SZN2, *Alkaliphilus* sp. SZN6, *Halomonas* sp. SZN1, *Pseudoalteromonas* sp. SZN3, *Epibacterium* sp. SZN4, and *Oceanicaulis* sp. SZN5. These were characterized respectively by 34, 15, 39, 35, 37, 30 genes for a total of 62 different proteins involved in mechanisms of metal detoxification (Fig. 3.36). The proteins were distributed heterogeneously in different draft genomes with only eight genes identified in all six draft genomes: Acriflavin resistance protein (specific for arsenic detoxification), two cobalt zinc cadmium efflux pumps, Copper homeostasis CutF, Magnesium and Cobalt efflux protein CorC, Multi Drug Resistance efflux pumps, and a transcriptional regulator (*MerR*) involved in mercury resistance.

The presence of such a heterogeneous set of genes, involved in mechanisms of resistance for multiple metals suggests that all the organisms investigated here have adapted to the high levels of pollution, developing detoxification systems over time. More specifically, of the 62 identified proteins, 24 code for efflux pumps capable of carrying ions selectively and non-selectively. Specifically, 15 proteins were identified that are able to carry ions non-selectively, of which 6 belong to the Resistance Nodulation Division (*RND*) efflux pump class and 7 to the multi drug resistance (*MDR*) class. Other genes coding for proteins able to co-selectively carry more ions have also been annotated such as *CzcA*, *CzcB*, *CzcC*, *CzcD* able to transport Cobalt, Zinc and Cadmium and CorC, specific for the transport of magnesium and cobalt.

From the automatic annotation 11 genes were identified that encode for proteins involved in the detoxification of copper, i.e. a copper chaperone, copper homeostasis

protein *CutE* and *CutF*, copper resistance protein B, D, *CopC* and *CopD*, a copper ATP ase, a multicopper and a blue multicopper oxidase and two regulator genes named “Copper sensing two component system response regulator *CusR*” and “Cu responsive transcriptional regulator”. Many of the efflux pumps and copper resistance proteins were identified in a single genic region in the genomes of *Pseudoalteromonas* sp. SZN3 and *Epibacterium* sp. SZN4 that are described below (Figs. 3.37 and 3.38).

The manual annotation of the region belonging to *Pseudoalteromonas* sp. SZN3 highlighted the presence of genes generally involved in the detoxification of metals (ORF 1 and ORF 8) and in the specific resistance mechanisms for copper (ORF 2, 3, 4, 5, 6), zinc, cadmium, cobalt and lead (ORF 10, 11, 12, 14) and mercury (ORF 9) confirming what has already been described by Qin et al. (2011) following the genome analysis of *Pseudoalteromonas* sp. SM9913.

Comparison with the homologous regions of *Pseudolalteromonas carragenovora* IAM 12662, KCTC 22325 and *Pseudolateromonas* sp. Xi13 displayed a degree of homology close to 100%. The only difference was with *Pseudoalteromonas* sp. Xi13 that exhibited a trypsin like serin protease (ORF 16) not currently believed to be involved in metal detoxification. The high homology suggests that this region is highly preserved at the evolutionary level in *Pseudoalteromonas* since the homologous species have been isolated in geographical areas far from each other, respectively in Cow Bay, Novo Scotia, Canada (*Pseudoalteromonas carragenovora* KCTC 22325; SAMN05271512/) and in Antarctica (*Pseudolateromonas* sp. Xi13). Unfortunately, it is not possible to know if and which stressors exerted evolutionary pressure as the characterization of the sampling sites are not available.

Similar to *Pseudolateromonas* sp. SZN3, the region comprising several genes for metal detoxification in *Epibacterium* sp. SZN4 also shows a high homology with the comparison sequences belonging to *Epibacterium mobile* EPIB1, *Pelagibaca abyssi* JLT2014 and *Ruegeria mobilis* F1926 suggesting that this region is highly preserved at the evolutionary level since the three microorganisms were isolated in different areas of the globe such as the Pacific Ocean (*E. mobile* EPIB1, and *P. abyssi* JLT2014; <https://www.ncbi.nlm.nih.gov/biosample/SAMEA4921595>) and Indian Ocean (*E. mobile* F1926, <https://www.ncbi.nlm.nih.gov/biosample/SAMN02471033>).

Further chemical characterization data are therefore desirable to understand if the presence of metal response genes are typical of such microorganisms or are selected following environmental stress.

In particular, the analysis of the gene region belonging to *Epibacterium* sp. SZN4 similarly to what reported by Matallana-Surget et al. (2018) following proteogenomic analysis of *Epibacterium Mobile* BBC367) identified the presence of genes codifying for detoxification in the presence of metals (ORF 4, 18, 25 and 28), specific genes for copper (ORF 1, 3, 4, 16, 22), a cadmium-zinc-cobalt efflux pump (ORF 19) and part of the genes constituting the operon involved in the detoxification of mercury (ORF 24, 26 and 27).

The entire mercury operon was also identified in *Halomonas* sp. SZN1 (Fig 3.39) whose coding sequence (from ORF 6 to ORF 11) was found to be highly conserved both in the reference organisms: *Halomonas axialiensis* Althf1 and *Halomonas* sp. ZM 3, isolated, respectively, from hydrothermal vents in the Pacific Ocean and from a mineral waste repository that was highly polluted with heavy metals in Poland (Dziewit et al. 2013). The typical structure of the mercury operon described by Boyd and Barkay (2012) was

also found in the sequence of *Halomonas* sp. SZN1 which shows two transcriptional regulator *MerR* (ORF 6 and 11), a mercuric transport protein *MerT* (ORF 7) able to transport Hg (II) to the cytoplasm, a periplasmic binding protein *MerP* (ORF 8), a mercuric reductase *MerA* (ORF 9), and an organic mercurial lyase *MerB* (ORF 10).

Finally also numerous proteins implicated in mechanisms of resistance to arsenic were found in the draft genomes. In particular, the genes coding for acriflavin resistance protein, arsenate reductase and arsenic resistance operon repressor were identified in almost all the genomes. However, these genes were organized in an operon like structure only in *Alcanivorax* sp. SZN2, *Halomonas* sp. SZN1, and *Epibacterium* sp. SZN4.

Sequences and relative comparisons with the regions of homologous microorganisms are shown in figures 3.40, 3.41 and 3.42. In particular, in the sequence belonging to *Alcanivorax* sp. SZN2, I identified an arsenical resistance protein *ArsH* (ORF 11), an oxidoreductase whose function is still not clear even if this enzyme is widely distributed among bacterial taxa (Chang, Yoon, and Kim 2018), an arsenic transporter *ArsB* (ORF 12), an arsenate reductase *ArsC* (ORF 13) capable of converting arsenate to arsenite by reduced glutathione (*GSH*) (Rosen and Liu 2009) and a transcription factor *ArsR*. Comparison with the sequences of *A. xenomutans* p 40, *A. Dieselsoi* B 5 and *A. sp. N3-2A* showed the conservation of more than 70% of the nucleotide residues coding for the operon proteins, even if the ORFs of *Alcanivorax xenomutans* p 40 code for different products compared to the other sequences, highlighting the absence of *ArsH* and *ArsC*. However, the presence of a high homology between the regions comprising the As operon and its flanking regions suggests that it is highly preserved at the evolutionary level in the genus *Alcanivorax*. Similarly, the region comprising the arsenic operon in

Halomonas sp. SZN1 also found a high degree of homology in the comparison sequences belonging to *Halomonas Olivaria* TYRc 17, *Halomonas* sp. R57-5, and *Halomonas ventosae* strain NRS2HaP1. Interestingly, the operon genes (ORF 6, 7, 10, 11, 12) in the draft genome of *Halomonas* sp. SZN1 are contiguous to each other while in the three genomes ORFs 6 and 7 are separated from the other ORFs by genes coding for non-identified products (ORF 8). The absence of these ORFs in the *Halomonas* sp. SZN1 draft genome suggests a possible removal of genes not involved in the detoxification of arsenic following evolutionary pressure given by the massive presence of this metalloid in the area in which it was isolated. This hypothesis, although it requires further experimental evidence, is supported by the observation that both *H. Olivaria* TYRC 17 and *H. sp.* R57-5 were isolated in areas that are not contaminated by this metal, including olive processing effluents (Nagata et al. 2019) and from Arctic marine waters (Williamson et al. 2016). Unfortunately there is no information about the site where *Halomonas ventosae* strain NRS2HaP1 (NCBI access: PRJNA397791) was isolated.

Finally the sequence identified in *Epibacterium* sp. SZN4, including genes for detoxification of arsenic, coding for a family transcriptional regulator *ArsR*, a novel transporter *ArsJ* (ORF 6), and another 2 transporters (ORF 7 and 8) showed a high homology with the homologous regions of *Epibacterium Mobile* EPIB1, *Ruegeria mobilis* F1926 and *Ruegeria* sp. TM1040. Interestingly, the flanking regions showed no correlation suggesting that the presence of arsenic resistance genes is due to horizontal gene transfer.



Figure 3.37. Heat map of genes and relative copy numbers identified by RAST in the six draft genomes analyzed. On the left column are indicated genes involved in “resistance to antibiotics and toxic compounds”. The different colour intensity is related to number of gene copies. (white: “no genes”; dark green “max. number of genes”)

Pseudoalteromonas sp. (metals resistance genes)

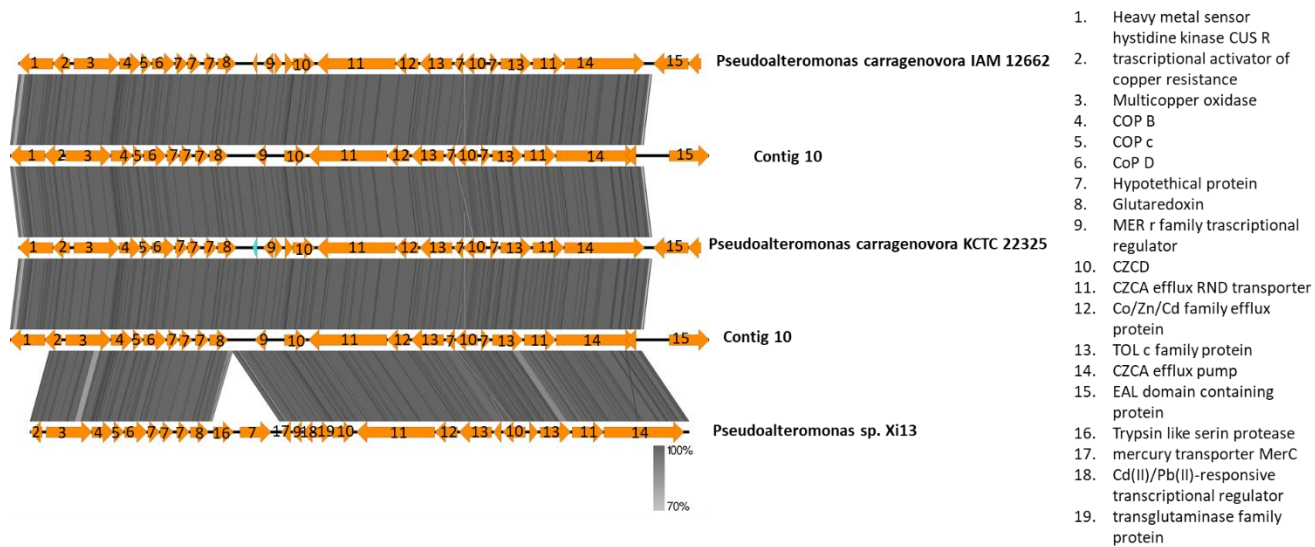


Figure 3.38. Comparison of strain sequences from my *Pseudoalteromonas* sp. SZN3 genome and the three closest sequences identified in the National Centre for Biotechnology Information (NCBI) data bank. The genes involved in metal resistance are indicated from ORF 2 to ORF 14. Contig 10 is the genomic region where the genes encoding for metal resistance were identified in my draft genome. The right panel lists genes that are encoded by the draft genome of *Pseudoalteromonas* sp. SZN3 (ORFs 1-15) and those that are encoded by reference genomes (ORFs 16-19)

Epibacterium sp. (metals resistance genes)

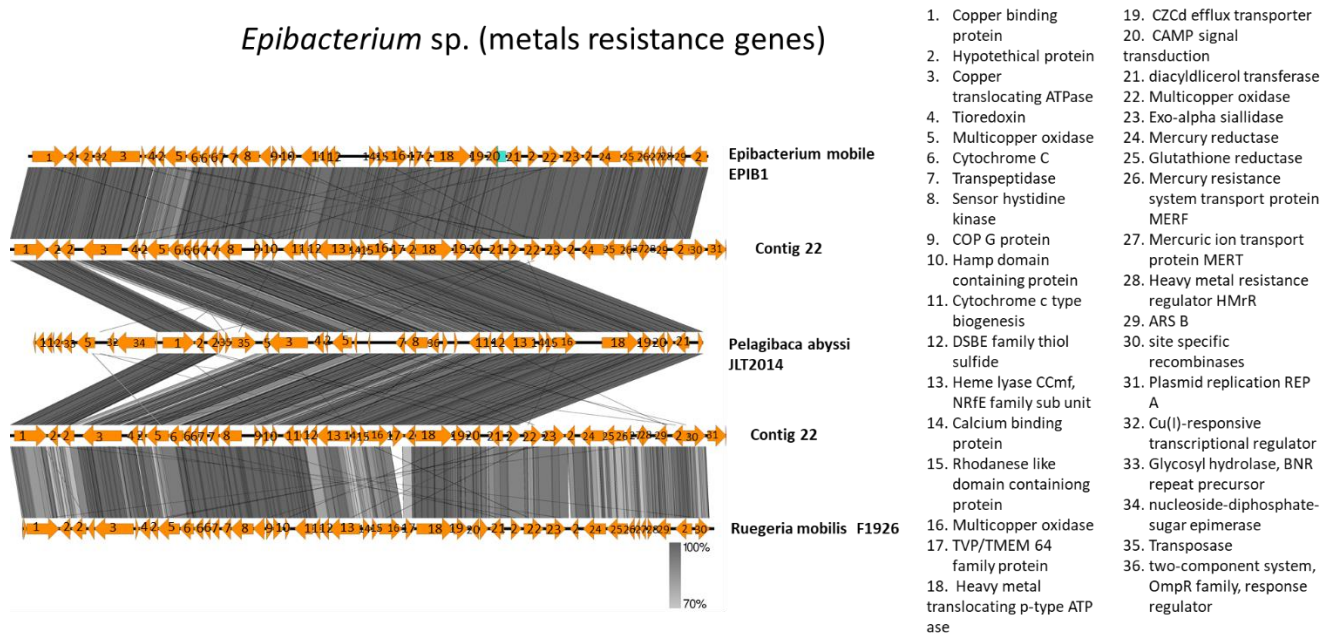


Figure 3.39. Comparison of strain sequences from my *Epibacterium* sp. SZN4 draft genome and the three closest sequences identified in the National Centre for Biotechnology Information (NCBI) data bank. The genes involved in metal resistance are indicated as ORF 1, 3, 4, 5, 16, 18, 19, 22, 24, 25, 26, 27, 28, 29. Contig 22 is the genomic region where the genes encoding for metal resistance were identified in my draft genome. The right panel lists genes that are encoded by the draft genome of *Epibacterium* sp. SZN4 (ORFs 1-31) and those that are encoded by reference genomes (ORFs 32-36)

Halomonas sp. (Mercury operon)

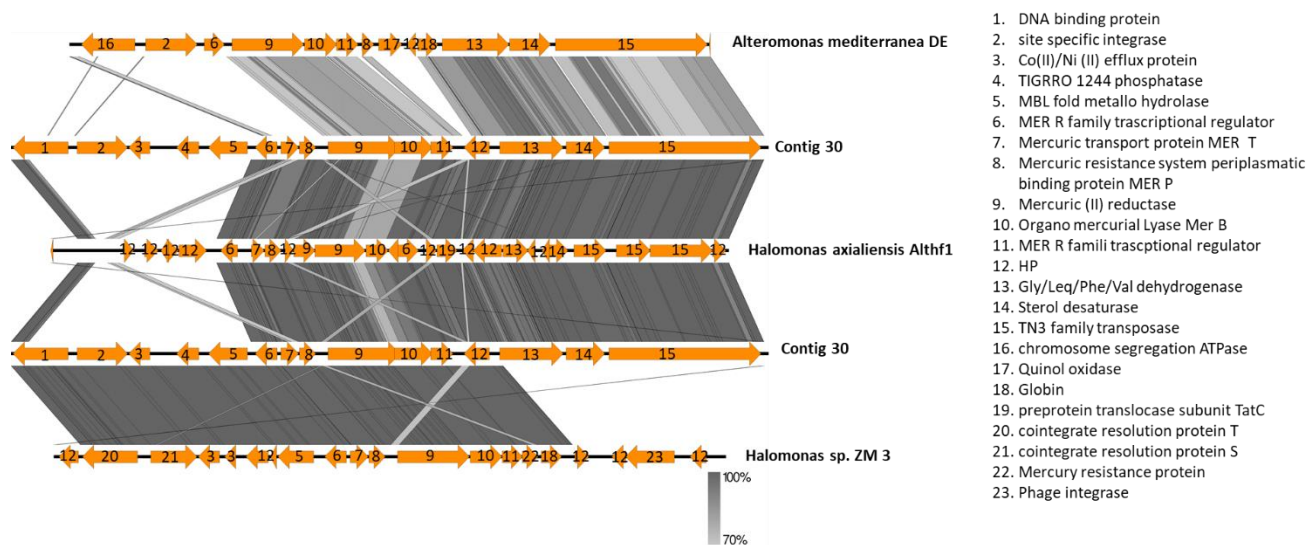


Figure 3.40. Comparison of strain sequences from my *Halomonas* sp. SZN1 genome and the three closest sequences identified in the National Centre for Biotechnology Information (NCBI) data bank. The genes involved in mercury resistance are indicated as ORF 6, 7, 8, 9, 10, 11. Contig 30 is the genomic region where the genes encoding for mercury esistance were identified in my draft genome. The right panel lists genes that are encoded by the draft genome of *Halomonas* sp. SZN1 (ORFs 1-15) and those that are encoded by reference genomes (ORFs 16-23)

Alcanivorax sp. (Arsenic operon)

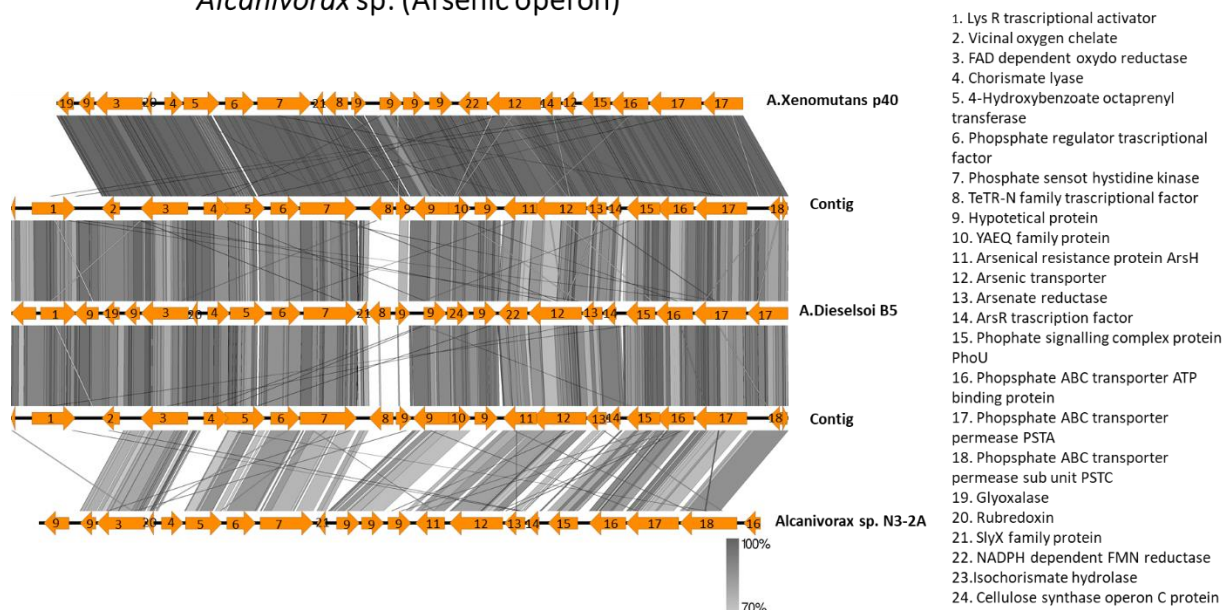


Figure 3.41. Comparison of strain sequences from my *Alcanivorax* sp. SZN2 genome and the three closest sequences identified in the National Centre for Biotechnology Information (NCBI) data bank. The genes involved in Arsenic resistance are indicated as ORF 11, 12, 13, 14. Contig 30 is the genomic region where the genes encoding for mercury resistance were identified in my draft genome. The right panel lists genes that are encoded by the draft genome of *Alcanivorax* sp. SZN2 (ORFs 1-18) and those that are encoded by reference genomes (ORFs 19-24)

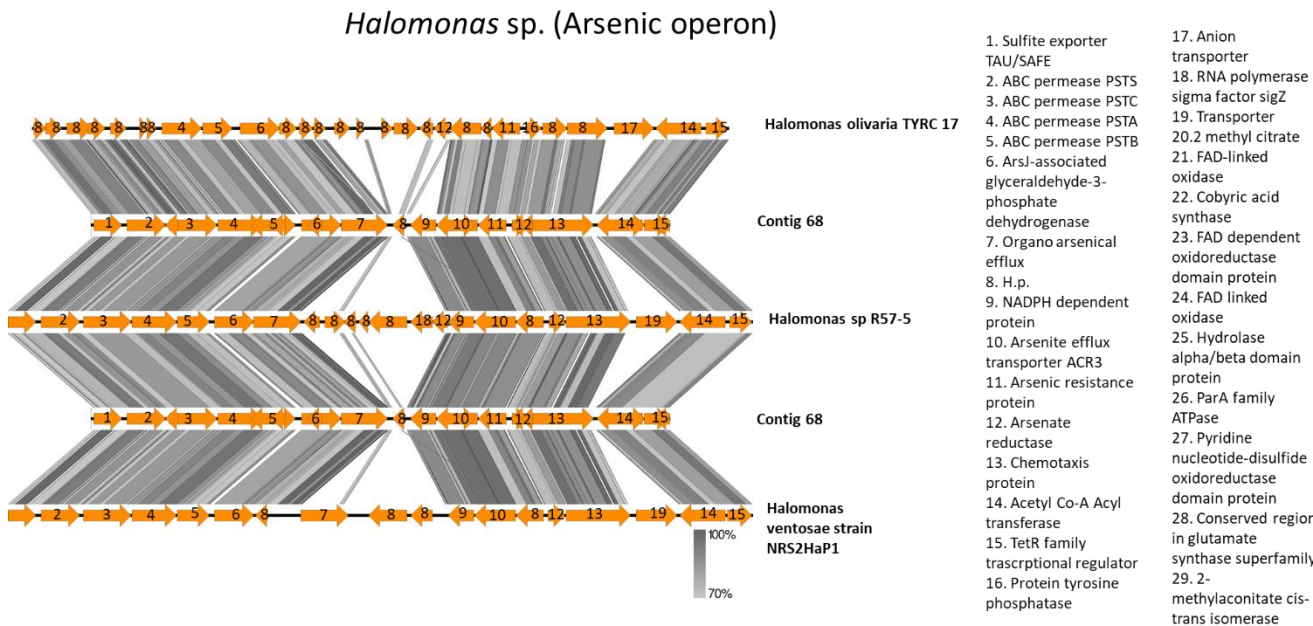


Figure 3.42. Comparison of strain sequences from my *Halomonas* sp. SZN1 genome and the three closest sequences identified in the National Centre for Biotechnology Information (NCBI) data bank. The genes involved in Arsenic resistance are indicated as ORF 6, 7, 10, 11, 12. Contig 68 is the genomic region where the genes encoding for Arsenic resistance were identified in my draft genome. The right panel lists genes that are encoded by the draft genome of *Halomonas* sp. SZN1 (ORFs 1-15) and those that are encoded by reference genomes (ORFs 16-29)

Epibacterium sp. (Arsenic operon)

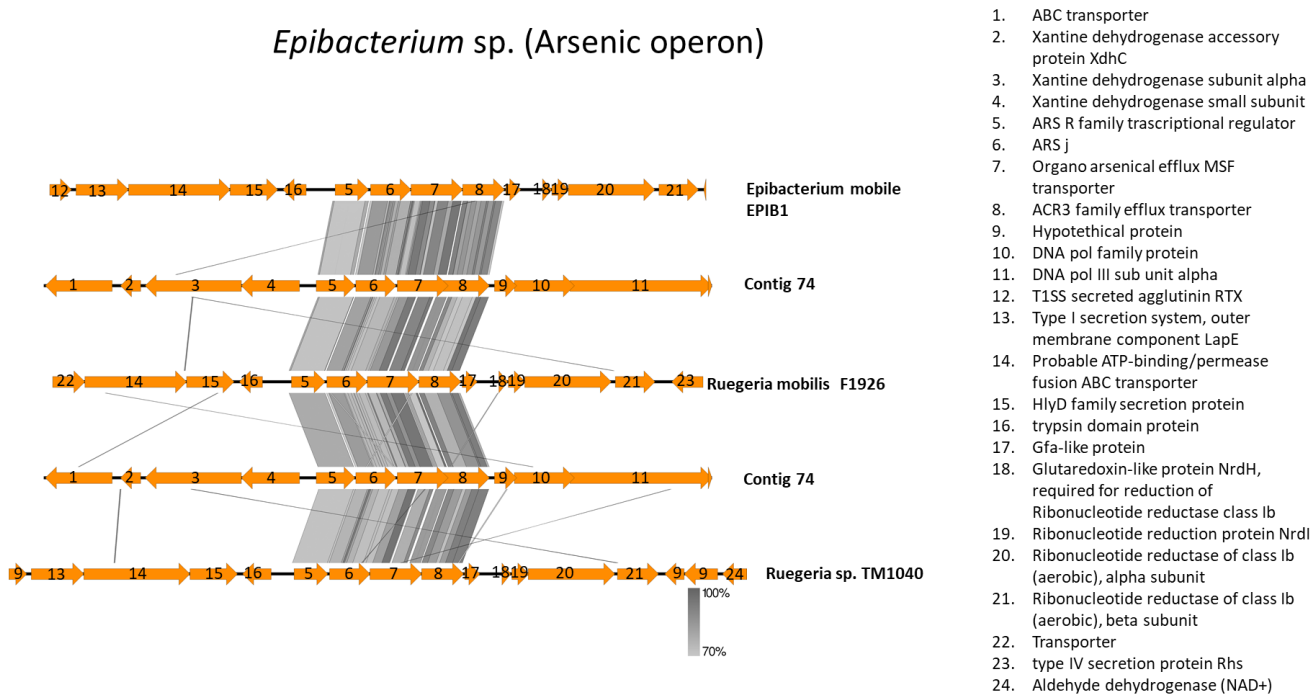


Figure 3.43. Comparison of strain sequences from my *Epibacterium* sp. SZN4 genome and the three closest sequences identified in the National Centre for Biotechnology Information (NCBI) data bank. The genes involved in Arsenic resistance are indicated as ORF 5, 6, 7, 18. Contig 74 is the genomic region where the genes encoding for Arsenic resistance were identified in my draft genome. The right panel lists genes that are encoded by the draft genome of *Epibacterium* sp. SZN4 (ORFs 1-11) and those that are encoded by reference genomes (ORFs 12-24)

4) Conclusion

Average Nucleotide Identity identified new species for the draft genomes of *Alkaliphilus* sp. SZN6, *Halomonas* sp. SZN1, *Oceanicaulis* sp. SZN5 and *Pseudoalteromonas* sp. SZN3 (Tab. 3.10). Indeed, the alignment of my draft genomes with the three closest genomes showed a reduced nucleotide conservation below 96%; the cutoff used to identify new species.

The analysis of the 6 draft genomes shown here denote a hydrocarbon degradative potential for 5 of the 6 genomes with the exception of *Alkaliphilus* sp. SZN6.

Furthermore, it is clear that the most promising organism in bioremediation processes is *Halomonas* sp. SZN1 as it is involved in all hydrocarbon degradation pathways as well as in mechanisms of metal detoxification, exhibiting almost all genes required for the metabolic routes here investigated (Tab. 10). Another two promising species are *Alcanivorax* sp. SZN2 and *Epibacterium* sp. SZN4 since both showed the presence of key enzymes such as Ring Hydroxylating dioxygenase and Cytochrome P450 as well as arsenic operon coding genes and numerous genes coding for metal efflux pumps involved in heavy metal resistance.

Additionally, intergenomic gene complementarity has been noted at the level of many hydrocarbon degradation pathways, since some genes belonging to a specific pathway were absent in a given microorganism but were present in others. These observations suggest that in the original environment, different bacteria work together to degrade toxic organic compounds. For this purpose, further analyzes are necessary to better understand the dynamics of microbial communities regulating these processes. Future

Transcriptome analysis of the most promising species (*Halomonas* sp. SZN1, *Alcanivorax* sp.SZN2, and *Epibacterium* sp.SZN4) is desirable to evaluate the presence of new proteins involved in the degradation / detoxification of toxic compounds since I already have the genomes sequenced and annotated. In details, the RNA seq will allow me to understand which genes in over expressed during a particular stressful condition.

Table 3.10. Summary table of the features shown by the draft genomes. In detail, ANI is the acronym of Average Nucleotide Identity; RHD is the acronym of Ring Hydroxylating Dioxygenase; CYP 450 is the acronym of Cytochrome P450

List of draft genomes	ANI < 96%	Genes and Pathway involved in Hydrocarbons Degradation							Genes And Operon involved in Metals resistance		
		RHDs	CYP 450	Catechol pathway	Protocatechuate pathway	Homogentisate pathway	Homoprotocatechuate pathway	Phenil acetic pathway	Arsenic operon	Mercury operon	Other metal resistance gene
<i>Alcanivorax</i> sp.		X	X				X		X		X
<i>Alkaliphilus</i> sp.	X										X
<i>Epibacterium</i> sp.		X	X		X	X			X		X
<i>Halomonas</i> sp.	X	X	X	X	X	X	X	X	X	X	X
<i>Oceanicaulis</i> sp.	X					X					X
<i>Pseudoalteromonas</i> sp.	X	X				X					X

Chapter 5

General conclusions

The results obtained during my PhD thesis work reveal the potential of some bacterial taxa/consortia for the bioremediation of heavy metals and/or organic pollutants. New information acquired in the present work on the biostimulation of the microbial communities and bioaugmentation experiments with autochthonous communities provide useful insights on how to enhance the removal rates of contaminants from the environmental matrix, for further technological development and applications in highly polluted sites, such as the Bagnoli-Coroglio sediments.

The possibility of designing an effective biostimulation strategy arises from the data obtained in my work and described in Chapter 2. Indeed, the extraction of environmental DNA from highly polluted sediments from Bagnoli-Coroglio, with its subsequent amplification and sequencing of 16s rRNA genes revealed the bacterial taxa assemblages thriving in such harsh environmental conditions. In detail, the most abundant classes identified in the Bagnoli-Coroglio sediments were Gammaproteobacteria, Alphaproteobacteria, Actinobacteria and Flavobacteria. These bacterial classes have already been identified as being capable of reducing organic contaminants by more than 80% by Al-Kindi and Abed (2016), and Al-Mailem, Elias, and Radwan (2018).

In the Bagnoli-Coroglio sediments, meta-barcoding analysis carried out on bacterial communities shows that the taxa distribution in the three different depth layers was not

affected directly by the concentration of contaminants. My results do not exclude that chronic chemical pollution has played a role in selecting a pool of resistant bacteria over a century of contamination by the activity of the ILVA steel plant but, rather, they suggest that the distribution of different toxic compounds does not affect the microbial composition in the studied area. Conversely, the concentration of Particulate Organic Matter released by sewage discharge and the grain size of the sediments are likely to have played a major role in shaping the microbial assemblages since only these two variables are correlated with the Bray-Curtis clusterization at the four stations. Cronin-O'Reilly et al. (2018) and Babcsányi, Meite, and Imfeld (2017) also found that a variety of factors, such as organic matter, N and P bioavailability, bioturbation and grain size play a major role in shaping the composition of bacterial assemblages even in areas polluted with inorganic contaminants.

Isolation and cultivation of promising cultures are discussed in Chapter 3 showing the capability of mix cultures (Consortia A2, 2B, 41, 4) and isolated taxa (*Halomonas* sp. SZN1, *Alcanivorax* sp. SZN2, *Pseudoalteromonas* sp. SZN3, *Epibacterium* sp. SZN4, and *Virgibacillus* sp. SZN7) to grow in presence of organic and inorganic pollutants. In particular, of the five heavy metals tested, Cd and Zn exerted the most toxic effects since all bacterial cultures, except *Alcanivorax* sp. SZN2 did not grow (Tab. 4.1). Conversely, all the isolated or mixed taxa were able to grow with PAH concentrations between 1000 and 10,000 ppm (Tab. 4.1).

Table 4.1. List of cultures and their ability to grow at different concentrations (100, 1000, 10000 ppm) of As, Pb, Cd, Zn, Cu and PAHs.

Cultures	Concentrations (ppm) of pollutants at which Cultures grow					
	As	Pb	Cd	Zn	Cu	PAHs
<i>Halomonas sp.</i>	100	100, 1000	-	-	100	100, 1000, 10000
<i>Alcanivorax sp.</i>	100, 1000	100	100	100	100	100, 1000
<i>Pseudoalteromonas sp.</i>	100, 1000	100, 1000	-	100	100	100, 1000, 10000
<i>Epibacterium sp.</i>	100, 1000, 10000	100	100, 1000	100	100	100, 1000
<i>Virgibacillus sp.</i>	-	100	-	100	100	100, 1000, 10000
Consortium A2	100, 10000	100, 1000, 10000	-	10000	-	100, 1000
Consortium 2B	100, 1000, 10000	10000	100	-	100	100, 1000
Consortium 41	100, 10000	10000	-	10000	100	100, 1000, 10000
Consortium 4	100, 1000, 10000	100, 1000	-	-	100	100, 1000

Interestingly, tests conducted in marine broth solutions highlighted the ability of all cultures, both mix and bacterial isolates, to remove PAH mixtures, with the highest removal performance observed in the presence of Naphtalene followed by Pyrene and Phenathrene. Moreover, my data demonstrate the ability of such microorganisms to enhance the precipitation of metals, mainly Lead, Cadmium and Copper. Only *Halomonas sp.* SZN1 promoted the precipitation of As and Zn (Tab. 4.2).

The ability shown by the cultures to precipitate heavy metals and degrade PAHs when incubated in liquid solution highlight their applicative interest and their potential usefulness for wastewater treatments, with adequate optimization of variables such as salinity and nutrient concentrations.

Table 4.2. List of cultures and their ability to precipitate heavy metals (As, Pb, Cd, Zn, Cu) and remove PAHs in marine broth solutions after 27 days of incubation.

Cultures	% of Metals precipitated by cultures					% of PAHs degraded by cultures		
	As	Pb	Cd	Zn	Cu	Pyrene	Phenantrene	Naphtalene
<i>Halomonas sp.</i>	11%	46%	57%	10%	-	99%	62%	99%
<i>Alcanivorax sp.</i>	-	34%	35%	-	-	99%	62%	99%
<i>Pseudoalteromonas sp.</i>	-	-	42%	-	65%	94%	63%	99%
<i>Epibacterium sp.</i>	-	-	51%	-	80%	47%	62%	99%
<i>Virgibacillus sp.</i>	-	-	38%	-	71%	99%	62%	98%
Consortium A2	-	54%	-	-	-	93%	67%	99%
Consortium 2B	-	47%	-	-	-	74%	28%	99%
Consortium 41	-	48%	-	-	-	88%	64%	99%
Consortium 4	-	20%	-	-	-	86%	64%	99%

Despite the treatments have been carried out in a rich broth such as Marine Broth, the ability of all the cultures, both mixed and bacterial isolates, to degrade hydrocarbons directly in the sediments suggests their possible use in an effective treatment of highly contaminated sediments being able to decrease the concentration of organic

contaminants, especially di Benzo anthracene, Benzo (g, h, i) perylene, Benzo (b) fluoranthrene, and Benzo anthracene by about 50% (Tab. 4.3).

Table 4.3. List of cultures and their ability to degrade hydrocarbons after 27 days of incubation in contaminated Bagnoli –Coroglio sediments.

Cultures	% of hydrocarbons degraded after adding cultures to Bagnoli Coroglio sediments										
	Pyrene	Indeno pyrene	di benzo anthracene	Chrysene	Benzo (k) fluoranthrene	Benzo (g,h,i) perylene	Benzo (b) fluoranthrene	Benzo (a) pyrene	Benzo anthracene	PAHs	Average degradation ability per Culture
<i>Halomonas sp.</i>	64%	52%	63%	56%	46%	70%	68%	51%	70%	63%	60%
<i>Alcanivorax sp.</i>	51%	38%	63%	38%	26%	63%	52%	36%	62%	51%	48%
<i>Pseudoalteromonas sp.</i>	6%	23%	25%	9%	30%	24%	26%	3%	40%	14%	20%
<i>Epibacterium sp.</i>	31%	-	39%	17%	-	34%	29%	13%	52%	29%	31%
<i>Virgibacillus sp.</i>	44%	28%	59%	30%	23%	56%	50%	30%	58%	42%	42%
Consortium A2	64%	63%	86%	55%	35%	67%	68%	70%	61%	62%	63%
Consortium 2B	20%	9%	38%	38%	11%	36%	48%	23%	35%	31%	29%
Consortium 41	5%	39%	96%	3%	41%	20%	-	59%	5%	48%	35%
Consortium 4	20%	45%	84%	44%	35%	55%	43%	65%	62%	51%	50%
Average compounds degradation for all the cultures	34%	37%	61%	32%	31%	47%	48%	39%	49%	43%	

The most suitable cultures for hydrocarbon degradation were *Halomonas sp.* SZN1 and Consortium A2 since both allowed to obtain, on average, a degradation yield about 60%.

In many cases, a different hydrocarbon degradation performance was observed comparing single isolates and the mixture of these taxa highlighting synergetic/antagonistic activities among taxa. Further studies addressing this aspect are needed.

Bacterial effects on the heavy metals present in the Bagnoli-Coroglio sediments highlighted the ability of all taxa to reduce the mobility (and thus its potential toxicity)

of As, although the most notable effects (> 30%) were found following treatment with Consortia A2, 41, 4 (Tab. 4.4).

Table 4.4. List of cultures and their ability to reduce Heavy Metal bioavailability (As, Pb, Cd, Zn, Cu) after 27 days of incubation with Bagnoli-Coroglio sediments.

strains	% of Heavy metals partitioned into a less bioavailable sediment fraction				
	As	Pb	Cd	Zn	Cu
<i>Halomonas sp.</i>	16%	-	-	-	-
<i>Alcanivorax sp.</i>	15%	-	-	-	-
<i>Pseudoalteromonas sp.</i>	15%	22%	-	-	-
<i>Epibacterium sp.</i>	20%	11%	-	-	-
<i>Virgibacillus sp.</i>	54%	-	-	-	-
Consortium A2	28%	22%	33%	-	-
Consortium 2B	20%	11%	-	-	-
Consortium 41	30%	27%	-	-	-
Consortium 4	43%	20%	32%	-	-

Similarly, all the Consortia along with *Pseudoalteromonas sp.* SZN3, and *Epibacterium sp.* SZN4, reduced Pb mobility in sediments, with the highest value obtained by Consortium 41 (27%). Only consortium A2 and 4 reduced Cd mobility in sediments, promoting a reduction of the Cd concentration associated with the exchangeable carbonate fraction of about 30% (Tab. 4.4).

Therefore, the effect mediated by Consortia A2, 4 e 41 in lowering the mobility of As, Cd and Pb heavy metals associated with sediments suggests that the bacterial taxa present

therein are suitable for the reduction of such harmful inorganic compounds. The mechanism used by these bacteria leading to different heavy metal partitioning need to be further investigated. A mechanism has been described for sulfur reducing bacteria (Jiang and Fan 2008), which generally are metabolically active in anaerobic conditions due to their ability to use sulfate as a terminal electron acceptor (Muyzer and Stams 2008). A possible hypothesis explaining the partitioning of heavy metals observed here may be due to modification of interactions between heavy metals and the different geochemical fractions of the sediment favoured by the addition of cultures. Indeed, as described by Kumari et al. (2016), bacteria are able to induce the partitioning of metals into different geochemical fractions through the production of enzymes capable of mediating chemical reactions such as the formation of carbonates, which may complex soluble heavy metals. To better understand this phenomenon, further studies combining metabolomics and transcriptomics coupled with the genome analysis are warranted.

In particular, the analysis of the genomes of promising bacterial taxa (Chapter 4), highlights that a similar pollution condition of the Sarno river and the Bagnoli-Coroglio area, characterized by hydrocarbons and heavy metals, has selected for two identical taxa: *Halomonas* sp. SZN1 and *Alcanivorax* sp. SZN2.

Halomonas sp. and *Alcanivorax* sp. from the Sarno river mouth showed 100% Average Nucleotide Identity with the homologous taxa from Bagnoli-Coroglio. This suggests that both *Halomonas* sp. SZN1 and *Alcanivorax* sp. SZN2 are capable of effectively degrading hydrocarbons, and could therefore be used for the possible *in-situ* bioremediation of these two areas. Furthermore, the cultures, isolated here, may be used for future ex-

situ bioremediation tests on sediment samples from other polluted areas in order to understand whether their bioremediation abilities are affected by the presence of a different contaminated matrix or if, instead, they are able to exhibit the same properties regardless of the matrix typologies.

Genome analysis described in Chapter 4 highlighted the genes involved in hydrocarbon degradation for 5 of the 6 genomes with the exception of *Alkaliphilus* sp. SZN6, whose role, within microbial communities capable to cope with high pollutant levels, still remains to be defined.

Genome analysis as well as culturing results (Tab 4.2 and Tab. 4.3) suggest, that *Halomonas* sp. SZN1 may be the most promising strain to be tested in a real bioremediation experiments. Indeed, it has been shown to be implicated in all the hydrocarbon degradation pathways as well as in mechanisms of metal detoxification, containing almost all the genes involved in the investigated metabolic routes. The distribution of genes belonging to the same pathway in different microorganisms suggest that different bacteria can have a complementary role in the degradation of toxic organic compounds.

Further analyses are necessary to understand the potential synergistic interactions among bacteria in hydrocarbon degradation processes. Finally, since the genomes of *Halomonas* sp. SZN1, *Oceanicaulis* sp. SZN5 and *Pseudoalteromonas* sp. SZN3 have been shown to differ markedly in terms of nucleotide conservation if compared to the closest genome deposited in the databases, the analysis of the transcriptomes would allow to evaluate the presence of potential new proteins/enzymes or even new pathways involved in the degradation / detoxification of toxic compounds.

6) Bibliography

- Abatenh, Endeshaw, Birhanu Gizaw, Zerihun Tsegaya, and Misganaw Wassie. 2017. "Application of Microorganisms in Bioremediation-Review." *Journal of Environmental Microbiology* 1 (1): 2–9.
- Abdel-Shafy, Hussein I., and Mona S.M. Mansour. 2016. "A Review on Polycyclic Aromatic Hydrocarbons: Source, Environmental Impact, Effect on Human Health and Remediation." *Egyptian Journal of Petroleum* 25 (1): 107–23.
<https://doi.org/10.1016/j.ejpe.2015.03.011>.
- Achal, Varenayam, Xiangliang Pan, and Daoyong Zhang. 2012. "Bioremediation of Strontium (Sr) Contaminated Aquifer Quartz Sand Based on Carbonate Precipitation Induced by Sr Resistant Halomonas Sp." *Chemosphere* 89 (6): 764–68.
<https://doi.org/10.1016/j.chemosphere.2012.06.064>.
- Adams, Godleads Omokhagbor, Prekeyi Tawari Fufeyin, Samson Eruke Okoro, Igelenyah Ehinomen, and Environmental Biology. 2015. "Bioremediation , Biostimulation and Bioaugmentation : A Review." *International Journal of Environmental Bioremediation & Biodegradation* 3 (1): 28–39. <https://doi.org/10.12691/ijebb-3-1-5>.
- Adriaens, P., M. Y. Li, and A. M. Michalak. 2006. "Scaling Methods of Sediment Bioremediation Processes and Applications." *Engineering in Life Sciences* 6 (3): 217–27.
<https://doi.org/10.1002/elsc.200520127>.
- Agius, Suzanne J, and Linda Porebski. 2008. "Towards the Assessment and Management of Contaminated Dredged Materials." *Integrated Environmental Assessment and Management* 4 (2): 255–60.
- Ahalya, N, T V Ramachandra, and R D Kanamadi. 2003. "Biosorption of Heavy Metals." *Research Journal Of Chemistry And Environment*. Vol. 7.
- Ahmad, Manzoor, Qingsong Yang, Yanying Zhang, Juan Ling, Wasim Sajjad, Shuhua Qi, Weiguo Zhou, et al. 2019. "The Distinct Response of Phenanthrene Enriched Bacterial Consortia to Different PAHs and Their Degradation Potential: A Mangrove Sediment Microcosm Study." *Journal of Hazardous Materials* 380: 120863.
<https://doi.org/10.1016/j.jhazmat.2019.120863>.
- Ahmed, Ayanleh Mahamoud, Emilie Lyautey, Chloé Bonnineau, Aymeric Dabrin, and Stéphane Pesce. 2018. "Environmental Concentrations of Copper, Alone or in Mixture with Arsenic, Can Impact River Sediment Microbial Community Structure and Functions." *Frontiers in Microbiology* 9 (AUG): 1–13. <https://doi.org/10.3389/fmicb.2018.01852>.
- Aiuppa, A., R. Avino, L. Brusca, S. Caliro, G. Chiodini, W. D'Alessandro, R. Favara, et al. 2006. "Mineral Control of Arsenic Content in Thermal Waters from Volcano-Hosted Hydrothermal Systems: Insights from Island of Ischia and Phlegrean Fields (Campanian Volcanic Province, Italy)." *Chemical Geology* 229 (4): 313–30.
<https://doi.org/10.1016/j.chemgeo.2005.11.004>.
- Ajayan, K. V., M. Selvaraju, and K. Thirugnanamoorthy. 2011. "Growth and Heavy Metals Accumulation Potential of Microalgae Grown in Sewage Wastewater and Petrochemical Emuents." *Pakistan Journal of Biological Sciences* 14 (16): 805–11.

<https://doi.org/10.3923/pjbs.2011.805.811>.

- Akcil, Ata, Ceren Erust, Sevda Ozdemiroglu, Viviana Fonti, and Francesca Beolchini. 2014. "A Review of Approaches and Techniques Used in Aquatic Contaminated Sediments: Metal Removal and Stabilization by Chemical and Biotechnological Processes." *Journal of Cleaner Production* 86: 24–36. <https://doi.org/10.1016/j.jclepro.2014.08.009>.
- Al-Kindi, Sumaiya, and Raeid M.M. Abed. 2016. "Effect of Biostimulation Using Sewage Sludge, Soybean Meal, and Wheat Straw on Oil Degradation and Bacterial Community Composition in a Contaminated Desert Soil." *Frontiers in Microbiology* 7: 1–14. <https://doi.org/10.3389/fmicb.2016.00240>.
- Al-Maillem, Dina M., Mohamed Eliyas, and Samir S. Radwan. 2018. "Ferric Sulfate and Proline Enhance Heavy-Metal Tolerance of Halophilic/Halotolerant Soil Microorganisms and Their Bioremediation Potential for Spilled-Oil under Multiple Stresses." *Frontiers in Microbiology* 9: 1–12. <https://doi.org/10.3389/fmicb.2018.00394>.
- Al-Turki, A. I. 2009. "Microbial Polycyclic Aromatic Hydrocarbons Degradation in Soil." *Research Journal of Environmental Toxicology*. <https://doi.org/10.3923/rjet.2009.1.8>.
- Ali, Syed Shahid, Iffat Habib, and Tanzeela Riaz. 2009. "Screening and Characterization of Alkaliphilic Bacteria from Industrial Effluents." *Punjab Univ. J. Zool* 24: 49–60.
- Alomary, Ahmed A., and Soraya Belhadj. 2007. "Determination of Heavy Metals (Cd, Cr, Cu, Fe, Ni, Pb, Zn) by ICP-OES and Their Speciation in Algerian Mediterranean Sea Sediments after a Five-Stage Sequential Extraction Procedure." *Environmental Monitoring and Assessment* 135 (1–3): 265–80. <https://doi.org/10.1007/s10661-007-9648-8>.
- Aly Salem, Dalia M.S., Azza Khaled, and Ahmed El Nemr. 2013. "Assessment of Pesticides and Polychlorinated Biphenyls (PCBs) in Sediments of the Egyptian Mediterranean Coast." *Egyptian Journal of Aquatic Research* 39 (3): 141–52. <https://doi.org/10.1016/j.ejar.2013.11.001>.
- Amoozegar, Mohammad Ali, Nooshinsadat Ghazanfari, and Maryam Didari. 2012. "Lead and Cadmium Bioremoval by Halomonas Sp., an Exopolysaccharide-Producing Halophilic Bacterium." *Progress in Biological Sciences Vol. 2* (1): 1–11.
- Anetor, John I., Hideki Wanibuchi, and Shoji Fukushima. 2007. "Arsenic Exposure and Its Health Effects and Risk of Cancer in Developing Countries: Micronutrients as Host Defence." *Asian Pacific Journal of Cancer Prevention* 8 (1): 13–23.
- Ara, Ismat, and Catherine N. Mulligan. 2008. "Conversion of Cr(VI) in Water and Soil Using Rhamnolipid." *Journal of Chemistry and Ecology* 31: 707–23.
- Arias-Barrau, Elsa, Elías R. Olivera, José M. Luengo, Cristina Fernández, Beatriz Galán, José L. García, Eduardo Díaz, and Baltasar Miñambres. 2004. "The Homogentisate Pathway: A Central Catabolic Pathway Involved in the Degradation of L-Phenylalanine, L-Tyrosine, and 3-Hydroxyphenylacetate in Pseudomonas Putida." *Journal of Bacteriology* 186 (15): 5062–77. <https://doi.org/10.1128/JB.186.15.5062-5077.2004>.
- Arienzo, Michele, Vincenzo Allocca, Ferdinando Manna, Marco Trifuoggi, and Luciano Ferrara. 2015. "Effectiveness of a Physical Barrier for Contaminant Control in an Unconfined Coastal Plain Aquifer: The Case Study of the Former Industrial Site of Bagnoli (Naples, Southern Italy)." *Environmental Monitoring and Assessment* 187 (12): 761. <https://doi.org/10.1007/s10661-015-4988-2>.

- Arjoon, Olaniran, and Pillay. 2013. "Co-Contamination of Water with Chlorinated Hydrocarbons and Heavy Metals: Challenges and Current Bioremediation Strategies." *International Journal of Environmental Science and Technology* 10 (2): 395–412. <https://doi.org/10.1007/s13762-012-0122-y>.
- Arsène-Ploetze, Florence, Philippe N. Bertin, and Christine Carapito. 2015. "Proteomic Tools to Decipher Microbial Community Structure and Functioning." *Environmental Science and Pollution Research* 22 (18): 13599–612. <https://doi.org/10.1007/s11356-014-3898-0>.
- Arunakumara, , Zhang Xuecheng, and Song Xiaojin. 2008. "Bioaccumulation of Pb 2+ and Its Effects on Growth, Morphology and Pigment Contents of Spirulina (Arthrospira) Platensis." *J. Ocean Univ. Chin. (Oceanic* 7 (4): 397–403. <https://doi.org/10.1007/s11802-008-0397-2>.
- Aşçi, Y., M. Nurbaş, and Y. Sağ Açıkel. 2007. "Sorption of Cd(II) onto Kaolin as a Soil Component and Desorption of Cd(II) from Kaolin Using Rhamnolipid Biosurfactant." *Journal of Hazardous Materials* 139 (1): 50–56. <https://doi.org/10.1016/j.jhazmat.2006.06.004>.
- Ayangbenro, Ayansina Segun, and Olubukola Oluranti Babalola. 2017. "A New Strategy for Heavy Metal Polluted Environments: A Review of Microbial Biosorbents." *International Journal of Environmental Research and Public Health* 14 (1). <https://doi.org/10.3390/ijerph14010094>.
- Aylagas, Eva, Ángel Borja, Michael Tangherlini, Antonio Dell'Anno, Cinzia Corinaldesi, Craig T. Michell, Xabier Irigoien, Roberto Danovaro, and Naiara Rodríguez-Ezpeleta. 2017. "A Bacterial Community-Based Index to Assess the Ecological Status of Estuarine and Coastal Environments." *Marine Pollution Bulletin* 114 (2): 679–88. <https://doi.org/10.1016/j.marpolbul.2016.10.050>.
- Ayse, B., Y., Oya, I., Selin, S. 2005. "Bioaccumulation and Toxicity of Different Copper Concentrations in Tetraselmis Chuii." *Journal of Fisheries & Aquatic Sciences* 22 (3–4): 297–301. http://50.6.25.94/pdf/2005-3-4/2005_22_3_4_8.pdf.
- Azubuiké, Christopher Chibueze, Chioma Blaise Chikere, and Gideon Chijioke Okpokwasili. 2016. "Bioremediation Techniques—Classification Based on Site of Application: Principles, Advantages, Limitations and Prospects." *World Journal of Microbiology and Biotechnology* 32 (11): 1–18. <https://doi.org/10.1007/s11274-016-2137-x>.
- Babcsányi, Izabella, Fatima Meite, and Gwenaël Imfeld. 2017. "Biogeochemical Gradients and Microbial Communities in Winogradsky Columns Established with Polluted Wetland Sediments." *FEMS Microbiology Ecology* 93 (8): 1–11. <https://doi.org/10.1093/femsec/fix089>.
- Bacosa, Hernando Pactao, Koichi Suto, and Chihiro Inoue. 2012. "Bacterial Community Dynamics during the Preferential Degradation of Aromatic Hydrocarbons by a Microbial Consortium." *International Biodeterioration and Biodegradation* 74: 109–15. <https://doi.org/10.1016/j.ibiod.2012.04.022>.
- Balaji, V., P. Arulazhagan, and P. Ebenezer. 2014. "Enzymatic Bioremediation of Polyaromatic Hydrocarbons by Fungal Consortia Enriched from Petroleum Contaminated Soil and Oil Seeds." *Journal of Environmental Biology* 35 (3): 521–29. <https://doi.org/10.13140/2.1.1528.3846>.
- Baldantoni, Daniela, Alessandro Bellino, Giusy Lofrano, Giovanni Libralato, Luca Pucci, and Maurizio Carotenuto. 2018. "Biomonitoring of Nutrient and Toxic Element

- Concentrations in the Sarno River through Aquatic Plants." *Ecotoxicology and Environmental Safety* 148 (October 2017): 520–27.
<https://doi.org/10.1016/j.ecoenv.2017.10.063>.
- Bargiela, R., Malpelli, F., [...] Ferrer, M. 2015. Bacterial population and biodegradation potential in chronically crude oil contaminated marine sediments are strongly linked to temperature. *Scientific Reports* 5, 11651.
- Barry, Sarah, and Gregory Challis. 2013. "Mechanism and Catalytic Diversity of Rieske Non-Heme Iron- Dependent Oxygenases." *ACS Catal.* 4 (3): 10.
<https://doi.org/10.1016/j.cortex.2009.08.003.Predictive>.
- Barton, Larry L., and Guy D. Fauque. 2009. *Chapter 2 Biochemistry, Physiology and Biotechnology of Sulfate-Reducing Bacteria. Advances in Applied Microbiology.* 1st ed. Vol. 68. Elsevier Inc. [https://doi.org/10.1016/S0065-2164\(09\)01202-7](https://doi.org/10.1016/S0065-2164(09)01202-7).
- Bashiardes, Stavros, Gili Zilberman-Schapira, and Eran Elinav. 2016. "Use of Metatranscriptomics in Microbiome Research." *Bioinformatics and Biology Insights* 10: 19–25. <https://doi.org/10.4137/BBI.S34610>.
- Bertelli, Claire, Matthew R. Laird, Kelly P. Williams, Britney Y. Lau, Gemma Hoad, Geoffrey L. Winsor, and Fiona S.L. Brinkman. 2017. "IslandViewer 4: Expanded Prediction of Genomic Islands for Larger-Scale Datasets." *Nucleic Acids Research* 45: 30–35.
<https://doi.org/10.1093/nar/gkx343>.
- Bertocci, I., A. Dell'Anno, L. Musco, C. Gambi, V. Saggiomo, M. Cannavacciuolo, M. Lo Martire, A. Passarelli, G. Zazo, and R. Danovaro. 2019. "Multiple Human Pressures in Coastal Habitats: Variation of Meiofaunal Assemblages Associated with Sewage Discharge in a Post-Industrial Area." *Science of the Total Environment* 655: 1218–31.
<https://doi.org/10.1016/j.scitotenv.2018.11.121>.
- Besaury, Ludovic, Florence Marty, Sylvaine Buquet, Valérie Mesnage, Gerard Muyzer, and Laurent Quillet. 2013. "Culture-Dependent and Independent Studies of Microbial Diversity in Highly Copper-Contaminated Chilean Marine Sediments." *Microbial Ecology* 65 (2): 311–24. <https://doi.org/10.1007/s00248-012-0120-0>.
- Beye, M., N. Fahsi, D. Raoult, and P. E. Fournier. 2018. "Careful Use of 16S RRNA Gene Sequence Similarity Values for the Identification of Mycobacterium Species." *New Microbes and New Infections* 22: 24–29. <https://doi.org/10.1016/j.nmni.2017.12.009>.
- Beyersmann, Detmar, and Andrea Hartwig. 2008. "Carcinogenic Metal Compounds: Recent Insight into Molecular and Cellular Mechanisms." *Archives of Toxicology* 82 (8): 493–512.
<https://doi.org/10.1007/s00204-008-0313-y>.
- Bharagava, Ram N., Diane Purchase, Gaurav Saxena, and Sikandar I. Mulla. 2019. *Applications of Metagenomics in Microbial Bioremediation of Pollutants. Microbial Diversity in the Genomic Era.* Elsevier Inc. <https://doi.org/10.1016/b978-0-12-814849-5.00026-5>.
- Bienhold, Christina, Lucie Zinger, Antje Boetius, and Alban Ramette. 2016. "Diversity and Biogeography of Bathyal and Abyssal Seafloor Bacteria." *PLoS ONE* 11 (1): 1–20.
<https://doi.org/10.1371/journal.pone.0148016>.
- Boechat, Cácio Luiz, Patricia Dörr De Quadros, Patrícia Giovanella, Ana Clecia Campos Brito, Filipe Selau Carlos, Enilson Luiz Saccol De Sá, and Flávio Anastácio De Oliveira Camargo. 2018. "Metal-Resistant Rhizobacteria Change Soluble-Exchangeable Fraction in Multi-

- Metalcontaminated Soil Samples." *Revista Brasileira de Ciencia Do Solo* 42: 1–11. <https://doi.org/10.1590/18069657rbcs20170266>.
- Bolyen, E, JR Rideout, MR Dillon, NA Bokulich, CC Abnet, GA Al-Ghalith, H Alexander, et al. 2019. "Reproducible , Interactive , Scalable and Extensible Microbiome Data Science Using QIIME 2." *Nature Biotechnology* 37: 852–857. <https://doi.org/10.1038/s41587-019-0209-9>.
- Bordas, François, Pierre Lafrance, and Richard Villemur. 2005. "Conditions for Effective Removal of Pyrene from an Artificially Contaminated Soil Using *Pseudomonas Aeruginosa* 57SJ Rhamnolipids." *Environmental Pollution* 138 (1): 69–76. <https://doi.org/10.1016/j.envpol.2005.02.017>.
- Boyd, Eric S., and Tamar Barkay. 2012. "The Mercury Resistance Operon: From an Origin in a Geothermal Environment to an Efficient Detoxification Machine." *Frontiers in Microbiology* 3 (OCT): 1–13. <https://doi.org/10.3389/fmicb.2012.00349>.
- Bradáčová, Klára, Andrea S. Florea, Asher Bar-Tal, Dror Minz, Uri Yermiyahu, Raneen Shawahna, Judith Kraut-Cohen, et al. 2019. "Microbial Consortia versus Single-Strain Inoculants: An Advantage in PGPM-Assisted Tomato Production?" *Agronomy* 9 (2). <https://doi.org/10.3390/agronomy9020105>.
- Brar, Amandeep, Manish Kumar, Vivek Vivekanand, and Nidhi Pareek. 2017. "Photoautotrophic Microorganisms and Bioremediation of Industrial Effluents: Current Status and Future Prospects." *3 Biotech* 7 (1): 1–8. <https://doi.org/10.1007/s13205-017-0600-5>.
- Bray, J. Roger, and J. T. Curtis. 1957. "An Ordination of the Upland Forest Communities of Southern Wisconsin." *Ecological Monographs* 27 (4): 325–49. <https://doi.org/10.2307/1942268>.
- Brezna, Barbara, Ohgew Kweon, Robin L. Stingley, James P. Freeman, Ashraf A. Khan, Bystrik Polek, Richard C. Jones, and Carl E. Cerniglia. 2006. "Molecular Characterization of Cytochrome P450 Genes in the Polycyclic Aromatic Hydrocarbon Degrading *Mycobacterium Vanbaalenii* PYR-1." *Applied Microbiology and Biotechnology* 71 (4): 522–32. <https://doi.org/10.1007/s00253-005-0190-8>.
- Brils, Jos. 2008. "Sediment Monitoring and the European Water Framework Directive." *Annali Dell'Istituto Superiore Di Sanita* 44 (3): 218–23.
- Brooijmans, Rob J.W., Margreet I. Pastink, and Roland J. Siezen. 2009. "Hydrocarbon-Degrading Bacteria: The Oil-Spill Clean-up Crew." *Microbial Biotechnology* 2 (6): 587–94. <https://doi.org/10.1111/j.1751-7915.2009.00151.x>.
- Bruns, Alke, and Luke Berthe-corti. 1999. "Slightly Halophilic Bacterium , Isolated From Intertidal Sediment." *International Journal of Systematic Bacteriology* 49: 441–48.
- Buah-Kwofie, Archibold, Marc S. Humphries, and Letitia Pillay. 2018. "Bioaccumulation and Risk Assessment of Organochlorine Pesticides in Fish from a Global Biodiversity Hotspot: ISimangaliso Wetland Park, South Africa." *Science of the Total Environment* 621: 273–81. <https://doi.org/10.1016/j.scitotenv.2017.11.212>.
- Buchan, Alison, José M. González, and Michelle J. Chua. 2019. "Aerobic Hydrocarbon-Degrading Alphaproteobacteria: Rhodobacteraceae (Roseobacter)." *Taxonomy, Genomics and Ecophysiology of Hydrocarbon-Degrading Microbes*, 1–13.

https://doi.org/10.1007/978-3-319-60053-6_8-1.

- Budiyanto, Fitri, Assad Thukair, Marwan Al-Momani, Musa M. Musa, and Alexis Nzila. 2018. "Characterization of Halophilic Bacteria Capable of Efficiently Biodegrading the High-Molecular-Weight Polycyclic Aromatic Hydrocarbon Pyrene." *Environmental Engineering Science* 35 (6): 616–26. <https://doi.org/10.1089/ees.2017.0244>.
- Burton, Edward D., Richard T. Bush, Leigh A. Sullivan, Scott G. Johnston, and Rosalie K. Hocking. 2008. "Mobility of Arsenic and Selected Metals during Re-Flooding of Iron- and Organic-Rich Acid-Sulfate Soil." *Chemical Geology* 253 (1–2): 64–73. <https://doi.org/10.1016/j.chemgeo.2008.04.006>.
- Bushnell, Brian, Jonathan Rood, and Esther Singer. 2017. "BBMerge – Accurate Paired Shotgun Read Merging via Overlap." *PLoS ONE* 12 (10): 1–15. <https://doi.org/10.1371/journal.pone.0185056>.
- Callahan, Benjamin J., Paul J. McMurdie, and Susan P. Holmes. 2017. "Exact Sequence Variants Should Replace Operational Taxonomic Units in Marker-Gene Data Analysis." *ISME Journal* 11 (12): 2639–43. <https://doi.org/10.1038/ismej.2017.119>.
- Calvo, C., M. Manzanera, G. A. Silva-Castro, I. Uad, and J. González-López. 2009. "Application of Bioemulsifiers in Soil Oil Bioremediation Processes. Future Prospects." *Science of the Total Environment* 407 (12): 3634–40. <https://doi.org/10.1016/j.scitotenv.2008.07.008>.
- Cameotra, Swaranjit Singh, and Randhir S. Makkar. 2010. "Biosurfactant-Enhanced Bioremediation of Hydrophobic Pollutants." *Pure and Applied Chemistry* 82 (1): 97–116. <https://doi.org/10.1351/PAC-CON-09-02-10>.
- Cao, Junwei, Qiliang Lai, Jun Yuan, and Zongze Shao. 2015. "Genomic and Metabolic Analysis of Fluoranthene Degradation Pathway in *Celeribacter Indicus* P73 T." *Scientific Reports* 5: 1–12. <https://doi.org/10.1038/srep07741>.
- Cao, Yong, and Charles P. Hawkins. 2019. "Weighting Effective Number of Species Measures by Abundance Weakens Detection of Diversity Responses." *Journal of Applied Ecology* 56 (5): 1200–1209. <https://doi.org/10.1111/1365-2664.13345>.
- Caporale, Antonio G., and Antonio Violante. 2016. "Chemical Processes Affecting the Mobility of Heavy Metals and Metalloids in Soil Environments." *Current Pollution Reports* 2 (1): 15–27. <https://doi.org/10.1007/s40726-015-0024-y>.
- Carmona, M., M. T. Zamarró, B. Blazquez, G. Durante-Rodríguez, J. F. Juárez, J. A. Valderrama, M. J. L. Barragan, J. L. Garcia, and E. Diaz. 2009. "Anaerobic Catabolism of Aromatic Compounds: A Genetic and Genomic View." *Microbiology and Molecular Biology Reviews* 73 (1): 71–133. <https://doi.org/10.1128/mubr.00021-08>.
- Caruso, Consolazione, Carmen Rizzo, Santina Mangano, Annarita Poli, Paola Di Donato, Barbara Nicolaus, Gaetano Di Marco, Luigi Michaud, and Angelina Lo Giudice. 2018. "Extracellular Polymeric Substances with Metal Adsorption Capacity Produced by *Pseudoalteromonas* Sp. MER144 from Antarctic Seawater." *Environmental Science and Pollution Research* 25 (5): 4667–77. <https://doi.org/10.1007/s11356-017-0851-z>.
- Carvalho, Fernando P. 2017. "Pesticides, Environment, and Food Safety." *Food and Energy Security* 6 (2): 48–60. <https://doi.org/10.1002/fes3.108>.
- Cases, Ildefonso, and Víctor De Lorenzo. 2005. "Genetically Modified Organisms for the Environment: Stories of Success and Failure and What We Have Learned from Them

Introduction: The Quest for the Superbug," 213–22.

- Casillo, Angela, Rosa Lanzetta, Michelangelo Parrilli, and Maria Michela Corsaro. 2018. "Exopolysaccharides from Marine and Marine Extremophilic Bacteria: Structures, Properties, Ecological Roles and Applications." *Marine Drugs* 16 (2). <https://doi.org/10.3390/md16020069>.
- Castro, Hector F., Aimée T. Classen, Emily E. Austin, Richard J. Norby, and Christopher W. Schadt. 2010. "Soil Microbial Community Responses to Multiple Experimental Climate Change Drivers." *Applied and Environmental Microbiology* 76 (4): 999–1007. <https://doi.org/10.1128/AEM.02874-09>.
- Catania, Valentina, Simone Cappello, Vincenzo Di Giorgi, Santina Santisi, Roberta Di Maria, Antonio Mazzola, Salvatrice Vizzini, and Paola Quatrini. 2018. "Microbial Communities of Polluted Sub-Surface Marine Sediments." *Marine Pollution Bulletin* 131 (April): 396–406. <https://doi.org/10.1016/j.marpolbul.2018.04.015>.
- Catania, Valentina, Santina Santisi, Geraldina Signa, Salvatrice Vizzini, Antonio Mazzola, Simone Cappello, Michail M. Yakimov, and Paola Quatrini. 2015. "Intrinsic Bioremediation Potential of a Chronically Polluted Marine Coastal Area." *Marine Pollution Bulletin* 99 (1–2): 138–49. <https://doi.org/10.1016/j.marpolbul.2015.07.042>.
- Chakraborty, Shatarupa, Abhishek Mukherjee, and Tapan Kumar Das. 2013. "Biochemical Characterization of a Lead-Tolerant Strain of *Aspergillus Foetidus*: An Implication of Bioremediation of Lead from Liquid Media." *International Biodeterioration and Biodegradation* 84: 134–42. <https://doi.org/10.1016/j.ibiod.2012.05.031>.
- Chang, Jin Soo, In Ho Yoon, and Kyoung Woong Kim. 2018. "Arsenic Biotransformation Potential of Microbial Arsenic Responses in the Biogeochemical Cycling of Arsenic-Contaminated Groundwater." *Chemosphere* 191: 729–37. <https://doi.org/10.1016/j.chemosphere.2017.10.044>.
- Chang, Yi Tang, Jiunn Fwu Lee, Keng Hua Liu, Yi Fen Liao, and Vivian Yang. 2016. "Immobilization of Fungal Laccase onto a Nonionic Surfactant-Modified Clay Material: Application to PAH Degradation." *Environmental Science and Pollution Research* 23 (5): 4024–35. <https://doi.org/10.1007/s11356-015-4248-6>.
- Chang, Yun Juan, John R. Stephen, Amy P. Richter, Albert D. Venosa, Julia Brüggemann, Sarah J. MacNaughton, George A. Kowalchuk, John R. Haines, Elizabeth Kline, and David C. White. 2000. "Phylogenetic Analysis of Aerobic Freshwater and Marine Enrichment Cultures Efficient in Hydrocarbon Degradation: Effect of Profiling Method." *Journal of Microbiological Methods* 40 (1): 19–31. [https://doi.org/10.1016/S0167-7012\(99\)00134-7](https://doi.org/10.1016/S0167-7012(99)00134-7).
- Chauhan, Nar Singh, Sonam Nain, and Rakesh Sharma. 2017. "Identification of Arsenic Resistance Genes from Marine Sediment Metagenome." *Indian Journal of Microbiology* 57 (3): 299–306. <https://doi.org/10.1007/s12088-017-0658-0>.
- Chekroun, Kaoutar Ben, Esteban Sánchez, and Mourad Baghour. 2014. "The Role of Algae in Bioremediation of Organic Pollutants." *International Research Journal of Public and Environmental Health* 1 (2): 19–32. <http://www.journalissues.org/irjpeh/>.
- Chen, Wen Jang, Lai Chun Hsiao, and Karen Kai Yun Chen. 2008. "Metal Desorption from Copper(II)/Nickel(II)-Spiked Kaolin as a Soil Component Using Plant-Derived Saponin Biosurfactant." *Process Biochemistry* 43 (5): 488–98. <https://doi.org/10.1016/j.procbio.2007.11.017>.

- Cheng, Bin, Yiwei Meng, Yanbing Cui, Chunfang Li, Fei Tao, Huijia Yin, Chunyu Yang, and Ping Xu. 2016. "Alkaline Response of a Halotolerant Alkaliphilic Halomonas Strain and Functional Diversity of Its Na⁺(K⁺)/H⁺ Antiporters." *Journal of Biological Chemistry* 291 (50): 26056–65. <https://doi.org/10.1074/jbc.M116.751016>.
- Cheng, K. Y., Z. Y. Zhao, and J. W.C. Wong. 2004. "Solubilization and Desorption of PAHS in Soil-Aqueous System by Biosurfactants Produced from Pseudomonas Aeruginosa P-CG3 under Thermophilic Condition." *Environmental Technology* 25 (10): 1159–65. <https://doi.org/10.1080/09593332508618382>.
- Chiellini, Carolina, Renato Iannelli, Franco Verni, and Giulio Petroni. 2013. "Bacterial Communities in Polluted Seabed Sediments: A Molecular Biology Assay in Leghorn Harbor." *The Scientific World Journal* 2013. <https://doi.org/10.1155/2013/165706>.
- Chon, Ho Sik, Dieudonné Guy Ohandja, and Nikolaos Voulvoulis. 2012. "The Role of Sediments as a Source of Metals in River Catchments." *Chemosphere* 88 (10): 1250–56. <https://doi.org/10.1016/j.chemosphere.2012.03.104>.
- Chun, Jongsik, Aharon Oren, Antonio Ventosa, Henrik Christensen, David Ruiz Arahall, Milton S. da Costa, Alejandro P. Rooney, et al. 2018. "Proposed Minimal Standards for the Use of Genome Data for the Taxonomy of Prokaryotes." *International Journal of Systematic and Evolutionary Microbiology* 68 (1): 461–66. <https://doi.org/10.1099/ijsem.0.002516>.
- Cicchella, Domenico, Lucia Giaccio, Annamaria Lima, Stefano Albanese, Antonio Cosenza, Diego Civitillo, and Benedetto De Vivo. 2014. "Assessment of the Topsoil Heavy Metals Pollution in the Sarno River Basin, South Italy." *Environmental Earth Sciences* 71 (12): 5129–43. <https://doi.org/10.1007/s12665-013-2916-8>.
- Coates, John D., Joan Woodward, Jon Allen, Paul Philp, and Derek R. Lovley. 1997. "Anaerobic Degradation of Polycyclic Aromatic Hydrocarbons and Alkanes in Petroleum-Contaminated Marine Harbor Sediments." *Applied and Environmental Microbiology* 63 (9): 3589–93.
- Colacicco, Antonio, Giorgia De Gioannis, Aldo Muntoni, Emanuela Pettinao, Alessandra Polettini, and Raffaella Pomi. 2010. "Enhanced Electrokinetic Treatment of Marine Sediments Contaminated by Heavy Metals and PAHs." *Chemosphere* 81 (1): 46–56. <https://doi.org/10.1016/j.chemosphere.2010.07.004>.
- Collins, Andrew J., Matthew S. Fullmer, Johann P. Gogarten, and Spencer V. Nyholm. 2015. "Comparative Genomics of Roseobacter Clade Bacteria Isolated from the Accessory Nidamental Gland of Euprymna Scolopes." *Frontiers in Microbiology* 6 (FEB): 1–15. <https://doi.org/10.3389/fmicb.2015.00123>.
- Corinaldesi, Cinzia, Michael Tangherlini, Eugenio Rastelli, Emanuela Buschi, Marco Lo Martire, Roberto Danovaro, and Antonio Dell'Anno. 2019. "High Diversity of Benthic Bacterial and Archaeal Assemblages in Deep-Mediterranean Canyons and Adjacent Slopes." *Progress in Oceanography* 171: 154–61. <https://doi.org/10.1016/j.pocean.2018.12.014>.
- Cosa, Sekelwa, Leonard V. Mabinya, Ademola O. Olaniran, Omobola O. Okoh, Kim Bernard, Shaun Deyzel, and Anthony I. Okoh. 2011. "Bioflocculant Production by Virgibacillus Sp. Rob Isolated from the Bottom Sediment of Algoa Bay in the Eastern Cape, South Africa." *Molecules* 16 (3): 2431–42. <https://doi.org/10.3390/molecules16032431>.
- Crini, Grégorio, and Eric Lichtfouse. 2018. "Wastewater Treatment : An Overview.Green Adsorbents for Pollutant Removal." *Springer Nature* 18: 1–22.

- Cronin-O'Reilly, Sorcha, Joe D. Taylor, Ian Jermyn, A. Louise Allcock, Michael Cunliffe, and Mark P. Johnson. 2018. "Limited Congruence Exhibited across Microbial, Meiofaunal and Macrofaunal Benthic Assemblages in a Heterogeneous Coastal Environment." *Scientific Reports* 8 (1): 1–10. <https://doi.org/10.1038/s41598-018-33799-9>.
- Czaplicki, Lauren M., and Claudia K. Gunsch. 2016a. "Reflection on Molecular Approaches Influencing State-of-the-Art Bioremediation Design: Culturing to Microbial Community Fingerprinting to Omics." *Journal of Environmental Engineering (United States)* 142 (10): 1–13. [https://doi.org/10.1061/\(ASCE\)EE.1943-7870.0001141](https://doi.org/10.1061/(ASCE)EE.1943-7870.0001141).
- Dahrazma, Behnaz, and Catherine N. Mulligan. 2007. "Investigation of the Removal of Heavy Metals from Sediments Using Rhamnolipid in a Continuous Flow Configuration." *Chemosphere* 69 (5): 705–11. <https://doi.org/10.1016/j.chemosphere.2007.05.037>.
- Danovaro, R., C. Corinaldesi, E. Rastelli, and A. Dell'Anno. 2015. "Towards a Better Quantitative Assessment of the Relevance of Deep-Sea Viruses, Bacteria and Archaea in the Functioning of the Ocean Seafloor." *Aquatic Microbial Ecology* 75 (1): 81–90. <https://doi.org/10.3354/ame01747>.
- Danovaro, Roberto, Joan Batista Company, Cinzia Corinaldesi, Gianfranco D'Onghia, Bella Galil, Cristina Gambi, Andrew J. Gooday, et al. 2010. "Deep-Sea Biodiversity in the Mediterranean Sea: The Known, the Unknown, and the Unknowable." *PLoS ONE* 5 (8). <https://doi.org/10.1371/journal.pone.0011832>.
- Danovaro, Roberto, Cinzia Corinaldesi, Gian Marco Luna, Mirko Magagnini, Elena Manini, and Antonio Pusceddu. 2009. "Prokaryote Diversity and Viral Production in Deep-Sea Sediments and Seamounts." *Deep-Sea Research Part II: Topical Studies in Oceanography* 56 (11–12): 738–47. <https://doi.org/10.1016/j.dsr2.2008.10.011>.
- Das, Nilanjana, and Preethy Chandran. 2011. "Microbial Degradation of Petroleum Hydrocarbon Contaminants: An Overview." *Biotechnology Research International* 2011: 1–13. <https://doi.org/10.4061/2011/941810>.
- Dash, HIRAK R., Neelam Mangwani, Jaya Chakraborty, Supriya Kumari, and Surajit Das. 2013. "Marine Bacteria: Potential Candidates for Enhanced Bioremediation." *Applied Microbiology and Biotechnology* 97 (2): 561–71. <https://doi.org/10.1007/s00253-012-4584-0>.
- Dastgheib, Seyed Mohammad Mehdi, Mohammad Ali Amoozegar, Khosro Khajeh, Mahmoud Shavandi, and Antonio Ventosa. 2012. "Biodegradation of Polycyclic Aromatic Hydrocarbons by a Halophilic Microbial Consortium." *Applied Microbiology and Biotechnology* 95 (3): 789–98. <https://doi.org/10.1007/s00253-011-3706-4>.
- Dell'Anno, A., M. L. Mei, C. Ianni, and R. Danovaro. 2003. "Impact of Bioavailable Heavy Metals on Bacterial Activities in Coastal Marine Sediments." *World Journal of Microbiology and Biotechnology* 19 (1): 93–100. <https://doi.org/10.1023/A:1022581632116>.
- Dell'Anno, Antonio, Francesca Beolchini, Massimo Gabellini, Laura Rocchetti, Antonio Pusceddu, and Roberto Danovaro. 2009. "Bioremediation of Petroleum Hydrocarbons in Anoxic Marine Sediments: Consequences on the Speciation of Heavy Metals." *Marine Pollution Bulletin* 58 (12): 1808–14. <https://doi.org/10.1016/j.marpolbul.2009.08.002>.
- Dell'Anno, Antonio, Francesca Beolchini, Laura Rocchetti, Gian Marco Luna, and Roberto Danovaro. 2012. "High Bacterial Biodiversity Increases Degradation Performance of Hydrocarbons during Bioremediation of Contaminated Harbor Marine Sediments."

- Environmental Pollution* 167: 85–92. <https://doi.org/10.1016/j.envpol.2012.03.043>.
- Desai, Chirayu, Hilor Pathak, and Datta Madamwar. 2010. “Advances in Molecular and ‘-Omics’ Technologies to Gauge Microbial Communities and Bioremediation at Xenobiotic/Anthropogen Contaminated Sites.” *Bioresource Technology* 101 (6): 1558–69. <https://doi.org/10.1016/j.biortech.2009.10.080>.
- Deshmukh, Radhika, Anshuman A. Khardenavis, and Hemant J. Purohit. 2016. “Diverse Metabolic Capacities of Fungi for Bioremediation.” *Indian Journal of Microbiology* 56 (3): 247–64. <https://doi.org/10.1007/s12088-016-0584-6>.
- Deutschbauer, Adam M., Dylan Chivian, and Adam P. Arkin. 2006. “Genomics for Environmental Microbiology.” *Current Opinion in Biotechnology* 17 (3): 229–35. <https://doi.org/10.1016/j.copbio.2006.04.003>.
- Devi, Upama, and Krishna G. Bhattacharyya. 2018. “Mobility and Bioavailability of Cd, Co, Cr, Cu, Mn and Zn in Surface Runoff Sediments in the Urban Catchment Area of Guwahati, India.” *Applied Water Science* 8 (1): 1–14. <https://doi.org/10.1007/s13201-018-0651-8>.
- Ding, Chao Qun, Kun Rong Li, Yun Xia Duan, Shi Ru Jia, He Xin Lv, He Bai, and Cheng Zhong. 2017. “Study on Community Structure of Microbial Consortium for the Degradation of Viscose Fiber Wastewater.” *Bioresources and Bioprocessing* 4 (1). <https://doi.org/10.1186/s40643-017-0159-3>.
- Dong, Biying, Lili Niu, Dong Meng, Zhihua Song, Litao Wang, Yue Jian, Xiaohong Fan, Mingzhu Dong, Qing Yang, and Yujie Fu. 2019. “Genome-Wide Analysis of MATE Transporters and Response to Metal Stress in *Cajanus cajan*.” *Journal of Plant Interactions* 14 (1): 265–75. <https://doi.org/10.1080/17429145.2019.1620884>.
- Dong, C., X. Bai, H. Sheng, L. Jiao, H. Zhou, and Z. Shao. 2015. “Distribution of PAHs and the PAH-Degrading Bacteria in the Deep-Sea Sediments of the High-Latitude Arctic Ocean.” *Biogeosciences* 12 (7): 2163–77. <https://doi.org/10.5194/bg-12-2163-2015>.
- Durairaj, Pradeepraj, Sailesh Malla, Saravanan Prabhu Nadarajan, Pyung Gang Lee, Eunok Jung, Hyun Ho Park, Byung Gee Kim, and Hyungdon Yun. 2015. “Fungal Cytochrome P450 Monooxygenases of *Fusarium oxysporum* for the Synthesis of ω -Hydroxy Fatty Acids in Engineered *Saccharomyces cerevisiae*.” *Microbial Cell Factories* 14 (1). <https://doi.org/10.1186/s12934-015-0228-2>.
- Dyksma, Stefan, Kerstin Bischof, Bernhard M. Fuchs, Katy Hoffmann, Dimitri Meier, Anke Meyerdierks, Petra Pjevac, et al. 2016. “Ubiquitous Gammaproteobacteria Dominate Dark Carbon Fixation in Coastal Sediments.” *ISME Journal* 10 (8): 1939–53. <https://doi.org/10.1038/ismej.2015.257>.
- Dziewit, Lukasz, Adam Pyzik, Renata Matlakowska, Jadwiga Baj, Magdalena Szuplewska, and Dariusz Bartosik. 2013. “Characterization of *Halomonas* Sp. ZM3 Isolated from the Zelazny Most Post-Flotation Waste Reservoir, with a Special Focus on Its Mobile DNA.” *BMC Microbiology* 13 (1). <https://doi.org/10.1186/1471-2180-13-59>.
- Dziewit, Lukasz, Adam Pyzik, Magdalena Szuplewska, Renata Matlakowska, Sebastian Mielnicki, Daniel Wibberg, Andreas Schlüter, Alfred Pühler, and Dariusz Bartosik. 2015. “Diversity and Role of Plasmids in Adaptation of Bacteria Inhabiting the Lubin Copper Mine in Poland, an Environment Rich in Heavy Metals.” *Frontiers in Microbiology* 6 (MAR): 1–12. <https://doi.org/10.3389/fmicb.2015.00152>.

- Edlund, Anna, Fredrik Hårdeman, Janet K. Jansson, and Sara Sjöling. 2008. "Active Bacterial Community Structure along Vertical Redox Gradients in Baltic Sea Sediment." *Environmental Microbiology* 10 (8): 2051–63. <https://doi.org/10.1111/j.1462-2920.2008.01624.x>.
- Eggleton, Jacqueline, and Kevin V. Thomas. 2004. "A Review of Factors Affecting the Release and Bioavailability of Contaminants during Sediment Disturbance Events." *Environment International* 30 (7): 973–80. <https://doi.org/10.1016/j.envint.2004.03.001>.
- Evans, Flavia F., Alexandre S. Rosado, Gina V. Sebastián, Renata Casella, Pedro L.O.A. Machado, Carola Holmström, Staffan Kjelleberg, Jan D. Van Elsas, and Lucy Seldin. 2004. "Impact of Oil Contamination and Biostimulation on the Diversity of Indigenous Bacterial Communities in Soil Microcosms." *FEMS Microbiology Ecology* 49 (2): 295–305. <https://doi.org/10.1016/j.femsec.2004.04.007>.
- Ezekwe, Clinton Ifeanyichukwu, and Israel Clinton Utong. 2017. "Hydrocarbon Pollution and Potential Ecological Risk of Heavy Metals in the Sediments of the Oturuba Creek, Niger Delta, Nigeria." *Journal of Environmental Geography* 10 (1–2): 1–10. <https://doi.org/10.1515/jengeo-2017-0001>.
- Farhadian, Mehrdad, Cédric Vachelard, David Duchez, and Christian Larroche. 2008. "In Situ Bioremediation of Monoaromatic Pollutants in Groundwater: A Review." *Bioresource Technology* 99 (13): 5296–5308. <https://doi.org/10.1016/j.biortech.2007.10.025>.
- Fasciglione, Paolo, Marco Barra, Angela Santucci, Sarah Ciancimino, Salvatore Mazzola, and Salvatore Passaro. 2016. "Macrobenthic Community Status in Highly Polluted Area: A Case Study from Bagnoli, Naples Bay, Italy." *Rendiconti Lincei* 27 (2): 229–39. <https://doi.org/10.1007/s12210-015-0467-5>.
- Fathpure, Babu Z. 2014. "Recent Studies in Microbial Degradation of Petroleum Hydrocarbons in Hypersaline Environments." *Frontiers in Microbiology* 5 (APR): 1–16. <https://doi.org/10.3389/fmicb.2014.00173>.
- Ferraroni, Marta, Jana Seifert, Vasili M. Travkin, Monika Thiel, Stefan Kaschabek, Andrea Scozzafava, Ludmila Golovleva, Michael Schlömann, and Fabrizio Briganti. 2005. "Crystal Structure of the Hydroxyquinol 1,2-Dioxygenase from *Nocardioides simplex* 3E, a Key Enzyme Involved in Polychlorinated Aromatics Biodegradation." *Journal of Biological Chemistry* 280 (22): 21144–54. <https://doi.org/10.1074/jbc.M500666200>.
- Festa, Sabrina, Bibiana Marina Coppotelli, Laura Madueño, Claudia Lorena Loviso, Marianela Macchi, Ricardo Martin Neme Tauil, María Pía Valacco, and Irma Susana Morelli. 2017. "Assigning Ecological Roles to the Populations Belonging to a Phenanthrene-Degrading Bacterial Consortium Using Omic Approaches." *PLoS ONE* 12 (9): 1–21. <https://doi.org/10.1371/journal.pone.0184505>.
- Fodelianakis, S., E. Antoniou, F. Mapelli, M. Magagnini, M. Nikolopoulou, R. Marasco, M. Barbato, et al. 2015. "Allochthonous Bioaugmentation in Ex Situ Treatment of Crude Oil-Polluted Sediments in the Presence of an Effective Degrading Indigenous Microbiome." *Journal of Hazardous Materials* 287: 78–86. <https://doi.org/10.1016/j.jhazmat.2015.01.038>.
- Fonti, Viviana, Antonio Dell'Anno, and Francesca Beolchini. 2015. "Biogeochemical Interactions in the Application of Biotechnological Strategies to Marine Sediments Contaminated with Metals." *Nova Biotechnologica et Chimica* 14 (1): 12–31. <https://doi.org/10.1515/nbec-2015-0010>.

- Franco, Diego C., Camila N. Signori, Rubens T.D. Duarte, Cristina R. Nakayama, Lúcia S. Campos, and Vivian H. Pellizari. 2017. "High Prevalence of Gammaproteobacteria in the Sediments of Admiralty Bay and North Bransfield Basin, Northwestern Antarctic Peninsula." *Frontiers in Microbiology* 8: 1–9. <https://doi.org/10.3389/fmicb.2017.00153>.
- Frazer, Lance. 2000. "Lipid Lather Removes Metals." *Environmental Health Perspectives* 108 (7): 320–23.
- Fuchs, Georg, Matthias Boll, and Johann Heider. 2011. "Microbial Degradation of Aromatic Compounds — from One Strategy to Four." *Nature Reviews Microbiology* 9 (11): 803–16. <https://doi.org/10.1038/nrmicro2652>.
- Fuentes-Gandara, Fabio, José Pinedo-Hernández, José Marrugo-Negrete, and Sergi Díez. 2018. "Human Health Impacts of Exposure to Metals through Extreme Consumption of Fish from the Colombian Caribbean Sea." *Environmental Geochemistry and Health* 40 (1): 229–42. <https://doi.org/10.1007/s10653-016-9896-z>.
- Fulekar, M H, and Jaya Sharma. 2008. "Bioinformatics Applied in Bioremediation." *Innovative Romanian For Biotechnology* 2 (2): 28–36.
- Gadd, Geoffrey Michael. 2010. "Metals, Minerals and Microbes: Geomicrobiology and Bioremediation." *Microbiology* 156 (3): 609–43. <https://doi.org/10.1099/mic.0.037143-0>.
- Ganesh Kumar, A., N. Nivedha Rajan, R. Kirubakaran, and G. Dharani. 2019. "Biodegradation of Crude Oil Using Self-Immobilized Hydrocarbonoclastic Deep Sea Bacterial Consortium." *Marine Pollution Bulletin* 146 (October 2018): 741–50. <https://doi.org/10.1016/j.marpolbul.2019.07.006>.
- Garbisu, Carlos, Olatz Garaiurrebaso, Lur Epelde, and Elisabeth Grohmann. 2017. "Plasmid-Mediated Bioaugmentation for the Bioremediation of Contaminated Soils." *Frontiers in Microbiology* 8: 1–13. <https://doi.org/10.3389/fmicb.2017.01966>.
- García de Llasera, Martha Patricia, José de Jesús Olmos-Espejel, Gabriel Díaz-Flores, and Adriana Montaña-Montiel. 2016. "Biodegradation of Benzo(a)Pyrene by Two Freshwater Microalgae *Selenastrum Capricornutum* and *Scenedesmus Acutus*: A Comparative Study Useful for Bioremediation." *Environmental Science and Pollution Research* 23 (4): 3365–75. <https://doi.org/10.1007/s11356-015-5576-2>.
- Garrido-Sanz, Daniel, Miguel Redondo-Nieto, María Guirado, Oscar Pindado Jiménez, Rocío Millán, Marta Martín, and Rafael Rivilla. 2019. "Metagenomic Insights into the Bacterial Functions of a Diesel-Degrading Consortium for the Rhizoremediation of Diesel-Polluted Soil." *Genes* 10 (6): 456. <https://doi.org/10.3390/genes10060456>.
- Geesink, Patricia, Olaf Tyc, Kirsten Küsel, Martin Taubert, Charlotte van de Velde, Swatantar Kumar, and Paolina Garbeva. 2018. "Growth Promotion and Inhibition Induced by Interactions of Groundwater Bacteria." *FEMS Microbiology Ecology* 94 (11): 1–8. <https://doi.org/10.1093/femsec/fiy164>.
- Genovese, Maria, Francesca Crisafi, Renata Denaro, Simone Cappello, Daniela Russo, Rosario Calogero, Santina Santisi, et al. 2014. "Effective Bioremediation Strategy for Rapid in Situ Cleanup of Anoxic Marine Sediments in Mesocosm Oil Spill Simulation." *Frontiers in Microbiology* 5 (APR): 1–14. <https://doi.org/10.3389/fmicb.2014.00162>.
- Ghosal, Debajyoti, Shreya Ghosh, Tapan K. Dutta, and Youngho Ahn. 2016a. "Current State of Knowledge in Microbial Degradation of Polycyclic Aromatic Hydrocarbons (PAHs): A

- Review." *Frontiers in Microbiology* 7 (AUG). <https://doi.org/10.3389/fmicb.2016.01369>.
- Gilbert, Jack A., Dawn Field, Paul Swift, Lindsay Newbold, Anna Oliver, Tim Smyth, Paul J. Somerfield, Sue Huse, and Ian Joint. 2009. "The Seasonal Structure of Microbial Communities in the Western English Channel." *Environmental Microbiology* 11 (12): 3132–39. <https://doi.org/10.1111/j.1462-2920.2009.02017.x>.
- Gillan, David C., Bruno Danis, Philippe Pernet, Guillemette Joly, and Philippe Dubois. 2005. "Structure of Sediment-Associated Microbial Communities along a Heavy-Metal Contamination Gradient in the Marine Environment." *Applied and Environmental Microbiology* 71 (2): 679–90. <https://doi.org/10.1128/AEM.71.2.679-690.2005>.
- Gnanamani, A., V. Kavitha, N. Radhakrishnan, G. Suseela Rajakumar, G. Sekaran, and A. B. Mandal. 2010. "Microbial Products (Biosurfactant and Extracellular Chromate Reductase) of Marine Microorganism Are the Potential Agents Reduce the Oxidative Stress Induced by Toxic Heavy Metals." *Colloids and Surfaces B: Biointerfaces* 79 (2): 334–39. <https://doi.org/10.1016/j.colsurfb.2010.04.007>.
- Gomila, Margarita, Arantxa Peña, Magdalena Mulet, Jorge Lalucat, and Elena García-Valdés. 2015. "Phylogenomics and Systematics in *Pseudomonas*." *Frontiers in Microbiology* 6 (MAR): 1–13. <https://doi.org/10.3389/fmicb.2015.00214>.
- Gorovtsov, Andrey Vladimirovich, Ivan Sergeevich Sazykin, and Marina Alexandrovna Sazykina. 2018. "The Influence of Heavy Metals, Polyaromatic Hydrocarbons, and Polychlorinated Biphenyls Pollution on the Development of Antibiotic Resistance in Soils." *Environmental Science and Pollution Research* 25 (10): 9283–92. <https://doi.org/10.1007/s11356-018-1465-9>.
- Gray, James P., and Russell P. Herwig. 1996. "Phylogenetic Analysis of the Bacterial Communities in Marine Sediments." *Applied and Environmental Microbiology* 62 (11): 4049–59.
- Guazzaroni, María Eugenia, Florian Alexander Herbst, Iván Lores, Javier Tamames, Ana Isabel Peláez, Nieves López-Cortés, María Alcaide, et al. 2013. "Metaproteogenomic Insights beyond Bacterial Response to Naphthalene Exposure and Bio-Stimulation." *ISME Journal* 7 (1): 122–36. <https://doi.org/10.1038/ismej.2012.82>.
- Guedes, R.N.C., L. C. Magalhães, and L. V. Cosme. 2009. "Stimulatory Sublethal Response of a Generalist Predator to Permethrin: Hormesis, Hormoligosis, or Homeostatic Regulation?" *Journal of Economic Entomology* 102 (1): 170–76. <https://doi.org/10.1603/029.102.0124>.
- Gupta, Pratima, and Batul Diwan. 2017. "Bacterial Exopolysaccharide Mediated Heavy Metal Removal: A Review on Biosynthesis, Mechanism and Remediation Strategies." *Biotechnology Reports* 13: 58–71. <https://doi.org/10.1016/j.btre.2016.12.006>.
- Gutierrez, Tony, David Berry, Tingting Yang, Sara Mishamandani, Luke McKay, Andreas Teske, and Michael D. Aitken. 2013. "Role of Bacterial Exopolysaccharides (EPS) in the Fate of the Oil Released during the Deepwater Horizon Oil Spill." *PLoS ONE* 8 (6): 1–18. <https://doi.org/10.1371/journal.pone.0067717>.
- Gutleben, Johanna, Maryam Chaib De Mares, Jan Dirk van Elsas, Hauke Smidt, Jörg Overmann, and Detmer Sipkema. 2018. "The Multi-Omics Promise in Context: From Sequence to Microbial Isolate." *Critical Reviews in Microbiology* 44 (2): 212–29.

<https://doi.org/10.1080/1040841X.2017.1332003>.

- Habe, Hiroshi, and Toshio Omori. 2003. "Genetics of Polycyclic Aromatic Hydrocarbon Metabolism in Diverse Aerobic Bacteria." *Bioscience, Biotechnology and Biochemistry* 67 (2): 225–43. <https://doi.org/10.1271/bbb.67.225>.
- Han, Na, Yujun Qiang, and Wen Zhang. 2016. "ANItools Web: A Web Tool for Fast Genome Comparison within Multiple Bacterial Strains." *Database : The Journal of Biological Databases and Curation* 2016: 1–5. <https://doi.org/10.1093/database/baw084>.
- Harayama, Shigeaki, Hideo Kishira, Yuki Kasai, and Kazuaki Shutsubo. 1999. "Petroleum Biodegradation in Marine Environments." *Journal of Molecular Microbiology and Biotechnology* 1 (1): 63–70.
- Hastings, D. W., P. T. Schwing, G. R. Brooks, R. A. Larson, J. L. Morford, T. Roeder, K. A. Quinn, T. Bartlett, I. C. Romero, and D. J. Hollander. 2016. "Changes in Sediment Redox Conditions Following the BP DWH Blowout Event." *Deep-Sea Research Part II: Topical Studies in Oceanography* 129: 167–78. <https://doi.org/10.1016/j.dsr2.2014.12.009>.
- Head, Ian M, D Martin Jones, and Wilfred F M Röling. 2006. "Marine Microorganisms Make a Meal of Oil." *Nature Reviews. Microbiology* 4 (3): 173–82. <https://doi.org/10.1038/nrmicro1348>.
- Hedlund, Brian P., and James T. Staley. 2006. "Isolation and Characterization of Pseudoalteromonas Strains with Divergent Polycyclic Aromatic Hydrocarbon Catabolic Properties." *Environmental Microbiology* 8 (1): 178–82. <https://doi.org/10.1111/j.1462-2920.2005.00871.x>.
- Herman, David C., Janick F. Artiola, and Raina M. Miller. 1995. "Removal of Cadmium, Lead, and Zinc from Soil by a Rhamnolipid Biosurfactant." *Environmental Science and Technology* 29 (9): 2280–85. <https://doi.org/10.1021/es00009a019>.
- Hochstein, Rebecca, Qian Zhang, Michael J. Sadowsky, and Valery E. Forbes. 2019. "The Deposit Feeder Capitella Teleta Has a Unique and Relatively Complex Microbiome Likely Supporting Its Ability to Degrade Pollutants." *Science of the Total Environment* 670: 547–54. <https://doi.org/10.1016/j.scitotenv.2019.03.255>.
- Horel, Agota, Behzad Mortazavi, and Patricia A. Sobczyk. 2015. "Input of Organic Matter Enhances Degradation of Weathered Diesel Fuel in Sub-Tropical Sediments." *Science of the Total Environment* 533: 82–90. <https://doi.org/10.1016/j.scitotenv.2015.06.102>.
- Hua, Fei, and Hong Qi Wang. 2014. "Uptake and Trans-Membrane Transport of Petroleum Hydrocarbons by Microorganisms." *Biotechnology and Biotechnological Equipment* 28 (2): 165–75. <https://doi.org/10.1080/13102818.2014.906136>.
- Ibarrolaza, Agustín, Bibiana M. Coppotelli, María T. Del Panno, Edgardo R. Donati, and Irma S. Morelli. 2009. "Dynamics of Microbial Community during Bioremediation of Phenanthrene and Chromium(VI)-Contaminated Soil Microcosms." *Biodegradation* 20 (1): 95–107. <https://doi.org/10.1007/s10532-008-9203-5>.
- Igiri, Bernard E, Stanley I R Okoduwa, Grace O Idoko, Ebere P Akabuogu, Abraham O Adeyi, and Ibe K Ejiogu. 2018. "Toxicity and Bioremediation of Heavy Metals Contaminated Ecosystem from Tannery Wastewater : A Review." *Journal of Toxicology*, 1–16.
- Imperato, Valeria, Miguel Portillo-Estrada, Breanne M. McAmmond, Yorben Douwen, Jonathan D. Van Hamme, Stanislaw W. Gawronski, Jaco Vangronsveld, and Sofie Thijs. 2019.

- “Genomic Diversity of Two Hydrocarbon-Degrading and Plant Growth-Promoting *Pseudomonas* Species Isolated from the Oil Field of Bóbrka (Poland).” *Genes* 10 (6). <https://doi.org/10.3390/genes10060443>.
- Iohara, K., R. Iiyama, K. Nakamura, S. Silver, M. Sakai, M. Takeshita, and K. Furukawa. 2001. “The Mer Operon of a Mercury-Resistant Pseudoalteromonas Haloplanktis Strain Isolated from Minamata Bay, Japan.” *Applied Microbiology and Biotechnology* 56 (5–6): 736–41. <https://doi.org/10.1007/s002530100734>.
- Islam, Md Shahidul, and Masaru Tanaka. 2004. “Impacts of Pollution on Coastal and Marine Ecosystems Including Coastal and Marine Fisheries and Approach for Management: A Review and Synthesis.” *Marine Pollution Bulletin* 48 (7–8): 624–49. <https://doi.org/10.1016/j.marpolbul.2003.12.004>.
- Izzo, Silvina A., Silvina Quintana, Mariela Espinosa, Paola A. Babay, and Silvia R. Peressutti. 2019. “First Characterization of PAH-Degrading Bacteria from Río de La Plata and High-Resolution Melting: An Encouraging Step toward Bioremediation.” *Environmental Technology (United Kingdom)* 40 (10): 1250–61. <https://doi.org/10.1080/09593330.2017.1420104>.
- Jaishankar, Monisha, Tenzin Tseten, Naresh Anbalagan, Blessy B. Mathew, and Krishnamurthy N. Beeregowda. 2014. “Toxicity, Mechanism and Health Effects of Some Heavy Metals.” *Interdisciplinary Toxicology* 7 (2): 60–72. <https://doi.org/10.2478/intox-2014-0009>.
- Jiang, Wei, and Wenhong Fan. 2008. “Bioremediation of Heavy Metal-Contaminated Soils by Sulfate-Reducing Bacteria.” *Annals of the New York Academy of Sciences* 1140: 446–54. <https://doi.org/10.1196/annals.1454.050>.
- Jing, Ran, and Birthe V Kjellerup. 2017. “Biogeochemical Cycling of Metals Impacting by Microbial Mobilization and Immobilization.” *Journal of Environmental Sciences*, 1–9. <https://doi.org/10.1016/j.jes.2017.04.035>.
- Jorfi, Sahand, Abbas Rezaee, Ghasem-ali Moheb-ali, and Nemat alah Jaafarzadeh. 2013. “Pyrene Removal from Contaminated Soils by Modified Fenton Oxidation Using Iron Nano Particles.” *Journal of Environmental Health Science and Engineering* 11 (1): 1. <https://doi.org/10.1186/2052-336x-11-17>.
- Joshi, P A, and G B Pandey. 2011. “Screening of Petroleum Degrading Bacteria from Cow Dung.” *Research Journal of Agricultural Sciences* 2 (1): 69–71.
- Junakova, Natalia, and Jozef Junak. 2017. “Sustainable Use of Reservoir Sediment through Partial Application in Building Material.” *Sustainability (Switzerland)* 9 (5): 1–13. <https://doi.org/10.3390/su9050852>.
- Juwarkar, Asha A., Kirti V. Dubey, Anupa Nair, and Sanjeev Kumar Singh. 2008. “Bioremediation of Multi-Metal Contaminated Soil Using Biosurfactant - A Novel Approach.” *Indian Journal of Microbiology* 48 (1): 142–46. <https://doi.org/10.1007/s12088-008-0014-5>.
- Kadri, Tayssir, Sara Magdouli, Tarek Rouissi, and Satinder Kaur Brar. 2018. “Ex-Situ Biodegradation of Petroleum Hydrocarbons Using *Alcanivorax Borkumensis* Enzymes.” *Biochemical Engineering Journal* 132: 279–87. <https://doi.org/10.1016/j.bej.2018.01.014>.
- Kamimura, Naofumi, and Eiji Masai. 2013. “The Protocatechuate 4,5-Cleavage Pathway: Overview and New Findings.” In *Biodegradative Bacteria*, 207–26.

<https://doi.org/10.1007/978-4-431-54520-0>.

- Kanehisa, Minoru, Miho Furumichi, Mao Tanabe, Yoko Sato, and Kanae Morishima. 2017. "KEGG: New Perspectives on Genomes, Pathways, Diseases and Drugs." *Nucleic Acids Research* 45 (D1): D353–61. <https://doi.org/10.1093/nar/gkw1092>.
- Kang, Seok Whan, Young Bum Kim, Jae Dong Shin, and Eun Ki Kim. 2010. "Enhanced Biodegradation of Hydrocarbons in Soil by Microbial Biosurfactant, Sophorolipid." *Applied Biochemistry and Biotechnology* 160 (3): 780–90. <https://doi.org/10.1007/s12010-009-8580-5>.
- Kauppi, Björn, Kyoung Lee, Enrique Carredano, Rebecca E. Parales, David T. Gibson, Hans Eklund, and S. Ramaswamy. 1998. "Structure of an Aromatic-Ring-Hydroxylating Dioxygenasenaphthalene 1,2-Dioxygenase." *Structure* 6 (5): 571–86. [https://doi.org/10.1016/S0969-2126\(98\)00059-8](https://doi.org/10.1016/S0969-2126(98)00059-8).
- Keren, Ray, Adi Lavy, and Micha Ilan. 2016. "Increasing the Richness of Culturable Arsenic-Tolerant Bacteria from *Theonella Swinhoei* by Addition of Sponge Skeleton to the Growth Medium." *Microbial Ecology* 71 (4): 873–86. <https://doi.org/10.1007/s00248-015-0726-0>.
- Keum, Young Soo, Jong Su Seo, Qing X. Li, and Jeong Han Kim. 2008. "Comparative Metabolomic Analysis of *Sinorhizobium* Sp. C4 during the Degradation of Phenanthrene." *Applied Microbiology and Biotechnology* 80 (5): 863–72. <https://doi.org/10.1007/s00253-008-1581-4>.
- Khullar, Shikha, and M. Sudhakara Reddy. 2019. "Cadmium and Arsenic Responses in the Ectomycorrhizal Fungus *Laccaria Bicolor*: Glutathione Metabolism and Its Role in Metal(Loid) Homeostasis." *Environmental Microbiology Reports* 11 (2): 53–61. <https://doi.org/10.1111/1758-2229.12712>.
- Kim, Hyun Soo, Yeo Jin Kim, and Young Rok Seo. 2015. "An Overview of Carcinogenic Heavy Metal: Molecular Toxicity Mechanism and Prevention." *Journal of Cancer Prevention* 20 (4): 232–40. <https://doi.org/10.15430/jcp.2015.20.4.232>.
- Kim, Mincheol, Hyun Seok Oh, Sang Cheol Park, and Jongsik Chun. 2014. "Towards a Taxonomic Coherence between Average Nucleotide Identity and 16S rRNA Gene Sequence Similarity for Species Demarcation of Prokaryotes." *International Journal of Systematic and Evolutionary Microbiology* 64 (PART 2): 346–51. <https://doi.org/10.1099/ijs.0.059774-0>.
- Kim, S.-J., and K. K. Kwon. 2010. "Marine, Hydrocarbon Degrading Alphaproteobacteria." In *Handbook of Hydrocarbon and Lipid Microbiology*. <https://doi.org/10.1007/978-3-540-77587-4>.
- Kim, Yong Hak, James P. Freeman, Joanna D. Moody, Karl Heinrich Engesser, and Carl E. Cerniglia. 2005. "Effects of PH on the Degradation of Phenanthrene and Pyrene by *Mycobacterium Vanbaalenii* PYR-1." *Applied Microbiology and Biotechnology* 67 (2): 275–85. <https://doi.org/10.1007/s00253-004-1796-y>.
- Korlević, M., P. Pop Ristova, R. Garić, R. Amann, and S. Orlić. 2015. "Bacterial Diversity in the South Adriatic Sea during a Strong, Deep Winter Convection Year." *Applied and Environmental Microbiology* 81 (5): 1715–26. <https://doi.org/10.1128/AEM.03410-14>.
- Kramer, James R., Russell A. Bell, and D. Scott Smith. 2007. "Determination of Sulfide Ligands and Association with Natural Organic Matter." *Applied Geochemistry* 22 (8 SPEC. ISS.):

- 1606–11. <https://doi.org/10.1016/j.apgeochem.2007.03.026>.
- Kumar, Baduru Lakshman, and D. V.R.Sai Gopal. 2015. "Effective Role of Indigenous Microorganisms for Sustainable Environment." *3 Biotech* 5 (6): 867–76. <https://doi.org/10.1007/s13205-015-0293-6>.
- Kumar, Sudhir, Glen Stecher, Michael Li, Christina Knyaz, and Koichiro Tamura. 2018. "MEGA X: Molecular Evolutionary Genetics Analysis across Computing Platforms." *Molecular Biology and Evolution* 35 (6): 1547–49. <https://doi.org/10.1093/molbev/msy096>.
- Kumar, Vivek, Manoj Kumar, and Ram Prasad. 2019. *Microbial Action on Hydrocarbons*. *Microbial Action on Hydrocarbons*. <https://doi.org/10.1007/978-981-13-1840-5>.
- Kumari, Deepika, Xin Yi Qian, Xiangliang Pan, Varenayam Achal, Qianwei Li, and Geoffrey Michael Gadd. 2016. *Microbially-Induced Carbonate Precipitation for Immobilization of Toxic Metals*. *Advances in Applied Microbiology*. Vol. 94. Elsevier Ltd. <https://doi.org/10.1016/bs.aambs.2015.12.002>.
- Kurniati, Evi, Novi Arfarita, Tsuyoshi Imai, Takaya Higuchi, Ariyo Kanno, Koichi Yamamoto, and Masahiko Sekine. 2014. "Potential Bioremediation of Mercury-Contaminated Substrate Using Filamentous Fungi Isolated from Forest Soil." *Journal of Environmental Sciences (China)* 26 (6): 1223–31. [https://doi.org/10.1016/S1001-0742\(13\)60592-6](https://doi.org/10.1016/S1001-0742(13)60592-6).
- Lacerda, C. M R, Leila H. Choe, and Kenneth F. Reardon. 2007. "Metaproteomic Analysis of a Bacterial Community Response to Cadmium Exposure." *Journal of Proteome Research* 6 (3): 1145–52. <https://doi.org/10.1021/pr060477v>.
- Lai, Qiliang, Weiwei Li, and Zongze Shao. 2012. "Complete Genome Sequence of Alcanivorax Dieselelei Type Strain B5." *Journal of Bacteriology* 194 (23): 6674–6674. <https://doi.org/10.1128/JB.01813-12>.
- Ławniczak, Łukasz, Roman Marecik, and Łukasz Chrzanowski. 2013. "Contributions of Biosurfactants to Natural or Induced Bioremediation." *Applied Microbiology and Biotechnology* 97 (6): 2327–39. <https://doi.org/10.1007/s00253-013-4740-1>.
- Lee, Sang Cheol, Seung Jin Lee, Sun Hee Kim, In Hye Park, Yong Seok Lee, Soo Yeol Chung, and Yong Lark Choi. 2008. "Characterization of New Biosurfactant Produced by Klebsiella Sp. Y6-1 Isolated from Waste Soybean Oil." *Bioresource Technology* 99 (7): 2288–92. <https://doi.org/10.1016/j.biortech.2007.05.020>.
- Lei, An Ping, Zhang Li Hu, Yuk Shan Wong, and Nora Fung Yee Tam. 2007. "Removal of Fluoranthene and Pyrene by Different Microalgal Species." *Bioresource Technology* 98 (2): 273–80. <https://doi.org/10.1016/j.biortech.2006.01.012>.
- Leinster, Thomas, and Christina Cobbold. 2012. "Measuring Diversity: The Importance of Species Similarity." *Ecology* 93 (3): 477–89.
- Lenk, Sabine, Julia Arnds, Katrice Zerjatke, Niculina Musat, Rudolf Amann, and Marc Mußmann. 2011. "Novel Groups of Gammaproteobacteria Catalyse Sulfur Oxidation and Carbon Fixation in a Coastal, Intertidal Sediment." *Environmental Microbiology* 13 (3): 758–74. <https://doi.org/10.1111/j.1462-2920.2010.02380.x>.
- Li, Xin, Youe Wu, Chang Zhang, Yunguo Liu, Guangming Zeng, Xinquan Tang, Lihua Dai, and Shiming Lan. 2016. "Immobilizing of Heavy Metals in Sediments Contaminated by Nonferrous Metals Smelting Plant Sewage with Sulfate Reducing Bacteria and Micro Zero Valent Iron." *Chemical Engineering Journal* 306: 393–400.

<https://doi.org/10.1016/j.cej.2016.07.079>.

- Liebgott, Pierre Pol, Marc Labat, Laurence Casalot, Agnès Amouric, and Jean Lorquin. 2007. "Bioconversion of Tyrosol into Hydroxytyrosol and 3,4-Dihydroxyphenylacetic Acid under Hypersaline Conditions by the New Halomonas Sp. Strain HTB24." *FEMS Microbiology Letters* 276 (1): 26–33. <https://doi.org/10.1111/j.1574-6968.2007.00896.x>.
- Lim, Hye Sook, Jin Soo Lee, Hyo Taek Chon, and Manfred Sager. 2008. "Heavy Metal Contamination and Health Risk Assessment in the Vicinity of the Abandoned Songcheon Au-Ag Mine in Korea." *Journal of Geochemical Exploration* 96 (2–3): 223–30. <https://doi.org/10.1016/j.gexplo.2007.04.008>.
- Lin, Hsin Hung, and Yu Chieh Liao. 2016. "Accurate Binning of Metagenomic Contigs via Automated Clustering Sequences Using Information of Genomic Signatures and Marker Genes." *Scientific Reports* 6 (March): 12–19. <https://doi.org/10.1038/srep24175>.
- Liu, Lu, Georg Pohnert, and Dong Wei. 2016. "Extracellular Metabolites from Industrial Microalgae and Their Biotechnological Potential." *Marine Drugs* 14 (10): 1–19. <https://doi.org/10.3390/md14100191>.
- Liu, Xin xin, Xin Hu, Yue Cao, Wen jing Pang, Jin yu Huang, Peng Guo, and Lei Huang. 2019. "Biodegradation of Phenanthrene and Heavy Metal Removal by Acid-Tolerant Burkholderia Fungorum FM-2." *Frontiers in Microbiology* 10 (MAR): 1–13. <https://doi.org/10.3389/fmicb.2019.00408>.
- Lladó, S., S. Covino, A. M. Solanas, M. Viñas, M. Petruccioli, and A. D'annibale. 2013. "Comparative Assessment of Bioremediation Approaches to Highly Recalcitrant PAH Degradation in a Real Industrial Polluted Soil." *Journal of Hazardous Materials* 248–249 (1): 407–14. <https://doi.org/10.1016/j.jhazmat.2013.01.020>.
- Lloyd-Jones, Gareth, and Peter C K Lau. 1997. "Glutathione S-Transferase-Encoding Gene as a Potential Probe for Environmental Bacterial Isolates Capable of Degrading Polycyclic Aromatic Hydrocarbons." *Applied and Environmental Microbiology* 63 (8): 3286–90.
- Lloyd, Jonathan R. 2003. "Microbial Reduction of Metals and Radionuclides." *FEMS Microbiology Reviews* 27 (2–3): 411–25. [https://doi.org/10.1016/S0168-6445\(03\)00044-5](https://doi.org/10.1016/S0168-6445(03)00044-5).
- Loflen, Chad L., Travis Buck, Autumn Bonnema, and Wesley A. Heim. 2018. "Pollutant Bioaccumulation in the California Spiny Lobster (*Panulirus Interruptus*) in San Diego Bay, California, and Potential Human Health Implications." *Marine Pollution Bulletin* 128 (February): 585–92. <https://doi.org/10.1016/j.marpolbul.2018.02.001>.
- Lofrano, Giusy, Giovanni Libralato, Floriana Giuseppina Acanfora, Luca Pucci, and Maurizio Carotenuto. 2015. "Which Lesson Can Be Learnt from a Historical Contamination Analysis of the Most Polluted River in Europe?" *Science of the Total Environment* 524–525: 246–59. <https://doi.org/10.1016/j.scitotenv.2015.04.030>.
- Loman, N. J., Chrystala Constantinidou, Martin Christner, Holger Rohde, Jacqueline Z M Chan, J Quick, J. C. Weir, et al. 2013. "A Culture-Independent Sequence-Based Metagenomics Approach to the Investigation of an Outbreak of Shiga-Toxigenic Escherichia Coli O104:H4." *Jama* 309 (14): 1502. <https://doi.org/10.1001/jama.2013.3231>.
- Lozada, Mariana, Magalí S. Marcos, Marta G. Commendatore, Mónica N. Gil, and Hebe M. Dionisi. 2014. "The Bacterial Community Structure of Hydrocarbon-Polluted Marine

- Environments as the Basis for the Definition of an Ecological Index of Hydrocarbon Exposure." *Microbes and Environments* 29 (3): 269–76.
<https://doi.org/10.1264/jsme2.ME14028>.
- Luna, Gian Marco, Cinzia Corinaldesi, Eugenio Rastelli, and Roberto Danovaro. 2013. "Patterns and Drivers of Bacterial α - and β -Diversity across Vertical Profiles from Surface to Subsurface Sediments." *Environmental Microbiology Reports* 5 (5): 731–39.
<https://doi.org/10.1111/1758-2229.12075>.
- Machado, Henrique, and Lone Gram. 2017. "Comparative Genomics Reveals High Genomic Diversity in the Genus Photobacterium." *Frontiers in Microbiology* 8 (JUN): 1–14.
<https://doi.org/10.3389/fmicb.2017.01204>.
- Madden, Tom. 2013. "NCBI_blast Information.Pdf." *The NCBI Handbook*, 1–15.
- Malik, Anushree. 2004. "Metal Bioremediation through Growing Cells." *Environment International* 30 (2): 261–78. <https://doi.org/10.1016/j.envint.2003.08.001>.
- Malla, Muneer A., Anamika Dubey, Shweta Yadav, Ashwani Kumar, Abeer Hashem, and Elsayed Fathi Abd-Allah. 2018. "Understanding and Designing the Strategies for the Microbe-Mediated Remediation of Environmental Contaminants Using Omics Approaches." *Frontiers in Microbiology* 9. <https://doi.org/10.3389/fmicb.2018.01132>.
- Mandal, F, C Chatterjee, and A Gosh. 2011. "ECOSYSTEMS AND HUMAN WELL-BEING." *J. Environ. & Sociobiol.* 8 (1): 25–42.
https://www.researchgate.net/publication/259443253_Ecosystems_and_Human_well-being.
- Mao, Jian, Yongming Luo, Ying Teng, and Zhengao Li. 2012. "Bioremediation of Polycyclic Aromatic Hydrocarbon-Contaminated Soil by a Bacterial Consortium and Associated Microbial Community Changes." *International Biodeterioration and Biodegradation* 70: 141–47. <https://doi.org/10.1016/j.ibiod.2012.03.002>.
- Markiewicz, M., J. Henke, A. Brillowska-Dąbrowska, S. Stolte, J. Łuczak, and C. Jungnickel. 2014. "Bacterial Consortium and Axenic Cultures Isolated from Activated Sewage Sludge for Biodegradation of Imidazolium-Based Ionic Liquid." *International Journal of Environmental Science and Technology* 11 (7): 1919–26. <https://doi.org/10.1007/s13762-013-0390-1>.
- Martin, Fergal J., and James O. McInerney. 2009. "Recurring Cluster and Operon Assembly for Phenylacetate Degradation Genes." *BMC Evolutionary Biology* 9 (1).
<https://doi.org/10.1186/1471-2148-9-36>.
- Martín, Héctor García, Natalia Ivanova, Victor Kunin, Falk Warnecke, Kerrie W. Barry, Alice C. McHardy, Christine Yeates, et al. 2006. "Metagenomic Analysis of Two Enhanced Biological Phosphorus Removal (EBPR) Sludge Communities." *Nature Biotechnology* 24 (10): 1263–69. <https://doi.org/10.1038/nbt1247>.
- Massara, Hafez, Catherine N. Mulligan, and John Hadjinicolaou. 2007. "Effect of Rhamnolipids on Chromium-Contaminated Kaolinite." *Soil and Sediment Contamination* 16 (1): 1–14.
<https://doi.org/10.1080/15320380601071241>.
- Matallana-Surget, Sabine, Johannes Werner, Ruddy Wattiez, Karine Lebaron, Laurent Intertaglia, Callum Regan, James Morris, et al. 2018. "Proteogenomic Analysis of Epibacterium Mobile BBCC367, a Relevant Marine Bacterium Isolated From the South

- Pacific Ocean." *Frontiers in Microbiology* 9 (December): 1–17.
<https://doi.org/10.3389/fmicb.2018.03125>.
- McKew, Boyd A., Frédéric Coulon, A. Mark Osborn, Kenneth N. Timmis, and Terry J. McGenity. 2007. "Determining the Identity and Roles of Oil-Metabolizing Marine Bacteria from the Thames Estuary, UK." *Environmental Microbiology* 9 (1): 165–76.
<https://doi.org/10.1111/j.1462-2920.2006.01125.x>.
- McKew, Boyd A., Frédéric Coulon, Michail M. Yakimov, Renata Denaro, Maria Genovese, Cindy J. Smith, A. Mark Osborn, Kenneth N. Timmis, and Terry J. McGenity. 2007. "Efficacy of Intervention Strategies for Bioremediation of Crude Oil in Marine Systems and Effects on Indigenous Hydrocarbonoclastic Bacteria." *Environmental Microbiology* 9 (6): 1562–71.
<https://doi.org/10.1111/j.1462-2920.2007.01277.x>.
- Meckenstock, Rainer U., Michael Safinowsk, and Christian Griebler. 2004. "Anaerobic Degradation of Polycyclic Aromatic Hydrocarbons." *FEMS Microbiology Ecology* 49: 27–36. <https://doi.org/10.1016/j.femsec.2004.02.019>.
- Megharaj, Mallavarapu, and Ravi Naidu. 2017. "Soil and Brownfield Bioremediation." *Microbial Biotechnology* 10 (5): 1244–49. <https://doi.org/10.1111/1751-7915.12840>.
- Méndez, Valentina, Loreine Agulló, Myriam González, and Michael Seeger. 2011. "The Homogentisate and Homoprotocatechuate Central Pathways Are Involved in 3- and 4-Hydroxyphenylacetate Degradation by Burkholderia Xenovorans LB400." *PLoS ONE* 6 (3). <https://doi.org/10.1371/journal.pone.0017583>.
- Mille, G., Mulyono, T., Jammal, EL., Bertrand, J-c. Effects of oxygen on hydrocarbon degradation studies *in vitro* in surficial sediments. 1988. *Estuarine coastal and shelf Science* 27, 3: 283-295..
- Molari, Massimiliano, Donato Giovannelli, Giuseppe D’Errico, and Elena Manini. 2012. "Factors Influencing Prokaryotic Community Structure Composition in Sub-Surface Coastal Sediments." *Estuarine, Coastal and Shelf Science* 97: 141–48.
<https://doi.org/10.1016/j.ecss.2011.11.036>.
- Mondal, S. K., B Lijon, R Reza, and T Ishika. 2016. "Isolation and Identification of *Vibrio Nereis* and *Vibrio Harveyi* in Farm Raised *Penaeus Monodon* Marine Shrimp." *International Journal of Biosciences (IJB)* 8 (4): 55–61. <https://doi.org/10.12692/ijb/8.4.55-61>.
- Montuori, P., P. Lama, S. Aurino, D. Naviglio, and M. Triassi. 2013. "Metals Loads into the Mediterranean Sea: Estimate of Sarno River Inputs and Ecological Risk." *Ecotoxicology* 22 (2): 295–307. <https://doi.org/10.1007/s10646-012-1026-9>.
- Moody, Joanna D., James P. Freeman, and Carl E. Cerniglia. 2005. "Degradation of Benz[a]Anthracene by *Mycobacterium Vanbaalenii* Strain PYR-1." *Biodegradation* 16 (6): 513–26. <https://doi.org/10.1007/s10532-004-7217-1>.
- Moran, M. A., R. Belas, M. A. Schell, J. M. González, F. Sun, S. Sun, B. J. Binder, et al. 2007. "Ecological Genomics of Marine Roseobacters." *Applied and Environmental Microbiology* 73 (14): 4559–69. <https://doi.org/10.1128/AEM.02580-06>.
- Morel, Mélanie, Edgar Meux, Yann Mathieu, Anne Thuillier, Kamel Chibani, Luc Harvengt, Jean Pierre Jacquot, and Eric Gelhaye. 2013. "Xenomic Networks Variability and Adaptation Traits in Wood Decaying Fungi." *Microbial Biotechnology* 6 (3): 248–63.
<https://doi.org/10.1111/1751-7915.12015>.

- Moreno-ulloa, Aldo, Victoria Sicairos Diaz, Javier A Tejada-mora, Marla I Macias Contreras, Fernando Díaz Castillo, Abraham Guerrero, Ricardo Gonzales Sanchez, Rafael Vazquez Duhalt, Alexei Licea-navarro, and Alexei Licea-navarro. 2019. "Metabolic and Metagenomic Profiling of Hydrocarbon-Degrading Microorganisms Obtained from the Deep Biosphere of the Gulf of México." *BioRxiv*.
- Morillo Pérez, José Antonio, Rafael García-Ribera, Teresa Quesada, Margarita Aguilera, Alberto Ramos-Cormenzana, and Mercedes Monteoliva-Sánchez. 2008. "Biosorption of Heavy Metals by the Exopolysaccharide Produced by *Paenibacillus Jamilae*." *World Journal of Microbiology and Biotechnology* 24 (11): 2699–2704. <https://doi.org/10.1007/s11274-008-9800-9>.
- Moron, Maria, Joseph Depierre, and Bengt Mannervik. 1979. "Levels of Glutathione-S-Transferase Activities in Rat Lung and Liver." *Biochimica et Biophysica Acta*, 582: 67–68.
- Mueller, J. G., P. J. Chapman, B. O. Blattmann, and P. H. Pritchard. 1990. "Isolation and Characterization of a Fluoranthene-Utilizing Strain of *Pseudomonas Paucimobilis*." *Applied and Environmental Microbiology* 56 (4): 1079–86.
- Mulligan, Catherine N. 2005. "Environmental Applications for Biosurfactants." *Environmental Pollution* 133 (2): 183–98. <https://doi.org/10.1016/j.envpol.2004.06.009>.
- Mulligan, Catherine N., and Suiling Wang. 2006. "Remediation of a Heavy Metal-Contaminated Soil by a Rhamnolipid Foam." *Engineering Geology* 85 (1–2): 75–81. <https://doi.org/10.1016/j.enggeo.2005.09.029>.
- Mulligan, Catherine N., Raymond N. Yong, and Bernard F. Gibbs. 1999. "Removal of Heavy Metals from Contaminated Soil and Sediments Using the Biosurfactant Surfactin." *Soil and Sediment Contamination* 8 (2): 231–54. <https://doi.org/10.1080/10588339991339324>.
- Mulligan, Catherine, Yong, Raimond, Gibbs, Bernard. 2001. "An Evaluation of Technologies for the Heavy Metal Remediation of Dredged Sediments." *Journal of Hazardous Materials* 85 (1–2): 145–63. [https://doi.org/10.1016/S0304-3894\(01\)00226-6](https://doi.org/10.1016/S0304-3894(01)00226-6).
- Mumtaz, Saqib, Claire Streten-Joyce, David L. Parry, Keith A. McGuinness, Ping Lu, and Karen S. Gibb. 2013. "Fungi Outcompete Bacteria under Increased Uranium Concentration in Culture Media." *Journal of Environmental Radioactivity* 120: 39–44. <https://doi.org/10.1016/j.jenvrad.2013.01.007>.
- Musat, Niculina, Ursula Werner, Katrin Knittel, Steffen Kolb, Tanja Dodenhof, Justus E.E. van Beusekom, Dirk de Beer, Nicole Dubilier, and Rudolf Amann. 2006. "Microbial Community Structure of Sandy Intertidal Sediments in the North Sea, Sylt-Rømø Basin, Wadden Sea." *Systematic and Applied Microbiology* 29 (4): 333–48. <https://doi.org/10.1016/j.syapm.2005.12.006>.
- Mußmann, Marc, Petra Pjevac, Karen Krüger, and Stefan Dyksma. 2017. "Genomic Repertoire of the Woeseiaceae/JTB255, Cosmopolitan and Abundant Core Members of Microbial Communities in Marine Sediments." *ISME Journal* 11 (5): 1276–81. <https://doi.org/10.1038/ismej.2016.185>.
- Muyzer, Gerard, and Alfons J.M. Stams. 2008. "The Ecology and Biotechnology of Sulphate-Reducing Bacteria." *Nature Reviews Microbiology* 6 (6): 441–54. <https://doi.org/10.1038/nrmicro1892>.

- Nagata, Shohei, Konosuke M. Ii, Tomoya Tsukimi, Masahiro C. Miura, Josephine Galipon, and Kazuharu Arakawa. 2019. "Complete Genome Sequence of Halomonas Olivaria, a Moderately Halophilic Bacterium Isolated from Olive Processing Effluents, Obtained by Nanopore Sequencing." *Microbiology Resource Announcements* 8 (18): 2–3. <https://doi.org/10.1128/mra.00144-19>.
- Nanca, Carolyn L., Kimberly D. Neri, Anna Christina R. Ngo, Reuel M. Bennett, and Gina R. Dedeles. 2018. "Degradation of Polycyclic Aromatic Hydrocarbons by Moderately Halophilic Bacteria from Luzon Salt Beds." *Journal of Health and Pollution* 8 (19): 1–10. <https://doi.org/10.5696/2156-9614-8.19.180915>.
- Nasser, B, AR Ramadan, RY Hamzah, ME Mohamed, and WA Ismail. 2017. "Detection and Quantification of Sulfate-Reducing and Polycyclic Aromatic Hydrocarbon-Degrading Bacteria in Oilfield Using Functional Markers and Quantitative PCR." *Journal of Petroleum & Environmental Biotechnology* 08 (05). <https://doi.org/10.4172/2157-7463.1000348>.
- Neagoe, Aurora, Virgil Iordache, and Ileana Cornelia Fărcășanu. 2012. "The Role of Organic Matter in the Mobility of Metals in Contaminated Catchments." In *Bio-Geo Interactions in Metal-Contaminated Soils.*, 297–325. https://doi.org/10.1007/978-3-642-23327-2_15.
- Nešvera, Jan, Lenka Rucká, and Miroslav Pátek. 2015. "Catabolism of Phenol and Its Derivatives in Bacteria: Genes, Their Regulation, and Use in the Biodegradation of Toxic Pollutants." *Advances in Applied Microbiology* 93 (October): 107–60. <https://doi.org/10.1016/bs.aambs.2015.06.002>.
- Ngara, Tanyaradzwa Rodgers, and Houjin Zhang. 2018. "Recent Advances in Function-Based Metagenomic Screening." *Genomics, Proteomics and Bioinformatics* 16 (6): 405–15. <https://doi.org/10.1016/j.gpb.2018.01.002>.
- Nikolopoulou, M., N. Pasadakis, H. Norf, and N. Kalogerakis. 2013. "Enhanced Ex Situ Bioremediation of Crude Oil Contaminated Beach Sand by Supplementation with Nutrients and Rhamnolipids." *Marine Pollution Bulletin* 77 (1–2): 37–44. <https://doi.org/10.1016/j.marpolbul.2013.10.038>.
- Nithya, Chari, and Shunmugiah Karutha Pandian. 2010. "Isolation of Heterotrophic Bacteria from Palk Bay Sediments Showing Heavy Metal Tolerance and Antibiotic Production." *Microbiological Research* 165 (7): 578–93. <https://doi.org/10.1016/j.micres.2009.10.004>.
- Novotnik, Breda, Jackie Zorz, Steven Bryant, and Marc Strous. 2019. "The Effect of Dissimilatory Manganese Reduction on Lactate Fermentation and Microbial Community Assembly." *Frontiers in Microbiology* 10 (MAY): 1–15. <https://doi.org/10.3389/fmicb.2019.01007>.
- Nuñal, Sharon N., Sheila Mae S. Santander-de Leon, Wei Hongyi, Adel Amer Regal, Takeshi Yoshikawa, Suguru Okunishi, and Hiroto Maeda. 2017. "Hydrocarbon Degradation and Bacterial Community Responses during Remediation of Sediment Artificially Contaminated with Heavy Oil." *Biocontrol Science* 22 (4): 187–203. <https://doi.org/10.4265/bio.22.187>.
- Ojuederie, Omena Bernard, and Olubukola Oluranti Babalola. 2017. "Microbial and Plant-Assisted Bioremediation of Heavy Metal Polluted Environments: A Review." *International Journal of Environmental Research and Public Health*. MDPI AG. <https://doi.org/10.3390/ijerph14121504>.
- Okoro, Oghenekevwe. 2007. "Biosurfactant Enhanced Remediation of a Mixed Contaminated

Soil." *Geoenvironmental Engineering Seminar*.

- Olaniran, Ademola O., Adhika Balgobind, and Balakrishna Pillay. 2013. "Bioavailability of Heavy Metals in Soil: Impact on Microbial Biodegradation of Organic Compounds and Possible Improvement Strategies." *International Journal of Molecular Sciences* 14 (5): 10197–228. <https://doi.org/10.3390/ijms140510197>.
- Oregaard, Gunnar, and Søren J. Sørensen. 2007. "High Diversity of Bacterial Mercuric Reductase Genes from Surface and Sub-Surface Floodplain Soil (Oak Ridge, USA)." *ISME Journal* 1 (5): 453–67. <https://doi.org/10.1038/ismej.2007.56>.
- Ostrem Loss, Erin M., and Jae Hyuk Yu. 2018. "Bioremediation and Microbial Metabolism of Benzo(a)Pyrene." *Molecular Microbiology* 109 (4): 433–44. <https://doi.org/10.1111/mmi.14062>.
- Overbeek, Ross, Robert Olson, Gordon D. Pusch, Gary J. Olsen, James J. Davis, Terry Disz, Robert A. Edwards, et al. 2014. "The SEED and the Rapid Annotation of Microbial Genomes Using Subsystems Technology (RAST)." *Nucleic Acids Research* 42 (D1): 206–14. <https://doi.org/10.1093/nar/gkt1226>.
- Overmann, Jörg, Birte Abt, and Johannes Sikorski. 2017. "Present and Future of Culturing Bacteria." *Annual Review of Microbiology* 71 (1): 711–30. <https://doi.org/10.1146/annurev-micro-090816-093449>.
- Paiva Magalhaes, Danielly de, Monica Regina da Costa Marques, Darcillio Fernandes Baptista, and Daniel Forsin Buss. 2015. "Metal Bioavailability and Toxicity in Freshwaters." *Environ Chem Lett* 13: 69–87. <https://doi.org/10.1007/s10311-015-0491-9>.
- Parks, D., Chuvochina, M., Waite, D. et al (2018). A standardized bacterial taxonomy based on genome phylogeny substantially revises the tree of life. *Nat Biotechnol* **36**, 996–1004.
- Parks, Donovan H., Michael Imelfort, Connor T. Skennerton, Philip Hugenholtz, and Gene W. Tyson. 2015. "CheckM: Assessing the Quality of Microbial Genomes Recovered from Isolates, Single Cells, and Metagenomes." *Genome Research* 25 (7): 1043–55. <https://doi.org/10.1101/gr.186072.114>.
- Patel, Vilas, Sravanthi Cheturvedula, and Datta Madamwar. 2012. "Phenanthrene Degradation by Pseudoxanthomonas Sp. DMVP2 Isolated from Hydrocarbon Contaminated Sediment of Amlakhadi Canal, Gujarat, India." *Journal of Hazardous Materials* 201–202: 43–51. <https://doi.org/10.1016/j.jhazmat.2011.11.002>.
- Patlolla, Anita K, C Barnes, C Yedjou, V. R Velma, and P. B Tchounwou. 2009. "Oxidative Stress, DNA Damage, and Antioxidant Enzyme Activity Induced by Hexavalent Chromium in Sprague-Dawley Rats." *Environmental Toxicology* 26: 146–52. <https://doi.org/10.1002/tox>.
- Pawlowski, Andrew C., Erin L. Westman, Kalinka Koteva, Nicholas Waglechner, and Gerard D. Wright. 2018. "The Complex Resistomes of Paenibacillaceae Reflect Diverse Antibiotic Chemical Ecologies." *ISME Journal* 12 (3): 885–97. <https://doi.org/10.1038/s41396-017-0017-5>.
- Pearce, Oliver M.T., Heinz Läubli, Andrea Verhagen, Patrick Secrest, Jiquan Zhang, Nissi M. Varki, Paul R. Crocker, Jack D. Bui, and Ajit Varki. 2014. "Inverse Hormesis of Cancer Growth Mediated by Narrow Ranges of Tumor-Directed Antibodies." *Proceedings of the National Academy of Sciences of the United States of America* 111 (16): 5998–6003.

<https://doi.org/10.1073/pnas.1209067111>.

- Peng, Jian-feng, Yong-hui Song, Peng Yuan, Xiao-yu Cui, and Guang-lei Qiu. 2009. "The Remediation of Heavy Metals Contaminated Sediment." *Journal of Hazardous Materials* 161: 633–40. <https://doi.org/10.1016/j.jhazmat.2008.04.061>.
- Peng, Ri He, Ai Sheng Xiong, Yong Xue, Xiao Yan Fu, Feng Gao, Wei Zhao, Yong Sheng Tian, and Quan Hong Yao. 2008. "Microbial Biodegradation of Polyaromatic Hydrocarbons." *FEMS Microbiology Reviews* 32 (6): 927–55. <https://doi.org/10.1111/j.1574-6976.2008.00127.x>.
- Peng, Weihua, Xiaomin Li, Shengtao Xiao, and Wenhong Fan. 2018. "Review of Remediation Technologies for Sediments Contaminated by Heavy Metals." *Journal of Soils and Sediments* 18 (4): 1701–19. <https://doi.org/10.1007/s11368-018-1921-7>.
- Pepi, Milva, Marco Borra, Stella Tamburrino, Maria Saggiomo, Alfio Viola, Elio Biffali, Cecilia Balestra, Mario Sprovieri, and Raffaella Casotti. 2016. "A *Bacillus* Sp. Isolated from Sediments of the Sarno River Mouth, Gulf of Naples (Italy) Produces a Biofilm Biosorbing Pb(II)." *Science of the Total Environment* 562: 588–95. <https://doi.org/10.1016/j.scitotenv.2016.04.097>.
- Perales-Vela, Hugo Virgilio, Julián Mario Peña-Castro, and Rosa Olivia Cañizares-Villanueva. 2006. "Heavy Metal Detoxification in Eukaryotic Microalgae." *Chemosphere* 64 (1): 1–10. <https://doi.org/10.1016/j.chemosphere.2005.11.024>.
- Piakong, MT, and Nur Zaida Z. 2018. "Effectiveness of Single and Microbial Consortium of Locally Isolated Beneficial Microorganisms (LIBeM) in Bioaugmentation of Oil Sludge Contaminated Soil at Different Concentration Levels: A Laboratory Scale." *Journal of Bioremediation & Biodegradation* 09 (02): 3–9. <https://doi.org/10.4172/2155-6199.1000430>.
- Plewniak, Frédéric, Simona Crognale, Simona Rossetti, and Philippe N. Bertin. 2018. "A Genomic Outlook on Bioremediation: The Case of Arsenic Removal." *Frontiers in Microbiology* 9 (APR): 1–8. <https://doi.org/10.3389/fmicb.2018.00820>.
- Polymenakou, Paraskevi N., Stefan Bertilsson, Anastasios Tselepidis, and Euripides G. Stephanou. 2005. "Bacterial Community Composition in Different Sediments from the Eastern Mediterranean Sea: A Comparison of Four 16S Ribosomal DNA Clone Libraries." *Microbial Ecology* 50 (3): 447–62. <https://doi.org/10.1007/s00248-005-0005-6>.
- Pourfakhraei, Elaheh, Jalil Badraghi, Fatemeh Mamashli, Mahboobeh Nazari, and Ali Akbar Saboury. 2018. "Biodegradation of Asphaltene and Petroleum Compounds by a Highly Potent *Daedaleopsis* Sp." *Journal of Basic Microbiology* 58 (7): 609–22. <https://doi.org/10.1002/jobm.201800080>.
- Preda, Micaela, and Malcolm E. Cox. 2005. "Chemical and Mineralogical Composition of Marine Sediments, and Relation to Their Source and Transport, Gulf of Carpentaria, Northern Australia." *Journal of Marine Systems* 53 (1–4): 169–86. <https://doi.org/10.1016/j.jmarsys.2004.05.003>.
- Pusceddu, Antonio, Silvia Bianchelli, and Roberto Danovaro. 2015. "Quantity and Biochemical Composition of Particulate Organic Matter in a Highly Trawled Area (Thermaikos Gulf, Eastern Mediterranean Sea)." *Advances in Oceanography and Limnology* 6 (1–2): 21–32. <https://doi.org/10.4081/aiol.2015.5448>.
- Qin, Qi Long, Yang Li, Yan Jiao Zhang, Zhe Min Zhou, Wei Xin Zhang, Xiu Lan Chen, Xi Ying

- Zhang, Bai Cheng Zhou, Lei Wang, and Yu Zhong Zhang. 2011. "Comparative Genomics Reveals a Deep-Sea Sediment-Adapted Life Style of *Pseudoalteromonas* Sp. SM9913." *ISME Journal* 5 (2): 274–84. <https://doi.org/10.1038/ismej.2010.103>.
- Quast, Christian, Elmar Pruesse, Pelin Yilmaz, Jan Gerken, Timmy Schweer, Pablo Yarza, Jörg Peplies, and Frank Oliver Glöckner. 2013. "The SILVA Ribosomal RNA Gene Database Project: Improved Data Processing and Web-Based Tools." *Nucleic Acids Research* 41: 590–96. <https://doi.org/10.1093/nar/gks1219>.
- Quero, Grazia Marina, Daniele Cassin, Margherita Botter, Laura Perini, and Gian Marco Luna. 2015. "Patterns of Benthic Bacterial Diversity in Coastal Areas Contaminated by Heavy Metals, Polycyclic Aromatic Hydrocarbons (PAHs) and Polychlorinated Biphenyls (PCBs)." *Frontiers in Microbiology* 6 (OCT): 1–15. <https://doi.org/10.3389/fmicb.2015.01053>.
- Quillet, Laurent, Ludovic Besaury, Milka Popova, Sandrine Paissé, Julien Deloffre, and Baghdad Ouddane. 2012. "Abundance, Diversity and Activity of Sulfate-Reducing Prokaryotes in Heavy Metal-Contaminated Sediment from a Salt Marsh in the Medway Estuary (UK)." *Marine Biotechnology* 14 (3): 363–81. <https://doi.org/10.1007/s10126-011-9420-5>.
- Rabus, Ralf, Matthias Boll, Johann Heider, Rainer U. Meckenstock, Wolfgang Buckel, Oliver Einsle, Ulrich Ermler, et al. 2016. "Anaerobic Microbial Degradation of Hydrocarbons: From Enzymatic Reactions to the Environment." *Journal of Molecular Microbiology and Biotechnology* 26 (1–3): 5–28. <https://doi.org/10.1159/000443997>.
- Radmann, Martha, Etiele Greque de Morais, Cibele Freitas de Oliveira, Kellen Zanfonato, and Jorge Alberto Vieira Costa. 2015. "Microalgae Cultivation for Biosurfactant Production." *African Journal of Microbiology Research* 9 (47): 2283–89. <https://doi.org/10.5897/ajmr2015.7634>.
- Rajkumari, Jina, L. Paikhomba Singha, and Piyush Pandey. 2018. "Genomic Insights of Aromatic Hydrocarbon Degrading *Klebsiella Pneumoniae* AWD5 with Plant Growth Promoting Attributes: A Paradigm of Soil Isolate with Elements of Biodegradation." *3 Biotech* 8 (2): 1–22. <https://doi.org/10.1007/s13205-018-1134-1>.
- Ranawat, Preeti, and Seema Rawat. 2018. "Metal-Tolerant Thermophiles: Metals as Electron Donors and Acceptors, Toxicity, Tolerance and Industrial Applications." *Environmental Science and Pollution Research* 25 (5): 4105–33. <https://doi.org/10.1007/s11356-017-0869-2>.
- Rappé, Michael S., Stephanie A. Connon, Kevin L. Vergin, and Stephen J. Giovannoni. 2002. "Cultivation of the Ubiquitous SAR11 Marine Bacterioplankton Clade." *Nature* 418 (6898): 630–33. <https://doi.org/10.1038/nature00917>.
- Ratzke, Christoph, and Jeff Gore. 2018. "Modifying and Reacting to the Environmental PH Can Drive Bacterial Interactions." *PLoS Biology* 16 (3): 1–20. <https://doi.org/10.1371/journal.pbio.2004248>.
- Rawlings, Douglas E., and D. Barrie Johnson. 2007. "The Microbiology of Biomining: Development and Optimization of Mineral-Oxidizing Microbial Consortia." *Microbiology* 153 (2): 315–24. <https://doi.org/10.1099/mic.0.2006/001206-0>.
- Regoli, F., S. Gorbi, G. Frenzilli, M. Nigro, I. Corsi, S. Focardi, and G. W. Winston. 2002. "Oxidative Stress in Ecotoxicology: From the Analysis of Individual Antioxidants to a More Integrated Approach." *Marine Environmental Research* 54 (3–5): 419–23. [https://doi.org/10.1016/S0141-1136\(02\)00146-0](https://doi.org/10.1016/S0141-1136(02)00146-0).

- Richter, Michael, and Ramon Rosselló-Móra. 2009. "Shifting the Genomic Gold Standard for the Prokaryotic Species Definition." *Proceedings of the National Academy of Sciences of the United States of America* 106 (45): 19126–31. <https://doi.org/10.1073/pnas.0906412106>.
- Rissanen, Antti J., Sari Peura, Promise A. Mpamah, Sami Taipale, Marja Tirola, Christina Biasi, Anita Mäki, and Hannu Nykänen. 2019. "Vertical Stratification of Bacteria and Archaea in Sediments of a Small Boreal Humic Lake." *FEMS Microbiology Letters* 366 (5): 1–11. <https://doi.org/10.1093/femsle/fnz044>.
- Roberts, Mark A.J., George H. Wadhams, Katie A. Hadfield, Susan Tickner, and Judith P. Armitage. 2012. "ParA-like Protein Uses Nonspecific Chromosomal DNA Binding to Partition Protein Complexes." *Proceedings of the National Academy of Sciences of the United States of America* 109 (17): 6698–6703. <https://doi.org/10.1073/pnas.1114000109>.
- Rodriguez-R, Luis, and Konstantinos Konstantinidis. 2016. "The Enveomics Collection: A Toolbox for Specialized Analyses of Microbial Genomes and Metagenomes." *PeerJ Preprints*. <https://doi.org/10.7287/peerj.preprints.1900>.
- Rognes, Torbjørn, Tomáš Flouri, Ben Nichols, Christopher Quince, and Frédéric Mahé. 2016. "VSEARCH: A Versatile Open Source Tool for Metagenomics." *PeerJ* 10: 1–22. <https://doi.org/10.7717/peerj.2584>.
- Röling, Wilfred F.M., Ivana R. Couto De Brito, Richard P.J. Swannell, and Ian M. Head. 2004. "Response of Archaeal Communities in Beach Sediments to Spilled Oil and Bioremediation." *Applied and Environmental Microbiology* 70 (5): 2614–20. <https://doi.org/10.1128/AEM.70.5.2614-2620.2004>.
- Röling, Wilfred F.M., Michael G. Milner, D. Martin Jones, Kenneth Lee, Fabien Daniel, Richard J.P. Swannell, and Ian M. Head. 2002. "Robust Hydrocarbon Degradation and Dynamics of Bacterial Communities during Nutrient-Enhanced Oil Spill Bioremediation." *Applied and Environmental Microbiology* 68 (11): 5537–48. <https://doi.org/10.1128/AEM.68.11.5537-5548.2002>.
- Romano, Elena, Antonella Ausili, Nadezhda Zharova, Maria Celia Magno, Bruno Pavoni, and Massimo Gabellini. 2004. "Marine Sediment Contamination of an Industrial Site at Port of Bagnoli, Gulf of Naples, Southern Italy." *Marine Pollution Bulletin* 49 (5–6): 487–95. <https://doi.org/10.1016/j.marpolbul.2004.03.014>.
- Romano, Elena, Luisa Bergamin, Antonella Ausili, Giancarlo Pierfranceschi, Chiara Maggi, Giulio Sesta, and Massimo Gabellini. 2009. "The Impact of the Bagnoli Industrial Site (Naples, Italy) on Sea-Bottom Environment. Chemical and Textural Features of Sediments and the Related Response of Benthic Foraminifera." *Marine Pollution Bulletin* 59 (8–12): 245–56. <https://doi.org/10.1016/j.marpolbul.2009.09.017>.
- Romano, Ida, Assunta Giordano, Licia Lama, Barbara Nicolaus, and Agata Gambacorta. 2005. "Halomonas Campaniensis Sp. Nov., a Haloalkaliphilic Bacterium Isolated from a Mineral Pool of Campania Region, Italy." *Systematic and Applied Microbiology* 28 (7): 610–18. <https://doi.org/10.1016/j.syapm.2005.03.010>.
- Rosen, Barry, and Zijuan Liu. 2009. "Transport Pathways for Arsenic and Selenium: A Minireview Barry." *Environ Int.* 35 (3): 512–15. <https://doi.org/10.1038/jid.2014.371>.
- Rothenstein, Dirk, Johannes Baier, Thomas D Schreiber, Vera Barucha, and Joachim Bill. 2012.

- "Influence of Zinc on the Calcium Carbonate Biomineralization of Halomonas Halophila." *Aquatic Biosystems* 8 (1): 31. <https://doi.org/10.1186/2046-9063-8-31>.
- Sabra, Nada, Henri Charles Dubourguier, Marie Nadège Duval, and Tayssir Hamieh. 2013. "Study of Canal Sediments Contaminated with Heavy Metals : Fungal versus Bacterial Bioleaching Techniques." *Environmental Technology* 32 (12): 1307–24. <https://doi.org/10.1080/09593330.2010.536782>.
- Salam, Lateef B., and Aisha Ishaq. 2019. "Biostimulation Potentials of Corn Steep Liquor in Enhanced Hydrocarbon Degradation in Chronically Polluted Soil." *3 Biotech* 9 (2): 1–20. <https://doi.org/10.1007/s13205-019-1580-4>.
- Satpute, Surekha K., Arun G. Banpurkar, Prashant K. Dhakephalkar, Ibrahim M. Banat, and Balu A. Chopade. 2010. "Methods for Investigating Biosurfactants and Bioemulsifiers: A Review." *Critical Reviews in Biotechnology* 30 (2): 127–44. <https://doi.org/10.3109/07388550903427280>.
- Senghor, B., S. Khelaifia, H. Bassène, E. H. Seck, P. E. Fournier, C. Sokhna, D. Raoult, and J. C. Lagier. 2017. "'Gracilibacillus Phocaeensis' Sp. Nov., 'Sediminibacillus Massiliensis' Sp. Nov. and 'Virgibacillus Ndiopensis' Sp. Nov., Three Halophilic Species Isolated from Salty Human Stools by Culturomics." *New Microbes and New Infections* 20: 51–54. <https://doi.org/10.1016/j.nmni.2017.08.006>.
- Shahsavari, Esmaeil, Alexandra Schwarz, Arturo Aburto-Medina, and Andrew S. Ball. 2019. "Biological Degradation of Polycyclic Aromatic Compounds (PAHs) in Soil: A Current Perspective." *Current Pollution Reports* 5: 84–92. <https://doi.org/10.1007/s40726-019-00113-8>.
- Sharma, Resham, Renu Bhardwaj, Neha Handa, Vandana Gautam, Sukhmeen Kaur Kohli, Shagun Bali, Parminder Kaur, et al. 2015. "Responses of Phytochelatins and Metallothioneins in Alleviation of Heavy Metal Stress in Plants: An Overview." *Plant Metal Interaction: Emerging Remediation Techniques*, 263–83. <https://doi.org/10.1016/B978-0-12-803158-2.00010-2>.
- Sharp, W. E., and Giuseppe Nardi. 1987. "A Study of the Heavy-Metal Pollution in the Bottom Sediments at Porto Di Bagnoli (Naples), Italy." *Journal of Geochemical Exploration* 29 (1–3): 31–48. [https://doi.org/10.1016/0375-6742\(87\)90069-0](https://doi.org/10.1016/0375-6742(87)90069-0).
- Shen, Liang, Yongqin Liu, Baiqing Xu, Ninglian Wang, Huabiao Zhao, Xiaobo Liu, and Fei Liu. 2017. "Comparative Genomic Analysis Reveals the Environmental Impacts on Two Arcticibacter Strains Including Sixteen Sphingobacteriaceae Species." *Scientific Reports* 7 (1): 1–12. <https://doi.org/10.1038/s41598-017-02191-4>.
- Shi, Junyi, Mitchell Huber, Ting Wang, Wang Dali, Zhifen Lin, and Yin Chun-Sheng. 2016. "Progress in the Studies on Hormesis of Low-Dose Pollutants." *Environmental Disease* 1 (2): 58. <https://doi.org/10.4103/2468-5690.185296>.
- Shoun, Hirofumi, Shinya Fushinobu, Li Jiang, Sang Wan Kim, and Takayoshi Wakagi. 2012. "Fungal Denitrification and Nitric Oxide Reductase Cytochrome P450nor." *Philosophical Transactions of the Royal Society B: Biological Sciences* 367 (1593): 1186–94. <https://doi.org/10.1098/rstb.2011.0335>.
- Singh, Om V. 2006. "Proteomics and Metabolomics: The Molecular Make-up of Toxic Aromatic Pollutant Bioremediation." *Proteomics* 6 (20): 5481–92. <https://doi.org/10.1002/pmic.200600200>.

- Singh, Pooja, and Swaranjit Singh Cameotra. 2004. "Potential Applications of Microbial Surfactants in Biomedical Sciences." *Trends in Biotechnology* 22 (3): 142–46. <https://doi.org/10.1016/j.tibtech.2004.01.010>.
- Singleton, David R., Jing Hu, and Michael D. Aitken. 2012. "Heterologous Expression of Polycyclic Aromatic Hydrocarbon Ring-Hydroxylating Dioxygenase Genes from a Novel Pyrene-Degrading Betaproteobacterium." *Applied and Environmental Microbiology* 78 (10): 3552–59. <https://doi.org/10.1128/AEM.00173-12>.
- Slizovskiy, Ilya B., Jason W. Kelsey, and Paul B. Hatzinger. 2011. "Surfactant-Facilitated Remediation of Metal-Contaminated Soils: Efficacy and Toxicological Consequences to Earthworms." *Environmental Toxicology and Chemistry* 30 (1): 112–23. <https://doi.org/10.1002/etc.357>.
- Song, Saisai, Lizhong Zhu, and Wenjun Zhou. 2008. "Simultaneous Removal of Phenanthrene and Cadmium from Contaminated Soils by Saponin, a Plant-Derived Biosurfactant." *Environmental Pollution* 156 (3): 1368–70. <https://doi.org/10.1016/j.envpol.2008.06.018>.
- Song, Yoon Jae. 2009. "Characterization of Aromatic Hydrocarbon Degrading Bacteria Isolated from Pine Litter." *Korean Journal of Microbiology and Biotechnology* 37 (4): 333–39.
- Stackebrandt, E., and B. M. Goebel. 1994. "Taxonomic Note: A Place for DNA-DNA Reassociation and 16S rRNA Sequence Analysis in the Present Species Definition in Bacteriology." *International Journal of Systematic Bacteriology* 44 (4): 846–49. <https://doi.org/10.1099/00207713-44-4-846>.
- Stagars, Marion H., Sonakshi Mishra, Tina Treude, Rudolf Amann, and Katrin Knittel. 2017. "Microbial Community Response to Simulated Petroleum Seepage in Caspian Sea Sediments." *Frontiers in Microbiology* 8 (APR): 1–16. <https://doi.org/10.3389/fmicb.2017.00764>.
- Stauffert, Magalie, Cristiana Cravo-Laureau, and Robert Duran. 2014. "Structure of Hydrocarbonoclastic Nitrate-Reducing Bacterial Communities in Bioturbated Coastal Marine Sediments." *FEMS Microbiology Ecology* 89 (3): 580–93. <https://doi.org/10.1111/1574-6941.12359>.
- Suja, Laura Duran, Stephen Summers, and Tony Gutierrez. 2017. "Role of EPS, Dispersant and Nutrients on the Microbial Response and MOS Formation in the Subarctic Northeast Atlantic." *Frontiers in Microbiology* 8 (APR): 1–15. <https://doi.org/10.3389/fmicb.2017.00676>.
- Sullivan, Mitchell J., Nicola K. Petty, and Scott A. Beatson. 2011. "Easyfig: A Genome Comparison Visualizer." *Bioinformatics* 27 (7): 1009–10. <https://doi.org/10.1093/bioinformatics/btr039>.
- Sun, Melanie Y., Katherine A. Dafforn, Emma L. Johnston, and Mark V. Brown. 2013. "Core Sediment Bacteria Drive Community Response to Anthropogenic Contamination over Multiple Environmental Gradients." *Environmental Microbiology* 15 (9): 2517–31. <https://doi.org/10.1111/1462-2920.12133>.
- Sungur, Ali, Mustafa Soylak, and Hasan Ozcan. 2014. "Investigation of Heavy Metal Mobility and Availability by the BCR Sequential Extraction Procedure: Relationship between Soil Properties and Heavy Metals Availability." *Chemical Speciation and Bioavailability* 26 (4): 219–30. <https://doi.org/10.3184/095422914X14147781158674>.

- Sutton, Dwayne J., Paul B. Tchounwou, Nanuli Ninashvili, and Elaine Shen. 2002. "Mercury Induces Cytotoxicity and Transcriptionally Activates Stress Genes in Human Liver Carcinoma (HepG 2) Cells." *International Journal of Molecular Sciences* 3 (9): 965–84. <https://doi.org/10.3390/i3090965>.
- Swannell, Richard P.J., Kenneth Lee, and Madeleine Mcdonagh. 1996. "Field Evaluations of Marine Oil Spill Bioremediation." *Microbiological Reviews* 60 (2): 342–65.
- Tabak, Henry H., Piet Lens, Eric D. Van Hullebusch, and Winnie Dejonghe. 2005. "Developments in Bioremediation of Soils and Sediments Polluted with Metals and Radionuclides - 1. Microbial Processes and Mechanisms Affecting Bioremediation of Metal Contamination and Influencing Metal Toxicity and Transport." *Reviews in Environmental Science and Biotechnology* 4 (3): 115–56. <https://doi.org/10.1007/s11157-005-2169-4>.
- Takáčová, Alžbeta, Miroslava Smolinská, Jozef Ryba, Tomáš Mackuľak, Jana Jokrllová, Pavol Hronec, and Gabriel Čík. 2014. "Biodegradation of Benzo[a]Pyrene through the Use of Algae." *Central European Journal of Chemistry* 12 (11): 1133–43. <https://doi.org/10.2478/s11532-014-0567-6>.
- Tan, H., J. T. Champion, J. F. Artiola, M. L. Brusseau, and R. M. Miller. 1994. "Complexation of Cadmium by a Rhamnolipid Biosurfactant." *Environmental Science and Technology* 28 (13): 2402–6. <https://doi.org/10.1021/es00062a027>.
- Tashla, Tamer, Radivoj Prodanovic, Jelana Boskovic, Milena Zuza, Dragan Solesa, Dragana Ljubojevic, and Nikola Puvaca. 2018. "Persistent Organic Pollutants and Heavy Metals and the Importance of Fish as a Bio-Indicator of Environmental Pollution." *Concepts of Dairy & Veterinary Sciences* 2 (2): 168–70. <https://doi.org/10.32474/cdvs.2018.02.000131>.
- Tchounwou, P. B., A. B. Ishaque, and J. Schneider. 2001. "Cytotoxicity and Transcriptional Activation of Stress Genes in Human Liver Carcinoma Cells (HepG2) Exposed to Cadmium Chloride." *Molecular and Cellular Biochemistry* 222 (1–2): 21–28. <https://doi.org/10.1023/A:1017922114201>.
- Telling, Jon, Alexandre M. Anesio, Martyn Tranter, Marek Stibal, Jon Hawkings, Tristram Irvine-Fynn, Andy Hodson, Catriona Butler, Marian Yallop, and Jemma Wadham. 2012. "Controls on the Autochthonous Production and Respiration of Organic Matter in Cryoconite Holes on High Arctic Glaciers." *Journal of Geophysical Research: Biogeosciences* 117 (1). <https://doi.org/10.1029/2011JG001828>.
- Thompson, Luke R., Jon G. Sanders, Daniel McDonald, Amnon Amir, Joshua Ladau, Kenneth J. Locey, Robert J. Prill, et al. 2017. "A Communal Catalogue Reveals Earth's Multiscale Microbial Diversity." *Nature* 551 (7681): 457–63. <https://doi.org/10.1038/nature24621>.
- Toes, Ann Charlotte M., Niko Finke, J. Gijs Kuenen, and Gerard Muyzer. 2008. "Effects of Deposition of Heavy-Metal-Polluted Harbor Mud on Microbial Diversity and Metal Resistance in Sandy Marine Sediments." *Archives of Environmental Contamination and Toxicology* 55 (3): 372–85. <https://doi.org/10.1007/s00244-008-9135-4>.
- Tornero, Victoria, and Georg Hanke. 2016. "Chemical Contaminants Entering the Marine Environment from Sea-Based Sources: A Review with a Focus on European Seas." *Marine Pollution Bulletin* 112 (1–2): 17–38. <https://doi.org/10.1016/j.marpolbul.2016.06.091>.
- Torres-Barceló, Clara, Blaise Franzon, Marie Vasse, and Michael E. Hochberg. 2016. "Long-Term Effects of Single and Combined Introductions of Antibiotics and Bacteriophages on

- Populations of *Pseudomonas Aeruginosa*." *Evolutionary Applications* 9 (4): 583–95. <https://doi.org/10.1111/eva.12364>.
- Tranum, Hilde Cecilie, Frode Olsgard, Jens M. Skei, Jane Indrehus, Sidsel Øverås, and Jonny Eriksen. 2004. "Effects of Copper, Cadmium and Contaminated Harbour Sediments on Recolonisation of Soft-Bottom Communities." *Journal of Experimental Marine Biology and Ecology* 310 (1): 87–114. <https://doi.org/10.1016/j.jembe.2004.04.003>.
- Tripathi, Manikant, Durgesh Singh, Surendra Vikram, Vijay Singh, and Shailendra Kumar. 2018. "Metagenomic Approach towards Bioprospection of Novel Biomolecule(s) and Environmental Bioremediation." *Annual Research & Review in Biology* 22 (2): 1–12. <https://doi.org/10.9734/arrb/2018/38385>.
- Ugbenyen, Anthony M., John J. Simonis, and Albertus K. Basson. 2018. "Screening for Biofloculant-Producing Bacteria from the Marine Environment of Sodwana Bay, South Africa." *Annals of Science and Technology* 3 (1): 16–20. <https://doi.org/10.2478/ast-2018-0010>.
- Vallenet, David, Alexandra Calteau, Stephane Cruveiller, Mathieu Gachet, Aurelie Lajus, Adrien Josso, Jonathan Mercier, et al. 2017. "MicroScope in 2017: An Expanding and Evolving Integrated Resource for Community Expertise of Microbial Genomes." *Nucleic Acids Research* 45 (D1): D517–28. <https://doi.org/10.1093/nar/gkw1101>.
- Valls, Marc, and Víctor De Lorenzo. 2002. "Exploiting the Genetic and Biochemical Capacities of Bacteria for the Remediation of Heavy Metal Pollution." *FEMS Microbiology Reviews* 26 (4): 327–38. [https://doi.org/10.1016/S0168-6445\(02\)00114-6](https://doi.org/10.1016/S0168-6445(02)00114-6).
- Vandieken, Verona, Niko Finke, and Bo Thamdrup. 2014. "Hydrogen, Acetate, and Lactate as Electron Donors for Microbial Manganese Reduction in a Manganese-Rich Coastal Marine Sediment." *FEMS Microbiology Ecology* 87 (3): 733–45. <https://doi.org/10.1111/1574-6941.12259>.
- Vela-Cano, María, Antonio Castellano-Hinojosa, Antonia Fernández Vivas, and María Victoria Martínez Toledo. 2014. "Effect of Heavy Metals on the Growth of Bacteria Isolated from Sewage Sludge Compost Tea." *Advances in Microbiology* 04 (10): 644–55. <https://doi.org/10.4236/aim.2014.410070>.
- Větrovský, Tomáš, and Petr Baldrian. 2013. "The Variability of the 16S rRNA Gene in Bacterial Genomes and Its Consequences for Bacterial Community Analyses." *PLoS ONE* 8 (2): 1–10. <https://doi.org/10.1371/journal.pone.0057923>.
- Vivo, Benedetto De, and Annamaria Lima. 2008. *Characterization and Remediation of a Brownfield Site. The Bagnoli Case in Italy. Environmental Geochemistry*. <https://doi.org/10.1016/B978-0-444-53159-9.00015-2>.
- Wang, Kai, Xiansen Ye, Huajun Zhang, Heping Chen, Demin Zhang, and Lian Liu. 2016. "Regional Variations in the Diversity and Predicted Metabolic Potential of Benthic Prokaryotes in Coastal Northern Zhejiang, East China Sea." *Scientific Reports* 6: 1–12. <https://doi.org/10.1038/srep38709>.
- Wang, S., and X. Shi. 2001. "Molecular Mechanisms of Metal Toxicity and Carcinogenesis." *Molecular and Cellular Biochemistry* 222 (1–2): 3–9. <https://doi.org/10.1023/A:1017918013293>.
- Watanabe, Kazuya. 2001. "Microorganisms Relevant to Bioremediation." *Current Opinion in*

- Biotechnology* 12 (3): 237–41. [https://doi.org/10.1016/S0958-1669\(00\)00205-6](https://doi.org/10.1016/S0958-1669(00)00205-6).
- Welch, B L. 1947. "The Generalization of 'Student's' Problem When Several Different Population Variances Are Involved." *Biometrika Trust* 34 (1): 28–35.
- Wharfe, Emma S., Roger M. Jarvis, Catherine L. Winder, Andrew S. Whiteley, and Royston Goodacre. 2010. "Fourier Transform Infrared Spectroscopy as a Metabolite Fingerprinting Tool for Monitoring the Phenotypic Changes in Complex Bacterial Communities Capable of Degrading Phenol." *Environmental Microbiology* 12 (12): 3253–63. <https://doi.org/10.1111/j.1462-2920.2010.02300.x>.
- White, C., J. A. Sayer, and G. M. Gadd. 1997. "Microbial Solubilization and Immobilization of Toxic Metals: Key Biogeochemical Processes for Treatment of Contamination." *FEMS Microbiology Reviews* 20 (3–4): 503–16. [https://doi.org/10.1016/S0168-6445\(97\)00029-6](https://doi.org/10.1016/S0168-6445(97)00029-6).
- Williamson, Adele, Concetta De Santi, Bjørn Altermark, Christian Karlsen, and Erik Hjerde. 2016. "Complete Genome Sequence of Halomonas Sp. R5-57." *Standards in Genomic Sciences* 11 (1): 1–9. <https://doi.org/10.1186/s40793-016-0192-4>.
- Wilmes, Paul, and Philip L. Bond. 2004. "The Application of Two-Dimensional Polyacrylamide Gel Electrophoresis and Downstream Analyses to a Mixed Community of Prokaryotic Microorganisms." *Environmental Microbiology* 6 (9): 911–20. <https://doi.org/10.1111/j.1462-2920.2004.00687.x>.
- Wolfe-Simon, Felisa, Jodi Switzer Blum, Thomas R. Kulp, Gwyneth W. Gordon, Shelley E. Hoefft, Jennifer Pett-Ridge, John F. Stolz, et al. 2011. "A Bacterium That Can Grow by Using Arsenic Instead of Phosphorus." *Science* 332 (6034): 1163–66. <https://doi.org/10.1126/science.1197258>.
- Wuana, Raymond A, and Felix E Okieimen. 2011. "Heavy Metals in Contaminated Soil: A Review of Sources, Chemistry, Risks and Best Available Strategies for Remediation." *ISRN Ecology* 2011: 1–20. <https://doi.org/10.5402/2011/402647>.
- Xu, Ran, Angelina N L Lau, Yong Giak Lim, and Jeffrey P. Obbard. 2005. "Bioremediation of Oil-Contaminated Sediments on an Inter-Tidal Shoreline Using a Slow-Release Fertilizer and Chitosan." *Marine Pollution Bulletin* 51 (8–12): 1062–70. <https://doi.org/10.1016/j.marpolbul.2005.02.049>.
- Xu, Xingjian, Wenming Liu, Shuhua Tian, Wei Wang, Qige Qi, Pan Jiang, Xinmei Gao, Fengjiao Li, Haiyan Li, and Hongwen Yu. 2018. "Petroleum Hydrocarbon-Degrading Bacteria for the Remediation of Oil Pollution Under Aerobic Conditions: A Perspective Analysis." *Frontiers in Microbiology* 9 (December). <https://doi.org/10.3389/fmicb.2018.02885>.
- Xu, Ying, Roland D. Kersten, Sang Jip Nam, Liang Lu, Abdulaziz M. Al-Suwailem, Huajun Zheng, William Fenical, Pieter C. Dorrestein, Bradley S. Moore, and Pei Yuan Qian. 2012. "Bacterial Biosynthesis and Maturation of the Didemnin Anti-Cancer Agents." *Journal of the American Chemical Society* 134 (20): 8625–32. <https://doi.org/10.1021/ja301735a>.
- Yakimov, Michail M., Renata Denaro, Maria Genovese, Simone Cappello, Giuseppe D'Auria, Tatyana N. Chernikova, Kenneth N. Timmis, Peter N. Golyshin, and Laura Giluliano. 2005. "Natural Microbial Diversity in Superficial Sediments of Milazzo Harbor (Sicily) and Community Successions during Microcosm Enrichment with Various Hydrocarbons." *Environmental Microbiology* 7 (9): 1426–41. <https://doi.org/10.1111/j.1462-5822.2005.00829.x>.

- Yakimov, Michail M., Kenneth N. Timmis, and Peter N. Golyshin. 2007. "Obligate Oil-Degrading Marine Bacteria." *Current Opinion in Biotechnology* 18 (3): 257–66. <https://doi.org/10.1016/j.copbio.2007.04.006>.
- Yakimov, Michail M, Peter N Golyshin, Siegmund Lang, Edward R B Moore, Wolf-rainer Abraham, Heinrich Lunsdorf, and Kenneth N Timmis. 1998. "A New , Hydrocarbon-Degrading and Surfactant-Producing Marine Bacterium." *International Journal of Systematic Bacteriology* 48: 339–48. <http://ijs.sgmjournals.org/cgi/doi/10.1099/00207713-48-2-339>.
- Yan, Shaomin, and Guang Wu. 2017. "Reorganization of Gene Network for Degradation of Polycyclic Aromatic Hydrocarbons (PAHs) in *Pseudomonas Aeruginosa* PAO1 under Several Conditions." *Journal of Applied Genetics* 58 (4): 545–63. <https://doi.org/10.1007/s13353-017-0402-9>.
- Yang, Lin, Hui Lin Yang, Zong Cai Tu, and Xiao Lan Wang. 2016. "High-Throughput Sequencing of Microbial Community Diversity and Dynamics during Douchi Fermentation." *PLoS ONE* 11 (12): 1–19. <https://doi.org/10.1371/journal.pone.0168166>.
- Yang, Si Zhong, Hui Jun Jin, Zhi Wei, Rui Xia He, Yan Jun Ji, Xiu Mei Li, and Shao Peng Yu. 2009. "Bioremediation of Oil Spills in Cold Environments: A Review." *Pedosphere* 19 (3): 371–81. [https://doi.org/10.1016/S1002-0160\(09\)60128-4](https://doi.org/10.1016/S1002-0160(09)60128-4).
- Yao, Jun, Wenbing Li, Fangfang Xia, Yuange Zheng, Chengran Fang, and Dongsheng Shen. 2012. "Heavy Metals and PCDD/Fs in Solid Waste Incinerator Fly Ash in Zhejiang Province, China: Chemical and Bio-Analytical Characterization." *Environmental Monitoring and Assessment* 184 (6): 3711–20. <https://doi.org/10.1007/s10661-011-2218-0>.
- Yedjou, Clement G., and Paul B. Tchounwou. 2007a. "In-Vitro Cytotoxic and Genotoxic Effects of Arsenic Trioxide on Human Leukemia (HL-60) Cells Using the MTT and Alkaline Single Cell Gel Electrophoresis (Comet) Assays." *Molecular and Cellular Biochemistry* 301 (1–2): 123–30. <https://doi.org/10.1007/s11010-006-9403-4>.
- Yedjou, Clement, Tchounwou, Paul. 2007b. "N-Acetyl-L-Cysteine Affords Protection against Lead-Induced Cytotoxicity and Oxidative Stress in Human Liver Carcinoma (HepG2) Cells." *International Journal of Environmental Research and Public Health* 4 (2): 132–37. <https://doi.org/10.3390/ijerph2007040007>.
- Yin, Huaqun, Jiaojiao Niu, Youhua Ren, Jing Cong, Xiaoxia Zhang, Fenliang Fan, Yunhua Xiao, et al. 2015. "An Integrated Insight into the Response of Sedimentary Microbial Communities to Heavy Metal Contamination." *Scientific Reports* 5 (September): 1–12. <https://doi.org/10.1038/srep14266>.
- Yu, S. H., L. Ke, Y. S. Wong, and N. F.Y. Tam. 2005. "Degradation of Polycyclic Aromatic Hydrocarbons by a Bacterial Consortium Enriched from Mangrove Sediments." *Environment International* 31 (2): 149–54. <https://doi.org/10.1016/j.envint.2004.09.008>.
- Zaki, Mona S., Mohammad M. N. Authman, and Hossan H. H. Abbas. 2015. "Bioremediation of Petroleum Contaminants in Aquatic Environments." *Life Science Journal* 12 (5): 109–21. <https://doi.org/10.1145/3132847.3132886>.
- Zanaroli, Giulio, Annalisa Balloi, Andrea Negroni, Luigimaria Borruso, Daniele Daffonchio, and Fabio Fava. 2012. "A Chloroflexi Bacterium Dechlorinates Polychlorinated Biphenyls in Marine Sediments under in Situ-like Biogeochemical Conditions." *Journal of Hazardous Materials* 209–210: 449–57. <https://doi.org/10.1016/j.jhazmat.2012.01.042>.

- Zengler, Karsten, Hans H. Richnow, Ramon Rosselló-Mora, Walter Michaelis, and Friedrich Widdel. 1999. "Methane Formation from Long-Chain Alkanes by Anaerobic Microorganisms." *Nature* 401 (6750): 266–69. <https://doi.org/10.1038/45777>.
- Zepeda, Vanessa K., Hans Jürgen Busse, Jan Golke, Jimmy H.W. Saw, Maqsudul Alam, and Stuart P. Donachie. 2015. "Terasakiispira Papahanaumokuakeensis Gen. Nov., Sp. Nov., a Gammaproteobacterium from Pearl and Hermes Atoll, Northwestern Hawaiian Islands." *International Journal of Systematic and Evolutionary Microbiology* 65 (10): 3609–17. <https://doi.org/10.1099/ijsem.0.000438>.
- Zgurskaya, Helen I., Cesar A. López, and S. Gnanakaran. 2016. "Permeability Barrier of Gram-Negative Cell Envelopes and Approaches to Bypass It." *ACS Infectious Diseases* 1 (11): 512–22. <https://doi.org/10.1021/acsinfecdis.5b00097>.
- Zhang, Chang, Zhi gang Yu, Guang ming Zeng, Min Jiang, Zhong zhu Yang, Fang Cui, Meng ying Zhu, Liu qing Shen, and Liang Hu. 2014. "Effects of Sediment Geochemical Properties on Heavy Metal Bioavailability." *Environment International* 73: 270–81. <https://doi.org/10.1016/j.envint.2014.08.010>.
- Zhang, Kai, Yongge Sun, Zhisong Cui, Di Yu, Li Zheng, Peng Liu, and Zhenmei Lv. 2017. "Periodically Spilled-Oil Input as a Trigger to Stimulate the Development of Hydrocarbon-Degrading Consortia in a Beach Ecosystem." *Scientific Reports* 7 (1): 1–9. <https://doi.org/10.1038/s41598-017-12820-7>.
- Zhang, Li, Yi Jin, Meng Huang, and Trevor M. Penning. 2012. "The Role of Human Aldo-Keto Reductases in the Metabolic Activation and Detoxication of Polycyclic Aromatic Hydrocarbons: Interconversion of PAH Catechols and PAH o-Quinones." *Frontiers in Pharmacology* 3 NOV (November): 1–12. <https://doi.org/10.3389/fphar.2012.00193>.
- Zhang, Wen, Jang Seu Ki, and Pei Yuan Qian. 2008. "Microbial Diversity in Polluted Harbor Sediments I: Bacterial Community Assessment Based on Four Clone Libraries of 16S rDNA." *Estuarine, Coastal and Shelf Science* 76 (3): 668–81. <https://doi.org/10.1016/j.ecss.2007.07.040>.
- Zhang, Ye, April Z. Gu, Tianyu Cen, Xiangyang Li, Miao He, Dan Li, and Jianmin Chen. 2018. "Sub-Inhibitory Concentrations of Heavy Metals Facilitate the Horizontal Transfer of Plasmid-Mediated Antibiotic Resistance Genes in Water Environment." *Environmental Pollution* 237: 74–82. <https://doi.org/10.1016/j.envpol.2018.01.032>.
- Zhao, Baisuo, Hui Wang, Xinwei Mao, and Ruirui Li. 2009. "Biodegradation of Phenanthrene by a Halophilic Bacterial Consortium under Aerobic Conditions." *Current Microbiology* 58 (3): 205–10. <https://doi.org/10.1007/s00284-008-9309-3>.
- Zheng, Binghui, Xingru Zhao, Lusan Liu, Zicheng Li, Kun Lei, Lei Zhang, Yanwen Qin, Zhifen Gan, Shizhen Gao, and Lixin Jiao. 2011. "Effects of Hydrodynamics on the Distribution of Trace Persistent Organic Pollutants and Macrobenthic Communities in Bohai Bay." *Chemosphere* 84 (3): 336–41. <https://doi.org/10.1016/j.chemosphere.2011.04.006>.
- Zhou, Weizhi, Hai'ou Zhang, Yuhong Ma, Jianpeng Zhou, and Yuzhong Zhang. 2013. "Bio-Removal of Cadmium by Growing Deep-Sea Bacterium *Pseudoalteromonas* Sp. SCSE709-6." *Extremophiles* 17 (5): 723–31. <https://doi.org/10.1007/s00792-013-0554-4>.
- Zhuang, Li, Ziyang Tang, Jinlian Ma, Zhen Yu, Yueqiang Wang, and Jia Tang. 2019. "Enhanced Anaerobic Biodegradation of Benzoate under Sulfate-Reducing Conditions with Conductive Iron-Oxides in Sediment of Pearl River Estuary." *Frontiers in Microbiology* 10:

1–13. <https://doi.org/10.3389/fmicb.2019.00374>.

Zouboulis, A. I., K. A. Matis, N. K. Lazaridis, and P. N. Golyshin. 2003. "The Use of Biosurfactants in Flotation: Application for the Removal of Metal Ions." *Minerals Engineering* 16 (11): 1231–36. <https://doi.org/10.1016/j.mineng.2003.06.013>.

Zouch, Hana, Léa Cabrol, Sandrine Chifflet, Marc Tedetti, Fatma Karray, Hatem Zaghdien, Sami Sayadi, and Marianne Quéméneur. 2018. "Effect of Acidic Industrial Effluent Release on Microbial Diversity and Trace Metal Dynamics During Resuspension of Coastal Sediment." *Frontiers in Microbiology* 9 (December). <https://doi.org/10.3389/fmicb.2018.03103>.